Meox2 is necessary for axial and appendicular tendon development

Acharya, Nikita Amit

Awarding institution:
King's College London

King's College London

FACULTY OF LIFE SCIENCE AND MEDICINE

Randall Division of Cell and Molecular Biophysics

Meox2 is necessary for axial and appendicular tendon development

by

Nikita Amit Acharya

Thesis for the degree of Doctor of Philosophy

March 2016

ABSTRACT

The development of complex musculoskeletal system requires essential interaction between muscles, bone, cartilage, soft connective tissue which includes tendons and ligaments and innervation of muscle by motor neurons. Tendon is a fibrous connective tissue that connects bone to muscle and bone to bone. Axial tendon progenitors arise from the syndetome in somites while limb tendons arise from lateral plate mesoderm. *Scleraxis*, a bHLH transcription factor is expressed in tendon cells.

Meox2 has been shown to express in the limb mesoderm. In this study, we found that *Meox2* is also necessary for the normal development of tendons and soft connective tissue. *Meox2*$^{-/-}$ neonatal mice had brittle, pale and thin tendons. Histological analysis showed mispatterned tendon tissue and reduced tendon mass. Using the *Scleraxis-GFP* reporter transgene, we found decreased expression of GFP in *Meox2*$^{-/-}$ in postnatal limb and tail tendons. In situ analysis of *Scx* RNA expression in *Meox2*$^{-/-}$ embryos confirmed the earliest tendon defects occurred at E12.5, preceding the defects observed in the *Scx*$^{-/-}$ mice.

To elucidate the mechanism, Meox2^{+} cells were analysed by antibody staining and compared with ScxGFP^{+} cells from E12.5-14.5. At E12.5, when tendon cells organise between prospective muscle and bone in the developing limb and trunk, we found Meox2 expression adjacent to (limbs) or overlapping (somites) but not co-expressed with Scx-GFP. During tendon cell condensation and differentiation at E13.5, Meox2^{+} cells were found in the connective tissue of the autopod and in non-overlapping expression with Scx-GFP^{+} cells in the zeugopod. However, at E14.5, the stage when the initial formation of mature tendons is complete, Meox2^{+} cells were found in Scx-GFP^{+} autopod tendons, whereas in the zeugopod Meox2^{+} cells remained non-overlapping with Scx-GFP^{+} cells revealing tendon diversity in the limb autopod and zeugopod. Analysis of a Meox2-nLacZ knock-in allele showed LacZ^{+} cells in tendons and connective tissue at E13.5, indicating that although these cells do not express endogenous Meox2 at that stage they are derived from Meox2-expressing

progenitors that have contributed to the tendon lineage. We also found reduction of $LacZ^{+}$ cells in the limb soft connective tissue and tendons at E15.5.

TGFβ signalling plays an essential role in the formation of muscle connective tissues and a severe tendon phenotype in TGFβ2/3 knockouts first manifest at E12.5 which coincides with the earliest tendon defect in *Meox2* mutants. Dynamic expression of TGFβ2 in the majority of musculoskeletal tissues and, its involvement in the recruitment of tendon cells led us to hypothesise that the defect in Meox2 mutants may be due to the down regulation of TGFβ2 signalling. Surprisingly, TGFβ2 RNA expression in $Meox2^{-/-}$ at E12.5 showed increased levels in the inter-limb somites and the expression domains were markedly expanded in zeugopod. Additionally, the overexpression of TGFβ2 in vitro showed differential expression of Meox2.

Collectively, these data provide a model on the biphasic necessity of Meox2 wherein it acts extrinsically during tendon induction and organisation while intrinsically during tendon maturation.

ACKNOWLEDGEMENTS

Gratitude is the memory of the heart. I have several reasons to be grateful to Dr. Baljinder Mankoo for which I could thank him all my life but it still wouldn't be enough. Yet I make this humble attempt at expressing my heartfelt gratitude to him for unfailingly supporting and patiently guiding me through every step of my journey.

I am also very thankful to Dr. Yin Biao-Sun and Dr. Elizabeth Ehler for sharing me with many thoughtful inputs. I am immensely thankful to Prof. Simon Hughes, Prof. Peter Zammit, Prof. Malcom Logan and all the members of Mankoo, Hughes, Zammit and Logan labs for making this an enjoyable learning experience and their gift of memories. Merci Dr. Nicolas Figeac for always lending me an ear and encouraging me at the lowest of times.

I am grateful to my friends Sweta, Dr. Emily, Dr. Fernanda, Roksana, Marta, Dee, Georgia, for showing me the rope when I am in doubt, showing their kindness and being so generous with their time. I am grateful for their friendship. A special thank you to my lovely sisters, Veronica for always being there and supporting me.

Having been blessed with in-laws, who are as dear as my own parents, I feel extremely lucky. Saying thanks to them and my parents would be too little for all the inexhaustible love, support and encouragement that they have given me! Thank you to Kamaxi, Nitesh and Shyamoli for their extreme support towards me.

My success would simply have not been possible without my dearest husband Amit. Thank you very much for always being there when I needed you and for believing in my dreams. Last but not the least, my inspiration, my son Kevin whom I love dearly. Thank you, thank you, thank you to both of you for coming in my life!

TABLE OF CONTENTS

List of figures

Chapter 1

Chapter 2

Chapter 3

Chapter 4

Chapter 5

Chapter 6

List of tables

Abbreviations

bHLH basic helix-loop-helix

BMP Bone morphogenetic protein

ECM Extracellular matrix

Egr Early growth response

ERK Extracellular signal- regulated kinases

Ets E26 transformation specific

FGF Fibroblast growth factor

Hox Homeotic gene

KI KI-N or $Meox2^{nLacZ}$ mouse line

KO *Meox2*$^{-/-}$ (original knockout) mouse line

MAPK Mitogen-activated protein kinase

MCP Metacarpophalangeal joints

MCT Muscle connective tissue

MRF Myogenic regulatory factors

MTJ Myotendinous junction

No Notochord

NT Neural tube

Pax Paired box genes

Sox SRY related HMG-box

Tbx T-box transciption factor

Tcf T-cell factor

TGF Transforming growth factor

TPC Tendon progenitor cells

Chapter 1

Introduction

1.1 Connective tissue- a component of musculoskeletal system

The musculoskeletal system serves as a tool that provides all vertebrates locomotion, movements and maintaining body positions. The accumulated knowledge based upon molecular characterization showed that the functional musculoskeletal system has diverse group of tissues. It includes muscle, bones, dense connective tissue (tendons and ligaments) and loose connective tissue (muscle connective tissue and fascia). The innervations of nerves then takes place to receive neuronal signals and vascularization by blood vessels that provide nutrients and signal to the growing tissues takes place. In order to understand this multicomponent system, it is necessary to comprehend basic development, which includes specification, differentiation and maturation of these diverse cell groups. In addition, it is also important to understand how these different tissues undergo coordinated morphogenesis by extrinsically influencing molecular machinery and thereby achieve an integrated functional system.

Furthermore, the musculoskeletal system acts as a great model of studying embryonic morphogenesis because it is composed of easily identifiable tissue types, which allow studying histology and patterning development. The development of a functioning musculoskeletal system is dependent on intricate signaling pathways along with the extrinsic and intrinsic gene regulation activity. During development these tissue must interact with high fidelity to give rise to a function musculoskeletal system (Figure 1.1). To date, much work has been focused on the muscle and bone development. However, several emerging studies provided insights on embryonic genesis of connective tissues and their spatial and temporal relationship with other tissues in musculoskeletal system.

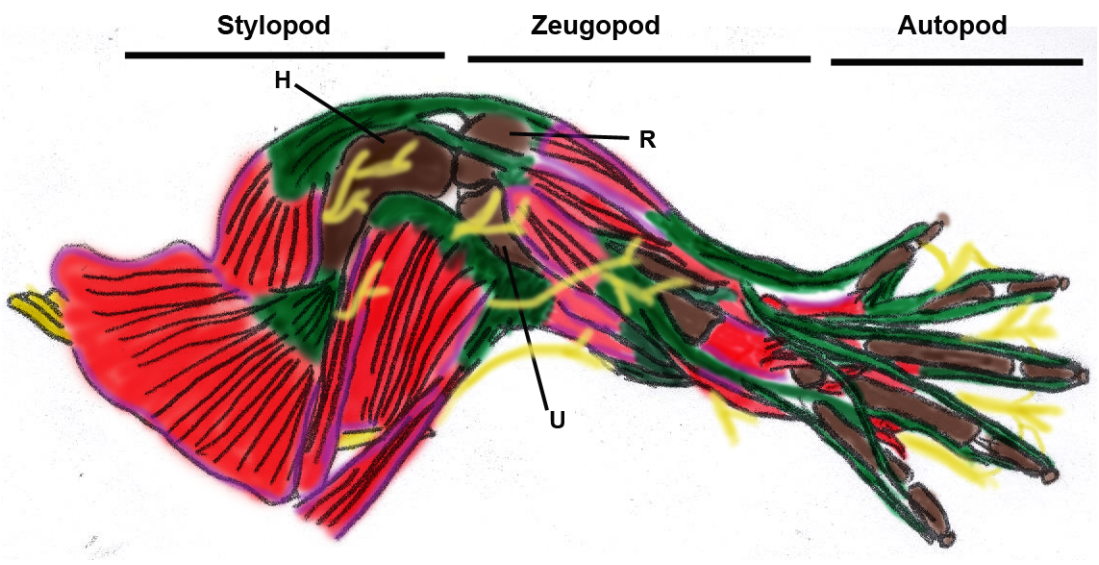

Figure 1.1: Illustration of the limb musculoskeletal system. The embryonic development of this system depends on the molecular signals from muscles (red), bone (grey), muscle connective tissue (purple), tendon (green) and nerve innervations (yellow). R, radius; U, ulna; H, humerus

1.2 Tendons- a dense connective tissue

Tendons are dense, fibrous connective tissues and are embedded in extracellular matrix (ECM). Tendon connects muscle to skeletal elements, and via these connecting attachments, it then passively transfer force generated by muscle thereby contributing to the overall integrity of the musculoskeletal system (Birk et al., 1989). The precise attachment site ensure that the bones are connected to the appropriate muscles by their respective tendons, and that the integrity of the joints is held together by the ligaments, while the individual muscle bundles are embedded within the loose connective tissue i.e. muscle connective tissue (MCT). Therefore, the tissues in direct contact with the final muscle are the tendons that are classified under dense connective tissue.

The mutual interactions between cells during embryonic development from somites lead to the formation of complex tissue, an example of which is the musculoskeletal system. Somites are the segmental blocks of mesoderm

present dorsally in the embryo and lie next to the neural tube and notochord. During the development, a naïve somite buds off as a columnar epithelial ball surrounding a central mesenchymal cavity from the presomitic mesoderm (PSM). The secreted signal from surrounding tissues results in epithelio-mesenchyme transition of the ventral part of somite. This event establishes the polarity in the somite along the dorsoventral and mediolateral axes. As a result, the somite derivatives are further subdivided into epaxial and hypaxial domains and these domains forms two separate compartments: sclerotome from the ventral mesenchyme and the dermomyotome from a dorsal epithelial layer. These distinct compartments in somites ultimately form muscles and dermis from dermomyotome, cartilage from sclerotome and tendons from syndetome, respectively (Brent et al., 2003; Kardon, 1998; Schweitzer et al., 2001; Tozer and Duprez, 2005). The dorso-medial dermomyotome expresses *Myf5* and these cells contribute to the underlying epaxial myotome, where the cells start to express *MyoD*, this region gives rise to the axial muscles. The ventro-lateral region of the dermomyotome forms hypaxial myotome that also expresses *MyoD*. This region forms intercostal and abdominal wall muscles. Finally, the central region of the dermomyotome develops into dermatome and forms dermis in the skin of neck, back, lateral and ventral surfaces of the trunk. Additionally cells from the central dermomyotome provide progenitors of future satellite cells – skeletal muscle stem cells. The ventro-lateral dermomyotome also gives rise to precursors of limb and extrinsic tongue muscles. Delamination, migration, proliferation, and differentiation occur in response to the cues available from the adjacent mesoderm. The delamination and migration of myoblasts are dependent on c-met, a tyrosine kinase receptor and its ligand SF/HGF expressed by limb mesoderm (Dietrich et al., 1999). In the absence of c-met or HGF, limbs muscles are absent (Bladt et al., 1995; Schmidt et al., 1995). Moreover, transcription of c-met is dependent on *Pax3* and in mutant mouse embryos that lack functional *Pax3* gene, myoblasts fail to delaminate from hypaxial dermomyotome and thus show a limb muscle phenotype (Borycki et al., 1999; Daston et al., 1996). Interestingly, epaxial myogenesis remained unaffected in $Pax3^{-/-}$ mutants (Borycki et al., 1999). Furthermore, another transcription factor, *Lbx1* is important for the migration but not delamination (Schafer and Braun, 1999). In $Lbx1^{-/-}$ mutant mice, the dorsal

limb muscle precursors followed their destined path whereas ventral limb myoblasts were disorientated (Brohmann et al., 2000; Gross et al., 2000; Schafer and Braun, 1999). Once delaminated, these cells express the receptors CXCR4 and EphA4 and respond to SDF1, the CXCR4 ligand, expressed in the limb mesoderm (Hunger et al., 2012; Vasyutina et al., 2005). Thereby, these regulators provide a defined path for the arrival of limb muscle precursors inside the limb mesoderm. In the absence of CXCR4 or SDF1, there is a reduction of *Lbx1*$^{+}$ muscle progenitor cells in the dorsal distal limb domain (Vasyutina et al., 2005). Finally, the migrated myoblasts in the limb then undergo differentiation and specification into dorsal and ventral muscle masses. Muscle patterning in the limb bud is perturbed in the absence of *Meox2* and loss of function in mice showed normal migration of muscle progenitors but impaired muscle patterning and specification in the limb (Mankoo et al., 1999).

Understanding normal mechanism of tendon development is important in order to generate functional and self-renewing tendon tissue. An optimal level of elasticity along with high mechanical strength and good flexibility makes tendon, unique connective tissues that have relatively few blood vessels and functions at low metabolic rate. Tendon injuries are common and affect a substantial portion of recreational and professional athletes and those in many occupations involving repetitive work (Brukner and Connell, 2016). This can be reasoned due to the classification of tendons amongst the heaviest loaded tissue type in the body (Harrison et al., 2010). Injuries in tendon clinically represent a serious and still unresolved problem since damaged tendon tissue heals very slowly and no surgical treatment can restore damaged tendon tissues to its normal structure integrity and mechanical strength (Sakabe and Sakai, 2011). Although events in the tendon healing are identical to most connective tissue, however, it occurs at a slower rate in tendon due to density of the tissue and hypocellularity. The total volume occupied by cells in tendon is only 5%. Tendinopathy, is characterised by activity related pain, focal tendon tenderness and decreased strength and movement of affected area. The acute traumatic flexor tendon injuries accounts for 25% of work related injuries and 75% of Achilles tendon injuries are reported in the individuals participating in sports (Raikin et al., 2013).

1.2.1 Tendon structure

The structure of tendons can be divided into six major compartments (Figure 1.2). The smallest component of a tendon is a collagen fibril, which is made up of longitudinally arranged chains of tropocollagen. A collagen fibril is a group of interconnected collagen strands that are bound together and are secreted by fibroblasts. One-step up in the tendon structure is the collagen fibre. The collagen fibre is a group of collagen fibrils bound in a sheath of endotenon (a substance that helps to stabilize and binds the fibrils). Fibre bundles represent the next level in the tendon. Fibre bundles are a group of collagen fibres bound together in a sheath of endotenon. A secondary fibre bundle is a group of fibre bundles bound together in a sheath of endotenon. A fascicle is the second largest component of tendon structure. Moreover, the group of secondary fibre bundles are bound together by endotenon. The endotenon that surrounds the fascicles is crimped in areas that may come under high stress. The tendon itself is the largest structure and is composed of a group of fascicles that are bound together by an interior sheath of endotenon and an exterior sheath of connective tissue called epitenon.

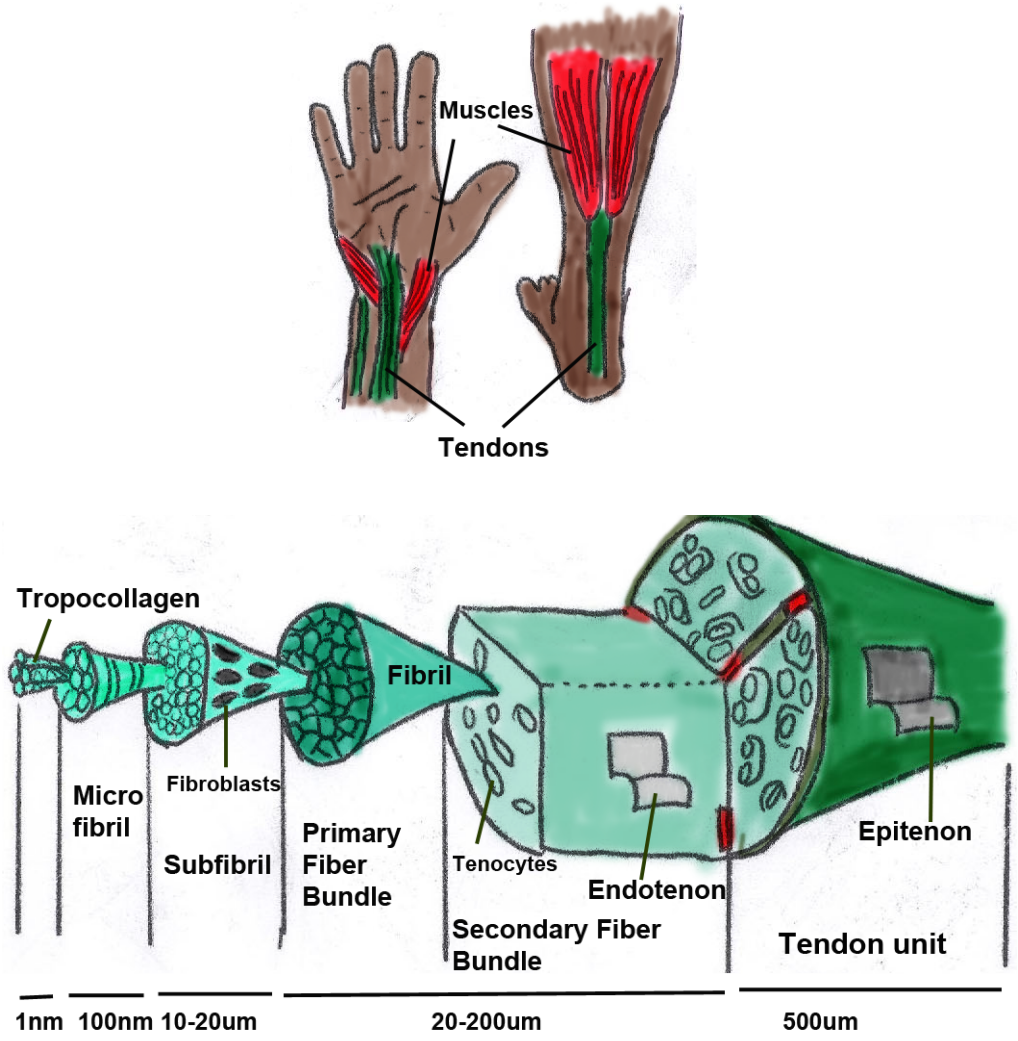

Figure 1.2: Illustration of the tendon position and organisation. Identical structural formats can be seen in either flexor tendon of hand or foot Achilles tendon. Tenocytes (tendon cell type) produce and secretes trihelical tropocollagen proteins that form collagen bundles and are arranged in cross-striated parallel fibrils. These collagen fibrils are enveloped by endotenon, which in turn surrounded by an exterior sheath called epitenon.

1.2.2 Composition of tendon

Water is predominant component at 55-70% in tendons. The collagen proteins, predominantly type I and small amounts of type III and V (Silver et al., 2003) comprises 70-80% of the dry weight. In addition, elastin, proteoglycans,

glycosaminoglycans and glycoproteins (e.g. fibronectin, thrombospondin) are also present. Collagen protein, an essential building block of musculoskeletal system can be found in both fibril and non-fibril forms. Type I collagen molecule is rod-like with little flexibility and high mechanical strength (Engel, 1997). Moreover, all of the fibril forming collagens self-assembles into cross-striated fibrils with a characteristic 67 nm repeat. They all share a triple helical region that is roughly 1000 amino acid residues long with a length of about 300nm (Reviewed by Silver et al., 2003). These collagens are synthesized within cells in a precursor form termed procollagen that has amino and carboxy-terminal non-helical ends that are about 15 and 10 nm long, respectively.

The cellular elements within tendons are known as tenocytes, which are type of fibroblasts, that synthesis, and secrete the collagen and all components of the extracellular matrix (ECM). These fibroblasts are termed “tenoblasts” when still immature. They are spindle-shaped. As they age, tenoblasts become elongated and transform into “tenocytes.” Together, tenocytes account for 90–95% of the cellular elements of tendons. The remaining 5–10% consists of chondrocytes at the bone attachment and insertion sites, synovial cells of the tendon sheath and vascular cells, including capillary endothelial cells and smooth muscle cells of arterioles (Reviewed by Hoffmann and Gross, 2007). Nonetheless, most of the mentioned molecules are not specific to tendons and virtually occurs throughout most ECM, and hence not considered as specific markers for tendon differentiation. However, there are extensive researches on the molecular architectural of tendon and its composition but not much in known about how this tissue is patterned and coordinated during development. Identification of early events in the tendon formation became possible with the gene, which encodes for a basic helix-loop-helix transcription factor *Scleraxis (Scx)*. It is a distinctive marker of tendon cells since it is expressed by both tendon progenitor cells (TPC) and mature differentiated tenocytes (Schweitzer et al., 2001). Recently stem cells have been discovered in tendon that show similar properties to tenoblast cells and are therefore specified but undifferentiated tendon progenitor cells. Tendon stem/progenitor cells (TSPCs) were isolated from adult tendons, and the stem cell niche of TSPCs is defined by the ECM of

tendons (Bi et al., 2007). These cells showed the characteristics of stem cells and also expressed combination of tendon cell markers, namely, Scx, TNMD, COMP and tenascin. TSPCs differ in their differentiation potential, morphology, proliferation and marker expression from tenocytes (Zhang and Wang, 2010); and TSPCs proliferate and increase collagen production in response to anabolic exercise, in a manner parallel to that shown by muscle stem cells (Zhang et al., 2010). In fact, Zhang et al. confirmed that these TSPCs express the known stem cell markers such as Oct-4, SSEA-4 and nucleostemin. The primary role of adult stem cells is to maintain homeostasis and repair of tissues, this function has yet to be demonstrated for TSPCs.

1.2.3 Embryonic morphogenesis of tendons

Comprehensive work has identified mechanisms, which regulates all stages of embryonic genesis of tendons. Still there are only few molecular factors shown to be crucial for tendon development when compared to those found in the genesis of muscles and skeleton. The tendon morphogenesis is a well-organised process. During the 10^{th} day of mouse development, tendon specific cells labelled by *Scx* gene, begin to induce in the limb mesoderm and in syndetome of somites. The cranial tendons are specified from neural crest cells (Schweitzer et al., 2010) Both compartments give rise to different group of tendons found in the appendicle and axial structure. These so-called “tendon progenitor cells” (TPC’s) that are specified to express tendon specific gene, *Scx*, exhibit three distinctive stages during the course of morphogenesis namely, (a) induction (E10.5-11.5), (b) alignment and organisation (E12.5), (c) maturation and differentiation (E13.5 onwards) as shown in figure 1.3 for limb tendon development.

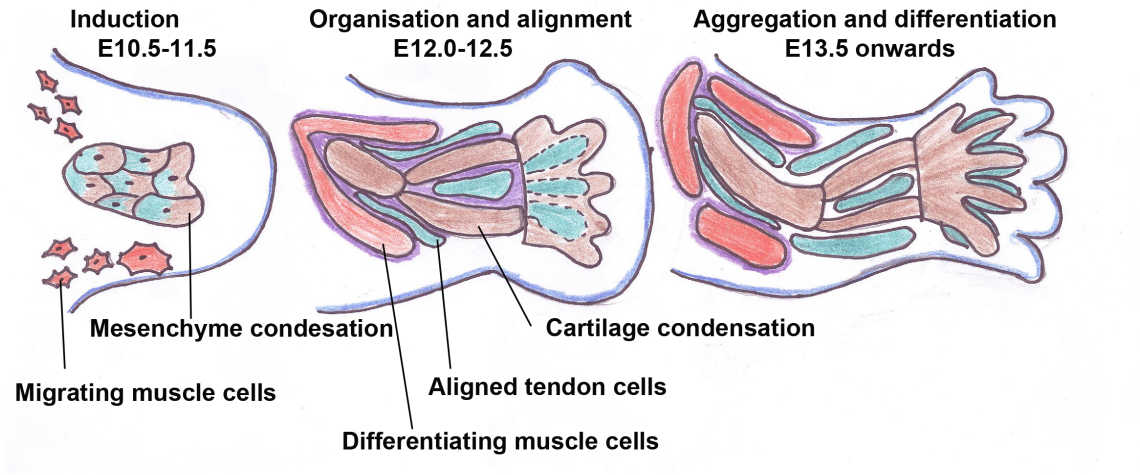

Figure 1.3: Diagram of the mouse limb tendon development. Induction of initial *Scx*-expressing tendon precursors occurs within the limb mesenchyme between E10.5-E11.5. During organisation and alignment of tendon progenitor cells between E12.0-E12.5, the cells are positioned at the presumptive functional site and a second wave of the recruitment of tendon cells occurs. Moreover, the intrinsic and extrinsic regulators are maintaining the tenoblastic identity. Eventually, from E13.5 onwards, mature tendons are formed due to combined activity of the extrinsic signals from the adjacent muscle and cartilage cells. In addition, *Scx* intrinsically favours the aggregation and differentiation of tendon cells to form the mature distinct tendon.

From the neonatal stage, the tendon tissues lose their ability to differentiate, instead, synthesize and secrete extra-cellular matrix (ECM) proteins that acts as scaffolding proteins for collagen fibril assembly. Moreover, an increase in collagen fibril diameter and changes in the morphology of fibroblast cells occur (Diamant et al., 1972).

The cellular dynamics and interactions of musculoskeletal components that regulate tendon development differ in the axial skeleton versus limb, and between autopod versus zeugopod. For example, the specification of TPC are autonomous in the limb mesoderm, however, for the proper organisation and maturation, signals from myogenic cell are crucial (Huang et al., 2015a; Kardon, 1998). In contrast, Scx-positive tendon cells in the somites are induced under the influence of FGF signalling emanating from adjacent myotome. A more

elaborated description on axial versus limb tendon development stages is discussed in the next section.

1.2.4 Inductive cues for axial versus limb tendon progenitor cells

Earlier chick-quail grafting orthotopic and heterotrophic transplantations showed that the non-myogenic components of the intricate musculoskeletal system of the limb, such as bones, cartilage, tendons, ligaments and connective tissue, are created *de novo* and are derived from the lateral plate or somatopleural limb mesenchyme (Wachtler et al., 1981). Radio-destruction of the somitic mesoderm showed that the absence of a given muscle results in the absence of corresponding tendons (Chevallier et al., 1977), providing the first evidence of a developmental relationships between these two distinct precursor populations. However, most of the subsequent analyses of tendon development concentrated on the distal autopod tendons. In a similar experiment, Kieny and Chevallier (1977) showed that despite the induced absence of flexor and extensor muscles, differentiation of the distal manus tendons still occurred. Although they were transient structures, it demonstrates an early autonomy of the tendons from the muscles. A requirement for subsequent interactions between the two tissues from maintenance and further development of the tendons was observed.

An axial tendon connects the muscles that are located near the spinal column to the vertebrae. As a result, this complex tissue helps in the stability of the spine and transfers force generated by muscles to the axial skeleton and assists in the extension, rotation, and flexion of the trunk. The progenitors for the axial tendons arise from the somites, unlike limb tendon progenitors that are derived from limb mesenchyme (Brent et al., 2003). However, current advances on proper steps in the trunk tendon development is limited due to the multiple complexities associated with the interaction between diverse tissues in the somites and their interdependence on each other (Schweitzer et al., 2010).

Trunk tendons: The axial tendon progenitors originate from syndetome that is a fourth compartment in somite and is located at the junction between two neighbouring myotomes and the sclerotome (Fig 1.4). Despite differences in the origin of muscle, cartilage, and tendon in somite compartments, their development is coordinated and interdependent. The bHLH transcription factor, *Scx* is an exclusive marker for both tendon progenitor cells and mature tenocytes. The double in situ hybridisation on mouse embryo at E10.5 for a myogenic marker MyoD and a tendon marker *Scx* revealed that indeed *Scx*-expressing cells are located in syndetome which is next to the myotome (Brent et al., 2003). Same study also showed that in the quail-chick chimera system the tendon progenitors are expressed between the myotome and sclerotome. In this experimental approach, the grafting of sclerotome from quail to chick resulted in the formation of sclerotome cells and Scx-expressing tendon precursors from the grafted quail. On the other hand, the surgical implantation of quail dermomyotome into the chick formed only dermomyotome and myotome but not *Scx*-expressing syndetome.

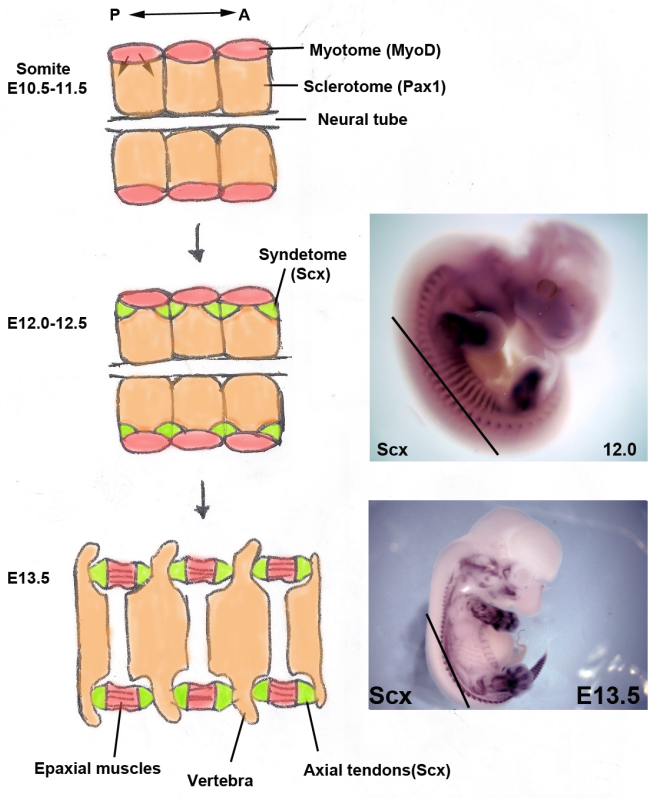

Figure1.4: Illustration of axial tendon development in mouse A depiction of the longitudinal trunk sections from the somite showing sclerotome (*Pax1*$^{+}$), myotome (*MyoD*$^{+}$), syndetome (*Scx*$^{+}$) and neural tube (NT). The whole mount in Scx in situ hybridisation is shown for the stages E12.0 (tendon organisation) and E13.5 (tendon condensation). The black line shows the level of longitudinal sections from the embryos. Myotome signals induce *Scx*$^{+}$ at anterior region of sclerotome that is known as syndetome from E12.0. Mature condensed tendons are then acting as connectors of the vertebrae and muscle cells from E13.5 onwards.

Myotomal fibroblast growth factors (FGFs) play a critical role in the induction of *Scleraxis* expressing tendon progenitors. FGF4 and FGF6 in mouse embryo while FGF4 and FGF8 in chick embryo have been shown to induce *Scleraxis* (Brent et al., 2005; Brent and Tabin, 2004; Tozer and Duprez, 2005). Brent and her colleagues further demonstrated the role of FGF signalling in Scx induction in 2003, where the expression of *Scx* was lost due to inhibition of FGF signalling in trunk culture of mouse embryo. FGFs activate Ets transcription factors, *Pea3* and *Erm,* which regulates directly or indirectly *Scx* transcription (Brent and Tabin, 2004) (Fig. 1.5). Another study also suggests that expression of *Scx* is also stimulated by FGF signalling via the mitogen activated ERK and MAPK kinase activity (Brent and Tabin, 2004; Smith et al., 2005). In chick embryos, the antibodies against active phosphorylated MAPK/ERK1 and MAPK/ERK2 detected active MAPK/ERK throughout dermomyotome, dorsal sclerotome, myotome and strong expression seen in adjacent sclerotome where *Scx* is expressed (Brent and Tabin, 2004).

In addition, the early development of tendons in somites is coordinated and interdependent on surrounding tissue i.e. muscle and cartilage. The muscle precursor region of somite is essential for tendon development since in MyoD and Myf5 double mutant mice where no muscles are formed, the *Scx* expression in the somite was completely abolished in syndetome (Brent et al., 2005). In the same study, it was revealed that in *Sox5*$^{-/-}$*; Sox6*$^{-/-}$ mutant embryos the loss of chondrocyte differentiation results in an expanded *Scx*$^{+}$ tendon progenitor cells.

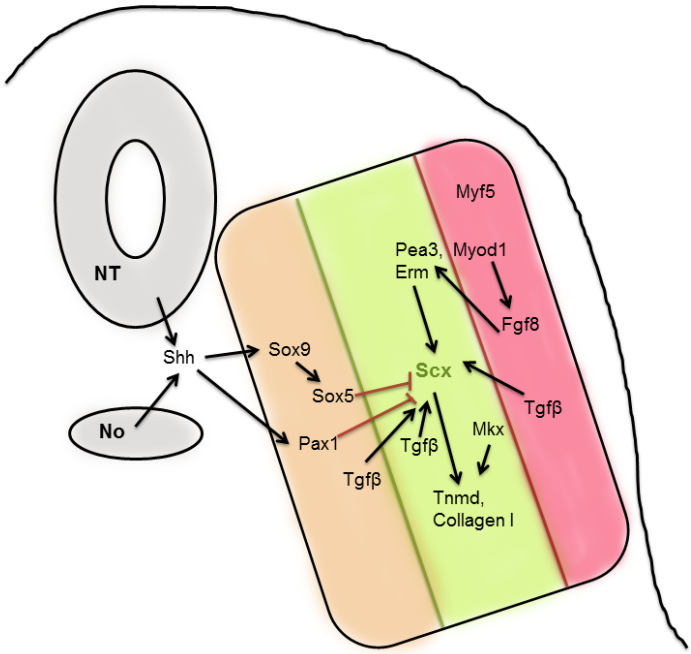

Figure1.5: Model of genes involved in axial tendon development- Myotomal signal FGF8 activates *Scx* via *Pea2* and *Erm* to induce tendon precursor cells in syndetome. Both Scx and Mkx can promote tendon differentiation factors e.g. tenomodulin (Tnmd). *Pax1* and *Sox5*, which are sclerotomal factors, inhibit *Scx* expression and promote development of cartilage in sclerotome. Myotome in pink, syndetome in green and sclerotome in brown. NT, neural tube; No, notochord.

Limb tendons: Limb tendons originate from lateral plate mesoderm. Once induced, the tendon progenitors are reorganised in the sub-ectodermal regions of ventral and dorsal areas of the limb (Schweitzer et al., 2001). Ectodermal signals have been shown to be involved in tendon progenitor induction for limb tendon precurssors. Removal of dorsal limb ectoderm in chick embryos results in loss of *Scleraxis* induction in limb mesenchyme (Schweitzer et al., 2001). The obvious signals from ectoderm are FGFs but to date no definitive evidence are available to show the involvement of FGF signalling in limb tendon development. Absence of *Fgf8* in proximal regions of limb makes it unlikely that it regulates induction of *Scx* in proximal mesenchyme of limbs (Schweitzer et

al., 2001). The induction of *Scleraxis* was found also in the absence of muscle cell, which expresse *Fgf4* (Edom-Vovard et al., 2002). However, in muscleless wings in chick embryos, *Scx* expression was eventually lost demonstrating muscle-dependent phase of tendon development. Hence, the molecular factor that leads to *Scleraxis* induction in limbs remains to be investigated. Furthermore, chondrogenesis was favoured in the absence of FGF signalling (Schweitzer et al., 2001).

Bone morphogenetic proteins (BMP) have negative influence on appendicular tendon development. The facilitation of chondrogenesis over tendon morphogenesis by BMP2 in developing limbs was shown in chick embryos (Edom-Vovard and Duprez, 2004; Edom-Vovard et al., 2002; Schweitzer et al., 2001). The application of endogenous BMP signalling inhibitor, *Noggin* up regulates *Scleraxis* expression in limb bud.

Interestingly, the dynamics of limb tendon development and patterning in contrast to axial tendons is independent of muscle and cartilage. As seen in Fig. 1.6, cartilage cell condensation is in the centre and in contrast to the somite (Fig. 1.5) where the tendon and muscle progenitors are well compartmented, both cell types are mixed together in the dorsal and ventral regions of limb buds.

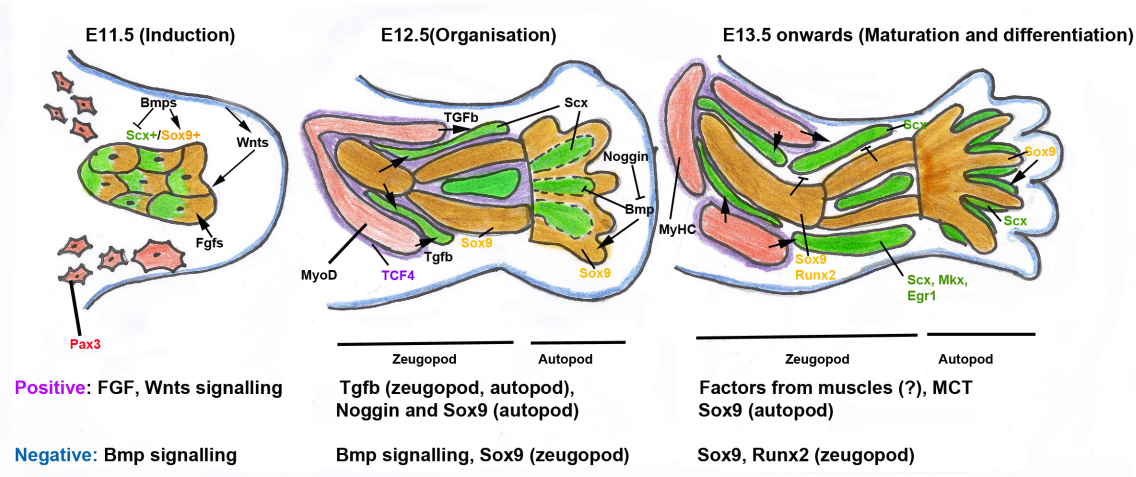

Figure1.6: Schematic of vertebrate tendon morphogenesis in the limbs. (A) Induction of initial *Scx*-expressing tendon precursors occurs under influence of Wnt signalling. (B) Organisation of tendon progenitors depends on TGFβ signalling which recruits a second wave of tendon cells and maintains tenoblastic identity. (C) *Scx* favours aggregation and differentiation of tendon progenitors to form mature distinct tendon occurs by E13.5. The positive and negative regulators are highlighted at the bottom of the stages of limb depiction.

Unlike axial tendons, which require myotome signals, *Scx* expressing tendon cells are clearly detected in muscle-less limbs of *Myf5/MyoD* mutant mice (Edom-Vovard et al., 2002; Kardon, 1998; Murchison et al., 2007; Schweitzer et al., 2001). In chick embryos, *Scleraxis* expression was seen in limbs even after the surgical removal of developing muscles (Edom-Vovard and Duprez, 2004; Schweitzer et al., 2001). Moreover, normal Scx expression was also found in Splotch embryos that have a defect in *Pax3* gene and failure in the migration of limb muscle progenitors from somite (Huang et al., 2015b). Altogether, these studies suggest that limb tendon induction does not require signals from myogenic cell population. However, for the continuous expression of *Scleraxis* signals from muscles is essential. It was discovered that in continued absence of myogenic cells, *Scx* expression was not maintained in chick embryos (Edom-Vovard et al., 2002). This clarified the role of muscles in limb tendon development where the initial establishment of *Scx* is independent on myogenic cells but they are essential at subsequent stages (Edom-Vovard et al., 2002; Kardon, 1998).

Recently, it was shown that the expression of transcription factor *Pea3,* a known effector molecule of FGF signalling is expressed by tendon cells at the site where myotendinous junction is present. When analysed in *Pax3* mutant mice limbs, there was complete loss of *Pea3* expression at E12.5 from defined tendon cells present at the close proximity to muscle cells (Eloy-Trinquet et al., 2009). This study has now further enhanced our understanding of muscle-dependent phase of tendon formation.

Based on the known molecular regulators for limb tendon development, a model is shown in Figure 1.7. Altogether, several sources of evidence are now available which show there are significant differences in limb tendon development when compared to axial tendons. Furthermore, in same study it was found that TGFβ signalling also helps in recruiting the additional *Scleraxis* expressing tendon progenitors at the site of condensation and might be involved in interaction between tendon precursors, adjacent muscle, and cartilage. Furthermore, the limb mesenchyme acts as a host for multipotent cells that can give rise to cartilage cells and connective tissues, which can be grouped into two categories, i.e. dense connective tissue (tendons and ligaments) and loose connective tissue (muscle connective tissue).

Recently, the modularity in the limb tendon development was established (Huang et al., 2015b). While the induction and proliferation of autopod tendons requires cues from cartilage, the zeugopod tendon development is dependent on muscle cells.

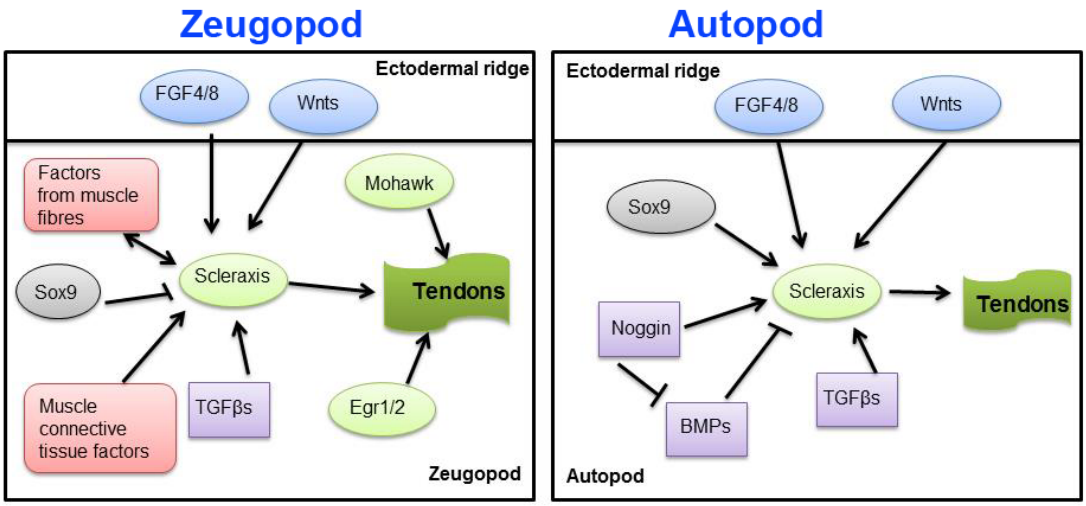

Figure1.7: Illustration of limb tendon induction and organisation. Induction of *Scx* expression in the limbs takes place in response to FGF and Wnt signalling. BMP signalling has negative effect on *Scx* while TGFβs promote tendon development by maintaining and recruitment of tendon precursor cells at the site of condensation. Other unknown positive regulator from muscle cells and MCT's extrinsically regulates *Scx* whereas *Sox9* from cartilage cells restricts *Scx* expression domains. Other transcription factors *Mohawk* (*Mkx*), *Egr1* and *Egr2* are required for tendon maturation.

Other important factors in regulation of tendon development in limbs include the transforming growth factor β (TGFβ) superfamily. The application of TGFβ2 - containing beads to mouse limbs in organ culture showed induction of *Scleraxis* at stages from E10.5 to E13.5 (Pryce et al., 2009). Additionally, surgical grafting of TGFβ2- loaded beads in somites of E10.5 embryos caused robust induction of *Scx.* In the absence of TGFβ signalling i.e. in Tgfβ2$^{-/-}$; Tgfβ3$^{-/-}$ mutant mice and TgfβRII mutant where deletion of the receptor blocked all TGFβ signalling, the initial induction of *Scx* remains unaffected but is subsequently lost, suggesting additional regulators are involved in induction of *Scleraxis*. In TGFβ2/3 double mutant mice, all limb tendon progenitors were lost at E12.5 (Fig.1.8). It was also found in cross sections, all long tendons of tail were missing but the intrinsic muscles and tendons persisted in Tgfβ2$^{-/-}$; Tgfβ3$^{-/-}$ mutant mice when observed at E15.5 (Pryce et al., 2009). Interestingly, this double ligand mutant of TGFβ displayed modularity in limb tendon phenotype whereby in E14.5 embryos, the digit tendons appeared normal but zeugopod tendons were abnormal. Moreover, the authors also detected TGFβ2 expression in differentiating cartilage and muscle cells that could explain severity of phenotype in zeugopod than autopod.

The same study also showed a role for TGFβ signalling in regulation of *Scx in vitro.* The mesenchymal-like cell line C3H10T1/2 expresses *Scx* at moderate level. By semi-quantitative RT-PCR it was observed that the mRNA level of *Scx* was significantly up regulated when TGFβ2 was added in the medium.

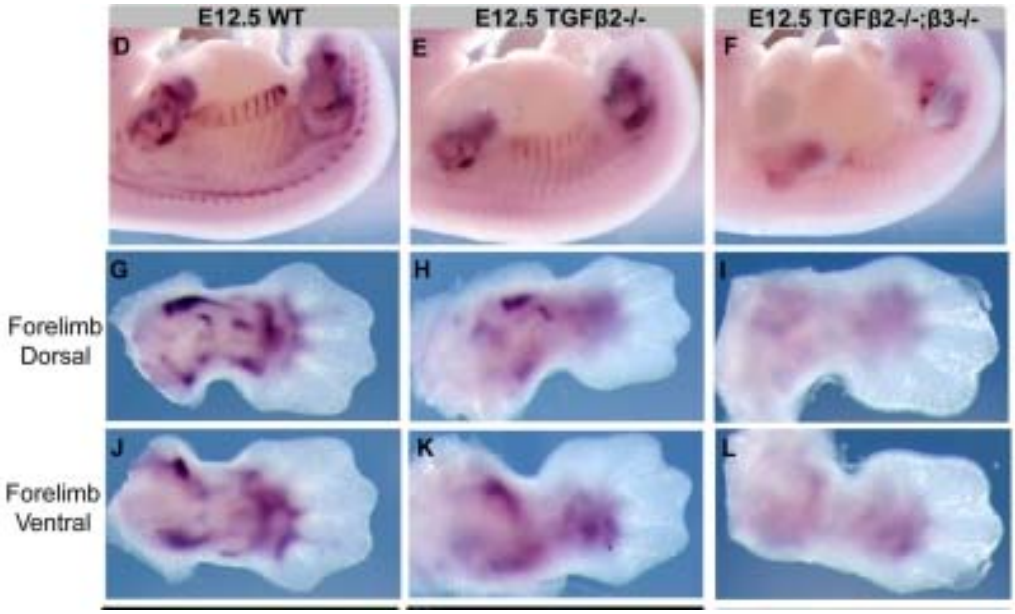

Figure 1.8 Whole-mount ISH for *Scx* on E12.5 The endogenous expression of Scx in the whole embryos and dorsal and ventral forelimbs in wild-type (D,G,J), *Tgfb2*$^{-/-}$ (E,H,K) and *Tgfb2*$^{-/-}$ and *Tgfb3*$^{-/-}$ embryos showed a severe phenotype in *Tgfb2*$^{-/-}$ and complete loss in compound mutants (Adapted from Pryce et al., 2009).

1.2.5 Organisation and differentiation of tendon cells

Murchison and his colleagues in 2007 provided the first evidence for the pivotal role of *Scleraxis* in tenocyte differentiation from E13.5 onwards. In *Scx* mutant mice, movement of paws was highly restricted and tail movement was completely lost. In addition, the long force-transmitting tendons and intermuscular tendons were the severely affected. However, the distribution of *ScxGFP*–positive cells in short range anchoring tendons such as intercostal tendon layer and ligaments were not affected in the mutant mice. The earliest defects were observed at E13.5 suggesting failure of condensation and aggregation of the tenocytes. This has been observed by loosely organised mesenchyme of tendon progenitors in the forelimbs (Fig. 1.9).

Moreover, flexor tendons were affected more in the absence of Scx than extensor tendons. Further analysis showed no significant changes in the apoptosis or cell proliferation events in the mutants. Additionally, the matrix organisation was significantly disrupted in the absence of Scx and it was also

shown that Scx directly regulates the expression of Col1a1 and Tenomodulin at tendon differentiation stages. In the absence of Scx function, by E18.5, the cellular components (tenocytes) of mature tendons were affected along with disorganised tendon sheath.

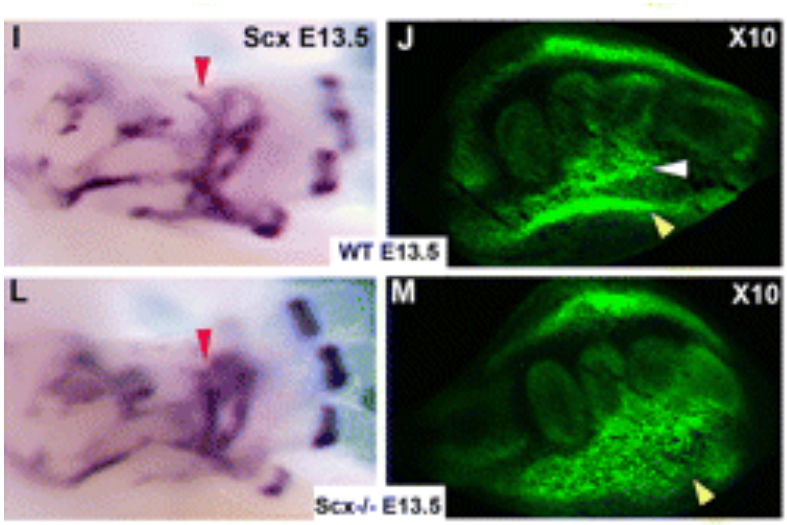

Figure 1.9 *ScxGFP* detected by in situ hybridization in wild type (I) and *Scx*$^{-/-}$ (L) forelimbs at E13.5. The tendon phenotype was first detected at E13.5 in mutant mice. (J,M) Sections through wild-type (J) and *Scx*$^{-/-}$ (M) forelimbs at E13.5 at a proximal metacarpal level (level 4 in A) (Adapted from Murchison et al., 2007).

Furthermore*, Scx* positively regulates the type I collagen through the tendon-specific element 2 of the procollagen, type1, alpha 1 (*Col1a1*) promoter (Lejard et al., 2007). Other genes shown to be positively regulated by *Scx* are tenomodulin and collagen XIV (Espira et al., 2009; Shukunami et al., 2006). Tenomodulin (*Tnmd*) is another important factor in tendon differentiation. It is type II transmembrane glycoprotein and is expressed by tendons and ligaments (Shukunami et al., 2001). A decrease in tenocyte proliferation and density was seen in targeted *Tnmd* mice. TNMD is required for maintaining proper network of collagen proteins in tendon.

Recently, it was discovered that another atypical homeobox gene *Mohawk (Mkx)* is expressed by tendon progenitors. It plays a critical role in tendon maturation (Anderson et al., 2006; Ito et al., 2010). *Mohawk*$^{-/-}$ mice show hypoplastic tendons at postnatal stages and reduction in type I collagen.

Interestingly, in *Mkx* null mice the tendon cell numbers remain unaffected even though there is a reduction in tendon mass.

Moreover, early growth response transcription factors *EGR1* and *EGR2* are now shown to increase collagen expression during vertebrate tendon differentiation (Lejard et al., 2011). In chick limbs, FGF4 signals positively regulate *Egr* gene expression. This was shown by bead experiments where ectopic *Egr1 and Egr2* transcripts could be detected after FGF4 bead implantation in dorsal chick wings. Moreover, *Egr* gene can induces tendon markers *Scx*, and the tendon collagen *Col1a1. Egr1* and *Egr2* double mutant mice at embryonic stage (E) 18.5 displayed decreased level of *Col1a1* transcripts and reduced collagen fibrils in embryonic tendons. When analysed by performing ChIP, the regulation of *Col1a1* by *Egr1* and *Egr2* were found by binding of *Egr1* to proximal 3.2kb segment, which also contains two tendon specific elements TSE1 and TSE2. These elements were shown to be essential for binding of Scx to regulate *Col1a1* expression (Lejard et al., 2007). In addition, the expression levels of the two DNA-binding factors, *Scx* and *Mkx* were also reduced in *Egr1*$^{-/-}$ mutant mice. *Fibin2* is a recently dicovered tendon marker strongly expressed in mature tendons (Liu et al., 2010). The expression analyses of Fibin 2 have shown a strong expression in the syndetome and continue to express through out the development in tendon cells. Thus, it can be considered as an additional marker for tendon specific cells for future investigations.

1.2.6 Tendon growth and maturation

The morphological events of tendon differentiation, growth, and maturation occur from E14.5 onwards until birth. During this phase, the correct connections between muscle-tendon (also called as myotendinous junctions) and tendon-bone attachment takes place. For this proper connections, ECM proteins acts as “glue” to join both cell types via integrin receptors found on cell membranes and are associated with cytoskeletal actin filaments present inside myocytes and tenocytes (Docheva et al., 2014; Mayer et al., 1997; Pan et al., 2013; Welser et al., 2009). The next segment in this chapter will discuss the several

ECM factors, which are coupled in spatio-temporal manner to mediate the force transmission at the myotendinous junction.

Moreover, tendon differentiation, maturation, and growth require muscle only in the zeugopod. For instance, in Splotch mouse embryos with a defect in migration of myogenic cells due to mutation of the *Pax3* locus showed down regulation of *Scx* and *Tnc* in zeugopod (Bonnin et al., 2005; Eloy-Trinquet et al., 2009; Huang et al., 2015b). The modularity in tendon development at this stage led to complete degeneration of differentiated tendons in the zeugopod segment (Kardon, 1998; Schweitzer et al., 2001). Recently, Huang and co-workers (2015) showed that in Splotch embryos, the autopod tendons are not only induced and differentiated but also survived throughout embryogenesis. Similar observations were also reported in chick embryos (Kardon, 1998). Therefore, we have now conclusive evidence that maintenance of zeugopod tendons requires physical interactions with muscles, and mechanical load applied by muscles also plays a pivotal role in overall growth and maturation of zeugopod tendons.

The tendons in digit segments are established in the regions where no muscle cells are normally found. The essential muscle-dependent signal for the tendon differentiation is replaced by cartilage-derived cues (Huang et al., 2015b). In $Sox9^{Prx1Cre}$ embryos, which contain the conditional deletion of *Sox9* gene from limb mesenchyme showed loss of Scx expression in the autopod at E13.5 whereas in $Gli3^{Xt/Xt}$ embryos, tendons were found in all the extra digits. *Gli3* is an important regulator of the digit formation and mutation of this gene in $Gli3^{Xt/Xt}$ embryos caused development of an extra digit (Vortkamp et al., 1992). Collectively, the tendon differentiation and maturation is dependent on skeletal condensation in the autopod whereas in zeugopod, myogenic cells help in the tenocyte differentiation.

1.3 Myotendinous junction

The transmission of force generated by muscles into skeletal elements takes place at myotendinous junctions (MTJ). Electron microscope analysis revealed that the establishment of MTJ occurs when cytoskeletal proteins of muscle cells and tendon ECM interact (Tidball, 1994; Tidball and Lin, 1989). These ECM proteins (e.g. collagens, laminins, thrombospondins) are accumulated between interacting myoblasts and fibroblasts (Figure 1.10) (Kuhl et al., 1986; Sanderson et al., 1996).

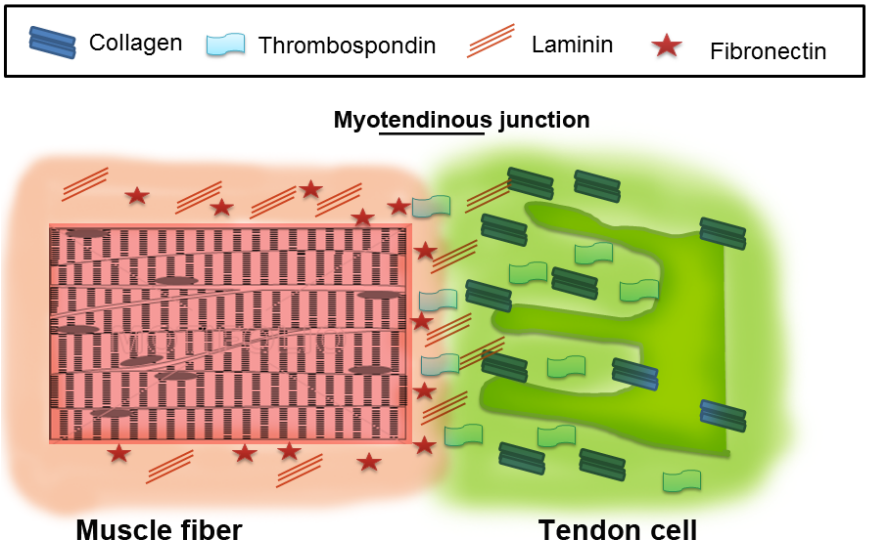

Figure 1.10 Schematic of myotendinous junction The extracellular matrices of muscle fibres (in red) and tendon cells (in green) interact at a sparse layer of ECM called myotendinous junction (MTJ). Distinguish molecular markers of muscle and tendon ECM are shown in red and green, respectively. Muscle ECM is composed of laminin trimers and fibronectin whereas tendon ECM contains collagen trimers and thrombospondin proteins.

While studies have shown that ECM proteins may enhance proliferation and growth of myogenic tissue (Lan et al., 2005; Langen et al., 2003; Stern et al.,

2009), they also modulate tendon maturation stage during development. The study that generate *Scx*$^{-/-}$ mutant mice, showed the disruption of tendon ECM at later stages of tendon morphogenesis (Murchison et al., 2007). The same study has further shown a severe down regulation of the expression of structural collagen proteins, Col1a1, Col1a2, Col3a1 and Col14a1 in Scx-/- mutant mice. Moreover, Scx is a direct regulator of *Col1a1* and *Col1a2* transcription (Espira et al., 2009; Lejard et al., 2007).

Likewise, *Mkx* also promotes expression of *Col1a1* and *Col1a2* and thus *Scx* and *Mkx* act as transcriptional activators of these collagen genes. Interestingly, in *Mkx*$^{-/-}$ that exhibit normal embryonic tendon formation, later showed a thinner collagen fibrils and reduction of fibromodulin (Fmod), decorin (Dcn), tenomodulin (Tnmd) (Ito et al., 2010; Liu et al., 2010). Moreover, the evidence suggests that the influence of *Scx* and *Mkx* on ECM proteins occurs via Smad mediated TGFβ signaling (Berthet et al., 2013; Hosokawa et al., 2010). Specifically, Berthet et al (2013) reported that the loss of Smad3 function resulted in reduction of *Scx*, *Tnc*, *Mkx* and matrix proteins such as *Col1a1*, *Col1a2*. Moreover, the authors showed that Smad3 physically interacting with *Scx* and *Mkx*. Furthermore, in *Wnt1-Cre;Tgfbr2 flox/flox* mice in which the derivatives of cranial neural crest cells were marked by Wnt1-Cre and Tgfbr2 conditional inactivation in these migratory cells was established by using *Tgfbr2flox/+* mice (Hosokawa et al., 2010). This conditional inactivation of Tgfbr2 resulted in loss of *Scx* expression from the tendons of tongue muscles that are derived from neural crest cells. Moreover, tongue explant assay demonstrated *Scx* induction in response to TGFb2 soaked bead. Therefore, it was concluded that TGFβ signalling regulates *Scx* expression and controls cranial neural crest derived cells.

Extensive research been carried out to understand the development of MTJ. Upon completion of muscle differentiation, ECM proteins direct myofibres to the attachment sites in MTJ (Kjaer, 2004). This site than undergoes maturation and imparts mechanical forces to maintain the function of mature tendon cells (Schwartz et al., 2013). The MTJ develops in two stages and with respect to tendon cell requirement; the stages are classified as tendon independent and

tendon dependent stages. First, induced tenoblasts secrete fibrilliar ECM components near the periphery of migrated myoblasts. The integrins on muscle cell membranes recognize signals emanating from tenocytes e.g. Thrombospondin (Tsp), laminins (Lama) (Gotwals et al., 1994; Martin-Bermudo, 2000; Subramanian et al., 2007). Additionally, muscle cells secrete Tiggrin that interacts with integrin receptors present on its surface membrane (Bokal and Brown, 2002; Fogerty et al., 1994).

Second, fusion of myoblast results in the formation of myotubes, which are then followed by extensive scaffolding of ECM proteins that produce basement membrane. There are a diverse set of extracellular proteins present in the basement membrane that includes laminins, perlecan, collagen IV, nidogen (Yao et al., 1996; Koch et al., 1999; Fox et al., 1991; Mayer et al., 1995; Hudson et al., 1993; Kuhn, 1994; Kruegel and Miosge, 2010). Last, a mechanical cross talk takes place between muscle and tendon cells. For the efficient delivery of mechanical load, the various groups of proteins are necessary at this stage. These are divided into three sub-groups: (a) collagen proteins secreted by tenocytes (Col1a1, Col1a2, Col2a1 and Col3a1); (b) proteins that can form scaffolds (e.g. Lama2, Comp, Tsp4) and (c) cross-linking proteins (e.g. Col6a1, Col12a1, decorin, Fmod, lumican, biglycan, alpha-dystroglycan and beta-dystroglycan). These altogether help in reducing frictions between fibers of ECM and disseminate the force appropriately (Wang et al., 2012; Dunkman et al., 2013). Interestingly, various studies have shown that misexpression of the gene coding for the cross-linking proteins produced an adverse outcome on tendon structure (Chakravarti, 2002; Corsi et al., 2002; Zhang et al., 2006). On a bigger scale, the ECM is critical for MTJ organization and plays a pivotal role by providing structural support and function.

1.4 Enthesis: Tendon-bone attachment

An enthesis is the site on the other end of a tendon where it attaches to the bone or cartilage. Starting at the tendon side, the first zone exhibits tendon

properties, including aligned type I collagen fibers and the proteoglycan decorin. The second zone comprises fibrocartilage that contains type II collagen, with only small amounts of type I collagen. The ECM of zone 2 contains, in addition, type III collagen, aggrecan and decorin. Next, zone 3 contains mineralized fibrocartilage that includes type II and type X collagens as well as aggrecan. Finally, zone 4 is bony and composed mostly of mineralized type I collagen (Reviewed by Schweitzer et al.,2010). Emerging studies have shown a close relationship between Scx expressing tenocytes and Sox9 positive chondrocytes in formation of enthesis (Soeda et al., 2010; Sugimoto et al., 2013a; Sugimoto et al., 2013b). Interestingly, Scx-/- mice lack entheses and its function was shown to be necessary for bone ridge initation (Blitz et al., 2013; Murchison et al., 2007). Moreover, BMP signalling and TGFb superfamily play key role in chondrocyte development (Blitz et al., 2009; Yoon et al., 2006).

Collectively, the summary of factors involved in the tendon development and the effects due to loss-of-function mutation in mice and humans are summarized in the following table:

Gene	Mouse	Chick	Zebrafish
Transcription factors			
1. Scleraxis (*Scx*)	*Scx* null mice • First tendon phenotype at E13.5 • Severe disruption of force-transmitting tendons but no defects in ligament and short-range anchoring tendons • Disorganised tendon matrix • Decrease of Tnmd, Col14a1, Col1a1 from E16.5	Overexpression in chick hindlimbs caused upregulation of Tnmd	
2. Mohawk (*Mkx*)	*Mkx* null mice • First tendon phenotype at E16.5 • Decrease of Tnmd, Col1a1, Col1a2, Tnmd, Fmod, Dcn from E16.5		*Mkx* morphants Myotendinous and muscle defects
3. Early growth response 1 (*Egr1*)	*Egr* null mice • First tendon phenotype at E18.5 • Decrease in Scx, Tnmd, collagen levels	Overexpression in chick embryos caused upregulation of Scx, Tnmd and collagen levels	
4. Sex determining region Y-box 9 (*Sox9*)	$Sox9^{f/f}$; $Prx1^{Cre}$ Complete loss of Scx expression in autopod but not in zeugopod from E12.5 onwards.		

Signalling pathways			
1. Wnt 2. TGFβ2 TGFβ3 3. GDF8/myostatin 4. GDF5 5. *Smad3* 6. BMP4	*Msx2*$^{Cre/+}$*/Wls*$^{c/c}$ Complete loss of Scx expression in autopod but not in zeugopod at E12.5. TGFβ2/TGFβ3 double mutant • Complete loss of tendons from E12.5. • TGFβ2 ectopic expression in mouse limbs and in vitro 10T1/2 cells upregulated *Scx* expression *Mstn* null mice • Postnatal tendon phenotype. • Abnormal mechanical properties and decrease in *Scx*, *Mkx*, collagen (Col1a2), Tnmd *Gdf5* null mice Limb shortening, joint dislocation and abnormal tendons *Smad3* null mice • Postnatal tendon phenotype • Decrease in Tnmd, Col1a1 *Bmp4*$^{fl/fl}$*;Prx1-Cre* • Enthesis formation inhibited. • Defective bone ridge formation	TGFβ1 overexpression up regulate Scx expression in E6 chick digits Overexpression of BMP in E4 chick limbs led to decrease in *Scx* expression FGF4/8 gain-of-function in somites and limbs led to	Smad2/3 pathway inhibition resulted in decrease in *Scx* expression

7. FGF4 FGF8	Ectopic expression of FGF4 caused upregulation of *Scx* expression	upregulation of *Scx*, *Tnc, Pea3, Spry2*, *Mkp3* expression Inhibition of ERK MAPK pathway result in loss of *Scx*, *Pea3* expression	
8. MAPK	Inhibition of MAPK pathways result in loss of *Scx* expression Inhibition of ERK MAPK pathway result in increase in *Scx* expression		
<u>Transmembrane proteins</u>			
Tenomodulin	*Tnmd* null mice • Loss of tenocyte proliferation and reduced tendon density • Postnatal defects in collagen fibrils • Defect in tendon stem cell proliferation		

Extracellular matrix protein(ECM)			
1. Type I collagen (Col1a1, Col1a2)	*Col1a1* null mice Postnatal decrease in collagen fibril diameter		
2. Biglycan	Disordered collagen fibril		
3. Comp	Short limb dwarfism and onset of osteoarthritis		
4. Decorin	Irregular collagen fibril		
5. Fibromodulin	Abnormal collagen fibrillogenesis in tendons		

1.5 Post-natal arrangement of limb tendons

The post-natal stage of tendon maturation involves assembly of monomeric units of collagen and fusion of collagen fibrils for fibril growth (Zhang et al., 2005). The unsheathing of the cell layers to form epitenon and paratenon takes place at birth (Benjamin and Ralphs, 1997, 1998; Birk et al., 1989). The organisation of major forelimb tendons at postembryonic stage was determined by Pryce and co-worker in 2007 using a *ScxGFP* transgene. The robust formation of the appropriate flexor and extensor tendon trajectories along the proximal-distal axis of the forelimb has been determined and the precise assemblage in the forelimb into a functional musculoskeletal system is achieved using *ScxGFP* (Watson et al., 2009). A major flexor tendon, the flexor digitorum profundus (FDP), trails down from the individual FDP muscle in the forearm as an elongated entity and reaches the carpal tunnel near the wrist and then splits into individual units on the palmar side of the phalanges (Figure 1.11). Within phalanx, each FDP tendon subunits insert into the distal interphalangeal joint, thereby, assisting in the movement of each fingers.

Moreover, inside the fingers, another superficial tendon is present above the FDP, known as, the flexor digitorum superficialis (FDS). At the interphalangeal joints of the digits, FDP tendons become volar whereas FDS tendon units are present at the bottom. In the mid-part of the forearm, FDS tendons are present as four bundles that split into two segments enclosing each FDP tendon cluster. Inside the wrist, each FDS tendons along with FDP travels through the carpal tunnel and reach the prospective FDS muscles that extends distally towards its origin sites inside the elbow.

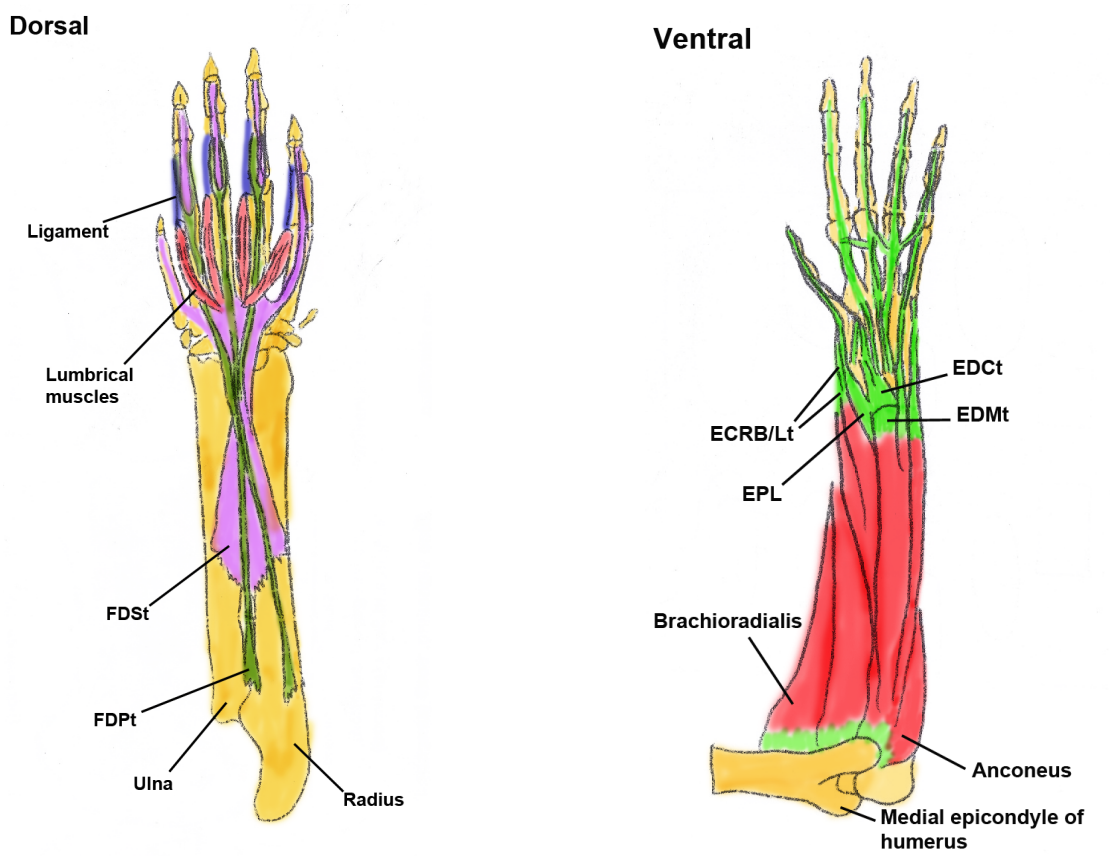

Figure 1.11: An illustration of the major flexor and extensor tendons in the forearm. Green represents *ScxGFP* expressing tendon cells of flexor digitorum profundus tendon (FDP); pink is tendon cells of flexor digitorium sublimis tendon (FDS); lumbrical muscles are shown in red; ligaments are shown in blue; ECRB, extensor carpi radialis brevis; EPL, extensor pollicis longus; EDC, extensor digitorum communis; EDM, extensor digiti minimi

In addition, the flexing of MCP joints are then achieved by interosseous and lumbrical muscles. Interosseous muscles arise from their metacarpal bone and present on both sides of the bone. On the other hand, lumbrical muscles reside within the palm and originate from FDP tendon, which is in contrast to the most muscles that originate from skeletal elements. Lumbricals pass through dorsally and laterally around each digit (Figure 1.11). The movement of thumb and little digit are due to the superficial thenar and hypothenar muscles. The thenar muscles are located at the base of thumb and produce a bulge. While, hypothenar muscles are muscular protrusions on the medial side of the palm, at the base of little finger. Lastly, transverse carpal ligament, a fibrous band acts as a roof of the carpal tunnel.

Furthermore, a prominent extensor tendon, the extensor digitorum communis (EDC) is position on the dorsal side of the forearm and is the key tendon on the backside of the palm. As individual bands, each EDC tendon subunits fans out from the digits and passes through the compartment formed by the extensor retinaculum and radius, after which they reach the origins at the lateral epicondyle of the humerus. Additionally, extensor digiti minimi after crossing over the wrist splits into two separate tendons called digiti quarti and digiti quinti. The extensor carpi ulnaris are located on the proximal side of the little finger near the meta-carpophalangeal joints and thereby helps in the extension of the little finger (Figure 1.11).

While a thorough knowledge is available on the forelimb tendon development, however, little is known about the hindlimb and axial tendon development. For instance, only recently the precise development and assemblage of flexor digitorum brevis (FDB) muscle-tendon unit inside the foot was established (Huang et al., 2013). Their study showed that in the hindlimb, three muscles gives rise to the FDB tendons at the metatarsophalangeal joint that then covers the flexor digitorum longus (FDL) tendon and eventually intercalate into the interphalangeal joint of the toes. Thereby, authors concluded a serial homology between the structure and formation of the FDS tendon in the forelimb with that of FDB tendons in the hindlimb.

Another prominent tendon in the foot is the Achilles tendon and is considered as the strongest and thickest tendon among all hindlimb tendon groups. The Achilles tendons has musculotendinous portion at the proximal side and insert into the bone on the distal end (Del Buono et al., 2013). However, the information available for the foot tendon development is still considered as generic and therefore, further research is required to dissect out the precise developmental pathways of hindlimb tendons.

Evidence has shown that FDS and FDB tendons share similar anatomical features based upon their positions the limbs, the only difference pertain in tendon patterning events (Huang et al., 2013). FDS tendon extends from distal

to proximal axis in the forelimb, and then translocation occurs into the zeugopod where they finally reside. No further studies has been conducted to provide genetic model for FDB tendon formation and at this point, we still lack the knowledge of FDB tendon formation in *Scx*$^{-/-}$ mutant mice.

1.6 Muscle connective tissue

Vertebrate muscle fibers are surrounded by muscle connective tissue (MCT) that is made up of fibroblasts and produce ECM. The studies have shown a pivotal role of MCT to partake in the muscle patterning and regulate their growth, type specification and differentiation (Chevallier and Kieny, 1982; Chevallier et al., 1977; Hasson et al., 2010; Kardon et al., 2003; Mathew et al., 2011; Stern et al., 2009; Swinehart et al., 2013; Wachtler et al., 1981). This is supported by the fact that muscle progenitors do not have a pre-determined fate as determined by quail-to-chick grafting where quail-derived muscle cells were able to develop in the chick limb-bud, suggesting that they receive environmental cues for muscle patterning which might implicate signals from the surrounding connective tissue (Chevallier et al., 1977). In this experimental strategy, the heterotopic transplantations in which the somite from chick wing level was replaced by quail neck level somite. There was a deep penetration of of cells from the quail graft into the distal limb level of chick and the proper limb muscle fiber was formed. Interestingly, this is very different from *Drosophila*, where the information pertaining muscle cell fate is intrinsic (see Abmayr and Pavlath, 2012).

Various molecular factors that are widely expressed by connective tissue have shown to regulate the events of muscle patterning. One such example is the protein Tcf4, from the TCF/LEF family (Kardon et al., 2003). Tcf4 is expressed in the lateral plate-derived limb mesoderm and tendons, and is a marker for muscle connective tissue important in generating a template for muscle

pattering (Kardon et al., 2003). Tcf4 acts downstream of the "canonical" β-catenin-dependent Wnt signaling pathway, determined to up regulate the myogenic commitment markers *Myf5* when *Myf5* activation was observed in mice embryos overexpressing an activated form of β-catenin (Borello et al., 2006; Daugherty and Gottardi, 2007; Kardon et al., 2003). *Tcf4*$^{-/-}$ mutants show reduced limb mobility and muscle mispatterning suggesting that Tcf4 expression generates a template for forming limb muscles. Tcf4 expression is maintained in the tissues that eventually form the endomysium, perimysium and epimysium surrounding the muscle fibres. Tcf4 also regulates myofibre type maturation and switch from foetal to adult muscles as evidenced by Tcf4 deletion or MCT ablation. This can be considered as first evidence of a cell autonomous and non-autonomous regulation of myosin heavy chain towards the end of neonatal stage and continue in the adults. BMP2 and BMP4 have been shown to repress Tcf4 expression showing that these three signalling molecules are important for the positioning of the premuscular masses. However, at some regions *Scx* that serve as a tendon marker (Schweitzer et al., 2001) also accompanied *Tcf4* expressions (Kardon et al., 2003).

T box transcription factors *Tbx4* and *Tbx5* are expressed in the forelimb- and hindlimb-generating regions respectively at the time of limb bud formation (Ahn et al., 2002; Chapman et al., 1996; Rallis et al., 2003). They are expressed in the limb mesenchyme post limb bud formation until late development (Hasson et al., 2010; Rallis et al., 2003). As development progresses, *Tbx5* expression becomes restricted to a subpopulation of MCT, some skeletal elements and tendons. *Tbx4* and *Tbx5* knockouts show limb muscle and tendon mis-patterning, myogenic differentiation and fusion proceeds, but the muscles demonstrate abnormal size, shape, splitting and localization; in *Tbx5*-only deletions, there is disorganized MCT and limb tendon patterning, with abnormal *Scx* expression. The muscle mis-patterning is accompanied by the reduced expression of *N*-cadherin and β-catenin as shown in figure 1.12 (Brand-Saberi et al., 1996; Hasson et al., 2010; Theveneau and Mayor, 2012).

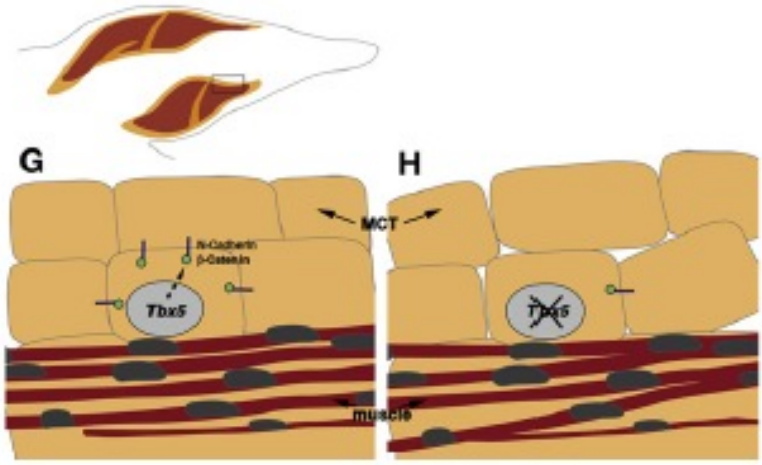

Figure 1.12: A schematic representation of regulation of MCT and muscle fibres by Tbx4/Tbx5. In the MCT (orange) of normal limbs, Tbx4/Tbx5 expression regulates the activity of N-cadherin and b-catenin in cell autonomous fashion as shown in G. In contrast, the deletion of Tbx4 or Tbx5 resulted in loss of N-cadherin and b-catenin due to which a mispatterning of the associated muscles and disruption of MCT occurred. (Adapted from Hasson et al., 2010)

However, Tbx4 and Tbx5 do not act upon the Tcf4-dependent β-catenin-mediated Wnt signalling as no changes in Tcf4 transcripts and protein were detected and β-catenin deletion results in a decrease in N-Cadherin expression in a Wnt-independent manner and implies that Tbx4 and Tbx5 function via a parallel Wnt-independent β-catenin pathway (Hasson et al., 2010).

More recently, *Hox11* expression was also found in the MCT of developing zeugopod of the forelimb (Swinehart et al., 2013). Despite the co-expression of Hox11 and Tcf4 in MCT, still Hox11 loss-of-function mutation resulted in normal Tcf4 expressions in the forelimb zeugopod. Interestingly, the regional loss of Hox11 gene from MCT led to disrupted muscle patterning that was restricted only to zeugopod segment. Hence, it emphasises the diversity found within the muscle connective tissue and further investigation will reveal the mechanisms controlling regional development of this tissues within the musculoskeletal system.

1.7 Myogenesis in the mouse embryo

Mice embryonic myogenesis occurs in two stages. In primary myogenesis, primary myofibres result from the fusion of embryonic myoblasts (see Biressi *et al.*, 2007). Secondary myogenesis follows with the fusion of fetal myoblasts, which develop from related progenitors and differ in proliferation and fusion capabilities, to form secondary myofibres in close proximity to primary myofibres (Duxson *et al.*, 1989; Hutcheson *et al.*, 2009). Differential expression in myofibres of myosin heavy chain isoforms for fast- and slow-contracting muscle takes place during secondary myogenesis (see Abmayr and Pavlath, 2012). In later development, satellite cells take their place between the basal lamina and myofibre cell membrane (Lepper and Fan, 2010).

Sine oculis-related homeobox factors Six1 and Six4 sit on the apex of the regulatory network driving myogenic differentiation, regulating early specification by targeting genes such as *Pax3* and basic helix-loop-helix (bHLH) genes such as *MyoD, MRF4* and *myogenin* (Grifone *et al.*, 2005). Paired-homeobox transcription factors *Pax3* and *Pax7* are influential for the undifferentiated state of precursor cells, *Pax3* being expressed in long-range migrating cells essential for limb development (Tremblay *et al.*, 1998). Key myogenic regulatory factors (MRFs) that mediate myogenesis via DNA binding are *Myf5, MyoD, myogenin* and MRF4 (see Massari and Murre, 2000). *MyoD* and *Myf-5*, commit myoblast traits into progenitor cells and have been observed to be individually redundant but cooperatively essential for myogenic determination (Braun *et* al., 1992). *Myogenin* and MRF4 are downstream MRFs that control terminal differentiation; *myogenin* is essential for the expression of myotube-specific genes such as myosin heavy-chain and MRF4 (Hasty *et al.*, 1993).

Initiation of migration of precursors is fundamentally controlled by the c-Met receptor and its ligand hepatocyte growth factor/scatter factor (HGF/SF) (Brand-Saberi *et al.*, 1996). Finally, different signalling mechanisms such as Wnt

signalling and Notch signalling, accompanied by the molecular activities of factors such as Sonic hedgehog and bone morphogenic proteins, also play a part in the self-renewal or differentiation of progenitor cells involved in muscle development (see Bentzinger *et al.*, 2012).

Myogenic differentiation

Following successful invasion of migratory precursor cells into the limb bud dorsal and ventral premuscular masses are formed. These premuscular masses subdivide in a proximal to distal gradient and each muscle mass eventually splits to individual muscles.

The premuscular masses consist of two layers. The superficial layer of proliferating muscle precursor cells express Pax3 and myf5 and the second deeper layer of differentiating myoblasts expressing MyoD and muscle proteins (Patel, Christ & Stockdale 2002). Quail premuscular masses grafted into chick limb buds show chick muscle patterning and because quail and chick patterning is different this suggests that muscle patterning is specified by somatopleural mesoderm of the limb bud and is not prespecified in the migratory cells from the dermomyotome (Grim, Wachtler 1991). FGFs, IGF-1, BMPs and follistatin have shown increased muscle size brought on by increased rate of proliferation suggesting their role in inducing proliferation. For example, using mouse model, the hypertrophy of muscle mass was observed when IGF-1 was overexpressed using a muscle-specific promoter (Musaro et al., 2001). Moreover, when injections of FGF2 were introduced into the anterior tibial muscles, it resulted in the increase in muscle weight (Iwata et al., 2006). Notch and SF/HGF have been implicated in the inhibition of muscle differentiation. Noggin, an antagonist of BMP signalling, reduces muscle mass (Amthor et al. 2002, Barton-Davis et al. 1998, Hannon et al. 1996). The MRF genes, MyoD, Myf5, Myogenin and MRF4 are essential for the determination and differentiation of the myoblasts because they encode bHLH transcription factors. Evidence includes overexpression of MyoD and Myf5 converting different cell types to the

myogenic fate. Previously, it was shown that the complete loss of function of *MyoD* and *Myf5* resulted in the lack of skeletal muscle cells (Rudnicki 1993). However, using a range of *Myf5* mutant alleles, Kassar-Duchossoy and colleagues (Kassar-Duchossoy et al. 2004) showed that the skeletal muscle cells were only affected in the absence of *MyoD* and *Myf5* when the expression of *Mrf4* gene was compromised. They generated a series of three allelic *Myf5* knockout mice i.e. $Myf5^{nLacZ}$, $Myf5^{GF-P}$ *and* $Myf5^{loxp}$. The $Myf5^{nLacZ}$ allele has an insertion of lacZ into the exon 1 that disrupts *Mrf4* expression. The $Myf5^{GFP-P}$ contain targeted insertion of GFP into exon 1 which resulted in the deletion of bHLH domain of *Myf5*. The $Myf5^{loxp}$ mutant had a loxP site inserted into exon 1 that deleted bHLH domain and lacked amino-terminal domain required for transactivation. Both $Myf5^{GFP-P}$ and $Myf5^{loxp}$ mutants showed normal *Mrf4* expression. $Myf5^{nLacZ}$; MyoD double mutants showed the same phenotype as those described by Rudnicki et al.(1993) , namely a lack of skeletal muscle development. When the $Myf5^{GFP-P}$ and $Myf5^{loxp}$ alleles were crossed with *MyoD* mutants, *Mrf4* expression was undisturbed and embryonic myogenesis occurred normally; however, these muscles are degenerated during the foetal stage of development and the mutant mice born without the skeletal muscles. Therefore, the phenotype of the original *Myf5*;*MyoD* (Rudnicki 1993) and the $Myf5^{nLacZ}$; MyoD double mutants (Kassar-Duchossoy et al., 2004)- was effectively a triple null of *Myf5*:*Mrf4*:*MyoD* where mutation of *Myf5* affected the expression of the neighbouring *Mrf4* gene in cis. Hence, it was concluded that *Myf5* and *Mrf4* both function upstream of *MyoD* to drive the embryonic multipotent cells into myogenic lineages (Kassar-Duchossoy et al., 2004).

Primary muscle fibres are formed by the fusion of myoblasts expressing MyoD. These fibres traversing the muscle anlage from tendon to tendon allow secondary fibre insertion near sites of innervation. The secondary fibres increase rapidly in number and nucleation and eventually separate from the primary fibres (Duxson, Sheard 1995). Fusion of the myoblasts requires N-CAM, N-cadherin and M-cadherin molecules (Arnold, Braun 1999).

1.8 Meox2 transcription factor

1.8.1 Meox2 in limb myogenesis

The *Meox* genes, *Meox1* and *Meox2* (also known as *Mox1* and *Mox2*), are members of a homeobox gene subfamily first characterised in the early mouse embryo during somitogenesis. They play distinctive role in somite regionalisation, patterning, and differentiation due to the differential localisation and characteristic expression in the somites and paraxial mesoderm during vertebrate development (Mankoo et al., 1999). The chromosomal localisation revealed that *Meox2* is not linked to any of the Hox clusters. The expression of Meox2 was first detected around 8th day after gestation and after half a day it is known to express throughout the entire epithelium of the somite. *Meox1* and *Meox2* showed highly overlapping patterns of transcript expression in the early epithelial somite, and *Meox1* was also expressed in the pre-somitic mesoderm posterior to the earliest somite. Following differentiation of the somites, *Meox2* expression appeared to be localised in the sclerotome labelling sclerotome derived cells, e.g. vertebral precursors from E10.5 onwards and *Meox1* in both the sclerotome and dermomyotome (Candia et al., 1992). However, Meox2 protein levels detectable by immunostaining are only found in differentiated somites up to E11.5 and in the limb bud thereafter (but not Meox1) (Candia and Wright, 1996). These studies provided initial clues into their respective roles during skeletomuscular development. Conversely, during limb bud development, Meox2 is expressed in the cells residing in the limb mesoderm (Figure. 1.12) along with the migrating myoblast that arrive into limb territory from lateral edge of the dermomyotome (Mankoo et al., 1999). This was further established by the expression of *Meox2* in limb mesoderm at E10.5 in Splotch embryos that lacks muscle cells in the limb due to point mutation in *Pax3* gene.

Previous work described that *Meox2* transcription factor is essential for the regulation of myogenic commitment and differentiation (Mankoo et al., 1999).

Indeed, mice homozygous for a null mutation of *Meox2* exhibit obvious defects in limb musculature, characterised by overall decrease of muscle mass and absence of specific muscles but have normal skeletal morphologies, highlighting the role of *Meox2* in controlling limb muscle development (Mankoo et al., 1999). Moreover, *Meox2*$^{-/-}$ mutant embryos at E10.5 show down regulation of genes Pax3 and Myf5, although MyoD expression was normal and collectively expressed by migrating muscle precursors from somites into the limb mesoderm. This finding places *Meox2* upstream of *Pax3* and *Myf5* in the genetic hierarchy regulating limb muscle development. Recently, it was shown that *Meox2* directly binds to 145-bp core element in the *Myf5* limb enhancer and thereby modulate the expression of *Myf5* during myogenesis (Daubas et al., 2015)

On the other hand, mice homozygous for a null mutation of Meox1 show abnormality in the axial skeleton, especially at the cranio-cervical joints, but have normal muscle development (Skuntz et al., 2009). *Meox1* mutants also show altered expression of Bapx1, Uncx and Tbx18, genes important for maintenance of somite polarity (Skuntz et al., 2009), supporting a previous in vitro finding that Meox1 directly activates Bapx1 expression in the sclerotome by binding to a homeobox-binding domain in Bapx1's promoter (Rodrigo et al., 2004).

While studies involving *Meox1* or *Meox2* homozygote mutants alone highlight their non-redundant roles in skeletal and muscular development, respectively, *Meox1;Meox2* double homozygous mutants display phenotypes characteristic of defective somitogenesis and patterning, lacking both normal axial skeleton and skeletal muscles(Mankoo et al., 2003). These double mutants exhibit loss of *Pax1* and *Twist* expression in the paraxial mesoderm as well as severe downregulation of *Pax9* expression. *Pax1* and *Pax9* are important for axial skeleton development while *Twist* is known to be involved in myogenic and chondrogenic differentiation (Mankoo et al., 2003). Putting it all together, these findings show that while *Meox1* can compensate for loss of *Meox2* in the sclerotome (but not in the myotome) and vice versa in differentiated somites,

both *Meox* genes are crucial upstream players in the genetic regulatory network that controls somite development.

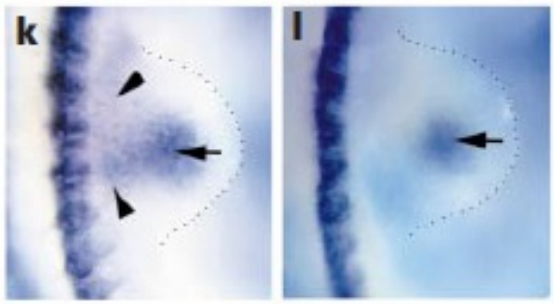

Figure 1.12: Whole mount Meox2 in situ hybridisation on E10.5 mouse forelimb bud

Image showing *Meox2* mRNA expression in E10.5 mouse control (k) and Splotch homozygous (l) embryos. Arrows show *Meox2* expression in the distal domain of control and mutant embryos i.e. in limb mesoderm. Arrowhead shows *Meox2* mRNA expression in proximal domain i.e. in migrated myogenic cells (Adapted from Mankoo et al., 1999).

Further analysis of Meox2 expression analysis in the *Splotch* embryos that have Pax3 mutation, which resulted in the absence of muscle revealed that Meox2 expression from the proximal limb is lost, but the distal domain from the limb mesoderm remained unaffected (Mankoo et al., 1999). The aforementioned *Meox2* is a potential candidate for MCT regulation of limb formation. While its mechanism, which was determined to be essential for limb muscle development, may be restricted within myoblasts and mediated via *Pax3* and *Myf5*, it could also have a role in the MCT where its expression may affect connective tissue development and can be speculated to have a downstream effect on the surrounding muscle (Mankoo et al., 1999).

1.8.2 *Meox2* transcription factor and TGFβ signalling

The *Meox2* transcription factor is a direct target of transforming growth factor β1 (TGFβ1) in epithelial cell growth (Valcourt et al., 2007). Interestingly, regulation by TGFβ1 is in biphasic manner where initial weak repression is then followed by strong robust induction of *Meox2* mRNA expression in normal mammary epithelial NMuMG cells and in normal immortalized HaCaT keratinocytes. Moreover, the regulation of *Meox2* expression by TGFβ is via Smad proteins. In HaCaT cells, when dominant negative mutants of Smad3 and Smad4 were used to block endogenous Smad signalling, the expression of Meox2 was completely abrogated even after stimulation with TGF- β1. Collectively, *Meox2* is involved in epithelial cell biology under the control of the morphogenetic cytokine TGF-β and *Meox2* play critical role along with Smad proteins to execute TGFβ's role in inhibition of epithelial cell growth.

Interestingly, *Meox2* has been shown to counteract the effects of TGFβ1 in adventitial fibroblasts by up regulating p15, p16 and p21 (Zhang et al., 2008). These results suggest *Meox2* may act as a direct target to provide negative feedback regulation of TGFβ1 signalling

1.9 Rationale

Ablation of Meox2 by targeted gene disruption in mice gives rise to a hypotrophic phenotype in the musculature of the limbs of neonates; the morphogenesis of these mutant limbs is further complicated by abnormal patterning of specific muscles, revealed by aberrant and failure of cleavage and invasion of tendon space by ectopic muscle. These muscle defects are embryonic in origin and in the absence of Meox, the earliest stages of myogenic differentiation are affected in the limb. Meox2 is expressed both in migratory muscle precursors delaminating into the limb bud, and more distally in the somatopleural limb mesoderm in the first stage of the forelimb bud development at E10.5.

As described in the previous sections, growing evidence shown the influence of tendons and muscle connective tissue on the series of the events involved in muscle patterning of the limb during development. Indeed the expression of Meox2 in limb mesoderm that hosts the progenitors for tendons and MCT indicate that Meox2 plays a role in differentiation of these tissues and thereby influence the various aspects of myogenic differentiation. Little is known about the implication of Meox2 mutation on limb mesenchyme derivatives. Preliminary observations showed thinner and extremely fragile limb and tail tendons in the $Meox2^{-/-}$ mutant animals and hence it opened up doorways to investigate *Meox2* functions during tendon morphogenesis.

1.10 Thesis hypothesis

We hypothesized that *Meox2* is necessary for normal axial and appendicular tendon development. Furthermore, we postulated that the role of *Meox2* could be intrinsic or extrinsic to regulate tendon progenitors. Finally, as TGFβ2 signals are important for tendon progenitor cells, we proposed an interaction between *Meox2* and TGFb2 during tendon development.

1.11 Project objectives

Therefore, this thesis has three research objectives:

1. To characterise the phenotype in *Meox2* mutant neonates in axial and appendicular tendons, using haematoxylin and eosin staining and ScxGFP expression analysis.

2. To identify whether the tendon defects are foetal or embryonic, and determine when the tendon phenotype first manifests, by *Scx* whole mount in situ hybridisation at E11.5-13.5 and ScxGFP expression analysis at E14.5

3. To determine whether Meox2 has an intrinsic or extrinsic role in tendon progenitors, and to elucidate the molecular mechanisms by which Meox2 fulfils this role. For this, Meox2 expression was compared to Scx expression in limb and axial tendons. Additionally, Meox2 derived cells were traced using *Meox2-nLacZ* reporter.

Chapter 2

Materials and Methods

All animal work in the thesis was carried out in accordance with the Animals (Scientific Procedures) Act 1986; project license PPL70/7341.

2.1 TRANSGENIC MICE, MATINGS AND HARVESTING EMBRYOS

2.1.1 *MEOX2^{KO} (-/-)* MICE

The knockout for the *Meox2* locus was described by Mankoo et al., (1999). The same transgenic line was maintained on a mixed129/SV and C57/BL6 background and was used in this study. The generation of mutant mice was by targeted disruption of the *Meox2* transcription and translation initiation sites, the first exon and part of the first intron, with PGK-neo-polyA cassette (fig 2.1). The *Meox2* heterozygous animals i.e. *Meox2$^{+/-}$* were used as controls.

2.1.2 *MEOX2^{nLacZ}* MICE

Generation of the *Meox2^{nLacZ}* allele was achieved by knockin of *nLacZ* into the exon1 whereas most of the 3' end of exon1 remained intact in *nLacZ* locus. The *Meox2^{nLacZ}* mice were generated by removing the *loxP* flanked *PGK-neo* cassette from the original *Meox2$^{nLacZ-neo}$* line generated on a 129/SV and C57/BL6 background and was produced by Dr. Mankoo. This was achieved by crossing the original *Meox2$^{nLacZ-neo}$* females with *Protamine-Cre* males. The latter mice express this recombinase transgene in the male germline, and homologous recombination to excise the *PGK-neo* cassette occurs upon fertilization (O'Gorman et al., 1997). The resulting recombinant mice have the *nLacZ* insert followed by an adjacent *loxP* site, disrupting *exon 1* and resulting in the same null phenotype as the original *Meox2$^{-/-}$* mice (fig 2.1). Therefore, the *Meox2^{nLacZ}* allele employed throughout this thesis corresponds to the recombinant allele without the *neo* cassette; the *Meox2$^{nLacZ-neo}$* mice were not used.

2.1.3 *SCLERAXIS-GFP* MICE

Scx is a unique marker expressed by tendon cells throughout tendon development (Brent et al., 2003; Schweitzer et al., 2001). The *ScleraxisGFP* (*ScxGFP*) transgenic mice were provided by Dr. Ronen Schweitzer (Oregon Health and Science University). The *ScxGFP* mice have GFP expression under the control of regulatory elements of *Scx* gene. After initiation sequence ATG for *Scx* gene, the open reading frame of GFP was cloned into the first exon of *Scx* gene and thereby removing most but not all of the first exon (Pryce et al., 2007). The retention of exon 2 in *Scx* gene locus along with first exon of splice donor sequence led to replicate an endogenous expression of *Scx* transcript. Because this transgene recapitulates endogenous *Scx* expression, all tendons appear green under fluorescence microscope. They were maintained by crossing with *Meox2*^{KO} and *Meox2*^{nLacZ} lines.

2.1.3 *SPLOTCH*^{2H} MICE

The splotch-delayed mice (*Splotch*^{2H}*)* mice were a gift from Prof.Andy Copp (Institute of Child Health), and this had been previously described in the literature (Franz et al., 1993). The genetic background of this line was unknown, and they were maintained by crossing with *Meox2*^{KO} line. The *Splotch*^{2H} mice have mutations in the *Pax3* gene and interfere with the limb muscle development. The homozygous splotch-delayed mice have spina bifida and are thus phenotypically distinguishable from heterozygous controls at embryonic stages.

2.1.5 TIMED MATINGS AND STAGING EMBRYOS

Mice were mated and vaginal plugs were monitored for five days. Noon on the day of vaginal plug observation was taken as 0.5 embryonic day of development. A neck dislocation method and carbon dioxide inhalation was used as per Home Office guidelines to cull pregnant females. All embryos were

staged according to The Atlas of Mouse Development (Kaufman, London 1992).For all experiments, at least three sets of embryos were used to produce the final results. Counting of the somites from the tail to the hindlimb and by comparing limb and head shape and size.

2.2 GENOTYPING OF TRANSGENIC MICE

2.2.1 GENOMIC DNA PURIFICATION

Tail clips of 0.2-0.4 cm were obtained from mice between 2 and 4 weeks of age and portions of yolk sac of embryos for genotyping. The amount of Tail Buffer added was 250 µl for tail and 500 µl for yolk sac. 5 µl proteinase K (20 mg/ml) was used for tails and yolk sac. Samples were then incubated at 50^{o}C overnight. Pellets of undigested hair from tails were obtained by centrifuging at 13000 rpm for 10 minutes. The supernatant was transferred into the fresh microfuge tubes and precipitated with an equal volume of isopropanol by mixing and then centrifuging for 10 minutes. The DNA pellet was washed with 200 µl 70% ethanol and spun for 3 minutes. The DNA pellet was air dried for 30 minutes and redissolved in 50 µl TE. DNA was then stored at -20 ^{o}C.

2.2.2 PCR FOR GENOTYPING TAIL AND EMBRYO

PCR reaction was done in a 30 µl sample volume consisting of 10X Hotstar buffer (Qiagen), 25 mM $MgCl_2$, 10 mM dNTPs, 6 µl of Q buffer, 1 unit of Hotstar polymerase, 100 ng/µl forward and reverse primer and 1 µl of extracted genomic DNA. The programme for Techne genius thermal cycle used was 94^{o}C 5 minutes, 3 cycles of 94^{o}C, 58^{o}C 60 seconds and 72^{o}C 60 seconds, followed by 35 cycles of 94^{o}C 60 seconds, 51^{o}C 60 seconds and 72^{o}C 60 seconds and lastly, one cycle for 5 minutes at 72^{o}C. The PCR products were analysed by 1.3% agarose gel electrophoresis/TAE and the absence or presence of a particular *Meox2* allele in each individual samples was determined using a UV transilluminator.

MEOX2 ALLELES PCR PRIMERS (See figure 2.1 for relative locations of the primers).

Table 2.1: Primer sequence used for genotyping

	Primer number	Sequence	Product size (bp)
1	612(*Meox2*^{WT} Forward primer)	5'GGCTCTGCAAAGCAACTGGCACC3'	255bp
2	1046((*Meox2*^{WT} Reverse primer)	5'CAGAGCGAGGAAAGGCTAGCAGC3'	255bp
3	86(*Meox2*^{KO} Forward primer)	5'CTAAAGCGCATGCTCCAGACTGCCTTGG 3'	400bp
4	592(*Meox2*^{KO} Reverse primer)	5'CCCAGTGCGTTCTGATGCCTTCTTAGG3'	400bp
5	618(*Meox2*$^{KI\text{-}N}$ Forward primer)	5'GAAGGCACATGGCTGAATATCG3'	600bp
6	613(*Meox2*$^{KI\text{-}N}$ Reverse primer)	5'GCTGTCGCTTTCCTTTTGCTGCCAC3'	600bp

2.3 GENERATION OF TEMPLATE cDNA FOR RNA SYNTHESIS

2.3.1 PREPARATION OF cDNA

Meox2 full-length cDNA was generated by B. Mankoo. *Scleraxis* was a gift from R. Schweitzer; *Sox9* was a gift from P. Koopman and *Tgfβ2* was an IMAGE clone (ID 4009682) obtained from Invitrogen.

2.3.2 BACTERIAL TRANSFORMATION OF PLASMID DNA

In order to obtain large amounts of cDNA for the synthesis of RNA probes, 50 µl of chemically competent *E.coli* DH10B (Invitrogen) cells were transformed with 10 ng plasmid DNA diluted in 20 µl of water. The cells were incubated on ice for 10-30 minutes. A heat shock was applied by transferring the cells directly to a 42°C heat block for 2 minutes. Cells were briefly incubated on ice and supplemented with 1 ml LB medium, without selection. The transformed cells were incubated at 37°C for 1 hour then plated onto LB-agar containing 100 ng/µl ampicillin to isolate ampicillin resistant single transformed colonies after overnight culture at 37°C.

2.3.3. PURIFICATION OF PLASMID DNA BY ZIPPY METHOD

Single bacterial clones were picked from the plates and grown in 5 ml cultures of LB medium containing 100 ng/µl ampicillin overnight in a shaking incubator at 37^0C. Next day, cultures were spun in a centrifuge for 10 minutes at 4000 rpm. The bacterial cell pellet was then resuspended in 0.7 ml of zippy buffer and 50 µl of 10 mg/ml lysozyme and transferred to microcentrifuge tubes. The tubes were heated at 90-120 sec at 95^0C in preheated heating block and then centrifuged for 10 minutes at maximum speed. A wooden toothpick was used to remove the gelatinous precipitate and to the remaining supernatant, an equal volume of 0.7 ml isopropanol was added. After vigorous shaking, DNA in pellet was obtained after centrifugation for 10 minutes. A DNA pellet was washed with

70% ethanol and centrifuged again for 3 minutes. Finally, DNA pellets were air-dried for 20 min at room temperature and then resuspended in 50 µl of TE and 3 µl of 100 ng/µl heat-treated RNase A. DNA was then stored at -20 ^{o}C.

2.3.4 ANALYSIS OF PURIFIED PLASMID DNA.

The production of correct DNA was verified by restriction digestions cleaving the individual insert from the vector, and analysed by 1.2% gel electrophoresis. The sizes of the fragments were determined using the λ DNA/BstEII fragments as a ladder (New England Biolabs). DNA concentration was estimated qualitatively by comparison with individual determined concentrations of ladder fragments and quantitatively by nanodrop spectrophotometer.

2.3.5 RESTRICTION ENZYME DIGESTION OF PLASMID DNA

All plasmid DNA were linearized to enable anti-sense RNA transcription from the promoter situated at the 3' end of all cDNAs. 20 µg of template cDNA was digested in a total volume of 200 µl with appropriate restriction enzymes, as summarised in table 2.2 and verified by 1% gel electrophoresis.

2.3.6. PURIFICATION OF LINEARISED cDNA

200 µl of linearized plasmid was purified by phenol-chloroform extraction. 120 µl of phenol-chloroform was added, and the tube was then mixed and centrifuged at 13000 rpm for 3 minutes; the DNA in aqueous phase was transferred to a fresh centrifuge tube and 120 µl of chloroform was added. This was mixed and centrifuged for 5 minutes. To this supernatant, 10% volume of 3M sodium acetate and 100% ethanol (2.5x DNA volume) were added. The tube was incubated at -20^{o}C for an hour and then centrifuged for 20 minutes to precipitate the DNA. The DNA pellet was washed with 70% ethanol, centrifuged for 3 minutes. The pellet was air dried and re-suspended in 20 µl of RNase-free water. Final concentration and purity of linearized template cDNA was determined by nanodrop spectrophotometer.

2.3.7 DIG LABELLED RNA PROBE SYNTHESIS

Labelling reaction: RNA synthesis reaction of 20 µl final volume comprised of 1µL of 1 µg/µl of linearized plasmid DNA in autoclaved ELGA water, 2 µl of 10X DIG-RNA labelling mix, 2 µl of RNA polymerase (Table 2.2) and 0.5 µl of RNase inhibitor (RNasin Roche).. The reaction was incubated at 37^{o}C for 2 hours and RNA synthesis was confirmed by analysis of 1 µl of reaction on 1% TAE agarose gel. Plasmid DNA was digested by adding 1 µl DNase1 (RNase free, Roche) was added and incubated for 1 hour at 37^{o}C. The activity of DNase1 was stopped by adding 1 µl of 0.5M EDTA.

Purification of RNA: To the above labelling reaction 2.5 µl 4M LiCl and 75 µl prechilled 100% ethanol were added and mixed. The samples were incubated at -80^{o}C for 30 min and centrifuged 13000 rpm for 20 minutes at 4^{o}C. RNA pellets were washed with using 50 µl chilled 70% ethanol. After air-drying for 20 min, riboprobes were dissolved in 50 µl sterile RNAse-free water and stored at -80^{0}C. Riboprobes were analysed using 1 µl on agarose-gel and concentration was determined using nanodrop spectrophotometer.

Table2.2: DIG-labelled cRNA probe synthesis from cDNA 3'UTR

cDNA	Restriction enzyme	RNA polymerase(Roche)	RNA product length
MEOX2	XbaI	T3	1400 nt
SCLERAXIS	SalI	T3	900 nt
TGF-β2	EcoRI	T7	1200 nt
SOX9	HindIII	T7	1400 nt

2.4 WHOLE MOUNT *IN SITU* HYBRIDIZATION

2.4.1 EMBRYO COLLECTION

Embryos of the required stage were collected as described in section 2.1.5 and fixed overnight in 4% paraformaldehyde at 4^0C. Washing with ice cold PBST for 5 minutes was carried out. Fixed embryos were then de-hydrated with gentle rocking in ascending concentration of methanol/PBST (25%, 50%, 75% and 100%) at room temperature until embryos sink at the bottom and finally stored in 100% methanol at -20^0C.

2.4.2 PRE-TREATMENTS AND HYBRIDISATION

Rehydration of embryo was performed on a rocker in 75%, 50% and 25% methanol/PBST mixture at room temperature and they were bleached with 6% H_2O_2 in PBT for 60 minutes. Proteinase K (10 µg/ml) made up in PBST was added for 50 minutes. The proteinase K activity was then stopped by adding 2 mg/ml glycine in PBST for 10 minutes. The bleached and porous embryos were washed twice in PBST for 5 minutes and post fixed for 20 minutes in 4% paraformaldehyde and 0.1% glutaraldehyde. Embryos were then rinsed with 1:1 PBST/hybridisation mixture and then with 1ml pre-warmed hybridisation mix. The tubes were then incubated horizontally in 1ml pre-warmed hybridisation mix for 1 hour at 70^0C. 0.2 µg/ml of DIG-labelled RNA probe in pre-warmed hybridisation mix was added to the tubes and incubated horizontally overnight on a rocker at 70^oC.

2.4.3 POST-HYBRIDISATION WASHES

After 15 hours of incubation, embryos were washed twice with pre-warmed hybridisation mix for 30 min each at 70^{o}C followed by 1:1 hybridisation mix/TBST for 20 minutes. Embryos were then rinsed and washed twice with TBST at room temperature. The tubes were then rinsed twice with MABT. Afterwards, embryos were pre-incubated with MABT plus 10% filtered heat-treated sheep serum for an hour. Subsequently, a 1/2000 dilution of anti-DIG antibody (Roche) in MABT plus 10% filtered heat-treated sheep serum was added and tubes were incubated at 4^{o}C overnight on a rocker.

2.4.4 POST-ANTIBODY WASHING

Next day, embryos were washed three times with MABT and then six times for 1 hour each with 2 ml MABT on a rocker. Tubes were incubated at room temperature overnight in MABT on a rocker.

2.4.5 COLOUR DEVELOPMENT

On Day 4, embryos were washed twice for 10 min with NTMT, and then incubated with 1.5 ml NTMT and 200µl NBT/BCIP mix (Roche) until colour developed to the desired extent. The colour reaction was then stopped by washing three times with PBT.

2.4.6 IMAGING

Images were taken with the digital camera (Leica) on the Leica MZ125 dissecting microscope and Openlab software and processed using Adobe Photoshop CS5.1.

2.5 *IN SITU* HYBRIDIZATION ON CRYOSECTIONS

All the reagents used in this method were pre-treated with 0.1% diethylpyrocarbonate (DEPC) overnight at room temperature followed by autoclaving.

2.5.1 EMBRYO COLLECTION AND CRYOSECTIONING

Fresh collected embryos were fixed in 4% paraformaldehyde at 4^0C for 2 hour. Embryos were then washed in ice-cold PBS and incubated overnight in 5% sucrose/PBS at 4^0C with gentle rocking. Next day, 15% sucrose/PBS was added for 2 hours at 4^0C and then embryos were transferred to 30% sucrose/PBS for 2 hours at at 4^0C. The embedding of embryos was done in OCT (Sakura) on dry ice at the appropriate orientation and they were stored at -80^0C. Transverse sections of 20 µm were obtained using the Leica CM1950 cryostat on the day of hybridization. The sections were collected on poly-lysine coated slides and air-dried for 3 hours at room temperature. GFP positive tissue sections were dried in the dark.

2.5.2 TISSUE PREHYBRIDIZATION AND HYBRIDIZATION

Slides were rinsed twice with PBST for 15 minutes. Also it was important to keep tissues wet all the time and therefore not allowed to dry out. Tissue sections were then washed with DEPC-treated 1:1 PBT/Hybridization mix (used in the section 2.4.2). The slides were then prehybridized in the hybridization mix for 1 hour at 65^0C in a moist atmosphere using 65^oC Wash Buffer to maintain humidity. Then, DIG-labelled RNA probe (0.1 µg/ml; 500 µl per slide) was added onto sections and slides were covered with RNase-free coverslip (Invitrogen, Catalog no. 10625983). Sections were left overnight at 65^oC in a humidified chamber using 65^oC Wash buffer.

2.5.3 POST-HYBRIDIZATION WASHES

The following day the slides were dipped into 65^{o}C Wash Buffer for the removal of the cover slips. Sections were then rinsed once and washed twice for 30 minutes at 65^{o}C with Wash Buffer. The slides were rinsed twice with MABT for 5 minutes followed by incubation of the slides in MABT and 10% filtered heat-treated sheep serum for 1 hour at room temperature. Subsequently, 200 µl of 1/2000 dilution of anti-DIG antibody (Roche) in MABT plus 10% filtered heat-treated sheep serum was added and slides were kept at 4^{o}C overnight in a humidified chamber using MABT.

2.5.4 POST-ANTIBODY WASHING AND COLOUR DEVELOPMENT

Slides were briefly rinsed three times and then washed six times for 5 minutes each with 2 ml MABT at room temprature. Sections were then washed twice for 10 minutes each with NTMT. The colour development on the sections was obtained by incubating with 1.5 ml NTMT and 200 µl NBT/BCIP mix (Roche) until the desired extent. The colour reaction was then stopped by washing three times with PBT. The slides were finally mounted with propyl gallate mounting medium containing DAPI (10 mg/ml).

2.5.6 IMAGING

Images were taken using the digital camera (Leica) on a Zeiss Axiovert 200M fluorescence microscope and processed by Adobe Photoshop CS5.1.

2.6 β-GALACTOSIDASE ANALYSIS

2.6.1 EMBRYO PROCESSING

The collection of appropriate staged embryos was done in ice-cold PBS followed by fixation in 4% paraformaldehyde at 4^{0}C for 2 hours. Embryos were then washed in ice-cold PBS and incubated overnight in ice-cold 5%

sucrose/PBS. Next day, 15% sucrose/PBS was added for 2 hours at 4^0C and then embryos were transferred to 30% sucrose/PBS for 2 hours at 4^0C. The embedding of embryos was done in OCT on dry ice at the required orientation and they were stored at -80^0C.

2.6.2 CRYOSECTIONING

Transverse sections of 20 µm were obtained using the Leica cryostat on the day of staining. The sections were collected on poly-lysine coated slides and were air-dried for 3 hours at room temperature. GFP positive tissue sections were dried in the dark.

2.6.3 X-GAL and S-GAL STAINING

Air dried slides of cryosections were washed thrice with *LacZ* wash buffer without X-gal or S-gal for 15 minutes at room temperature. *LacZ* staining solution was added for 20 minutes. Slides were then washed in PBS for 5 minutes and then submerged in *LacZ* staining solution containing 0.5ml of 40mg/ml X-gal (dissolved in dimethyl formamide) (Thermofischer) or 0.1mg/ml S-gal (6-chloro-3-indolyl- β-D-galactopyranoside, Apollo Labs) overnight at 37^0C. Subsequently, sections were washed in PBS and rinsed in water for 5 minutes. S-gal, a β-gal substrate produces pink-colour precipitate when hydrolysed by β-galactosidase and was preferred, as S-gal precipitates do not quench DAPI unlike X-gal that gives blue colour precipitate and therefore interferes with the DAPI signal.

2.7 HAEMATOXYLIN AND EOSIN STAINING

Tissue histology at post-natal stages was studied using haematoxylin and eosin staining. Air-dried cryosections (section 2.6.2) were stained for 3 minutes with haematoxylin stain and then rinsed with distilled water. In order to lessen the background colour, slides were washed in tap water for 5 minutes. Destaining was then performed using an acid rinse (2% glacial acetic acid in distilled water)

by fast dipping for 8-12 times. The slides were rinsed with tap water and then with distilled water for 2 minutes. After that, eosin staining was performed on the same slides. Eosin stain (0.1% eosin in 95% ethanol) was added for 30 seconds. The slides were then dehydrated in 95% ethanol and 100% ethanol for 3 minutes each. Subsequently, slides were air dried for 30 minutes. Finally, the slides were mounted with propyl gallate mounting medium containing DAPI (10 mg/ml).

2.8 GENERAL IMMUNOFLUROSCENCE

20 µm cryosections were processed as mentioned in 2.6.2. The cryosections were rinsed thrice in PBS at room temperature followed by blocking with PBST and 10% goat serum for 2 hours. The primary antibody diluted in 5% goat serum/PBST was then applied on sections and incubated overnight at 4^{o}C in an atmosphere humidified with PBS. Next day, the sections were washed thrice for 5 minutes in PBST. Secondary antibody diluted in 5% goat serum/PBST was then added onto the sections for 2 hours at room temperature. The slides were then rinsed thrice for 5 min in PBST. The slides were finally mounted with propyl gallate mounting medium containing DAPI and examined with a Zeiss Axiovert 200M fluorescence microscope. Adobe Photoshop CS5.1 was used for image processing. The above described immunofluorescence method was used for all antibodies except the listed Meox2 antibodies (discussed in next section). Primary and secondary antibody details are tabulated in Table 2.3 and Table 2.4.

2.9 *MEOX2* IMMUNOFLUORESCENCE

The optimisation of Meox2 antibody protocol was required for this project, as the general immunofluorescence method described did not produced any signal for this antibody.

2.9.1 EMBRYO PROCESSING

Mouse embryos of E12.5-E14.5 were fixed in ice-cold solution 1 containing 0.2% paraformaldehyde overnight at 4^{o}C. On day 2, the embryos were washed twice in cold PBS then incubated in solution 1 without 0.2% paraformaldehyde overnight at 4^{o}C. After 24 hours, the embryos were washed in cold PBS and incubated in solution 2 overnight at 4^{o}C. Finally, on day 4, the embryos were rotated in solution 3 for 1 hour at 37^{o}C, followed by embedding in OCT with appropriate orientation and stored at -80^{0}C

2.9.2 CRYOSECTIONING

As described in section 2.6.2.

2.9.3 *Meox2* ANTIBODY STAINING

The sections were fixed in pre-cooled 100% methanol at -20^{0}C for 5 minutes. The slides were then rinsed twice with PBSX for 5 minutes. The permeabilization was then performed using PBSX for 20 minutes. The sections were then blocked in PBSX plus 10% sheep serum for 1 hour. Meox2 antibody (table 2.3) diluted in PBSX and 10% sheep serum was added onto the sections for overnight incubation at 4^{0}C in moist atmosphere using PBS. Next day, the sections were washed at least 5 times for 5 minutes with PBSX at room temperature. Secondary antibody diluted in PBSX plus 10% sheep serum was added for 2 hours at room temperature. After washing with PBSX for 5 minutes, slides were air-dried and were finally mounted with propyl gallate mounting medium containing DAPI.

2.9.4 IMMUNODETECTION

The stained sections were documented using a Zeiss Axiovert 200M fluorescence microscope and a Zeiss LSM Exciter confocal microscope. (S Hughes lab). Adobe Photoshop CS5.1 was used for image processing as shown in Fig 2.2.

Table 2.3: Primary antibodies

Name	Supplier	Catalogue no.	Species	Dilution
Anti-Meox2	GenWay	Custom-made	Rabbit	1:100
Anti-Myosin heavy chain	Upstate (Millipore)	A4.1025	Mouse	1:100
Anti-Caspase 3	BD Biosciences	559565	Rabbit	1:300
Anti-GFP	Abcam	ab13970	Chicken	1:2000
Anti-Ki67	Abcam	ab15580	Rabbit	1:200
Rabbit pre-immune IgG	GenWay	Custom-made	Rabbit	1:100

Table 2.4: Secondary antibodies

Name	Supplier	Catalogue no.	Species	Dilution
Cy2 conjugated Anti-chicken IgG	Jackson Immuno Research	703-225-155	Donkey	1:500
DyLight 488 conjugated Anti-rabbit	Jackson Immuno Research	111-485-003	Goat	1:500
DyLight 594 conjugated Anti-rabbit	Bethyl Laboratories	A120-601D4-1	Goat	1:500
DyLight 550 conjugated Anti-mouse	Bethyl Laboratories	A90-231D3	Goat	1:500

2.10 *IN VITRO* ANALYSIS

2.10.1 C3HT10$^{1/2}$ CULTURE

A murine cell line considered to represent a mesenchymal progenitor state C3HT10$^{1/2}$ was used in this project (Pinney and Emerson, 1989). The stock was kindly provided by Hughes lab and was stored in liquid nitrogen. The cells were stored in liquid nitrogen and in freezing media containing 10% FCS, 1% PS, herewith, referred as growth medium (DMEM+FCS+PS) with 10% dimethylsulfoxide, DMSO. The cryovial containing the cells was thawed quickly and the cells transferred to 5 ml of growth medium in a 15 ml conical falcon tube. This was then centrifuged for 5 min at 1000 rpm. The supernatant was removed and the cell pellet was resuspended in 1 ml growth medium. The cells were then re-plated as indicated by the storage instructions. Routinely, C3HT10$^{1/2}$ cells were frozen in aliquots equivalent to 1/6th of a T75 flask and replated onto a T75 flask.

2.10.2 CELL SPLITTING

When necessary (>80% confluency for C3HT10$^{1/2}$ cells) the cells were split by first removing the medium and washing the cells twice with sterile PBS. The cells were detached from the bottom of the flask using 2 ml of 1x Trypsin-EDTA, incubated for 3-5 minutes. Cells were further dislodged by hitting hard on the sides of the flask and checked under a microscope for roundness. 2 ml of sterile PBS was added and used to detach the cells from plastic and dispersed into a single cell suspension. 8 ml DMEM+FCS+PS was added to quench the Trypsin-EDTA and the cell suspension was transferred to a 15 ml sterile Falcon tube. Cells were pelleted by centrifuging for 5 minutes at 1000 rpm and the supernatant was discarded. The cell pellet was then resuspended in a fresh growth medium and plated as described in next section

2.10.3 CELL PLATING FOR *IN VITRO* ANALYSIS

C3H10T1/2 were seeded in a 24-well plate at a cell density of $1X10^5$ cells/well in growth medium. After 24 hours, the medium was supplemented with a freshly thawed aliquot of 20 ng/ml TGFβ2 (Peprotech, Catalog no. 100-35B) or 25 ng/ml FGF4 (Peprotech, Catalog no. 100-31) and 1 ng/µl BSA. The cells were incubated for 1 hour, 4 hours, 8 hours and 24 hours. Subsequently, cell lysates were collected after each time point and processed for RNA purifications.

2.10.4 RNA PURIFICATION BY TRIZOL METHOD

After the desired time point, cells were washed with PBS and 0.25 ml of Trizol reagent was added to obtain cell lysates. The adherent cells were collected by using a cell scraper (BD Falcon) and transferred into the sterile eppendorf tubes. 0.25 ml chloroform was added and 15 sec of vigorous shaking was performed. The tubes were then incubated at room temperature for 3 minutes and spun at 13000 rpm for 15 minutes at 4^oC. RNA in supernatant was collected in an eppendorf tube and 0.125 ml isopropanol was added. The mixture was incubated for 10 minutes at room temperature. The tubes were spun at 13000 rpm for 15 minutes at 4^oC. The RNA pellets were washed with 1 ml of 70% ethanol and mixed properly. After centrifugation for 5 minutes at 4^0C, RNA pellets were collected and air dried for 15-20 minutes. Finally, RNA was dissolved in 50 µl of RNase-free water and the concentration was measured at 260 nm using Nanodrop spectrophotometer and stored at -80^0C.

2.10.5 PREPARATION OF cDNA

Reverse transcription of purified RNA was performed as per the manufacturer's standard protocol using the QuantiTect Reverse Transcription kit (Qiagen). Briefly, the template RNA and Quantiscript reverse transcriptase was thawed on ice. The gDNA wipeout buffer, Quantiscript reverse transcription buffer, reverse transcription primer-mix were thawed at room temperature. The genomic DNA elimination reaction was then prepared in an eppendorf using 2 µl gNDA wipe out buffer, 1 µg of template RNA and then the volume of the mixture was levelled for 14 µl using RNase free water. The tubes were incubated for 2 minutes at 42^{o}C and then placed on ice immediately. Following this, the reverse transcriptase master mix on ice was prepared. In a fresh eppendorf tube, 14 µl of genomic DNA elimination reaction was added along with 1 µl of Quantiscript reverse transcriptase, 4 µl of 5X Quantiscript reverse transcription buffer and 1 µl reverse transcription primer-mix was added. The tubes were mixed properly and incubated at 42^{o}C for 15 minutes. The tubes were then incubated at 95^{o}C for 3 minutes to inactivate Quantiscript reverse transcriptase. Finally, 1 µl sample was added for semi-quantitative PCR reaction and rest of the sample was stored at -80 ^{o}C.

2.10.6 SEMI-QUANTITATIVE PCR

The PCR reaction was done in 30 µl sample volume consisting of 10XHotstar buffer (Qiagen), 25 mM $MgCl_2$, 10 mM dNTPs, 6 µl of Q buffer, 1 unit of Hotstar polymerase, 5 µM forward and reverse primer and 1 µl of cDNA. The programme for thermal cycle used was 95^{o}C for 5 minutes, 3 cycles of 94^{o}C for 50 seconds, 60.2 ^{o}C for 30 seconds and 72^{o}C 40 seconds, followed by 35 cycles of 94^{o}C 50 seconds, 57^{o}C 30 seconds and 72^{o}C for 40 seconds and, lastly, one cycle for 5 minutes at 72^{o}C. The PCR products were analysed on 0.8% agarose gel electrophoresis.

PCR primers were:

a) Scleraxis forward 5'CTTCCACAGCGGTCGTGCGGC3'
b) Scleraxis reverse 5'AGCGTGCTCTTGGGGACCTGCGCT3'
c) Meox2 forward 5'GCGACAGCTCAGATTCCCAGG3'
d) Meox2 reverse 5'CCAGTTCCTTTTCTCGGGCAG3'

SOLUTIONS

Unless otherwise stated, all solutions were made with autoclaved MilliQ double distilled H20.

$CaCl_2$ 1M 14.7 g $CaCl_2.2H_2O$ in 100 ml of H_2O.

Deoxynucleotide triphosphates (dNTPs) 10mM 2.5 mM each of dDNTP, dCTP,

dGTP, and dTTP (Omega). Stored at 20°C.

DEPC-H_2O MilliQ water treated overnight with 0.1% (v/v) diethyl dicarbonate (diethylpyrocarbonate) then autoclaved.

EDTA stock 500mM EDTA, adjusted to pH 8.0 with NaOH.

Freezing media DMEM (Dulbecco's Modifies Eagle Medium) and glutamax (Invitrogen), Stored at 4°C.

FGF4 recombinant protein (25 µg/ml) 5 µg dissolved in 200 µl 1 mg/ml BSA. 20 µl Aliquots stored at -20°C.

Growth medium DMEM+FCS+PS i.e. DMEM containing 10%FCS and 1%PenStrep. Prepared under sterile hood. Stored at 4°C.

Hybridization mixture 50% formamide, 1.3X SSC pH 5, 5mM EDTA, 50 µg/ml Yeast RNA, 0.2% Tween-20, 1% SDS, 100 µg/ml Heparin in water. Stored at -20°C.

LB 85mM NaCl, 0.5% (w/v) yeast extract, 1% (w/v) bacto-tryptone. Autoclaved and stored at 4°C.

LB+AMP LB supplemented with 1x ampicillin.

LB-agar LB supplemented with 1.5% (w/v) agar. Cast into 10 cm petriplates. Stored at 4°C.

LB-agar+AMP LB-agar supplemented with 1x ampicillin. Stored inverted at 4°C.

***LacZ* wash buffer** PBS, 0.02% Nonidet P-40

***LacZ* stain** PBS, 0.02% Nonidet P-40, 2mM $MgCl_2$, 0.01% Sodiumdeoxycholate, 40mg potassium-ferrocyanide, 30mg potassium-ferricyanide.

MABT 100mM Maleic acid, 150mM NaCl pH7.5, 1%Tween-20

Na_2HPO_4 0.2M 28.4 g Na_2HPO_4 in 1000 ml of ddH_2O.

NaH_2PO_4 0.2M.H_2O 27.6 g $NaH_2PO_4.H_2O$ in 1000 ml of ddH_2O.

NBT stock 50mg/ml NBT in 70% (v/v) DMF. Stored at -20°C.

NTMT 100mM Tris-HCl pH9.0, 100mM NaCl, 50mM MgCl2, 0.1% (v/v) Tween-20 in sterile water.

Optimal Cutting Temperature (OCT) Sakura, Catalog no.4583.

10x HotStar PCR Buffer Proprietary formula (Qiagen).

PBS (5x) 137mM NaCl, 2.7mMKCl, 10mM Na2HPO4, 1.76mM KH2PO4, pH 7.4. Prepared with 5 tablets (Oxoid) per 100ml MilliQ H20 and autoclaved.

PBST 1xPBS with 0.1% (v/v) Tween-20.

PBSX 1xPBS plus 0.1% (v/v) Triton X-100

Phosphate buffer stock solution 0.24M, pH 7.2 6.4 gm $NaH_2PO_4.H_2O$ + 27 gm Na_2HPO_4 in 1000ml ddH_2O. Autoclaved.

Propyl gallate mounting medium 2.5 g (Sigma P3130) dissolved in 35 ml glycerol overnight at room temperature on a roller and 1 µl of DAPI was added next day. Aliquotes stored at -20°C.

Paraformaldehyde (4%PFA) 4 gm PFA powder (stored at 4°C) in 1x PBS.

Poly-lysine coated slides (Thermo-scientific, Catalog no.J2800AMNZ)

QuantiTect Reverse Transcription kit (Catalog no. 205310 Qiagen)

Sodium Saline Citrate (SSC, 20X) 3 M NaCl, 0.3 M Na citrate, pH 5. Autoclaved.

Solution 1 (Meox2 antibody staining) 8 gm Sucrose, 0.12mM of 1M $CaCl_2$, 0.2M Na_2HPO_4, 0.2M $NaH_2PO_4.H_2O$. Adjusted the pH 7.4 and aliquotes stored at -20°C.

Solution 2 (Meox2 antibody staining) 0.12M phosphate buffer pH 7.2/15% sucrose. Aliquots stored at -20°C.

Solution 3(Meox2 antibody staining) 0.12M phosphate buffer/15% sucrose/7.5% gelatin. Dissolved at 37ºC and aliquotes stored at -20°C.

TAE 40mM Tris-HCl pH 8.0, 20mM acetic acid, 1mM EDTA.

Tail Buffer 100mM Tris-HCl pH 8.0, 5mM EDTA, 200mM NaCl, 0.2%SDS.

10x TBS 1.37M NaCl, 27mM KCl, 0.25M Tris-HCl pH 7.5. Autoclaved.

TBST 1xTBS with 1% (v/v) Tween-20. Freshly made from 10x TBS on the day of requirement.

Tris-EDTA buffer (TE) 10mM Tris-HCl, 1mM EDTA. Prepared at pH 7.5 and pH 8.0.

Tris stock 1M Trizma-HCl at pHs of 6.5, 7.0, 7.5, 8.0, 8.5, 9.0, 9.5 in ddH_2O . Autoclaved and stored at RT.

Triton buffer 0.25% Triton 100, 10mM Tris pH 8.0, 10mM EDTA, 0.5mM EGTA.

2.5% Trypsin-EDTA (10x) 146.55mM NaCl, 1.05mM Trypsin (Invitrogen).

TGFβ2 recombinant protein (20 µg/ml) 1 µg dissolved in 50 µl 1 mg/ml BSA. Aliquots stored at -20°C.

Wash buffer 50% formamide, 1X SSC pH 5 and 0.1% Tween 20 used at 65°C.

Zippy buffer 8 % sucrose, 0.5% Triton X-100, 0.5 M EDTA, 1M Tris pH 8.0 in autoclaved distilled water. Autoclaved.

All restriction endonucleases were obtained from New England Biolabs. Majority of the chemicals were obtained from Sigma-Aldrich unless otherwise stated. Integrated DNA Technologies synthesized all oligonucleotides. Solutions were stored at room temperature (RT) unless otherwise stated. Where applicable, reagents have been named in accordance with the naming conventions of the International Union of Pure and Applied Chemistry (IUPAC).

Meox2 Wildtype and *Meox2 KO* alleles

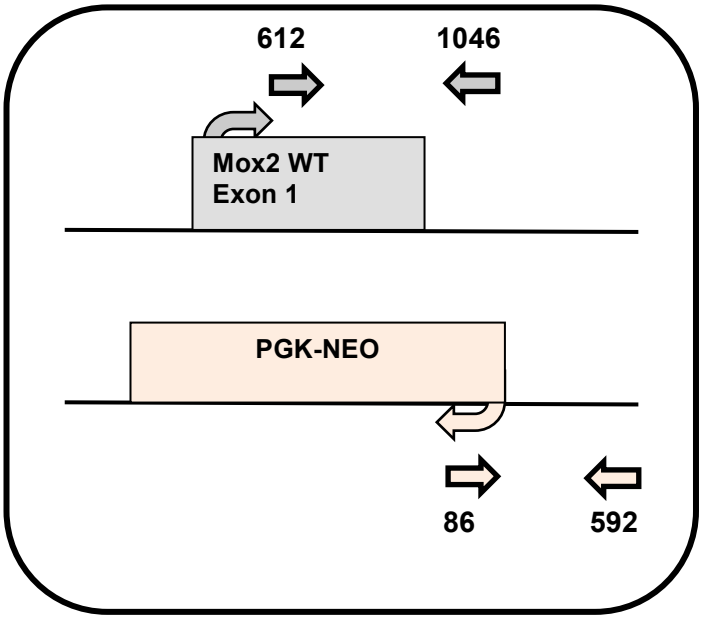

Meox2 Wildtype and *Meox2 KI-N* alleles

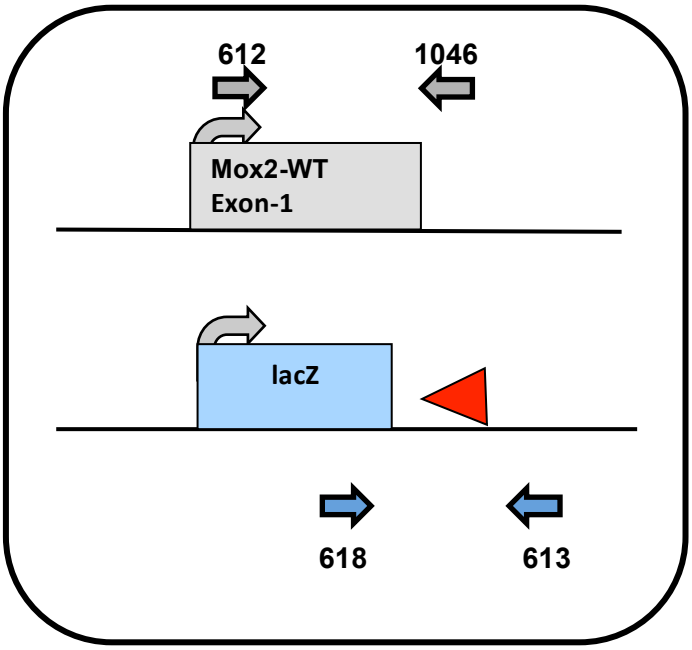

Figure 2.1. Schematic of the *Meox2* transgenic lines and corresponding PCR primers

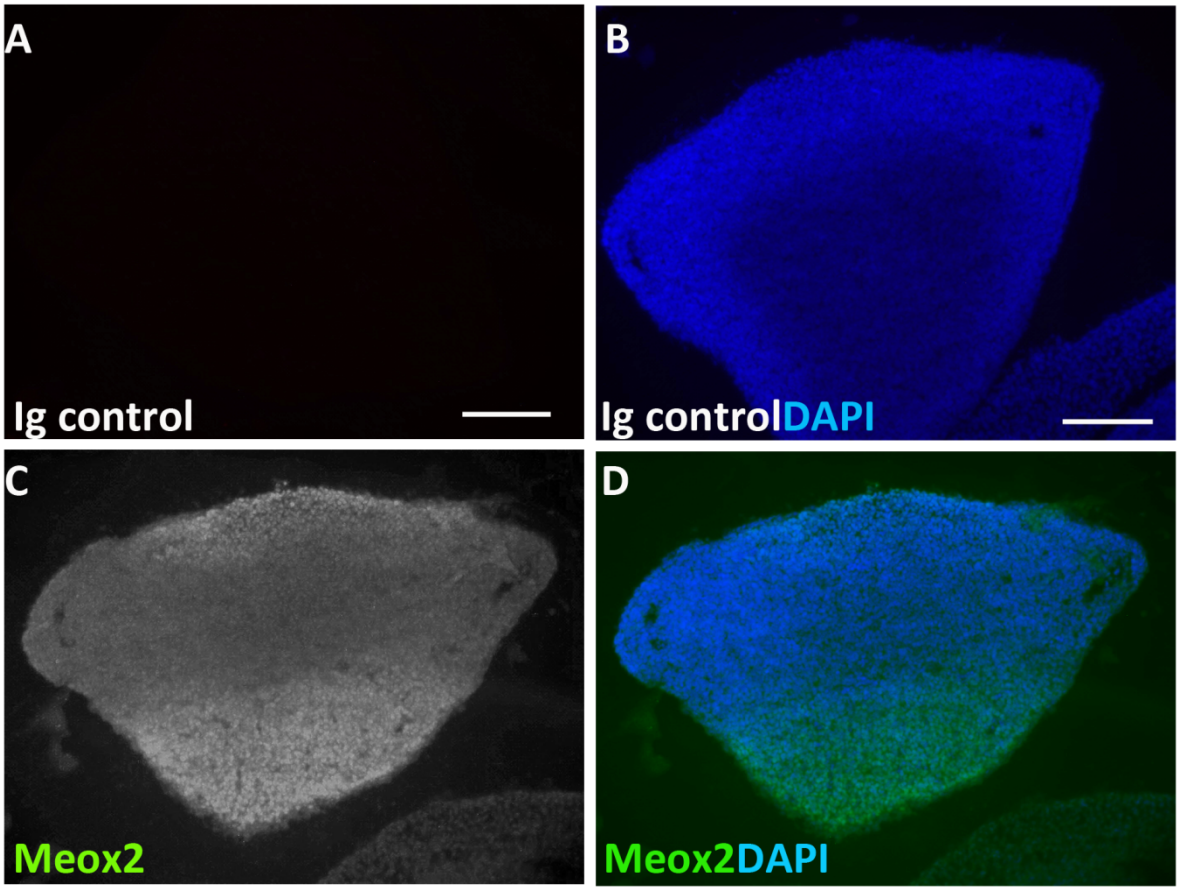

Figure 2.2 Optimization of the Meox2 antibody staining: The transverse cryosection of the limb was immunostained with rabbit pre-immune IgG as a control (A and B) whereas Meox2 antibody was added to the equivalent limb section (C and D). The sections were observed under a Zeiss Axiovert 200M fluorescence microscope. Scale bar= 100 µm.

Chapter 3

Phenotypic analysis of the tendons in *Meox2* mutant mice

3.1 Introduction

The requirement of *Meox2* during limb muscle patterning has been reported before. Muscle abnormalities included overall reduction in skeletal muscle mass of the limb and mutant animals displayed normal axial and appendicular skeleton (Mankoo et al., 1999). *Meox2*$^{-/-}$ embryos at E10.5 show down regulation of genes previously known to be expressed in myogenic precursors that eventually populate the limb mesenchyme *Pax3* and *Myf5*, although *MyoD* expression was normal (Mankoo et al., 1999). This finding places *Meox2* upstream of *Pax3* and *Myf5* in the genetic hierarchy regulating limb muscle development. Interestingly, during the limb bud development, distal *Meox2* expression was found to be normal in *Splotch*^{2H} embryos in which all limb muscles are lost due to a point mutation in the *Pax3* gene resulting in the failure in migration of muscle progenitor cells into the limb buds. It was suggested that the *Meox2* expressing cells from the limb mesenchyme might cause the muscle patterning defects in *Meox2*$^{-/-}$ animals.

Several studies have shown that the interactions between muscle and tendon tissues are mandatory for their patterning and development (Chevallier et al., 1977; Kardon, 1998). The initial stages of tendon and muscle progenitor cells induction are autonomous; however, the patterning, growth and maintenance of both tissues require the local extrinsic cues within the limb bud. For instance, in the chick, when the tendons were surgically altered in the limb, the migration of muscle cells were found normal and likewise, tendon precursors were originated in the muscle-less limbs (Kardon, 1998). However, in the absence of myotendinous interactions, muscles and tendon cells failed to develop and hence, degeneration of both tissue occurred. This observation found similar results with a classical quail-chick chimera study (Chevallier et al., 1977) that demonstrated the requirement of external cues for muscle development in the limbs.

The interdependency of both tissues during embryogenesis led us to hypothesize that the muscle defects in *Meox2*$^{-/-}$ could be the result of loss of *Meox2* expression in the limb tendons. The bone and cartilage were normal in these mutants suggesting normal cartilage development, however, tendons were thinner, fragile and hypoplastic. Thus, we characterised the tendon tissue defects in *Meox2*$^{-/-}$ neonates.

3.2 Aims

Our aim was to describe the tendon distribution along the proximal-distal axis of the forearm in the heterozygous animal and homozygous neonates and this analysis was carried out using *ScxGFP* transgene to identify tendon fibres. Tendon histology was performed on transverse sections of paraffin-embedded limbs that were obtained from a control and mutant new born animals and counterstained with Haematoxylin and eosin stain. Due to the complexity of the stylopod segment of the limb, the focus of this analysis has been restricted to the autopod and zeugopod. Tendon nomenclature is tabulated in Table 1 and the limb tendon atlas used here was in accordance with Watson et al., 2009.

3.3 Results

3.3.1 REDUCED *SCXGFP* IN TENDON CELLS IN *MEOX2* NULL MUTANTS

The *ScxGFP* transgenic reporter was shown to recapitulate the endogenous *Scx* expression domains in the tendon cells (Pryce et al., 2007). Thus, to visualize whole tendons, the *ScxGFP* transgene was used to compare tendons in controls and mutants. Mice heterozygous for the *Meox2* mutation (*Meox*$^{+/-}$) and crossed to the *ScxGFP* transgene displayed no tendon abnormalities (Fig. 3.3.1A,C). When intercrossed, the homozygous mutant animals (*Meox2*$^{-/-}$*; ScxGFP*) were born with the expected Mendelian transmission rate of these alleles. Newborn *Meox2*$^{-/-}$*; ScxGFP* litters showed severe limb tendon defects and extremely thin tendon trajectories were evident. In forelimbs of the mutants, the GFP expression was dramatically reduced from the extensor digitorium communis (EDC) on the dorsal side but only partially reduced on the ventral side (T3, Fig. 3.3.1B,C). Interestingly, EDC tendon was completely missing at the wrist level on the ventral side that could probably explain the abnormal extension and abduction of the wrist and paw in the absence of Meox2. Additionally, other extensor tendons i.e. carpi radialis longus and carpi radialis brevis remained completely invisible (T7 and T8, Fig. 3.3.1B,C). Moreover, only the trails of the extensor digiti quarti/quinti tendons were present in the mutants (T9a and T9b, Fig. 3.3.1A,B,C,D). In addition, extensor pollicis (T5) and extensor carpi ulnaris tendon (T6) were detectable but thin and reduced in the size. In conclusion, the various levels of complexity in tendon defects could be responsible for the locked dorsal flexur in the forelimb.

Together, the *ScxGFP* expression in *Meox2* mutants demonstrated the major structural defects in the forelimb tendons whereby flexor tendons were more

affected than extensor tendons and hence the degree of severity in the tendon phenotype was concluded.

3.3.2 REDUCED *SCXGFP* SIGNAL FROM THE HINDLIMB TENDONS

The hindlimb tendons undergo similar tissue developmen and patterning compare to the forelimbs (Popesko et al., 2003). The serial homology between forelimb and hindlimb tendon tissue was recently uncovered and it was shown that the FDS tendon development in forelimb and the flexor digitorium brevis (FDB) tendons were developmentally delayed compared to the other tendon groups (Huang et al., 2013). Therefore, the absence of the FDS tendon from the forelimb in *Meox2* mutants prompted us to investigate FDB tendons. For this, hindlimb tendons were once again visualised using the *ScxGFP* marker. As predicted in the mutants, the FDB tendon was completely disrupted on the dorsal side as observed by loss of *ScxGFP* (Fig. 3.3.2A,B).

In control hindlimbs, the Achilles tendon, one of the major tendons of the hindlimb, exhibited bright *ScxGFP* fluorescence both dorsally and ventrally. However, the mutant mice exhibited greatly diminished GFP fluorescence from Achilles tendon and revealed that it was thinner (Fig. 3.3.2A,B,C and D). In fact, to acquire the images for comparing control and mutant tendons, we had to increase the exposure by four times for the mutant limbs. Additionally, the extensor digitorium longus (EDL) tendon was also completely missing (Fig. 3.3.2A,B,C and D).

Therefore, hindlimb tendons also showed reduced *ScxGFP* expression in the absence of *Meox2* suggesting an overall requirement of *Meox2* in the limb tendon development.

3.3.3 DISRUPTION OF AXIAL AND TAIL TENDONS

Tendons progenitor cells of the epaxial and hypaxial muscles are derived from the syndetome that are found in between two adjacent somites. Therefore, *ScxGFP* fluorescence was used to visualize tendons of axial musculature in this study.

The distinctive structure of epaxial tendon in a skinned *Meox2* heterozygous animal showed normal *ScxGFP* expression and fine long fibres of tendons were evident. However, the mutant counterparts displayed severe disruption of GFP fluorescence from trunk tendon cells (Fig. 3.3.3A and B, white arrows). Moreover, the loss of ScxGFP expression indicated intercostal tendons were completely lost (Fig. 3.3.3A and B, red arrowheads). Despite sharing a common origin with tendons of axial musculature in syndetome, the dramatic loss of tail tendons was evident in the absence of *Meox2* gene while the control littermates showed complete dorsal and ventral sides of long tail tendons (Fig. 3.3.6C and D). In contrast, annulus fibrosus ligament in the tail was recognised (Fig. 3.3.6C) and remained unaffected in the mutant tails (Fig. 3.3.6D).

In summary, the limb tendons as well as axial tendons at postnatal stage were had severe abnormalities in *ScxGFP* expression. Since, *ScxGFP* faithfully replicates the endogenous *Scx* expression from tendon cells; our data indicate defects in tendon development in *Meox2*$^{-/-}$ animals. The intercostal and tail tendons were completely lost. *Meox2* mutants did not exhibit any change in the cartilage and ligaments. This suggests a role of *Meox2* in tendon development independent of cartilage condensation both in the limbs and in trunk.

3.3.4 SEVERE FORELIMB AUTOPOD TENDON DEFECTS

Although *ScxGFP* is a useful tool to visualize whole tendon, still it fails to impart the important information associated with the morphology of the tendon tissue.

Therefore, we decided to analyse the tendon structure using haematoxylin and eosin staining of the forelimb sections at P0. The evaluation of morphology was carried out in the distal autopod (digit tendons) and proximal autopod (metacarpal tendons), which has revealed significant tendon differences between controls and mutants tendon tissues (Fig. 3.3.4A'-D'). The FDS tendon was completely lost in the *Meox2* mutants along the proximal-distal axis of the forearm (T2 in Fig. 3.3.4A,A',B,B'). In contrast, only a remnant of the FDP was found (T1 in Fig. 3.3.4A,A',B,B'). The primary extensor tendon, EDC remained unaffected in the absence of *Meox2* (T3 in Fig. 3.3.4A,A',B,B'). Moreover, the proximal segment of the paw showed a more profound tendon phenotype in the *Meox2* mutants. The reduced mass of the other extensor tendons was also found, namely, extensor carpi radialis longus and extensor carpi radialis brevis (T7 and T8 in Fig. 3.3.4C,C',D,D'). Another two groups of extensor tendons, namely, extensor digiti quarti/quinti were reduced in size (T9a and T9b Fig 3.3.4B,B',C,C').

Furthermore, the flexor carpi radialis tendon was present as loose extensions in contrast to the compact round bundle in the heterozygous controls (T10Fig. 3.3.4C,C'). Notably, the fusion of interosseous muscle and lumbricals muscle occurred in the absence of *Meox2* (Fig.3.3.4B,B', blue arrowheads, blue arrows). There was also a significant disruption of the superficial paw muscles i.e. thenar muscles and hypothenar muscles (Fig.3.3.4D,D', yellow arrowheads, yellow arrows). However, the collateral ligament metacarphophalangeal joint (MCP) and transverse carpal ligament were unaffected in the mutants (Fig.3.3.4A,A',D,D', pink arrowheads).

Collectively, it is apparent from the autopod histology that in *Meox2*$^{-/-}$ animals, flexor digitorum superficialis (FDS) tendon in the forelimb was lost and other tendons that were present showed abnormal histology. In addition, the muscles were disorganised but the bone and ligaments were normal.

3.3.5 DEFECTIVE FORELIMB ZEUGOPOD TENDONS

Depiction of the major zeugopod tendons in the histological examination along the proximo-distal axis revealed significant differences in the heterozygous control and homozygous mutant forearm (Fig.3.3.5A-D and A'-D'). The forelimb bones, radius and ulna remained unaffected in the zeugopod. The FDS tendon (T2 Fig.3.3.5A-D and A'-D') was not present throughout the zeugopod in mutants indicating complete failure of the FDS tendon morphogenesis in the absence of *Meox2*. Furthermore, only the remnants of FDP tendon mass was present in the mutants (T1 in Fig.3.3.5A-D and A'-D'). In controls, a major extensor tendon, EDC crosses over the entire length of the zeugopod as four tendon bundles and they travel along with another tendon called extensor indicis proprius (T3, T4 in Fig.3.3.5A-D) within a common sheath. Conversely, in *Meox2*$^{-/-}$ forelimb zeugopod, the fusion of EDC tendon bundles was evident throughout the sets of the sections and a considerable loss of extensor indicis proprius was observed (T3, T4 Fig.3.3.5A'-D'). We found the abnormal muscle fibres replacing the regions of EDC and indicis proprius tendon tissues in the mutant sections (Fig.3.3.5C,C',D,D'). The majority of the other extensor tendons, namely, carpi ulnaris (T6) and pollicis (T5) were also small and disorganised. Furthermore, significant reduction in the tendons mass and fusion of two separate but closely associated extensor tendons i.e. carpi radialis longus and carpi radialis brevis (T7 and T8 in Fig.3.3.5A-D and A'-D') was clearly observed. While, the extensor digiti quarti/quinti remained as two separate tendon bundles in the control, in the mutants both tendons were fused into one small tissue mass (T9a and T9b in Fig.3.3.5A-D and A'-D'). Interestingly, the dislocation of palmaris longus tendon was found in the mutants (T12 Fig.3.3.5C, C', D and D'). For instance, in controls palmaris longus tendon was located between flexor carpi radialis and flexor carpi ulnaris (T10, T12, T11 Fig.3.3.5C,D). While the equivalent mutant zeugopod section showed presence of a small palmaris longus tendon tissue at a different location (T10, T12 Fig.3.3.5C',D'). Noticeably, the flexor carpi radialis tendon showed loosely organised tendon fibres in the mutants in contrast to the tight compaction found in controls (T10 Fig.3.3.5A-D and A'-D'). Finally, flexor carpi

ulnaris (T11) which is adjacent to the palmaris longus (T12) in controls was missing in the absence of *Meox2* in (Fig.3.3.5A-D and A'-D').

In conclusion, the tendon phenotype in zeugopod was more dramatic than autopod with almost all tendon groups (flexors and extensors) severely affected. This suggests that *Meox2* contribute to the normal zeugopod tendon formation and or maintenance of tendon cells during embryonic genesis of tendons.

3.3.6 IRREGULAR FASCIA IN THE PROXIMAL FORELIMB ZEUGOPOD

Fascia is a form of the connective tissues that are derived from undifferentiated mesenchymal cells. They form a layer of fibrous tissue which envelopes and separates different muscle groups (Benjamin and Ralphs, 1998). The fascia in the proximal sections of the forelimb zeugopod in heterozygous controls and homozygous mutants showed multiple differences. The well-defined separation of individual muscle groups into the compartments by fascia was evident in the controls, whereas, the intermixing of abnormal muscles resulted and the defective fascia in the mutants was observed (Fig.3.3.6A-C'). For example, the fascia of FDP tendon was present as thick sheets separating FDP and FDS muscles in the controls (Fig.3.3.6A,B,C, black arrowhead). On the contrary, the fascia in the mutants were severely redundant resulting in intermingling of loosely organised muscle fibres (Fig.3.3.6A', B' and C'). In *Meox2* mutants, tendon tissues were replaced by abnormal muscle fibres (Fig.3.3.6A, A'). The individuated tendon bundles of EDC was present in controls whereas only residues were found in the mutants (T3 Fig.3.3.6A, B, A',B'). Other extensor tendons i.e. pollicis, carpi radialis longus and carpi radialis brevis (T5, T7 and T8 in Fig.3.3.6A, B, A' and B') were abnormal and more compact in the more proximal zeugopod.

Therefore, it can be proposed that *Meox2* is required for the proper formation of fascia. At post-natal stage, more proximally, the failure of fascia development in

the absence of *Meox2* could be responsible for the muscle and tendon abnormality.

3.3.7 DEFECTIVE HINDLIMB AUTOPOD TENDONS

To understand the tendon defects inside the hindlimb autopod, we obtained the serial cross sections from the paw region and counter stained for studying tissue histology of major hindlimb tendons. We found major morphological modifications of the hindlimb tendons in the absence of *Meox2* similar to those in the forelimbs. In controls, the cup-like structure of FDB tissue surrounding another tendon group called flexor digitorium longus (FDL) was present (T14 and T18 in Fig 3.3.7A,C,E). Conversely, the disappearance of a major flexor tendon known as flexor digitorium brevis (FDB) due to *Meox2* mutation was obvious (T14 in Fig 3.3.7 A-F). In addition to the complete loss of FDB, there was reduction in the FDL tendon mass due to the *Meox2* mutation (T18 Fig.3.3.7B,D,F). Another flexor tendon known as flexor hallucis longus was highly reduced in size compared to the controls neonates (Fig.3.3.7A-F, black arrowhead). Interestingly, the extensor digitorium longus (EDL) tendon remained unaffected in the mutants (Fig.3.3.7A-F black arrows). Moreover, the lumbrical muscle defects in the hindlimb showed defective muscle patterning similar to that in the forelimb (Fig.3.3.7A-F yellow arrowheads).

Taken together, it is evident that *Meox2*$^{-/-}$ mutant animals show remarkable degrees of abnormalities in limb tendons. The *ScxGFP* and histology data demonstrated the complete loss FDB tendon tissue and suggesting an important requirement of *Meox2* in the normal patterning and growth.

3.3.8 DISRUPTED ACHILLES TENDON AND FASCIA IN THE ZEUGOPOD OF HINDLIMB

The histological analysis further confirmed the tendon defects in the zeugopod segment of the hindlimb. A sharp decrease in the size of Achilles tendon was identified in the mutant that corresponds to the highly reduced *ScxGFP*

fluorescence from this tendon cells (T13 in Fig 3.3.8 A,B). Moreover, only a fragment of flexor digitorium longus was found in the mutants in comparison to the thick tendon mass in controls (T18 in Fig.3.3.8 A,B). The extensor hallucis longus tendon was also found to be severely reduced in size (T17 in Fig.3.3.8 A,B). In addition, defects in the fascia were evident in the more proximal section (Fig.3.3.8 C,D, black arrows).

Therefore, similar to the forelimbs, overall defects in the hindlimb tendon resulted in *Meox2*$^{-/-}$ animals. Interestingly, in both appendicular musculatures, cells of fascia were disorganised.

3.3.9 INTERCOSTAL MUSCLES ARE NORMAL IN *MEOX2*$^{-/-}$ NEONATES

Using tissue histology for muscles, we found normal epaxial and hypaxial muscles in the absence of *Meox2* gene function. These muscle groups were examined on the thin sections obtained from trunk of control and mutants embryos (Fig. 3.3.9 A and B). The muscle morphology and fiber arrangement remained unaltered in all muscles on the sections.

Hence, the overall hypaxial muscles in the trunk that includes intercostal and abdominal wall along with epaxial muscles that encompasses right serratus anterior muscles were normal.

3.4. Discussion

Our detailed analysis on the role of *Meox2* in tendon morphogenesis provided a new insight in understanding genetic control of tendon development. Although *Meox2*$^{-/-}$ animals are viable, the severe tendon defects were found in addition to the reported muscle defects. A detailed investigation of the phenotype was performed at a neo-natal stage. The histological analysis of all tendon tissues in the limb from post-natal mice revealed that these tissues were abnormal and disorganised. *ScxGFP* expression from the tendon cells showed *Meox2* mutant mice display an overall impaired tendon structure including failure in the formation of correct shape and size. Altogether, the axial and limb tendon defects in our mutant mice model, once again, featured the structural and molecular divergence in the relatively unexplored complex tissue like tendons.

Gross appendicular tendon defect in the absence of *Meox2*

In order to visualize the whole limb tendons in the *Meox2* null mice, we utilized the *ScxGFP* transgene. The fluorescent signals from this transgene revealed thinner tendons at all levels in the mutant limb. In agreement with the histological analysis, some subsets of tendons were completely missing e.g. extensor digiti quarti/quinti and an extensive loss of GFP signal from EDC tendon on the dorsoventral aspects of the forelimb. Furthermore, the *ScxGFP* analysis in the hindlimb showed complete loss of FDB tendon and only small tissue mass of Achilles tendon.

We further investigated this profound limb tendon malformation by histological examination in *Meox2*$^{-/-}$ mice. The most dramatic aspect of this mutation was a complete loss of tendons, FDS in the forelimb and FDB in the hindlimb. The

developmental pathway of this tendon groups are unique compare to other limb tendons. The data from previous studies has shown that while the pattern and position of all other tendons was established by E14.5, the induction of FDS and FDB tendon cells initiates at this stage and mature form is only acquired at E16.5. (Huang et al., 2013; Pryce et al., 2009). Our data indicate complete failure of FDS and FDB tendon formation suggesting a role of *Meox2* during late induction and maturation of these tendon groups in the forelimb and hindlimb. Moreover, Huang and co-workers show that FDS and FDB tendons share similar anatomical features based upon their position in the limbs, the only difference in tendon patterning steps is FDS tendon extends from distal to proximal axis in the forelimb, and then translocation occurs into the zeugopod that acts as the final location. In contrast, FDB tendon cells originate and differentiate within the hindlimb autopod. In agreement with this, our data conclude that the failure in formation of FDS and FDB confirm the requirement of *Meox2* transcription factor in the developmental machinery for both tendon groups. In $Scx^{-/-}$ mutants, FDS tendons was absent in the digits and metacarpal level indicating an exclusive requirement of the *Scx* gene in the FDS tendon formation (Huang et al., 2013; Murchison et al., 2007). Despite sharing anatomical homology between FDS and FDB, in $Scx^{-/-}$ mutants, there is no analysis available on developmental effects *Scx* mutation on FDB tendons. Therefore, to date in our knowledge, *Meox2* is the only known transcription factor that is critical for FDB tendon formation in hindlimb. We can conclude that in addition to *Scx*, *Meox2* is also an important molecular regulator of FDS tendon development.

Another major flexor tendon in forelimbs i.e. FDP, though present, was rudimentary. This observation is consistent with $Scx^{-/-}$ mutants, in which FDP tendons were smaller (Murchison et al., 2007). A recent lineage tracing analysis using $Six2^{CreERT2}$ deleter along with *Rosa-TdTomato* Cre reporter showed the co-expression of $Six2^{+}$ and $ScxGFP^{+}$ cells in the autopod FDP tendons (Huang et al., 2015b). However, the zeugopod segment for FDP only expressed *ScxGFP*. Thereby, separate groups of progenitor cells in the autopod and zeugopod to form FDP was concluded. Interestingly, in the absence of *Meox2*,

both of these FDP tendon progenitors in the autopod and zeugopod are affected.

Huang et al. (2015) have also shown that the cartilage is necessary and sufficient for the formation of normal FDS tendons in the autopod. The distal formation of FDS tendon in the autopod is dependent on the cues from the metacarpophalangeal (MCP) joint whereas the proximal development in the zeugopod is dependent on the FDS muscles. Notably, *Meox2*$^{-/-}$ mutants showed the regular bilateral symmetry of the MCP joint despite the loss of FDS digit tendon. The normal chondrocyte differentiation due to *Meox2* mutation could not explain the complete loss of FDS tendons in distal segments of the digit. This indicates that in addition to the cartilage, a distinct but concurrent signal dependent on *Meox2* is also required for normal FDS tendon formation.

Moreover, the proximal stretch of FDS tendon anlage was also absent. During late development of FDS muscles, the shifting of differentiated muscle fibres from the autopod towards zeugopod takes place by retraction at distal end that is attached to FDS tendon and proximal elongation once inside the zeugopod (Huang et al., 2013). The same study showed that in *Scx*$^{-/-}$ mutant embryos, there was a complete loss of distal retraction and restricted proximal elongation of FDS muscle. Conversely, *Mdg* embryos in which muscle paralysis occurred due to a mutation in voltage-gated calcium channels, there was a defective FDS muscle retraction and translocation along the proximodistal axis. Thereby, authors concluded that a coordinated response from the FDS tendon at distal end is necessary for the FDS muscle contractility. Previously, it was shown that Meox2$^{-/-}$ mice exhibit disrupted FDS muscle in the proximal zeugopod (Mankoo et al., 1999). Our data on the complete loss of FDS tendon explain the disruption FDS muscles and thereby indicates a crucial role of *Meox2* in the formation of FDS muscle-tendon unit.

Closer examination of histology sections demonstrated that the EDC tendon was present in the autopod but reduced in size and like controls, were found as individual units on the top of each digit. Conversely, the EDC tendons inside the zeugopod showed a dramatic phenotype. The anatomical position of EDC

tendon tissue is known to present on the dorsal side of the forearm and is the key tendon on the dorsal aspect of the paw. As individual bands, each EDC tendon subunit fans out from the digits and passes through the compartment formed by the extensor retinaculum and radius, after which they reach the origins at the lateral epicondyle of the humerus. Other subsets of extensor tendon groups along the proximodistal axis i.e. extensor digiti quarti/quinti were fused into a highly reduced tendon tissue in *Meox2*$^{-/-}$ animals. Moreover, the dislocation and fusion of the flexor carpi radialis longus tendon occurred in these animals with another extensor tendon groups i.e. carpi radialis longus and carpi radialis brevis within the zeugopod region. Recently, analogous observations were made where the fusion of tendon groups namely, EDC, extensor longus/brevis and extensor digiti quarti/quinti occurred due to muscle inactivity in the zeugopod (Huang et al., 2015b). Due to inactivation of *Pax3* gene, in *Splotch* embryos myoblast migration was disrupted. In these embryos, the autopod tendons were found normal, whereas, at the wrist level of zeugopod segment showed coalescence of the fused extensor tendons.

Similarly, the fusion of EDC tendon bundles and other extensor tendon groups, carpi radialis longus/brevis and digiti quarti/quinti was also found in the *Muscular dysgenesis* (*Mdg*) embryos at E16.5. The embryos of *Mdg* contains a mutation in voltage-gated calcium channels resulting in the paralysis of all muscles, although, the muscle patterning remained unaffected (Chaudhari, 1992; Huang et al., 2015b; Huang et al., 2013). Therefore, it could be reasoned that the zeugopod tendon phenotype in *Meox2* mutants is due to an extrinsic role of Meox2 gene from the muscle cells onto the zeugopod tendon morphogenesis. In addition, *Meox2* gene is critical for the modular development of extensor tendons at the wrist level. However, the exact mechanism to address this issue is described in the subsequent results chapter. A summary of comparison of the development of major flexor and extensor tendons in the absence of *Meox2*$^{-/-}$ mutants with the *Scx*$^{-/-}$, *Sp*^{d}, *Mdg* and *Sox5*$^{-/-}$*; Sox6*$^{-/-}$ mutants are listed in table 3.3 and 3.4. For instance, in the absence of *Meox2* and *Scx*, FDP tendon cells showed similar defective phenotype in the digits whereas the paralysis of muscle in *Mdg* embryos or loss of cartilage in *Sox5*$^{-/-}$*; Sox6*$^{-/-}$ mutants does not affect FDP tendon development in digit autopod.

Conversely, the metacarpal location of FDP tendon cells showed severe abnormality in *Meox2*$^{-/-}$ and *Sp*^{d} but normal morphology was reported in *Scx*$^{-/-}$ and *Sox5*$^{-/-}$*; Sox6*$^{-/-}$ mutants. Moreover, the most remarkable tendon phenotype for FDS tissue was a complete loss throughout the proximodistal axis of the forearm due to loss of the *Meox2* gene. In contrast, rudiments of FDS tendon was present *Scx*$^{-/-}$ and *Sp*^{d} mutants. Majority of the extensor tendons showed tissue fusion in the transgenic mice with defective expression of *Meox2*, *Scx*, *and Pax3* or muscle inactivity. However, no defects of extensor tendons were observed in the proximal segment of the forearm in *Sox5*$^{-/-}$*; Sox6*$^{-/-}$ mutants.

Furthermore, previous work that evaluated the developmental requirement of *Meox2* by muscle cells also established disrupted forelimb flexor muscles namely, flexor digitorium profundus, flexor carpi ulnaris and flexor carpi radialis (Mankoo et al., 1999). Consistently, the data reported here, revealed the fusion of the interosseous and lumbricals muscles in the autopod of mutants. Additionally, the superficial paw muscles i.e. thenar and hypothenar were disarranged.

It has been shown that the cartilage cells express *Sox9* gene and are derived from limb mesenchyme (Suzuki and Kuroiwa, 2002). Recent studies revealed the presence of a unique population in the early mesenchyme that express both *Scx* and *Sox9* (Blitz et al., 2013; Sugimoto et al., 2013a). The divergent fates of generation of either cartilage primordia or tendon primordia are due to the extrinsic signals received by these early progenitors during subsequent differentiation and maturation stage of development in the limb (Schweitzer et al., 2001). The inductive factors for tendon progenitors could be either TGFβ signalling emanated from nearby cartilage or ectoderm derived Wnt signalling and repressed by BMP signalling from surrounding limb mesenchyme cells (Pryce et al., 2009; Yamamoto-Shiraishi and Kuroiwa, 2013;(Schweitzer et al., 2001). *Meox2* is expressed in the early limb mesenchyme at E10.5 where multipotent chondro-tendo progenitor population exists expressing both *Scx* and *Sox9*, therefore it would be useful to analyse the Sox9 expression (cartilage marker) in *Meox2*$^{-/-}$ mutants during embryonic stages. Analysis of this proposed experiment could provide a better understanding of the specific role of Meox2

only on *Scx*$^{+}$*/Sox9* and not *Scx*$^{+}$*/Sox9*$^{+}$ progenitor cells. Extrapolation of the results would direct us to explain the normal cartilage but defective tendon formation in *Meox2*$^{-/-}$ animals at birth. Together, we conclude that *Meox2* plays a significant and dual role in the tendon and muscle development.

Meox2 is necessary for the intercostal and tail tendon at P0

A pioneer study in chick using Scleraxis as a marker for tendon cells exposed details of axial and tail tendon development (Schweitzer et al., 2001). In both groups of tissue, the progenitors are derived from the compartment of somite called syndetome as opposed to the limb tendons whose developmental origins are limb bud mesenchyme. The robustness of *ScxGFP* fluorescence from all tendon cells offered a tool to characterise the morphological consequences of the *Meox2* mutation on the axial and tail tendons. Similar to our limb analysis, the whole mount *ScxGFP* expression in the *Meox2* deficient mice showed an extensive loss of axial tendon. We could not able to detect any *ScxGFP* expression from the intercostal tendons in the *Meox2* mutants. This tendon connects the adjacent ribs and assists in joining the intercostal muscles to the ribs. In *Scx*$^{-/-}$ mutant embryos, the intercostal tendon layer remained unaffected, however, all force-transmitting and intermuscular tendons connecting two muscles throughout the body were abnormal (Murchison et al., 2007). To our knowledge, the data presented in this thesis provide the first evidence for a requirement of specific transcription factor for the intercostal tendon development. Interestingly, our histological analysis showed normal intercostal muscles in the mutants that could explain the viability of these animals despite absence of tendon layer in the thorax.

The substantial loss of tail tendons in *Meox2* mutants was evident due to the absence of *ScxGFP* signal from long tendons in the tails. However, the highly organised ligament of tail tendon, annulus fibrosus, remained unaffected due to *Meox2* mutation. The role of this ligament is to connect the adjacent vertebrae. The cells in the annulus fibrosus contain collagen fibres that are arranged

perpendicularly to the tendons and display criss-cross pattern. This observation is similar to the tail tendon phenotype of *Scx*$^{-/-}$ mutants (Murchison et al., 2007). It is not yet clear how exactly the *Meox2* dependent cues in these anatomical similar tissues (axial and tail tendons) led to discrete outcome and hence, elucidating the exact mechanism needs further investigation. *Meox2* and *Scx* genes might be functioning independently or in a complementary manner for the proper formation of tail tendons. Evidence from data shown in this study suggests that the *Meox2* dependent signals are necessary for the post-natal tendon growth and maintenance. Interestingly, *TGFβ2* mutant mice also show loss of all axial and tail tendons due to failure in the maintenance and recruitment of tendon progenitors by TGFβ signalling during embryonic stages (Pryce et al., 2009). Additionally, an analogous phenotype was reported in *Scx*$^{-/-}$ mice that showed severe disruption of the force-transmitting from the trunk (Murchison et al., 2007). A plausible explanation of the comparable phenotype in all these mutants could be the requirement of a cross talk of these molecular regulators during normal tendon development. For instance, complete loss of *ScxGFP* expression from trunk tendons in *TGFβ2*$^{-/-}$*; TGFβ3*$^{-/-}$ mutant mice was reported. Additionally, TGFβ signalling acts as a potent inducer of *Scx* in both cell culture and organ culture. Besides, this study showed that TGFβ signalling regulates *Scx* expression during key stages of tendon morphogenesis (Pryce et al., 2009). Likewise, in future, it would be interesting to observe if Meox2 could directly regulate Scx and or regulating TGFβ signalling pathway to execute its function for the normal tendon development.

Furthermore, changes in the collagen fibril growth and extracellular matrix (ECM) deposition towards the end of embryogenesis are the hallmark of post-natal tendon growth. It includes further accumulation of the collagen matrix and maturation of collagen proteins. Recently, the *Mohawk* gene was shown to be involved in the tendon cell differentiation and maturation stage in addition to the *Scx* (Anderson et al., 2006; Ito et al., 2010; Liu et al., 2010). While the defects in collagen matrix in the absence of *Mkx*$^{-/-}$ mice is appeared only after birth, the embryonic genesis of tendon is normal, highlighting the differences in the embryonic and post-natal tendon morphogenesis (Liu et al., 2010). Interestingly, *Scx*$^{-/-}$ mice show a less and disorganised collagen matrix towards the end of

embryogenesis (Murchison et al., 2007). A unique role of *Scx* in regulating cardiac fibroblast was shown via its DNA-binding mechanism in promoting collagen 1α2 expression (Espira et al., 2009). This suggests an important function of *Scx* in regulating ECM proteins. Moreover, *in situ* analysis show *Mkx* expression in tendons and surrounding cells and therefore authors concluded that *Scx* could be considered as the key embryonic regulator of collagen proteins whereas *Mkx* determines the postnatal maturation and growth of these matrix proteins (Liu et al., 2010; Ito et al., 2010).

Furthermore, the reduction in overall tendon size and defective collagen matrix is also observed in a transgenic mice deficient of the *Egr*1 transcription factor (Guerquin et al., 2013). Although *Scx* expression along with collagen protein expression is relatively normal in the absence of *Egr1*, fragile tendons are evident after birth and mutant mice show a modest tendon phenotype. The importance of *Egr* gene in tendon biology is emphasised due to its capacity to convert the mesenchymal stem cells into tenogenic cells *in vitro* (Liu et al., 2015). Moreover, GDF6/BMP13 and GDF5/ BMP14 deficiencies in mice are associated with altered compositional, ultrastructural, and mechanical properties of tendons (Mikic et al., 2009).

Prior to the discovery of *Scx*, a type II transmembrane glycoprotein, Tenomodulin (Tnmd) served as faithful marker for the tendon cells (Shukunami et al., 2001). *Tnmd*$^{-/-}$ mutant mice show no tendon defects during embryonic stages and only a small reduction in tenocyte proliferation and tenocyte density was observed in tendon cells after birth (Docheva et al., 2005). However, it can still be considered, as an ideal marker for later stages of tendon development due to exclusive expression and is known to be positively regulated by *Scx* (Shukunami et al., 2006). Myostatin/GDF8 knockout mice show defects in muscle integrity and performance, and evidence indicates this is exacerbated by increased tendon stiffness (Mendias et al., 2008). The spatiotemporal expression of Myostatin during development, in conjunction with the observation that tendon fibroblasts continue to express both the Myostatin and receptors into adulthood and that *Scx* is a direct downstream target of Myostatin

signalling, strongly suggest that Myostatin plays a role in both the prenatal and postnatal development and regulation of tendons.

A hallmark of tendon differentiation after birth include expression of several proteins in the collagen matrix of tendon fibres, namely, type I collagen, biglycan, decorin, fibromodulin, fibrillin 2, lumican and tenomodulin (Ansorge et al., 2009; Birk and Mayne, 1997; Birk et al., 1989; Boregowda et al., 2008; Elliott and Crawford, 1965; Trelstad et al., 1983). Evidence suggests that these proteins have key role in tendon differentiation, however, tendon induction and maturation remained normal in the absence of any of these proteins. For instance, mice double deficient for the Small Leucine Rich Proteoglycans (SLRPs) Biglycan and Fibromodulin show disruption in disturbed collagen fibril structures of tendons, with reduced stiffness (Young et al., 2002). Similarly, Lumican and Fibromoulin double mutants have defects in tendon integrity (Jepsen et al., 2002). Loss of Biglycan and Fibromodulin also impairs tendon formation in vivo by disrupting BMP signalling in the stem cell niche of TSPCs (Bi et al., 2007). So far, this is the only knockout model where a defect in tendon integrity has been linked to abnormalities in tendon stem cell function. Fibrillin2 is located in the pericellular matrix of interior tenocytes, and knockout mice have decreased collagen cross-linking of tendons (Boregowda et al., 2008). Mutations in Fibrillin2 result in muscle weakness and regenerative myopathy, a likely consequence of connective tissue abnormalities (Miller et al., 2010).

3.5. Conclusion

We finally conclude that our evidence represents the first demonstration of a requirement of *Meox2* for normal tendon genesis in axial and appendicular tissue. The summary of the phenotype is tabulated in table 3.1 and 3.2 for the forelimbs and hindlimbs respectively. This provide, to our knowledge, the first direct evidence of a role *Meox2* in the important and often neglected complex tissue i.e. tendon. Moreover, the detailed characterization reported for all individual tendons could provide a direction for the future studies to understand a diverse role of *Meox2* in tendon morphogenesis. However, further

investigation is needed to understand whether the failure of tendon formation is an outcome of deteriorated tendon morphogenesis during the embryonic stages. Therefore, the experimental observations in next chapter focus embryonic stages of tendon development.

Meox2 is an important regulator of tendon development in axial and appendicular tissue. The tendon phenotype in zeugopod was more profound than the autopod segment demonstrating a unique regional role of *Meox2* in the modular limb tendon morphogenesis. Furthermore, our analyses from mutant mice highlighted the loss of FDS in the forelimb and FDB tendons from the hindlimb and hence, an exclusive role of *Meox2* in these anatomically similar tendons can be concluded. Interestingly, there was no discernible defect in cartilage and ligaments of *Meox2*$^{-/-}$ null mice. Together, *Meox2* is a key component of the cellular mechanisms that govern growth and maturation of highly disparate tissue i.e. tendons.

Table 3.1: Summary of the defects in the forelimb tendon in *Meox2*$^{-/-}$ animal

	TENDON CLASSIFICATION	LOST	ABNORMAL
	Flexors		
Autopod	Flexor digitorum profundus (FDP) T1		✓ Reduced size
Autopod	Flexor digitorum superficialis (FDS) T2	✓	
Zeugopod	Flexor carpi radialis T10		✓ Reduced size
Zeugopod	Flexor carpi ulnaris T11	✓	
Zeugopod	Palmaris longus T12		✓ Dislocated
	Extensors		
Autopod and Zeugopod	Extensor digitorum communis (EDC) T3		✓ a)Normal in autopod b) Fusion of individual bundles and reduced size in zeugopod
Zeugopod	Extensor Indicis Proprius T4	✓	
Zeugopod	Extensor pollicis T5		✓ Dislocation and fusion with carpi radialis longus/brevis tendons
Zeugopod	Extensor carpi ulnaris T6	✓	
Zeugopod	Extensor carpi radialis longus T7		✓ Fusion with carpi radialis longus/brevis tendons
Zeugopod	Extensor carpi radialis brevis T8		✓ Fusion with carpi radialis longus/brevis tendons
Zeugopod	Extensor digiti quarti/quinti T9a/T9b		✓ Fusion of both tendon groups and reduced size

Table 3.2: Summary of the defects in hindlimb tendons in the *Meox2*$^{-/-}$ animal

TENDON CLASSIFICATION	LOST	ABNORMAL
Flexors		
Flexor digitorum brevis (FDB) T14	✓	
Flexor digitorum longus(FDL) T18		✓ Reduced size
Extensors		✓
Extensor digitorum longus (EDL) T16		✓ Reduced size
Extensor hallucis longus tendon T17		✓ Reduced size
Achilles tendon T13		✓ Reduced size

Table 3.3: Summary of the flexor tendon phenotype in the various mouse models (Huang et al., 2015)

Tendons		*Meox2*$^{-/-}$	*Scx*$^{-/-}$	*Sp*^{d}	*Mdg*	*Sox5*$^{-/-}$; *Sox6*$^{-/-}$
Flexor digitorum profundus (FDP)	Digits	Reduced	Reduced	Normal	Normal	Normal
	Metacarpal	Reduced	Normal	Lost	Normal	Normal
	Zeugopod	Reduced	?	?	?	?
Flexor digitorum superficialis (FDS)	Digits	Lost	Reduced	Reduced	Reduced	Lost
	Metacarpal	Lost	Reduced	Lost	Reduced	Present
	Zeugopod	Lost	Reduced	Lost	?	?

Table 3.4: Summary of the extensor tendon phenotype in the various mouse models (Huang et al.,2015)

Tendons		Meox2-/-	Scx-/-	Sp^d	Mdg	Sox5-/-; Sox6-/-
Extensor digitorum communis (EDC)	Digits Metacarpal: Zeugopod	Normal Lost Fused	Reduced Lost Fused	Reduced Lost Fused	Reduced Reduced ?	Lost Normal Normal
Extensor carpi ulnaris	Zeugopod	Lost	?	Lost	?	?
Extensor carpi radialis longus	Zeugopod	Fused	Fused	Fused	Fused	?
Extensor digiti quarti/quinti	Zeugopod	Fused	Fused	Fused	Fused	?

Nomenclature of tendons in *Meox2*$^{+/-}$ and *Meox2*$^{-/-}$ neonates and embryos

No.	Tendon classification
T1	Flexor digitorum profundus (FDP)
T2	Flexor digitorum superficialis (FDS)
T3	Extensor digitorum communis (EDC)
T4	Extensor Indicis Proprius
T5	Extensor pollicis
T6	Extensor carpi ulnaris
T7	Extensor carpi radialis longus
T8	Extensor carpi radialis brevis
T9a	Extensor digiti quarti
T9b	Extensor digiti quinti
T10	Flexor carpi radialis
T11	Flexor carpi ulnaris
T12	Palmaris longus
T13	Achillies tendon
T14	Flexor digitorum brevis (FDB)
T15	Peroneous longus brevis
T16	Extensor digitorum longus
T17	Extensor hallucis longus tendon
T18	Flexor digitorum longus(FDL)

Fig 3.3.1 Decreased ScleraxisGFP expression from the forelimb tendons in Meox2 null neonates

The heterozygous and homozygous alleles for Meox2 were maintained on a ScxGFP transgenic background. Whole-mount view of ScleraxisGFP in the heterozygous and homozygous forelimb dorsal (A and B) and ventral (C and D) confirmed the limb tendon abnormality. Numerical tendon assignments are tabulated in Table 2. Marked decrease in the GFP levels can be seen in mutant forelimbs and absence of extensor digiti quarti/quanti subsets of tendons (T9a and T9b) in the mutant zeugopod. Scale bar=50um

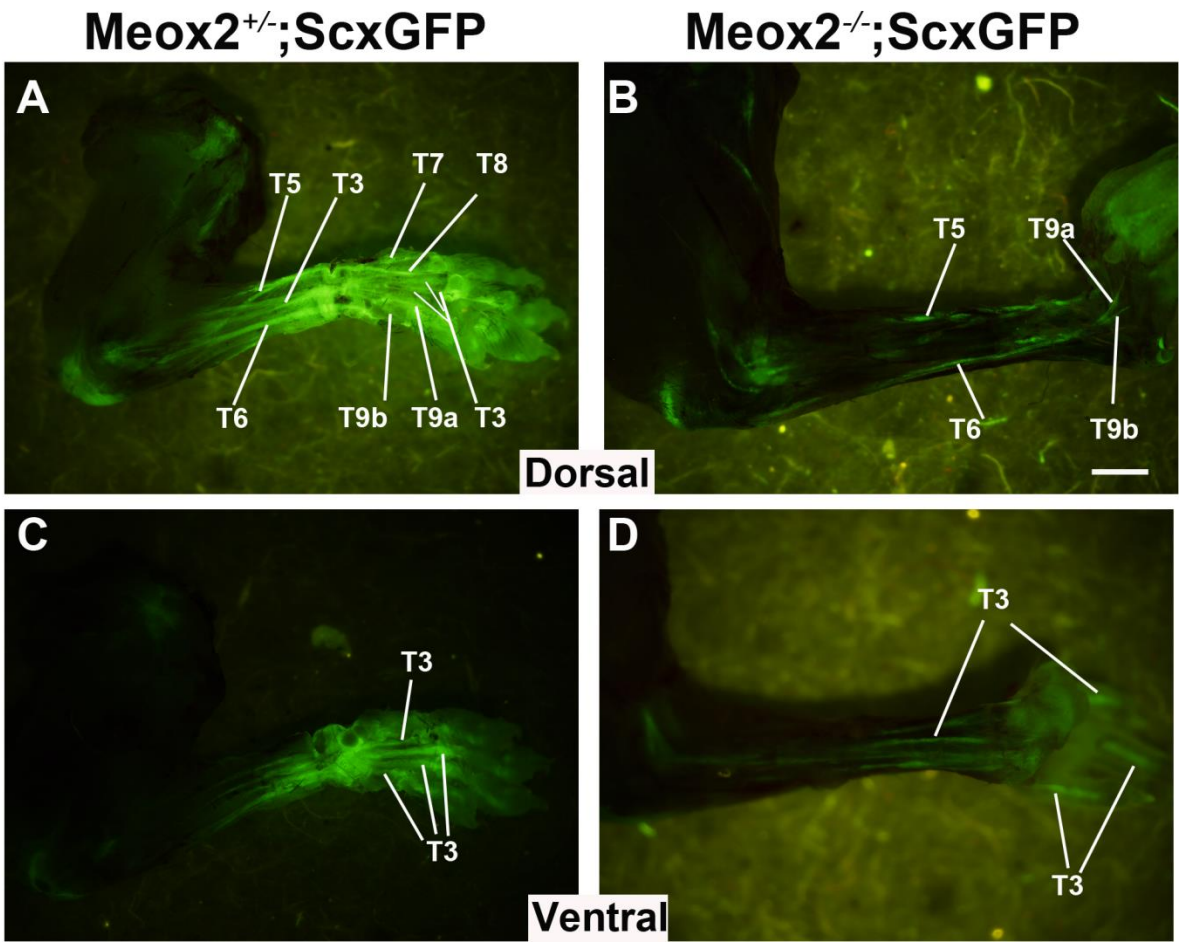
Meox2+/-;ScxGFP
Meox2-/-;ScxGFP
A
T5
T3
T7
T8
T6
T9b
T9a
T3
B
T5
T9a
T6
T9b
Dorsal
C
T3
T3
D
T3
T3
Ventral

Fig 3.3.2 Absence of major hindlimb tendons in Meox2 null neonates

The heterozygous and homozygous alleles for Meox2 were maintained on a ScxGFP transgenic background. Whole-mount view of *ScleraxisGFP* was compared in the dorsal and ventral aspects of heterozygous (A, C) and homozygous (A and B) and ventral (C and D). The tendon names are as follow:; (EDL) , (EHL), (PLB) and *achilles tendon* (AT). The apparent reduction in an overall GFP expression from hindlimb tendons can be seen.

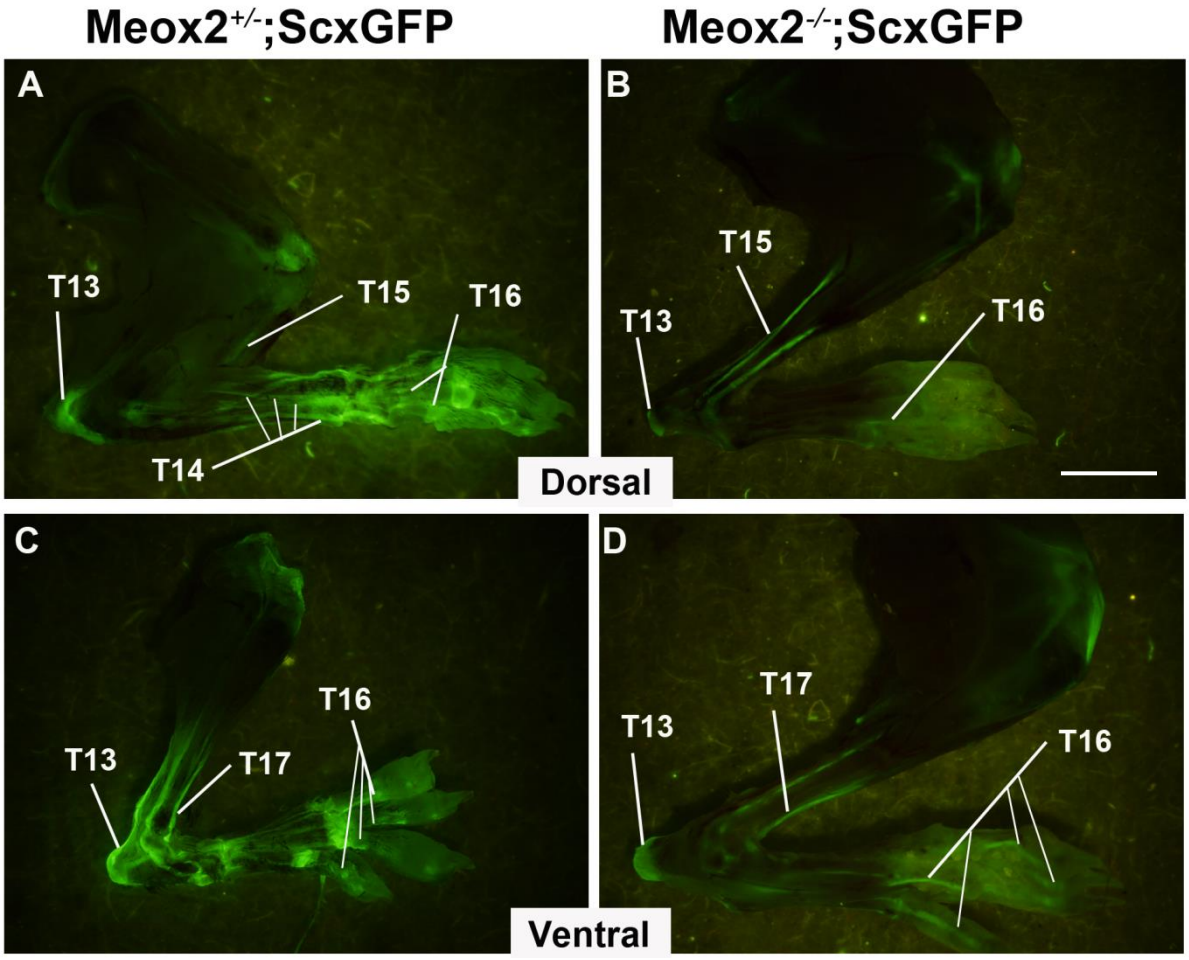
Meox2+/-;ScxGFP
Meox2-/-;ScxGFP
A
B
T13
T15
T16
T14
T15
T13
T16
Dorsal
C
D
T16
T13
T17
T17
T13
T16
Ventral

Fig 3.3.3 Axial and tail tendons showed diminished ScxGFP expression in the absence of Meox2 at neonatal stage

Axial and limb tendons of Meox2 heterozygous and homozygous littermates are directly visualized in skinned tissue using ScxGFP transgenic reporter. Axial tendons (A and B) showed significant reduction in GFP levels. The intercostal tendons were completely lost as shown by red arrowheads. In contrast, all tail tendons (C and D) are lost in mutants as shown by white arrows. White arrowhead indicates unaffected ligaments in the tail. Scale bars=100um

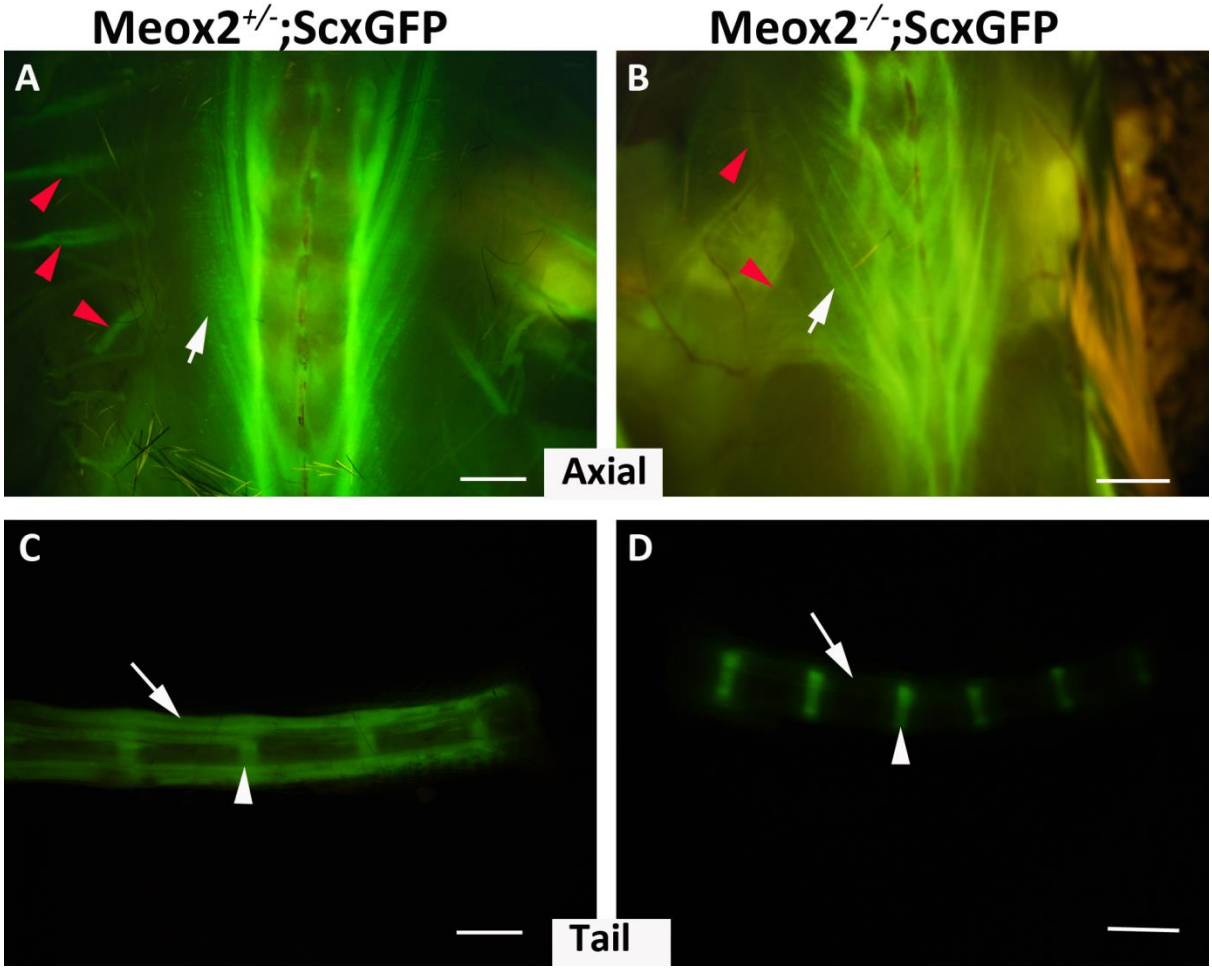
Meox2+/-;ScxGFP
Meox2-/-;ScxGFP
A
B
Axial
C
D
Tail

Fig 3.3.4 Forelimb autopod of *Meox2*$^{-/-}$ neonates showed tendon deformities

Sequential transverse sections of a forelimb autopod stained for Haematoxylin & eosin from a heterozygous control (A, B, C and D) and Meox2 homozygous (A', B', C' and D'). Tendon classifications are shown with black numerals except Flexor digitorium superficialis (FDS, T2) in red for its absence in the mutants. The nomenclature is described in Table 1. Majority of other tendons are reduced in size in mutants e.g. Flexor digitorium profundus (T1), extensor digiti quarti/quanti subsets of tendons (T9a and T9b). Red arrowheads indicate FDS tendon, Pink arrowheads indicate collateral ligament metacarphophalangeal joint (MCP), blue arrows head indicate interosseous muscle , blue arrows indicate lumbricals muscle, yellow arrowhead show thenar muscle , yellow arrow show hypothenar muscle and white arrow indicates transverse carpal ligament. Scale bars= 100um.

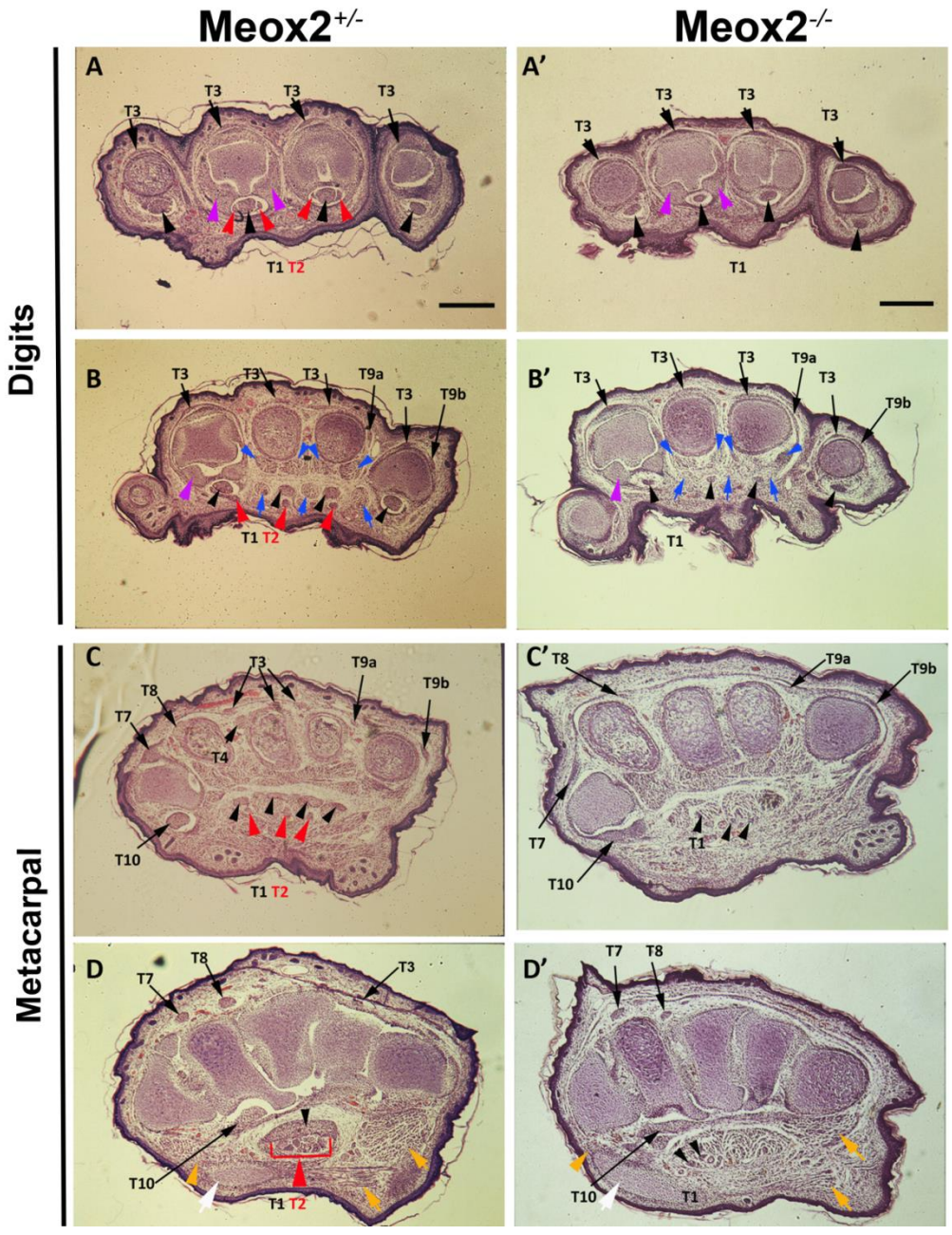
Meox2+/-
Meox2-/-
Digits
Metacarpal
A
A'
B
B'
C
C'
D
D'
T1 T2
T3
T4
T7
T8
T9a
T9b
T10

Fig 3.3.5 Reduction of zeugopod tendon mass in Meox2-/- postnatal mice

Transverse sections through the zeugopod of heterozygous control (A, B, C and D) and Meox2 mutant (A', B', C' and D') at P0. Haematoxylin & eosin staining show abnormality in tendon histology in *Meox2* mutants including severe reduction in tendon mass and tendon fusion. Tendon classifications are shown with black numerals. Notice the absence of FDs tendons (T2 in red) the mutant zeugopod. Tendon classification as shown with black numerals is named in Table 2. Red arrowheads indicate missing FDP tendon. Scale bars=100um

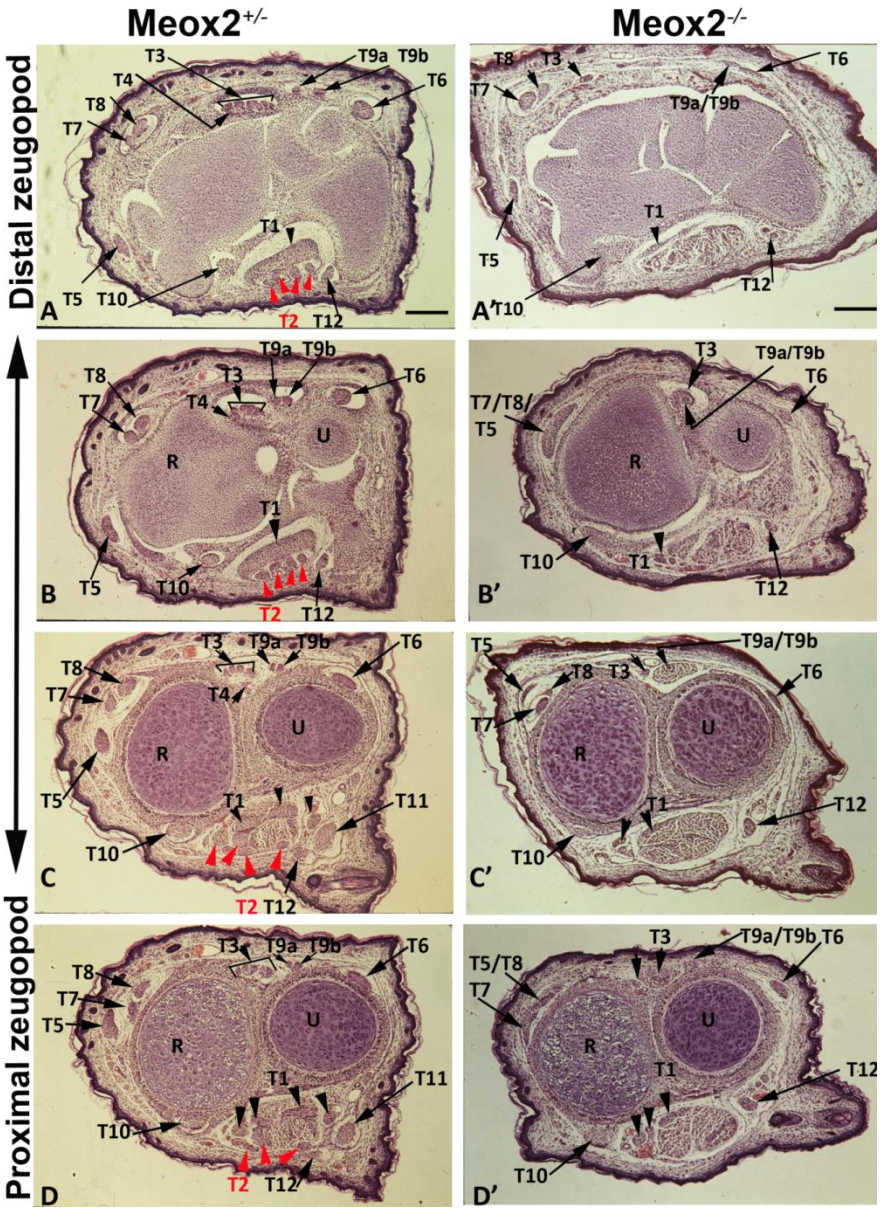
Meox2+/-
Meox2-/-
Distal zeugopod
Proximal zeugopod
A
A'
B
B'
C
C'
D
D'
T1
T2
T3
T4
T5
T6
T7
T8
T9a
T9b
T9a/T9b
T10
T11
T12
T5/T8
T7/T8/
R
U

Fig 3.3.6 Irregular fascia in the forelimb zeugopod of Meox2 mutants

Transverse sections through the forearm of the heterozygous control (A, B, C and D) and Meox2 mutant (A', B', C' and D') at P0. Haematoxylin & eosin staining show drastic reduction of the thick fascia at the wrist level which includes several extensor and flexor tendons. Blue arrow shows *m. flexor digitorium profundus*; blue arrowheads show *m. flexor digitorium sublimis* and red arrowheads indicate *t. flexor digitorium sublimis.* Notably, in the absence of Meox2, defective fascia was observed in the majority of tendon-muscle attachment. Tendon classification as shown with black numerals is named in Table 2.

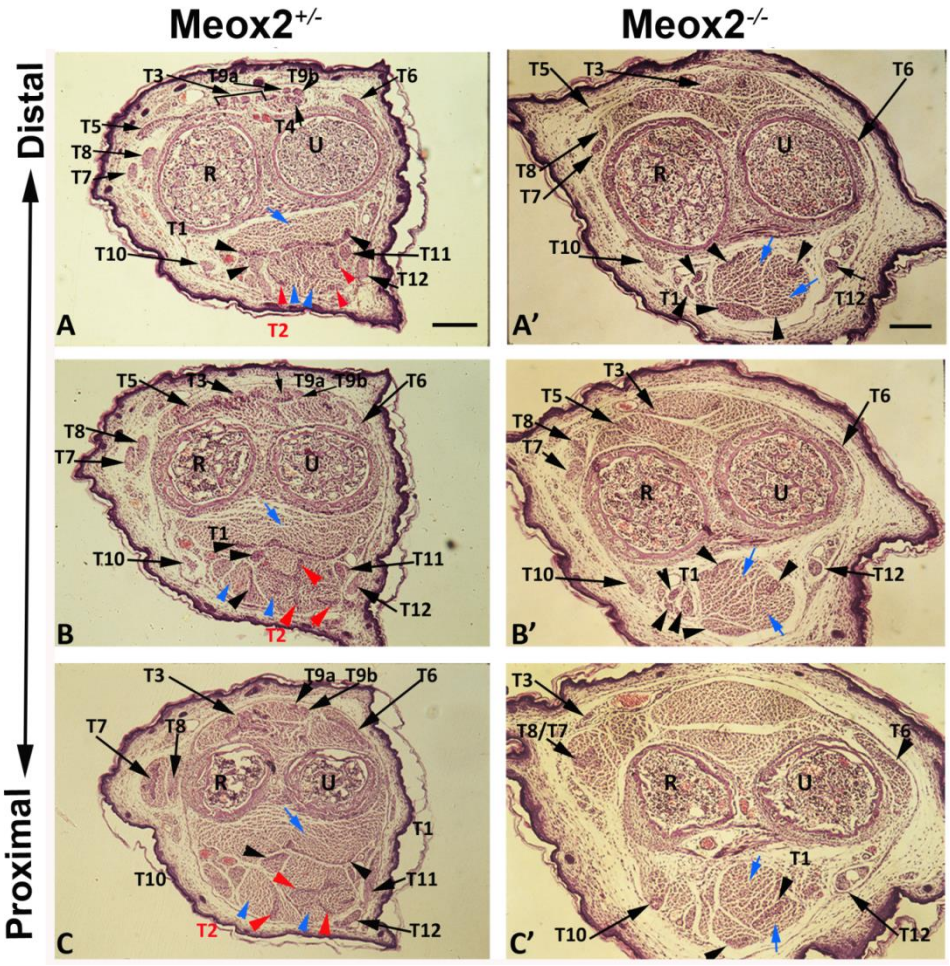
Meox2+/-
Meox2-/-
Distal
Proximal
T3
T9a
T9b
T6
T5
T4
T8
T7
R
U
T1
T10
T11
T12
T2
A
A'
B
B'
C
C'
T8/T7

Fig 3.3.7 Hindlimb autopod showed severe tendon defects

Sequential transverse sections of a hindlimb autopod stained for Haematoxylin & eosin from a heterozygous control (A, C, E) and Meox2 homozygous (B, D, F). Tendons are shown by arrow and classifications are as follow: red arrowhead indicate *flexor digitorum brevis* (FDB), blue arrowhead show *flexor digitorum longus* (FDL), black arrow head indicate *flexor hallucis longus* tendon and black arrows assign *extensor digitorum longus* tendons. The meta-tarsal joint is shown by yellow arrowhead and lumbricals muscle indicated by yellow arrowhead. FDB tendons, a serial homologues of FDS tendon in the forelimb found missing in the $Meox2^{-/-}$ mutants. Scale bars= 100um.

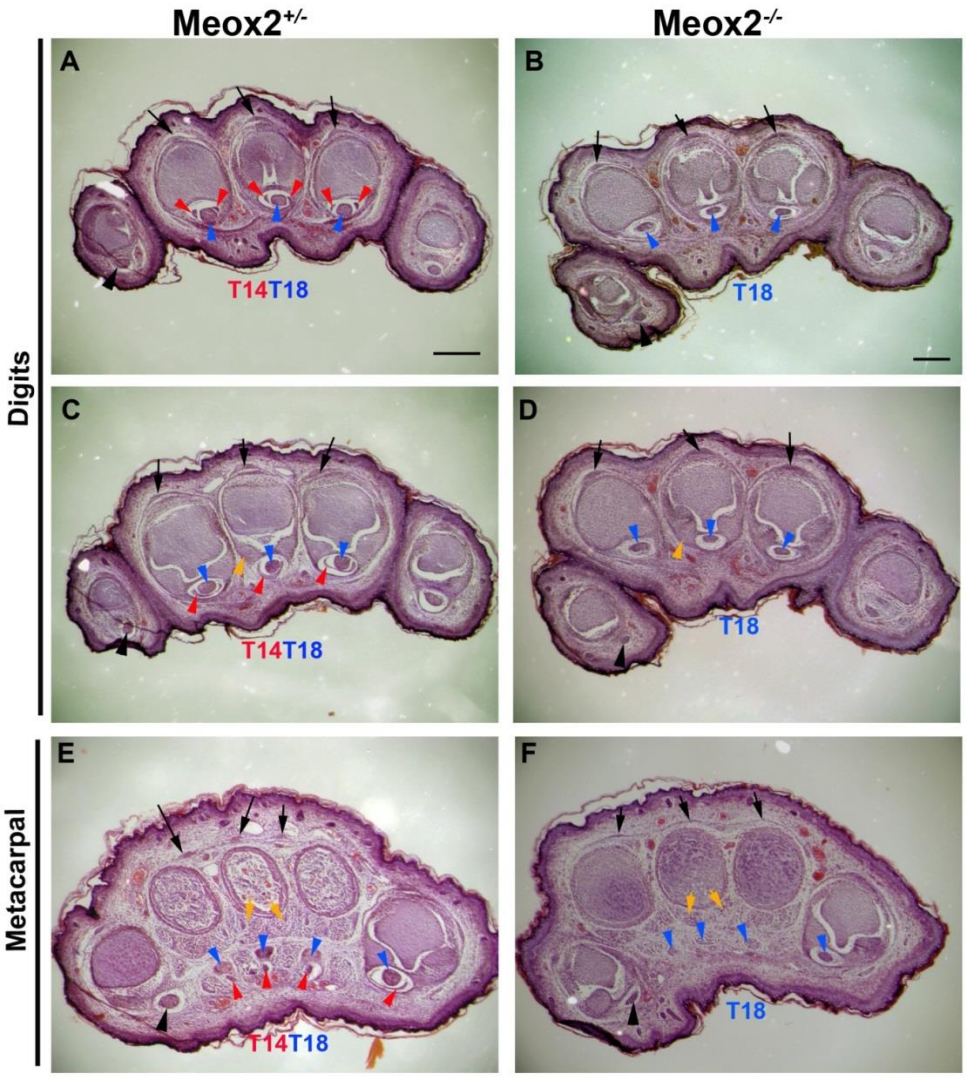
Meox2+/-
Meox2-/-
A
B
C
D
E
F
T14T18
T18
T14T18
T18
T14T18
T18
Digits
Metacarpal

Fig 3.3.8 Abnormal zeugopod tendon mass and defective fascia in the hindlimb

Transverse sections through the zeugopod of heterozygous control (A, C) and Meox2 mutant (B, D) at P0. Haematoxylin & eosin staining show abnormality in the tendon histology including severe reduction in tendon mass and loss of fascia. The zeugopod bones are t, tibia and f, fibula. Individual tendon and muscles indicated by numbers:; 5, *m*, *extensor digitorum longus*; 6, *m. biceps femoris*; 7, *m. soleus*. Black arrowheads indicate fascia separating the muscle compartments in the proximal end of zeugopod. Considerable loss of thick fascia is evident in the mutant hindlimb. Scale bar=100um.

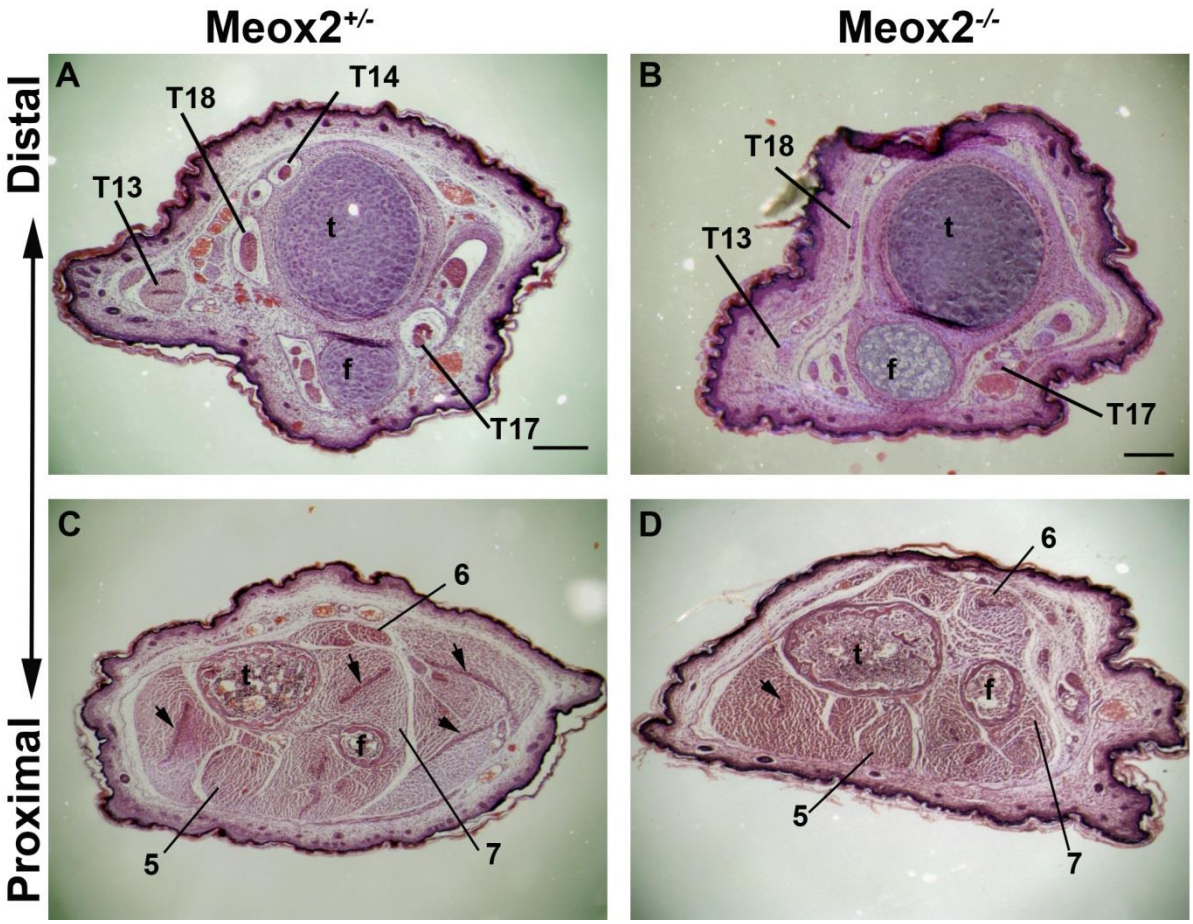
Meox2+/-
Meox2-/-
Distal
Proximal
A
B
C
D
T18
T14
T13
T17
t
f
6
5
7

Fig 3.3.9 Normal intercostal muscles in the *Meox2* null neonates

Transverse sections through the trunk of heterozygous control (A) and Meox2 mutant (B) at P0. Haematoxylin & eosin staining show normal epaxial muscle i.e. *right serratus anterior muscles* shown by yellow arrows and hypaxial muscles i.e. *intercostal muscle* (external and internal layers) shown by black arrows. The brown fact overlying the shoulder muscles were also normal as shown by white arrows. H, heart; Sc, spinal cord; C, cartilage primordium. Scale bar=100μm.

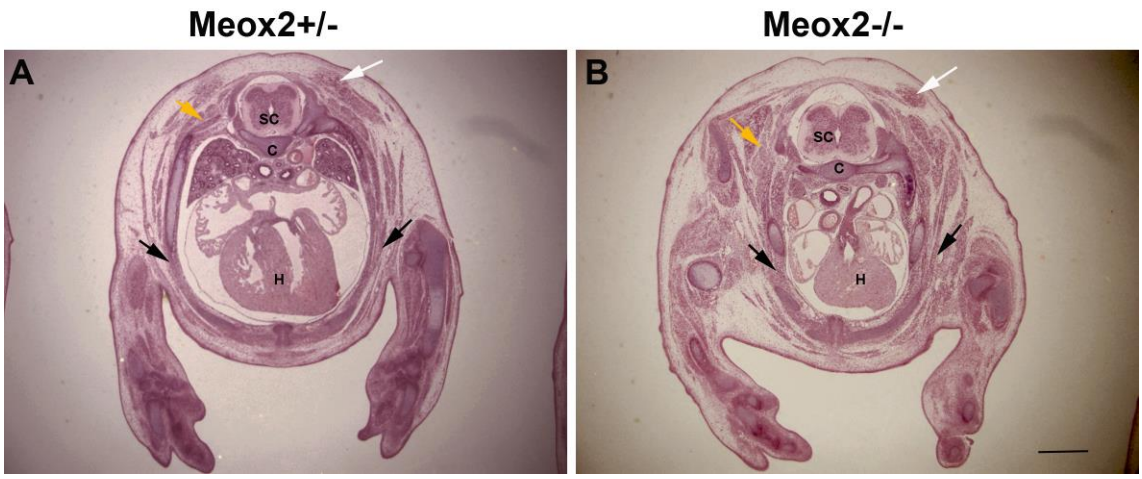
Meox2+/-
Meox2-/-
A
B
SC
C
H
SC
C
H

Chapter 4

Embryonic tendon defects in the absence of *Meox2*

4.1 Introduction

Vertebrate tendon development is multistep processes that include three stages in modular fashion: a) induction of tendon progenitors b) recruitment and organisation c) aggregation and differentiation of these tendon precursors. In mouse, the initial induction of committed tendon progenitor cells occurs in somite and limb mesenchyme between E10.5-11.5 and in somites that is associated with FGF signalling (Edom-Vovard et al., 2002; Eloy-Trinquet et al., 2009). At this stage, the limb bud progression occurs from the proximal to the distal axis and *Scx* expression is found in dorsal and ventral sub-ectoderm patches (Murchison et al., 2007; Schweitzer et al., 2001). By E12.5, a loose cellular organisation of tendon progenitors and muscle connective tissue occurs throughout the body between differentiating muscles and cartilage tissue. This phase of limb tendon development is dependent on TGFβ signals emanating from the skeletal elements and muscles, which contributes towards recruiting more tendon progenitors at the site of condensation. Additionally, TGFβ signals emitted from the induced tendon progenitors are involved to maintain the tenoblastic identity of the committed progenitors and are recruiting more committed precursors to undergo tendon cell fate at E12.5 (Pryce et al., 2009). Finally, in some tendon groups, the differentiation and aggregation from E13.5 depends on the presence of muscles (Bonnin et al., 2005; Edom-Vovard and Duprez, 2004; Eloy-Trinquet et al., 2009; Kardon, 1998; Schweitzer et al., 2001). *Scx*, which is expressed in all tendon progenitors, plays an essential role as molecular regulator for tendon cell differentiation in force-transmitting tendons (Murchison et al., 2007).

Tendon progenitor cells from E14.5 onwards are also known as tenocytes and are fibroblast-like characteristics that form the mature tendons. These tenocytes are capable of synthesizing the extra-cellular matrix including the assembly of early collagen fibres, which acts as fundamental units of a mature tendon. From E14.5, onwards tendon growth occurs and is a tightly regulated balance

between collagen fibrillogenesis and cellular processes that package the collagen fibrils into a higher order structure forms.
Recent evidence indicates that tendon development in the autopod and zeugopod is modular (Huang et al., 2015b), whereby the autopod progenitors are induced and organised in the developing digits (Schweitzer et al., 2001). Interestingly, the zeugopod tendon cells are induced near the presumptive wrist and then extend proximally to form various tendon groups (Huang et al., 2015b). While the axial tendon progenitor induction occurs in the somite under the influence of FGF signalling, the subsequent stages are then assumed similar to the limb tendon development. (Brent et al., 2003; Brent and Tabin, 2002; Schweitzer et al., 2001; Schweitzer et al., 2010).

In the previous chapter, we established that *Meox2* mutant mice display a neonatal tendon phenotype. This indicated a primary defect in embryonic or foetal stages of tendon development, which could be in induction (E11.5), organisation (E12.0-12.5), maturation (E13.5), or maintenance (E14.5 onwards). To identify when the primary defect occurs, we closely monitored the entire embryonic stages that are relevant to axial and appendicular tendon development. We performed analysis starting from E11.5 (induction of tendon progenitors) until E14.5 (mature tendon formation) in *Meox2*$^{-/-}$ embryos. From this, we also aimed to suggest if Meox2 has a role in the developmental modularity by comparing defects in the autopod and zeugopod segments in our mutant model.

4.2 Aim

The tendon progenitor cells were identified by expression of the *ScxGFP* transgene and whole mount in situ hybridization detected *Scx* mRNA expression in the *Meox2* heterozygous controls and homozygous mutants during the key tendon developmental stages starting from induction at E11.5 until maturation and growth stage at E14.5.

4.3 Results

4.3.1 NORMAL TENDON CELL INDUCTION AT E11.5

The induction of tendon progenitors in the axial and appendicular regions occurs at E11.5 (Schweitzer et al., 2001). To determine if there is a requirement for *Meox2* at this stage we performed *Scx* whole-mount in situ hybridization at E11.5 (Fig. 4.3.1). We found normal tendon progenitor distribution in the syndetome that is present in intersomitic region of mutant embryos (Fig. 4.3.1A-D, yellow arrows). When analysed at higher magnification, the proximal sclerotome showed orderly strips of *Scx* expressing cells in both controls and mutants (Fig. 4.3.1C-D, yellow arrows). The *Scx* positive committed tendon progenitors were also normally induced in the mesodermal cells residing in the limb bud (Fig. 4.3.1A-B, red arrows).

Therefore, we conclude that the induction of tendon precursors in trunk and limbs at embryonic stage 11.5 does not depend on *Meox2* gene activity.

4.3.2 FAILURE OF INITIAL ALIGNMENT OF TENDON CELLS IN FORELIMB AT E12.0

The expression analysis of *Scx* at E12.0 shows that tendon cells are aligned and distributed evenly on the proximomedial axis and beneath surface ectoderm of growing limb bud (Schweitzer et al., 2001). We observed a significant loss of *Scx* expression using whole mount in situ hybridisation on the dorsal and ventral sides of the forelimb at E12.0 (Fig 4.3.2A-D). These included a reduction in the anterior and posterior domains in the presumptive autopod and zeugopod. The substantial loss of a chevron-shaped *Scx* domain was observed in the medial region of zeugopod (Fig 4.3.2A,B, yellow arrows).

Moreover, the ventral side of the limb showed severely reduced *Scx* expressing tendon progenitor cells indicating defective positioning of induced tendon progenitor cells at their functional site in the limbs (Fig. 4.2C, D).
Furthermore, the control and mutant hindlimbs showed a similar expression of *Scx* transcripts that were present as a small patch of tendon progenitors on the dorsal side (Fig 4.3.2E-H). However, there was a small reduction of *Scx* mRNA on the ventral aspects of the hindlimb (Fig 4.3.2E-H, yellow arrows).

Together, our results indicate that the first tendon phenotype is at E12.0 in the forelimb of *Meox2*$^{-/-}$ embryos, and suggests *Meox2* is necessary for the normal resolution of the initial alignment of tendon progenitors in the limbs. The hindlimbs are developmentally delayed by half a day, and this may reflect the absence of severe phenotype in the hindlimbs at this stage.

4.3.3 LOSS OF FORELIMB LIMB TENDONS AT E12.5

Having established a failure of tendon cell alignment at E12.5 in the absence of *Meox2*, we asked does the phenotype persist in the forelimb after half a day. To answer this, we next examined *Scx* expression at E12.5, the stage when tendon progenitors undergo expansion and reorganisation between the skeletal elements i.e. muscle and cartilage (Murchison et al., 2007; Pryce et al., 2009). To determine whether *Meox2* is involved in these events, whole mount *in situ* hybridisation of *Scx* was performed in the control and *Meox2*$^{-/-}$ mutant limbs. The results showed a sequential loss of tendon precursors at E12.5 (Fig. 4.3.3A-C').

The degree of disruption for *Scx* expression domains varied in the presumptive zeugopod and autopod. For instance, the *Scx* expression was obvious in the autopod segment that gives rise to the distal digit tendons in heterozygous controls (Fig 4.3.3A, C, yellow arrowheads). In the mutants, a profound loss of *Scx* mRNA transcripts in the autopod tendon cells was noticeable (Fig 4.3.3B, D, yellow arrowheads).

Furthermore, despite the presence of *Scx* positive cells near the presumptive wrist of *Meox2*$^{-/-}$ forelimbs, overall levels of *Scx* expression were much reduced compared to the control limbs. Moreover, the arrangement of *Scx* positive domains in the zeugopod showed striking differences between the control and mutant limbs. The chevron-shaped *Scx* domain first observed to be completely missing at E12.0 was also absent at E12.5 in the absence of *Meox2* (Fig.4.3.3A, B and B', red arrowheads). There was also an overall reduction of *Scx* expression throughout the zeugopod in the dorsal and ventral aspects of the forelimbs (Fig.4.3.3A-D', yellow arrows).

Collectively, these observations indicate that in *Meox2*$^{-/-}$ mutants at E12.5 the tendon precursors failed to position correctly between the developing muscles and cartilage. Moreover, due to the loss of *Meox2* derived cues, the alignment, and integration of the functional musculoskeletal tendon tissue was defective at this stage.

4.3.4 LOSS OF HINDLIMB TENDON PROGENITOR CELLS AT E12.5

As hindlimbs are developmentally delayed by half a day with respect to forelimbs, and showed no abnormality at E12.0, we decided to analyse the *Scx* expression in the tendon progenitors of the hindlimb at E12.5. In *Meox2*$^{-/-}$, we found a more dramatic loss in the arrangement of tendon cells within presumptive zeugopod displayed on the dorsal and ventral aspects of the hindlimb (Fig. 4.3.4A-D, black arrows). There was also a decrease in Scx transcripts in the developing autopod of *Meox2*$^{-/-}$ mutant hindlimbs (Fig. 4.3.4A-D, black arrowheads).

Hence, the loss of tendon progenitors from the hindlimbs at E12.5 indicated a catastrophic outcome of an earlier breakdown during the stages in the alignment of tendon precursors.

4.3.5 AXIAL TENDON PROGENITORS ARE DISRUPTED IN *MEOX2*$^{-/-}$ AT E12.5

Our initial analysis of *Scx* mRNA expression in the trunk could not detect any significant changes at E12.0 and thus we analysed any axial tendon phenotype begin to emerge at E12.5. For this purpose, we took advantage of the *ScxGFP* transgene to analyse the distribution of tendon precursors in the control and mutant embryos (Fig. 4.3.5A, B). Using this tool, we found the GFP reporter expression in the dorsoventral regions of two adjacent somites in control embryos (Fig. 4.3.5A, white arrow). Additionally, control embryos also showed the expression of *ScxGFP* in the condensing mesenchyme (Fig. 4.3.5A, white arrowhead). In contrast, a profound reduction of GFP fluorescence from the condensing mesenchyme was evident in the *Meox2*$^{-/-}$ embryos (Fig. 4.3.5B, white arrowhead). There was also a widespread reduction of *ScxGFP* in the syndetome of the mutants (Fig. 4.3.5B, white arrow).

At E12.5, ScxGFP expression is comparable to the endogenous Scx expression only for axial tendon cells (Pryce et al., 2007). The reduction of the *Scx*GFP in the proximal sclerotome prompted us to evaluate this region using Scx gene expression by whole mount in situ hybridisation (Fig. 4.3.5C-H). In controls, *Scx* mRNA was detected in the vertebral bodies (Fig 4.3.5C, black arrowhead) and stripes of transcripts were found in the condensing mesenchyme of the proximal ribs that form from the posterior sclerotome (Fig. 4.3.5C, black arrowhead). The cartilaginous rib primordia are shown to express *Scx* and *Sox9* at high levels and hence are denoted as multipotent cells (Sugimoto et al., 2013a; Sugimoto et al., 2013b). The domains of *Scx* expression were markedly reduced in the somites of *Meox2*$^{-/-}$ embryos (Fig 4.3.5D, F, and H). The most dramatic reduction of *Scx* was seen in the regions of condensing mesenchyme in the posterior sclerotome that gives rise to the ribs and (Fig. 4.3.5H, black arrows). In addition, the *Scx* expression was lost in proximal regions of somites of the mutants near neural tube (Fig. 4.3.5H, black arrowhead).

Therefore, a tendon defects were first manifest in axial tissues, similar to that of hindlimbs, at E12.5, in contrast to the forelimbs where abnormalities in *Scx* expression were first detected at E12.0.

4.3.6 MODULARITY IN THE TENDON PHENOTYPE DUE TO THE *MEOX2* MUTATION

The classification of various tendon groups begins to emerge at E13.5. In *Meox2*$^{-/-}$ embryos, the examination of a cross section from autopod using ScxGFP transgene showed normal GFP expression and cellular arrangement when compared with a wild type section (Fig. 4.3.6A, B). Additionally, the two distinct condensed layers that form FDP tendon (Murchison et al., 2007) were found normal in *Meox2*$^{-/-}$ autopod at this stage (Fig. 4.3.6A, B, yellow arrowheads). This could explain the residual FDP found in the post-natal autopod of *Meox2*$^{-/-}$ animals (Result section 3.3.1). Moreover, the EDC tendon precursors also showed normal *ScxGFP* fluorescence and the alignment of cells on top of the digits (Fig. 4.3.6A, B, white arrows).

Furthermore, our observations of transverse sections from the proximal zeugopod segments at E13.5 showed significant differences in contrast to the normal *ScxGFP* expression from the proximal regions. The *ScxGFP* fluorescence from the identified tendons groups at this stage in zeugopod showed reduced signal in the mutants suggesting the presence of fewer tendon cells in these groups (Fig. 4.3.6C, D). *Meox2*$^{-/-}$ embryos showed fewer flexor digitorum profundus (FDP) tendon cells near the cartilage (T1 in Fig. 4.3.6C, D). Conversely, EDC tendon precursors were found normal (T3 in Fig. 4.3.6C, D). Additionally, a reduction in the condensation of tendon cell numbers for digiti quinti/quarti and pollicis were observed that could explain the abnormality of these tendon groups in postnatal mutant mice (T5, T9a and T9b in Fig. 4.3.6).

These results overall demonstrate that the autopod tendon individuation was not affected and normal FDP tendon cells anlagen were present at E13.5 even in the absence of *Meox2*. In addition, *Meox2* gene regulates some aspects of

zeugopod tendon condensation and maintenance. Therefore, we conclude the autopod and zeugopod modularity of the tendon phenotype begins to emerge at E13.5 in *Meox2*$^{-/-}$ mutant embryos.

4.3.7 DEFECTS IN TENDON CELL DIFFERENTIATION IN *MEOX2*$^{-/-}$ EMBRYOS

As *ScxGFP* analysis showed the beginning of modularity in tendon phenotype in autopod and zeugopod at E13.5, here we performed whole mount analysis of *Scx* mRNA along the proximal-distal axis of the developing limb. The *Scx* expression from the distal segments of the digit tendon cells was severely reduced in both dorsal and ventral sides of the limb in the *Meox2*$^{-/-}$ embryos (Fig. 4.3.7A-D, black arrows). Furthermore, in the hand plate of a heterozygous control limbs showed the wider expression of *Scx* in both dorsal and ventral aspects (Fig. 4.3.7A-D). The examination of the wrist region in a homozygous limb showed extended and disorganised domains of *Scx* expressing tendon cells (Fig. 4.3.7B, D, red arrowhead).

We conclude that the initial stages of the tendon cell condensation and differentiation were perturbed in the absence of *Meox2*. Thus the defective formation of load bearing tendons cells already existed at E13.5 in the *Meox2*$^{-/-}$ and there was an early irregularity of the tendon individualisation in the autopod and zeugopod of the *Meox2*$^{-/-}$ limbs resulting in defective long tendon formation.

4.3.8 LOSS OF *SCXGFP* EXPRESSION IN SOMITES AT E13.5

We evaluated *ScxGFP* expression in longitudinal sections obtained from the trunk of heterozygous controls and homozygous mutant embryos at E13.5 (Fig. 4.3.8A, B). In the somites of heterozygous control, strong *ScxGFP* expression was present at the junction between adjacent myotomes (Fig 4.3.8A). However, a considerable loss of *ScxGFP* expression from mutant somites was evident

(Fig 4.3.8B). Therefore, the failure of axial tendon cell condensation at E13.5 in the absence of *Meox2* could serve as plausible explanation for the post-natal tendon phenotype where all *ScxGFP* expression was disrupted.

4.3.9 FAILURE OF FORELIMB FLEXOR TENDON DIFFERENTIATION IN *MEOX2*$^{-/-}$ EMBRYO AT E14.5

By E14.5, the majority of the tendons in the limb have achieved their developmental maturity except FDS and FDB tendons. Tendon tissues from this stage onwards, while preserving their mature arrangement, only undergo growth and differentiation. In mouse, tendons that are associated with muscles are identifiable at this stage and can be considered as a miniature of the tendon of an adult animal. Therefore, we decided to evaluate the limb autopod tendons using the *ScxGFP* transgene to identify tendon cells. Myosin-heavy chain antibody was used to detect terminally differentiated muscles on the same sections. The deletion of *Meox2* led to the disruption of FDP tendons at the metacarpal level, which were severely disorganised, in contrast to the controls, which showed a tight compact arrangement of *ScxGFP*$^{+}$ tendon fibres in the FDP (T1 in Fig. 4.3.9A-F).

The failure of the cell condensation process in the presumptive wrist region at E13.5 could explain a profound *ScxGFP* loss at E14.5 (Fig. 4.3.9, white arrowhead). Although examination at lower magnification of EDC tendons showed slight differences in GFP levels between controls and mutants; higher magnification levels revealed the normal cell condensation for this tendon group in the autopod and therefore this explains the presence of normal EDC tendon morphology in the digits after birth (T3 in Fig. 4.3.9G-H; see chapter 3).

Furthermore, the staining for muscle fibres revealed mispatterend and loosely organised interosseous and lumbrical muscles in the palm (Fig. 4.3.9C and D, red arrowhead and red arrows). Cartilage formation in the mouse limbs is considered complete at E14.5 in all individual digits (Martin, 1990). When

analysed in *Meox2*$^{-/-}$, the individuation for cartilage formation in each digits was found normal at this stage (Fig. 4.3.9A-F).

Therefore, we conclude that there is continuous requirement of *Meox2* gene during embryonic tendon morphogenesis through to E14.5. The tendon defects seen at this stage are the outcome of earlier breakdown of tendon cell condensation.

4.3.10 DEFECTIVE ZEUGOPOD TENDON CELL DIFFERENTIATION IN *MEOX2*$^{-/-}$ EMBRYOS

Although rudimentary flexor tendons in the autopod were formed in the mutants when analysed using ScxGFP expression, these flexor tendons along with extensors in zeugopod were severely reduced in the mutants. Analysis of transverse sections through the zeugopod showed strong *ScxGFP* expression in the FDP tendons of the control limb (Fig. 4.3.10A). However, in distal sections of mutant zeugopod, *ScxGFP* expression was completely absent from the FDP tendon bundles (T1 in Fig. 4.3.10B). Interestingly, an even more striking phenotype was evident in a proximal zeugopod section where mispatterning of FDP tendon cells occurred in this segment of *Meox2*$^{-/-}$ embryos (Fig. 4.3.10C, D).

In contrast to the autopod, EDC tendon cells were loosely organised and muscle fibres replaced tendon cells, which could potentially explain the similar phenotype found at P0 (T3 in Fig. 4.3.10C, D; T3 in Fig. 3.3.6A, A'). At this level of section, the loss of other extensor tendons namely, carpi radialis brevis and carpi radialis longus was observed in *Meox2*$^{-/-}$ embryos (T7, T8 in Fig 4.3.10C, and D). Furthermore, a severe reduction in the size of extensor carpi ulnaris was noticeable that was lost completely at P0 (T6 in Fig 4.3.10C, D). Additionally, muscle patterning defects and splitting of muscle cells was also observed in the mutant zeugopod. The chondrification of the proximal limb elements was normal and resulted in the orderly formation of radius and ulna seen in the *Meox2*$^{-/-}$ embryos.

Together, these results demonstrate that *Meox2* regulates the tendons of the zeugopod segment and coordinates in muscle patterning at E14.5. Additionally, the differential outcome of *Meox2* mutation in the autopod and zeugopod was fully manifested by E14.5 since zeugopod tendons were profoundly affected then autopod tendons. It supports the notion of modularity in limb tendon development described by Huang et al., 2015.

4.3.11 DISRUPTED INTERCOSTAL MUSCLE/TENDON UNIT AT E14.5

The defects in the neonatal axial tendons prompted us to examine the organisation of trunk tendons at E14.5. The analysis of *ScxGFP* fluorescence from sagittal section of the trunk represented clear differences in the heterozygous and homozygous embryos. Consistent with the limb data, trunk tendon cells of control embryos showed strong *ScxGFP*$^{+}$ cells near the cartilage in the ribs and thereby assisting in the joining of the intercostal muscles to the ribs (Fig. 4.3.11A). Conversely, *ScxGFP* expression was completely lost from intercostal tendons in a homozygous mutant embryo (Fig. 4.3.11B). This observation explains with the loss of GFP^{+} cells from intercostal tendons in the *Meox2*$^{-/-}$ neonates (see chapter 3).

The intercostal muscles of control embryos appeared as highly organized in a meshwork of parallel muscle fibers divided in layers and formed muscle mass boundaries in between adjacent cartilages of the trunk (Fig. 4.3.11C, yellow arrows). However, in the *Meox2*$^{-/-}$ embryos, a sharp disruption of these muscles were observed (Fig. 4.3.11D, yellow arrows). Strikingly, the internal intercostal muscle that connect the two adjacent cartilages in the rib cage was completely missing in the mutants, whereas, other intercostal muscles layers showed loosely organised muscle fibres (Fig. 4.3.11D). Collectively, these observations indicate an exclusive role of *Meox2* expression in the development of intercostal muscle-tendon units at embryonic stages.

4.3.12 LOSS OF SKELETAL MUSCLE PROGENITORS REFLECTS THE ZEUGOPOD TENDON DEFECT AT E12.5

In previous findings, *Meox2*$^{-/-}$ embryos show a down regulation *Pax3*, which is expressed in somitic myogenic precursors that eventually populate the limb mesenchyme (Mankoo et al., 1999). The *Pax3* transcription factor is required for the myogenic progenitor cells to migrate into the limb bud mesenchyme (Goulding et al., 1994; Williams et al., 1994). *Meox2* is expressed by these muscle precursors when migrating from somite to limbs between E9.5-E10.5; however, it is down regulated soon after entering into limb territory (Mankoo et al., 1999). In addition, *Meox2* is also known to be upstream of *Pax3* in the genetic hierarchy and thereby to regulate limb skeletal muscle development (Bismuth and Relaix, 2010).

All this led us to investigate whether the limb tendon phenotype could be an indirect consequence of the *Meox2* activity due to defective migration of muscle cells. For this purpose, we utilized a *Sp*^{d} muscle-less embryo that has a mutation in the *Pax3* gene locus to examine *Scx* expression at E12.5. Consistent with a recent study, we found normal distribution of *Scx* transcripts in the presumptive autopod of both control and mutant forelimbs (Fig. 4.3.12A-D) (Huang et al., 2015b). However, in the zeugopod, the tendon progenitor cells that differentiate and form a chevron-shaped domains were severely reduced (Fig. 4.3.12A,B, yellow arrowhead) This specific tendon phenotype of the zeugopod was found to be similar to *Meox2*$^{-/-}$ forelimbs at E12.5 (Fig. 4.3.8). Although in absence of *Meox2*, this chevron-shaped domain remained invisible whereas loss of *Pax3* results in remnants of this *Scx* expressing domain in the zeugopod. Once again, our data showed the spatial relationship that exists between the diverse musculoskeletal tissues in these early stages.
Hence, we conclude that *Meox2* expressing cells could be acting indirectly via developing muscles to regulate the zeugopod tendon development during embryonic stages.

4.3.13 NORMAL CHONDROGENESIS IN *MEOX2*$^{-/-}$ AT E12.5

A recent study revealed the necessity of cartilage derived cues for autopod tendon development (Huang et al., 2015b). The authors showed that in the absence of Sox9, the autopod tendon cells were failed to form at E12.5, whereas, zeugopod tendon cells were properly aligned at their functional positions. Thereby, it was concluded that the cartilage cells are necessary and sufficient for autopod tendon induction. Moreover, it has been shown that during musculoskeletal development, at E12.5, a subpopulation of tendon progenitor cells express Scx and Sox9 in axial and appendicular regions (Sugimoto et al., 2013a; Sugimoto et al., 2013b). Specifically, in *ScxCre-H;Ai14;ScxGFP* at E12.5, the endogenous Scx and Sox9 expression was located in the cartilaginous rib primordia and intervertebral regions (Sugimoto et al., 2013a). Further analysis in this genetic model revealed overlapping expression domains of Scx and Sox9 also in the limb region.

We found that due to Meox2 mutation, there was complete loss of forelimb autopod tendons at E12.5, highly reduced Scx expression from the syndetome (Scx+/Sox9-) and diminished Scx regions in the proximal sclerotome (Scx+/Sox9+). Therefore, we aimed to evaluate the consequences of *Meox2* alteration on the cartilage cells labelled by Sox9, which could provide better explanation of tendon phenotype in Meox2-/- mutant embryos at E12.5. We performed *Sox9* whole mount in situ hybridisation on Meox2+/- heterozygous controls and Meox2-/- homozygous mutant embryos at E12.5. The patterns of *Sox9* expression were found indistinguishable between control and mutant embryos (Fig. 4.3.13A-D). In the limb buds at this stage, the *Sox9* transcripts were found normal in the cartilage primordia of the digits. Therefore, it seems that Meox2 dependent autopod tendon development is independent but parallel to the skeletal derived regulation for the tendon cells in this segment of the limb.

Furthermore, in axial regions, we found similar expression pattern in the vertebrae, ribs, cranial cartilage and tail tip vertebrae suggesting normal

progression of cartilage condensation even in the absence of *Meox2*. This could explain the presence of normal skeleton in the *Meox2*$^{-/-}$ newborn littermates (Mankoo et al., 1999). In conclusion, the data indicate that the process of chondrogenesis in the axial and appendicular tissues remained unaffected in the *Meox2*$^{-/-}$ embryos at E12.5 when there was a profound loss of *Scx*$^{+}$ tendon cells.

4.4 Discussion

In this study, we showed that the defects seen in *Meox2*$^{-/-}$ neonates are preceded by a dramatic loss of tendon progenitor cells during embryonic stages. In *Meox2*$^{-/-}$ mutant embryos, *Scleraxis* expressing tendon cells were induced normally at E11.5. However, the proliferative phase of tendon precursors was impaired. The earliest limb tendon phenotype was found in the forelimb at E12.0, the stage when committed tendon cells initiate to align between muscle and cartilage cells and at E12.5 for hindlimb and axial tendon tissues. Moreover, we found differential outcome of *Meox2* mutation on tendon development whereby a profound defect of all zeugopod tendons occurred in contrast to the autopod tendons. This observation is in agreement with the developmental modularity established for limb tendon morphogenesis. Further analysis of Meox2$^{-/-}$ mutant embryos revealed a sustained role of Meox2 in alignment and organisation (E12.5), maturation (E13.5), integration, and differentiation (E14.5) of tendon progenitor cells to form the musculoskeletal system. In somites, disruption of *Scx* expression occurred both in sclerotome (*Scx*$^{+}$/*Sox9*$^{+}$) and in the syndetome (*Scx*$^{+}$/*Sox9*$^{-}$). The intercostal muscle-tendon unit was severely affected where tendon layer connecting adjacent ribs were lost. We found normal cartilage formation that persisted through the embryogenesis.

Meox2 promotes organisation and alignment of tendon progenitor cells

Whole mount Scx expression analysis in *Meox2*$^{-/-}$ embryos indicates that tendon precursor cells are induced normally in the limb mesoderm and syndetome, and that *Meox2* plays an essential role in the maintenance of committed tendon precursors after the induction. In the absence of *Meox2*, a significant loss of *Scx* expression in the forelimbs of *Meox2*$^{-/-}$ embryos occurred from E12.0 onwards. The experimental data in this study using *Scx* labelled tendon precursors strongly indicate that *Meox2* is also required for the proper organisation and alignment of tendon cells. Interestingly, these tendon defects precede the tendon phenotype found in *Scx*$^{-/-}$ embryos where the tendon disruption was first apparent at E13.5 (Murchison et al., 2007).

Moreover, in *TGFβ2*$^{-/-}$*;TGFβ3*$^{-/-}$ and *TGFβ*RII embryos, the first indication of a tendon loss was seen at E12.5 and thereby demonstrated an absolute necessity of TGFβ signalling for the alignment of tendon primordia between the differentiating muscles and cartilage. Our observations suggest a dynamic role of *Meox2* in tendon genesis, which is upstream of *Scx* and presumably parallel or downstream to TGFβ signalling. Furthermore, *TGFβ2* signalling encompasses a second wave of tendon cell recruitment at E12.5 (Pryce et al., 2009). In line with this report, our data provide substantial evidence that supports the notion that along with TGFβ signalling, *Meox2* could also actively participate in maintaining the tenoblastic identity and recruitment of a second wave of committed progenitors. This alignment then begins to resolve into the tendon-like elements from E13.5 under the influence of *Scx* gene and the appropriate trajectories of all tendon groups found by E14.5. However, it is unclear at this point that whether *Meox2* and TGFβ signals act in a reciprocal fashion whereby *Meox2* synergies with TGFβ signals or *Meox2* stimulates TGFβ signals to produce a similar outcome on tendon development by maintaining the committed identity and incorporating more cells to form mature tendons.

Murchison and colleagues (2007) reported an important role of *Scx* function during tendon development. In *Scx*$^{-/-}$ mutant embryos the majority of the progenitors were lost by E13.5 and the rudimentary tendon cells that were, still present exposed their loosely organised mesenchyme identity as opposed to tight compaction of tendon cell mass found in control embryos. *Meox2* ablation led to very similar outcome in forelimb tendon differentiation with severe loss of autopod flexor tendon and a significant disruption of zeugopod tendons. The defective flexor tendons at metacarpal level show similar phenotype in *Meox2*$^{-/-}$ and *Scx*$^{-/-}$ embryos at E13.5. However, unlike *Scx*$^{-/-}$ mutant embryos, the extensor tendons in the forelimbs were normal in *Meox2*$^{-/-}$ mutant embryos. This demonstrates a divergent role of Meox2 in the extensor and flexor tendon formation. Notably, we found an overall complex phenotype at E13.5 along the proximodistal axis of the limb in three ways: first, the significant loss of all zeugopod tendons revealed by gross reduction in *ScxGFP* expression. Second, an unaffected autopod EDC tendon cell segment demonstrated by normal condensation of *ScxGFP*$^{+}$ cells. Third, reduction in the digit FDP tendons defined by reduced endogenous *Scx* in the distal autopod segment.

To gain a better understanding of Meox2 gene function, we also performed analysis on the hindlimbs of mutant embryos that are developmentally delayed by half a day. The hindlimb shares similar developmental sequences to that of the forelimb. The observations in a *Meox2*$^{-/-}$ mutant hindlimb found a reduction in *Scx* expression emphasising an overall failure of tendon development machinery that was visible at E12.5. In favour of limb tendon modularity during development (Huang et al., 2015b), our hindlimb data showed an apparent reduction in zeugopod than the autopod similar to autopod. This suggests that the tendon alignment disruption that was appeared in the forelimb at E12.5 could be a consequence of an even earlier defect during the transition from induction to the alignment stage of tendon progenitors, which is at E12.0.
Furthermore, the data presented here on axial tissues lends to support the hypothesis that *Meox2* is necessary for both axial and appendicular tendon development, at different anatomical locations. The syndetome is a sub compartment of sclerotome in which the *Scx*-expressing axial tendon progenitors are concentrated; in contrast to the appendicular tendon cells that

are induced from undifferentiated limb mesenchyme (Brent et al., 2003; Schweitzer et al., 2001). The reduction of axial tendon tissue marked by endogenous *Scx* expression and ScxGFP transgene due to *Meox2* loss-of-function from E12.5 onwards provided a conclusive evidence for the substantial role of Meox2 in overall tendon genesis. Moreover, a similar phenotype of tendon cells in axial musculature was also observed in $Scx^{-/-}$ embryos (Murchison et al., 2007). Similar to $Meox2^{-/-}$ embryos, $Scx^{-/-}$ embryos also displayed reduction in tendon cells at E13.5. Therefore, we can extrapolate that in addition to *Scx*, *Meox2* play a decisive role in axial tendon morphogenesis.

The multipotent progenitors for tendons and cartilage are initially intermixed in the somites and limbs (Brent et al., 2005; Sugimoto et al., 2013a; Sugimoto et al., 2013b). Interestingly, in somites, a mutual repression of cartilage forming sclerotome cells labelled by *Sox9* and promoting the tendon-forming *Scx* cells present in the syndetome is due to FGF signalling from adjacent myotome (Brent et al., 2005; Brent et al., 2003; Tozer and Duprez, 2005). Further evidence has shown an implication of TGFβ signalling during tendon induction, which promotes Scx^{+} cells to differentiate (Pryce et al., 2009). Sugimoto and co-workers (2013 a,b) more recently showed that the sclerotome is comprised of $Scx^{+}/Sox9^{+}$ cells whereas the syndetome has $Scx^{+}/Sox9^{-}$ cell population.

We found that in $Meox2^{-/-}$ mutant embryos, the severe loss of *Scx* expression in the sclerotome that could be from the loss of Scx^{+} in $Scx^{+}/Sox9^{+}$ multipotent cells. However, *Scx* expression was slightly reduced in the syndetome suggesting a milder effect of the *Meox2* mutation on $Scx^{+}/Sox9^{-}$ cell population. Our data of *ScxGFP* expression in somites demonstrate complete loss of GFP signals from the proximal sclerotome that reinforced our observation of complete loss of Scx^{+} only in $Scx^{+}/Sox9^{+}$ cell population. Normally, *Scx* expression can be found in the anterior and posterior somite borders (Brent et al., 2003). Previously, it was shown that *Meox2* expression is restricted to dermomyotome and sclerotome at stage 16 chick embryos (Reijntjes et al., 2007) and therefore, it might be possible that *Meox2* loss-of function targeted the Scx^{+} cells in the sclerotome. The syndetome expression though present was found to be severely reduced. Nevertheless, the extensive loss of *Scx*

transcripts in the somites represented a gross embryonic tendon defect due to *Meox2* ablation at E12.5.

The residual expression of *Scx* at E12.5 in *Meox2*$^{-/-}$ embryos suggests that *Meox2* is could be directly or indirectly regulating *Scx* expression and thereby commencing the tendon phenotype. The analysis to understand the expression domains of *Meox2* and *Scx* during the formation of a mature tendon segments in the autopod and zeugopod are investigated in the next chapter.

Meox2 specifies condensation and differentiation of tendon cells

By E14.5, the tendons and muscles appear as a miniature of mature musculoskeletal system (Pryce et al., 2009). Although some features e.g. FDS and FDB tendon units are incomplete and the final development of these tissues are achieved by E16.5 (Huang et al., 2013). Our results suggest the disorganised tendon cell-condensation and differentiation due to *Meox2* mutation at E14.5 in the forelimbs. This could be a most likely explanation of the tendon phenotype in the *Meox2*$^{-/-}$ mutant new-borns. It emphasizes the continuous requirement of *Meox2* gene in the later stages of tendon development. In the autopod segment, *ScxGFP* expression showed that despite defect in both tendon categories, flexor tendons were more affected than extensor tendons. An essential function of *Meox2* was also evident for the zeugopod tendons since we found a severe reduction of *ScxGFP* expression in all tendon cells. Consequently, we propose that a unique cue from *Meox2*$^{+}$ cells is necessary alongside the muscle cells for normal zeugopod tendon development (Huang et al., 2015b). Additionally, loose fibers of interosseous and lumbrical muscles in the palm was evident, highlighting, a pivotal role of *Meox2* in muscle and tendon development during embryonic stage.

Similar to the limb tendons, we also found defects in the axial tendons at E14.5, despite anatomical differences between both tendon categories. In the absence of *Meox2* derived clues, the intercostal muscle-tendon unit were severely

affected. The absence of tendon layer from this unit during embryogenesis explains the complete loss in neonates (chapter 3). Intercostal tendons are grouped in anchoring tendon tissues that mediate connection between associated muscle and ribs. While the *Scx* loss of function did not affected intercostal tendons, all force-transmitting and inter-muscular tendons showed phenotype (Murchison et al., 2007). Notably, our findings suggest an identical role of *Meox2* for the development of all tendon categories. On the other hand, it also suggests a significant role of *Meox2* in the development of anchoring tendons.

It has been shown that intercostal muscles were lost in *Myf5*$^{-/-}$ embryos at E12.5 (Tajbakhsh and Buckingham, 1994). While the *Myf5*$^{-/-}$ mutant embryos show delay in hypaxial myogenesis (Braun et al., 1994); still these embryos displayed lung hypoplasia due to complete lack of intercostal muscles and rib cage (Inanlou and Kablar, 2005a, b). Similar abnormality due to defect of these muscles was also found in *myogenin* null mice (Tseng et al., 2000). Interestingly, *Meox2* mutation targeted the down regulation of *Myf5* (Mankoo et al., 1999) and a subsequent study showed that the concerted role of *Meox* transcription factors is necessary to maintain *Myf5* and *myogenin* expression (Mankoo et al., 2003). While this study showed non-redundant roles of Meox genes in skeletal musculature, the Meox1; Meox2 double homozygous mutant foetuses at E16.5 lacked both epaxial (back) and hypaxial (intercostal) muscles. Therefore, the disruption of intercostal muscles in *Meox2*$^{-/-}$ embryo in our report indicates an essential requirement of *Meox2* gene activity in hypaxial myogenesis.

Collectively, these data are an important contribution to the evidence for the role of *Meox2* in modular limb tendon formation. In general, it emphasizes the distinctive role of *Meox2* in segmental and complex dense connective tissue such as tendons. Furthermore, a transgenic approach would be required to generate conditional inactivation of *Meox2* gene. *Prx1-Cre* mediated loss-of-function (Logan et al., 2002) of *Meox2* allele would result in the ubiquitous loss of Meox2 protein from limb bud mesenchyme that gives rise to connective tissue and cartilage cells.

Furthermore, to evaluate the outcome of defective migration of *Meox2*$^{+}$ muscle cells on the limb tendon development, mating *Meox2* heterozygous animals with *Splotch* animals that has defective *Pax3* gene restricting the migration of myogenic cells from somites in to the limb territory could be achieved. The observations from this approach would be useful to gain a better understanding of *Meox2* gene function in modular tendon development along the proximodistal axis of the limbs.

Orderly cartilage condensation in the absence of *Meox2*

In the primitive mesenchyme, *Sox9* gene labels the cells undergoing cartilage condensation (Wright et al., 1995). Due to the shared progenitors for tendons and cartilage cells in the limb mesenchyme at E10.5 and subsequently the overlapping expression of *Sox9* labelled cartilage cells and *Scx* positive tendon cells in the axial and appendicular tissue at E12.5 was reported (Blitz et al., 2013; Sugimoto et al., 2013a). Previously, it has been shown that the expansion of tendon progenitors occured in the absence of cartilage differentiation in *Sox5*$^{-/-}$*; Sox6*$^{-/-}$ double mutants in sclerotome (Brent et al., 2005). However, a recent study from the embryos of *Sox9*^{Prx1Cre} mutants revealed complete failure of autopod tendon formation in the absence of cartilage and authors concluded that cartilage is necessary and sufficient for the induction of autopod tendon progenitors (Huang et al., 2015b). In our study, we found that *Meox2* ablation does not affected Sox9 expressing cartilage cells at E12.5, in fact, we found normal chondrogenesis throughout the embryonic stages and at neo-natal stage (see chapter 3). Despite normal cartilage cells in the autopod of Meox2-/- mutant embryos, we found gross tendon defects in the digits and metacarpal segment of the limb.

Moreover, Sugimoto and coworkers found that all tendons are derived from early precursor cells that are either Scx+/Sox9+ near the joints or Scx+/Sox9- in all other regions due to presence of bipotent cells in the limb mesenchyme and sclerotome. Using loss-of-function assays, they further showed that the tendon

cells closer to the cartilage primordia were originated from Scx+/Sox9+ (Sugimoto et al., 2013a; Sugimoto et al., 2013b). The normal *Sox9* expression in the limbs and axial cartilage tissue of Meox2-/- mutant embryos at E12.5, suggest the substantial effects of *Meox2* derived clues are restricted to Scx+/Sox9- cell population.

Furthermore, in autopod segment of the forelimb, reports have shown that Wnt signalling from the ectoderm can induce *Scx* expression (Yamamoto-Shiraishi and Kuroiwa, 2013) and TGFβ signalling secreted from the condensing autopod cartilage can also potently induce *Scx* expression (Pryce et al., 2009). Therefore, we could anticipate that these signalling pathways might affect the spatial and temporal expression of *Meox*2^{+} cells during regulation of autopod tendon genesis. However, current study is limited to address this issue, as it would require in vitro analysis using mesenchymal cell line and in vivo analysis using bead soaked in the recombinant protein solution and implanted in to the chick or mouse limb to monitor the effect on Meox2 transcripts. From these experiments, we aimed to understand the Meox2 expression in response to TGFb and Wnt signalling that can help in elucidating the mechanism behind the autopod tendon defects in Meox2-/- mutants.

Together, the tendon and muscle phenotype in our mutant model, demonstrate that these defects are not secondary to the skeletal perturbations but represent an independent role of *Meox2* gene on the tendon cells either intrinsic or extrinsic during the tendon morphogenesis.

An indirect role of *Meox2* in the zeugopod tendon development

Various comprehensive studies had identified diversity in the segmental development limb tendons along the proximodistal axis (Bonnin et al., 2005; Huang et al., 2015b; Kardon, 1998; Swinehart et al., 2013). The data from the chick experiments showed that muscle and tendon induce autonomously in the

limb (Chevallier et al., 1977). However, for continuous growth and differentiation, both tissues are highly dependent on each other. This interdependence in the generation of functional musculoskeletal system has revealed an increased complexity during the limb tendon development. In addition, the distinct and independent developmental cues of the autopod tendons from skeletal cells and zeugopod tendons from muscle cells are established by Huang and co-worker (2015).

Previous work has shown that in the earliest stages of limb development, *Meox2* plays an important role in limb myogenesis and positively regulate the onset of *Pax3* and *Myf5* expression. During the subsequent stages, *Meox2* is necessary to restrict uncontrolled MyoD-dependent terminal muscle differentiation at the time of patterning and splitting of muscle masses during limb development (Bismuth and Relaix, 2010; Mankoo et al., 1999). Furthermore, role of muscles in tendon development was revealed using Sp^{d} mutants in which *Pax3* point mutation resulted in loss of all muscle cells (Huang et al., 2015b; Vogan et al., 1993). The tendon progenitors of presumptive autopod and zeugopod are induced normally in the absence of muscles but the differentiation and maintenance of zeugopod tendon progenitors were lost at E13.5 (Bonnin et al., 2005; Huang et al., 2015b; Kardon, 1998).

Our analysis of *Scx* expression in Sp^{d} embryos at E12.5 showed severe reduction of chevron-shaped tendon domain in the medial region of the presumptive zeugopod that was lost in the $Meox2^{-/-}$ embryos. This indicates a secondary defect of *Meox2* mutation on Scx+ tendon cells in zeugopod. It could provide us to hypothesis an indirect role of *Meox2* gene activity from the muscle connective tissue on the zeugopod tendon development and muscle patterning. Cohort studies have shown a pivotal role of muscle connective tissue on limb muscle patterning and tendon formation (Hasson et al., 2010; Kardon et al., 2003; Mathew et al., 2011; Swinehart et al., 2013). The evidence showed ectopic splitting of the dorsal and ventral limb muscle masses in the absence of *Tbx5* gene from muscle connective tissue (Hasson et al., 2010). The limb tendon organisation was also affected due to loss of Tbx5 function in the muscle connective tissue. In another report, authors showed that an over

expression of *Tcf4* gene in muscle connective tissue, resulted in ectopic muscle formation (Kardon et al., 2003). There is also demonstration that *Hox11* gene coordinates in the maintenance and differentiation of zeugopod tendon and muscle formation (Swinehart et al., 2013). It therefore follows that the retrospective analysis of Meox2 function in zeugopod requires the generation of conditional knockout mice by removing the limb specific expression of *Meox2* by mating with prx1Cre animal (Logan et al., 2002) and thereby examining zeugopod tendon development.

4.5 Conclusions

In summary, we found that induction of axial and appendicular tendon progenitor cells does not required Meox2 function. Forelimb tendon phenotype was first manifested at E12.0, whereas, the hindlimb and axial tendon phenotype emerged at E12.5. The limb tendon phenotype was more profound in autopod than in zeugopod segments. In our mutant model, the proximal sclerotome ($Scx^{+}/Sox9^{+}$) and the syndetome ($Scx^{+}/Sox9^{-}$) showed reduction in *Scx* expressing tendon progenitor cells. At E14.5, in $Meox2^{-/-}$ mutant embryos, flexor digitorium profundus (FDP) was severely affected whereas extensor digitorium communis (EDC) remained normal in the autopod. An overall disruption of all tendons including extensors and flexors in zeugopod segment occurred. There was a complete loss of intercostal tendon layer and disrupted intercostal muscle in Meox2-/- mutant embryos. Lastly, our data indicate the fact that *Meox2* is crucial for the normal limb muscle patterning and tendon formation. In conclusion, the embryonic tendon defect in the $Meox2^{-/-}$ embryos has uncovered various previously unexplored role of *Meox2* in the tendon development. The following chapter investigates the possible mechanism by determining whether Meox2 acts intrinsically or extrinsically from tendon during embryogenesis.

Fig 4.3.1 Normal tendon induction in the absence of *Meox2* at embryonic day (E) 11.5

Whole-mount in situ analysis for *Scx* at E11.5 in a wild-type embryo (A and C) and in *Meox2*$^{-/-}$ embryo (B and D). Red arrows represent normal induction of *Scx* positive tendon progenitors in the limb buds. Yellow arrows indicate normal *Scx* transcripts in the interlimb somites. C and D is a higher magnification of interlimb somites.

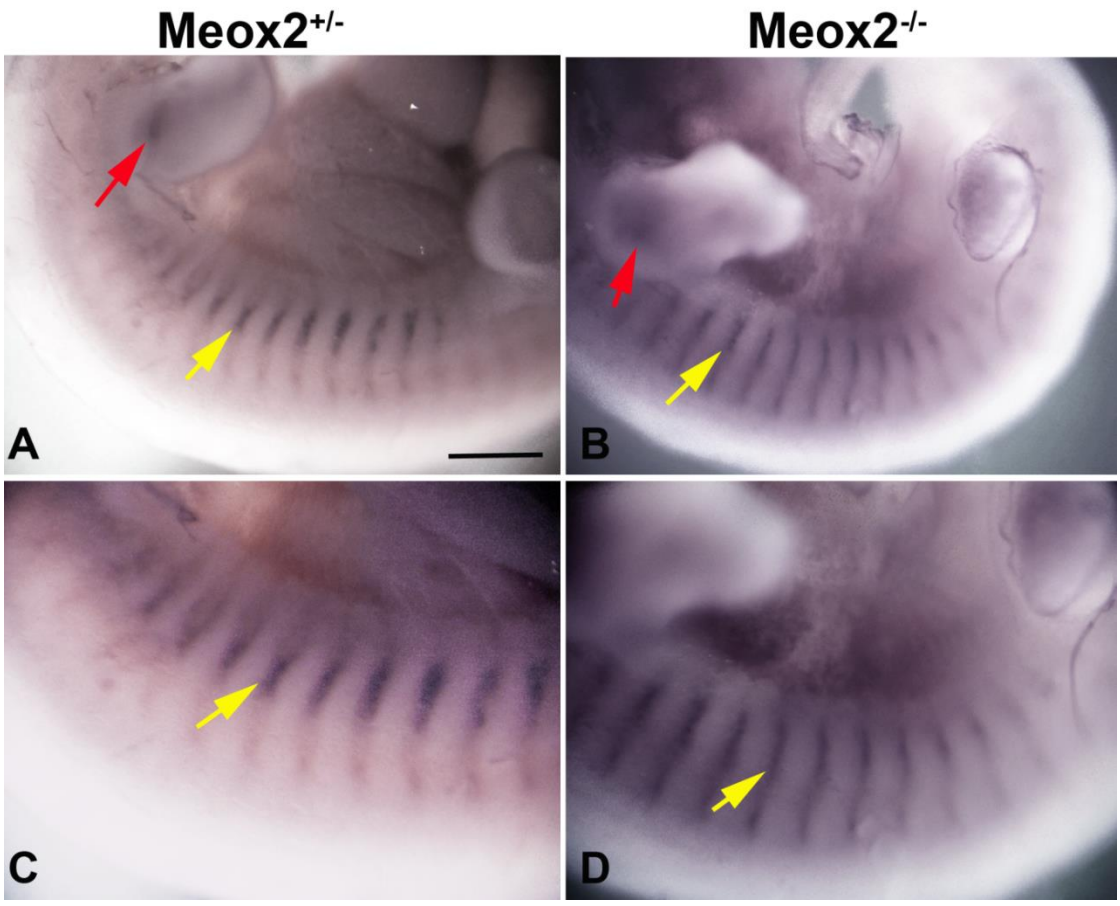
Meox2+/-
Meox2-/-
A
B
C
D

Fig.4.3.2 Aberrant *Scleraxis* expression restricted for only forelimb tendon precursor cells at E12.0

Whole-mount in situ analysis for *Scx* at E12.0 in a wild-type forelimb dorsal and ventral (A and C) and in the *Meox2*$^{-/-}$ embryo dorsal and ventral forelimb (B and D) was performed. Yellow arrowhead indicates a missing chevron-shaped *Scx* expression domain and yellow arrows on the ventral side showed overall considerable reduction of Scx levels in the absence of *Meox2*. In addition, Scx whole-mount in situ analysis on the hindlimb dorsal and ventral (E and G) and in *Meox2*$^{-/-}$ embryo dorsal and ventral (F and H) was performed. Yellow arrows in ventral side represent reduced Scx expression domain in the presumptive autopod of hindlimb.

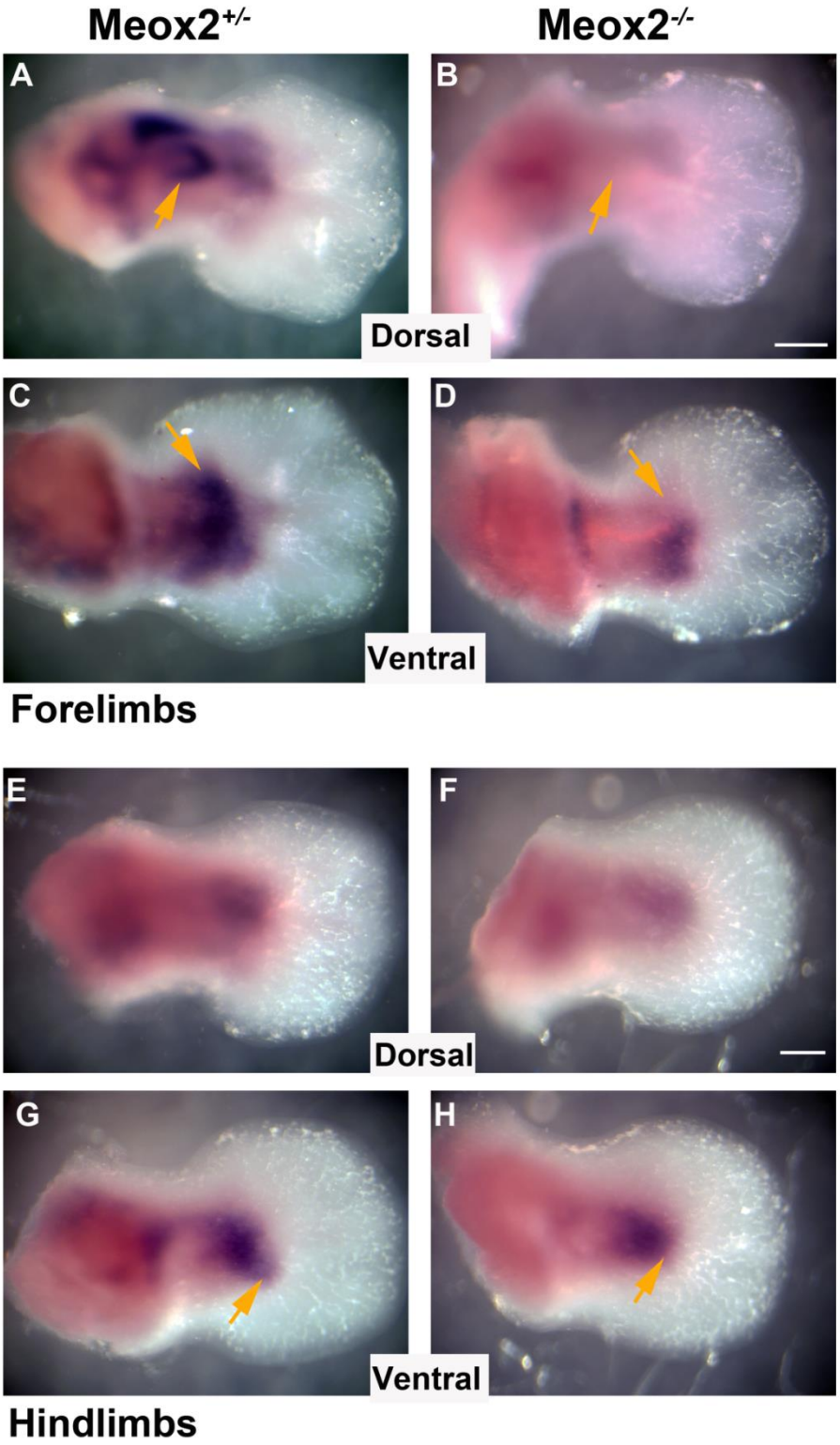
Meox2+/-
Meox2-/-
A
B
Dorsal
C
D
Ventral
Forelimbs
E
F
Dorsal
G
H
Ventral
Hindlimbs

Fig 4.3.3 Disordered organization of tendon progenitors in the absence of *Meox2* at E12.5

Whole-mount in situ analysis for *Scx* at E12.5 in a wild-type forelimb dorsal and ventral (A and C) and in the two separate *Meox2*$^{-/-}$ embryos 1 and 2 dorsal forelimbs (B, B') and ventral forelimbs (D, D'). Red arrows indicate a missing chevron-shaped Scx expression domain in the *Meox2* mutants. Yellow arrow heads indicate considerable reduction of Scx levels in the presumptive autopod; yellow arrows indicate reduction in zeugopod tendon progenitors.

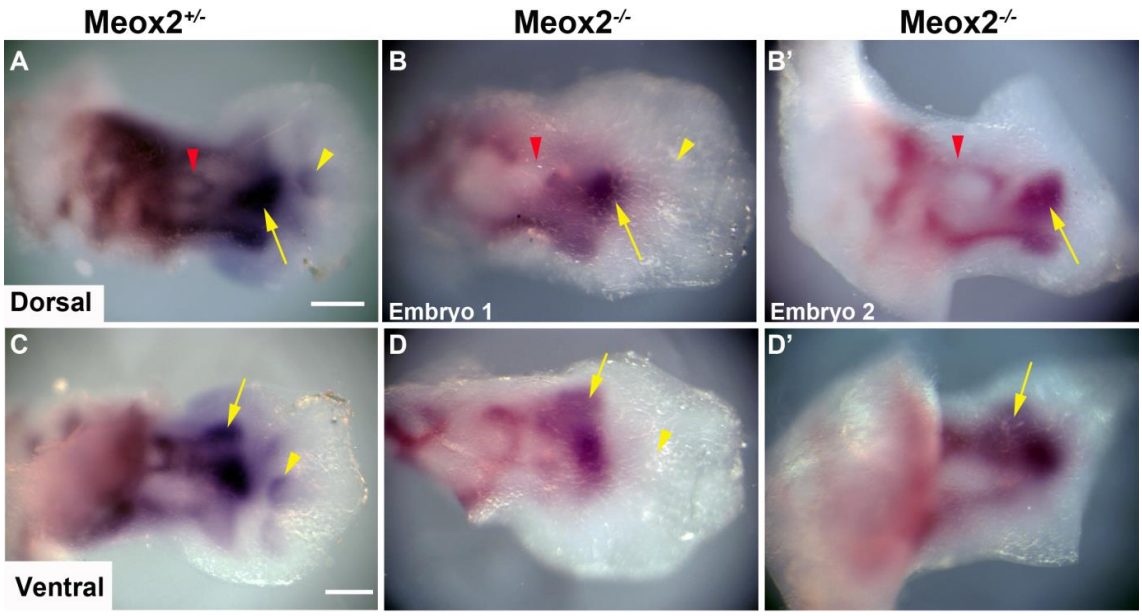
Meox2+/-
Meox2-/-
Meox2-/-
A
B
B'
Dorsal
Embryo 1
Embryo 2
C
D
D'
Ventral

Fig 4.3.4 Depleted Scleraxis levels in the hindlimbs of *Meox2*$^{-/-}$ at E 12.5

Whole-mount in situ analysis for Scx at E12.5 in a wild-type hindlimb dorsal and ventral (A and C) and in *Meox2*$^{-/-}$ embryo dorsal and ventral (B and D) was performed. Black arrows represent reduced *Scx* expression domain in the presumptive zeugopod of hindlimb whereas black arrowhead showed considerable reduction of *Scx* levels in the hindlimb autopod.

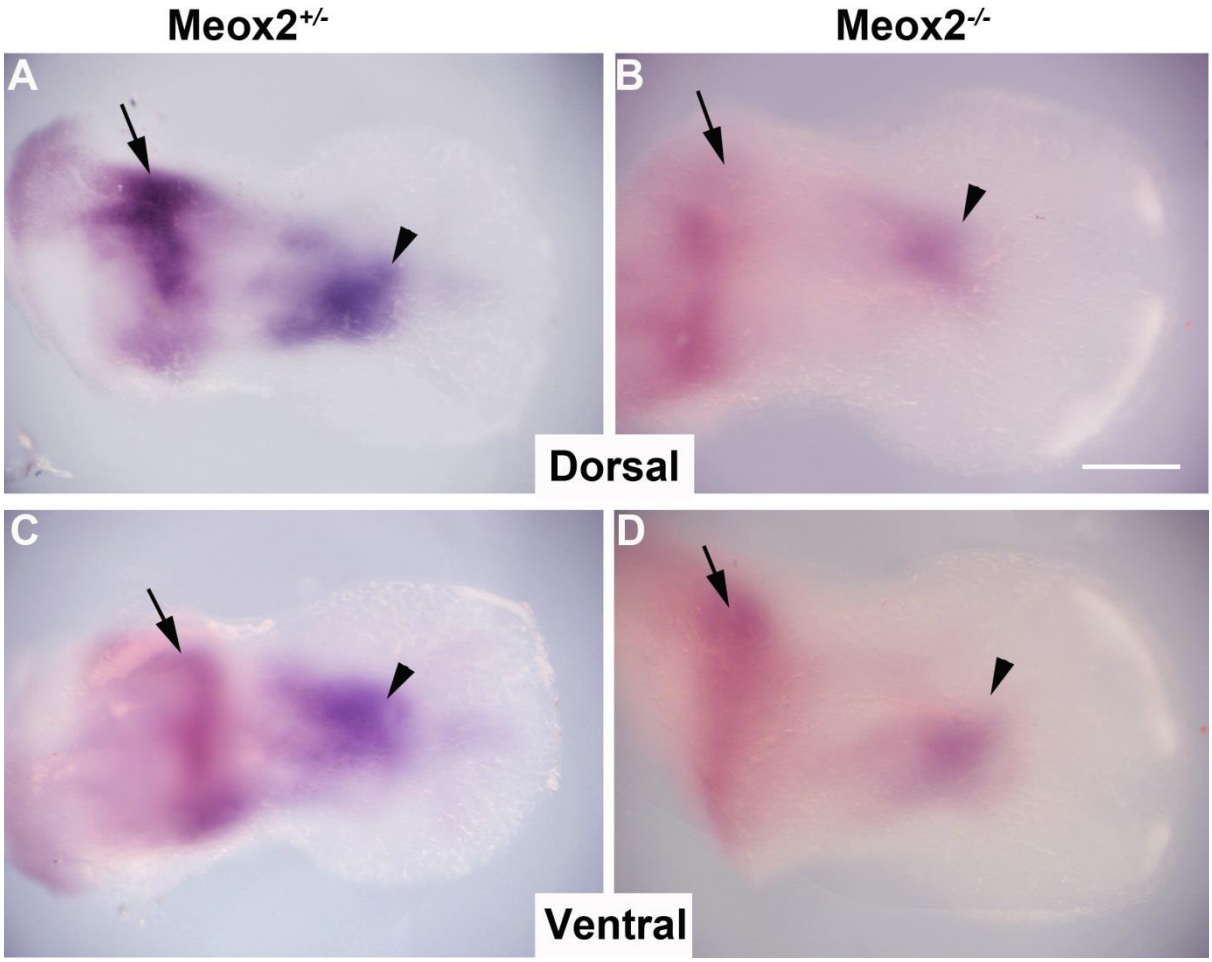
Meox2+/-
Meox2-/-
A
B
Dorsal
C
D
Ventral

Fig 4.3.5 Disordered axial tendon progenitors in the absence of *Meox2* at embryonic day (E) 12.5

Analysis of *ScxGFP* on longitudinal sections of the trunk at E12.5 in a heterozygous embryo (A) and in homozygous mutant embryo (B) revealed important differences for axial tendon progenitors. White arrowheads represent complete loss of *ScxGFP* expression domains in the proximal sclerotome in the mutants; white arrows indicate reduction in GFP expression from syndetome. Endogenous Scx expression was observed by whole mount in situ hybridisation in a *Meox2*$^{+/-}$ heterozygous control (C,E and G) and in *Meox2*$^{-/-}$ homozygous mutant embryo (D, F and H). Black arrowheads represent severe loss of *Scx* mRNA expression domains in the somite whereas black arrows indicate decreased *Scx* expressing domains.

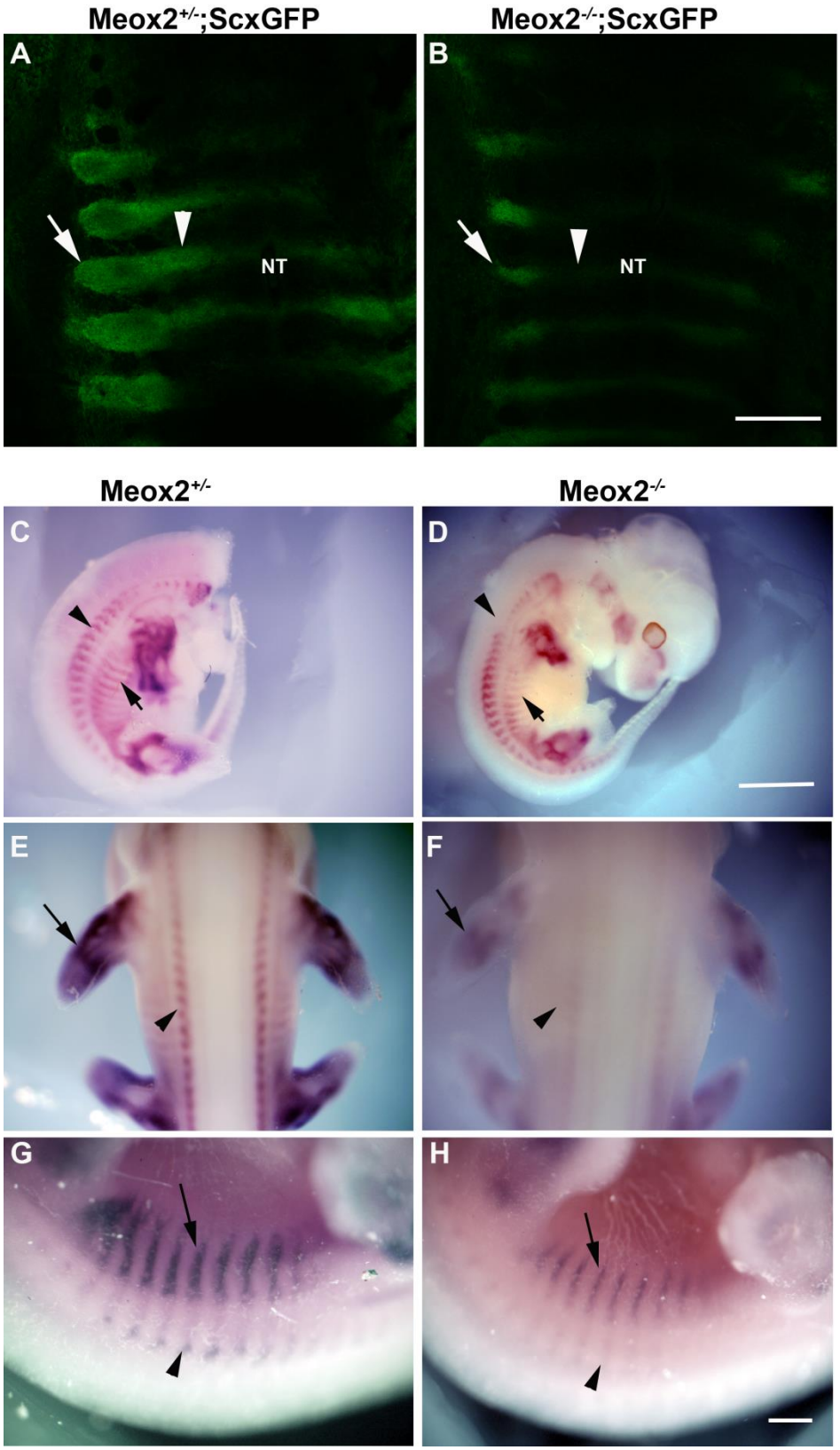
Meox2+/-;ScxGFP
Meox2-/-;ScxGFP
A
B
NT
NT
Meox2+/-
Meox2-/-
C
D
E
F
G
H

Fig 4.3.6 *ScxGFP* expression at E13.5 remained unaffected in autopod but reduced in zeugopod of *Meox2* mutant mice

The heterozygous and homozygous alleles for *Meox2* were maintained on a *ScxGFP* transgenic background. The cross sections of autopod in the heterozygous embryo (A) and homozygous embryo (B) were observed for ScxGFP expression domains. The GFP signals from extensor and flexor tendons were found normal. T1, flexor digitorium profundus indicated by yellow arrowheads; T3, extensor digitorium communis tendon progenitors showed by white arrows. Additionally, the cross sections of zeugopod in the heterozygous (C) and homozygous (D) at E13.5 showed reduction in ScxGFP tendon cells, visualised as green cells. Tendon nomenclatures are listed in table 3.1.

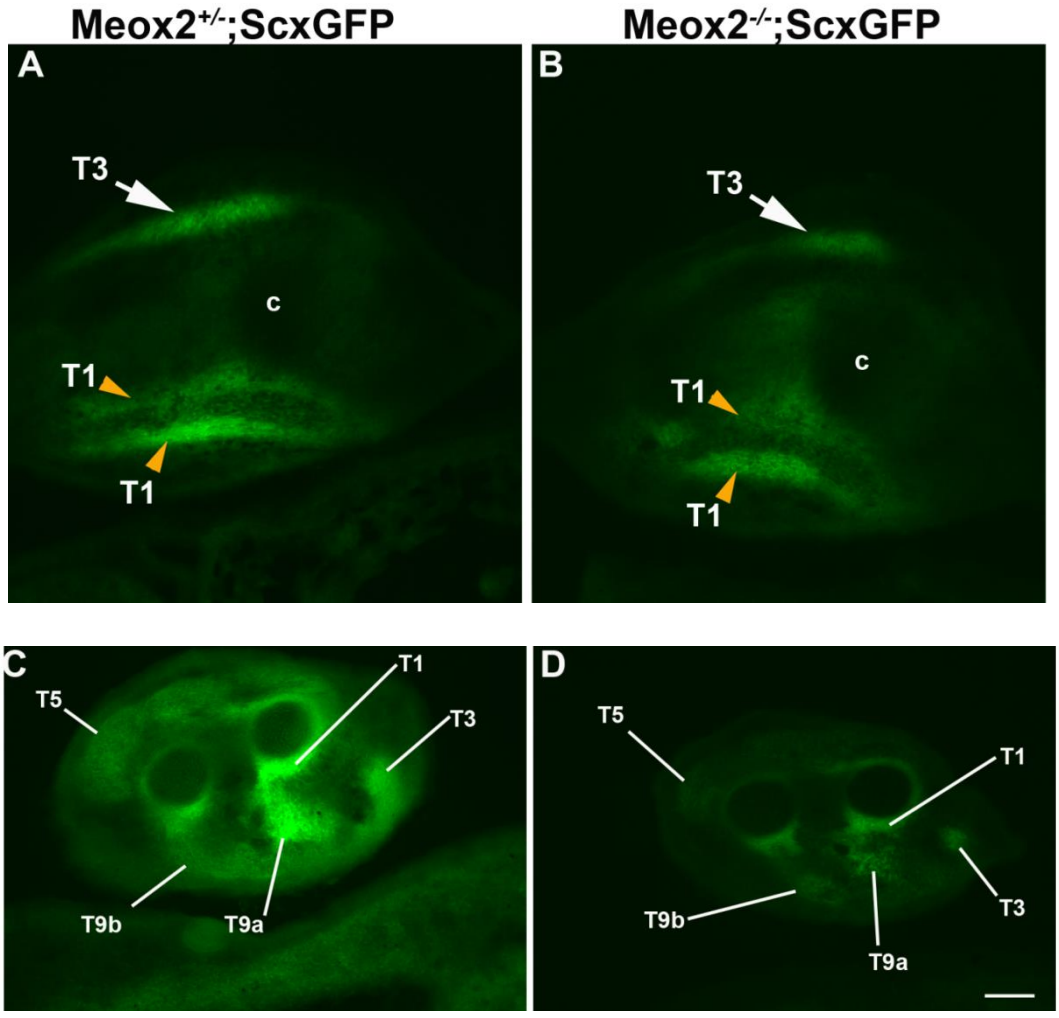
Meox2+/-;ScxGFP
Meox2-/-;ScxGFP
A
B
T3
c
T1
T1
T3
c
T1
T1
C
D
T5
T1
T3
T9b
T9a
T5
T1
T9b
T3
T9a

Fig 4.3.7 Endogenous *Scx* expression at E13.5 showed disrupted expression patterns in both autopod and zeugopod

Whole-mount in situ analysis was performed using Scx antisense cRNA probe on a heterozygous control forelimbs (A and C) and in homozygous *Meox2*$^{-/-}$ *mutant* embryo (B and D). The dorsal aspect of the limb is shown as A and C whereas the ventral aspects is shown in B and D. Red arrowhead indicate an expansion of Scx mRNA domain in the *Meox2* mutants. Black arrows show reduced Scx expression in the autopod.

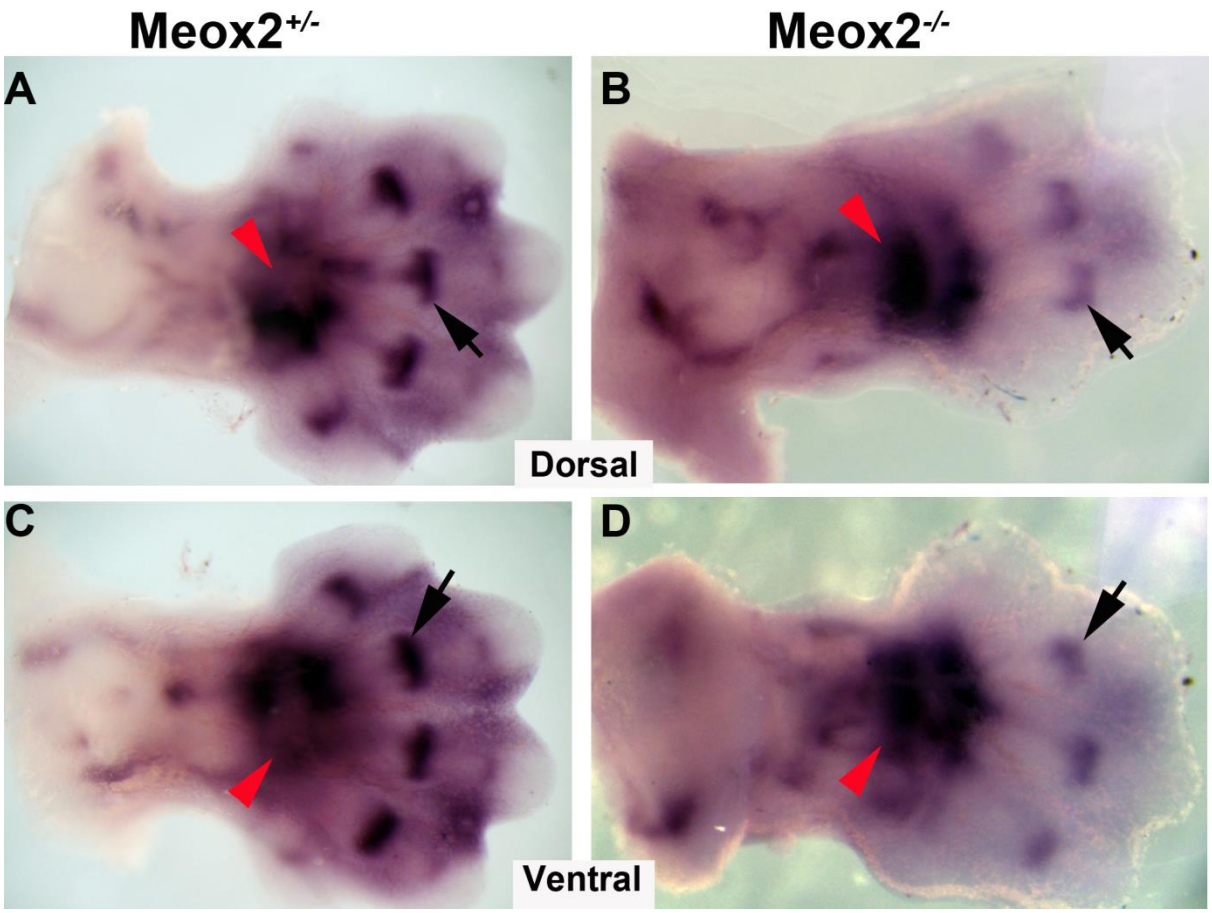
Meox2+/-
Meox2-/-
A
B
Dorsal
C
D
Ventral

Fig 4.3.8 Decreased ScxGFP expression in tendon precursors of somite at E13.5

Frontal sections of the trunk from *Meox2*$^{+/-}$*;ScxGFP* (A) and *Meox2*$^{-/-}$*;ScxGFP* (B) embryos observed under fluorescence microscope for ScxGFP signal (green) in tendon precursors residing in the somite.

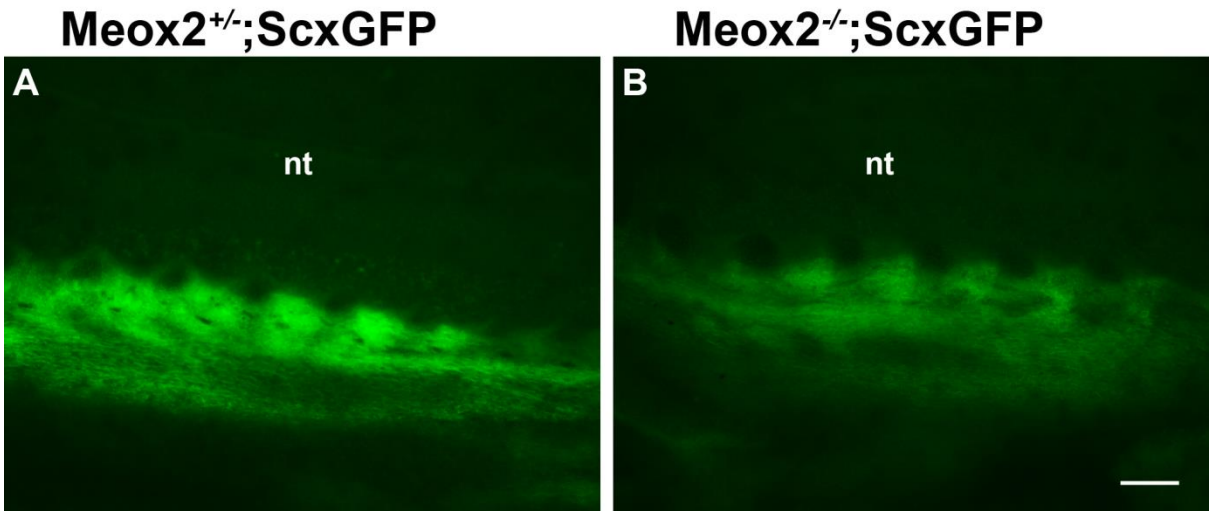
Meox2+/-;ScxGFP
Meox2-/-;ScxGFP
A
nt
B
nt

Fig 4.3.9 Disruption of autopod tendons at E14.5 in *Meox2* mutant mice

The heterozygous and homozygous alleles for Meox2 were maintained on a *ScxGFP* transgenic background. The cross sections of autopod in the heterozygous embryo (A,C,E and G) and homozygous embryo (B,D,F and H) were stained for myosine heavy chain (C and D) red immunofluorescence and *ScxGFP* tendon cells are in green (A and B). Merged image shown in E and F. The EDC tendon (T3) was found normal at higher magnification in G and H. Tendon nomenclature are tabulated in Table 2. Yellow arrowhead indicates interosseous muscle and yellow arrow show lumbricals muscle. Scale bars=100um

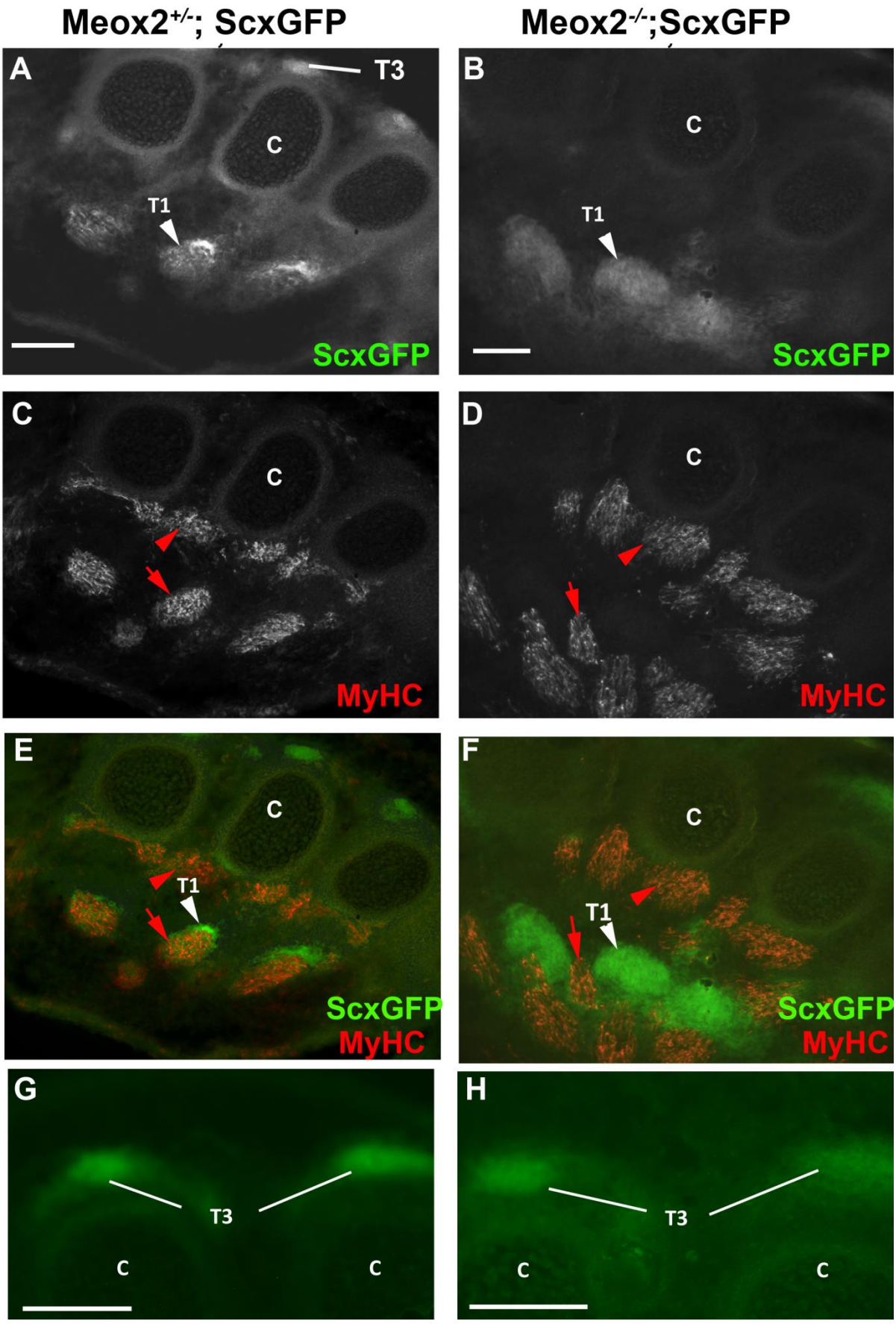
Meox2+/-; ScxGFP
Meox2-/-;ScxGFP
A
T3
C
T1
ScxGFP
B
C
T1
ScxGFP
C
C
MyHC
D
C
MyHC
E
C
T1
ScxGFP
MyHC
F
C
T1
ScxGFP
MyHC
G
T3
C
C
H
T3
C
C

Fig 4.3.10 Loss of zeugopod tendons at E14.5 in *Meox2$^{-/-}$;ScxGFP*

The heterozygous and homozygous alleles for *Meox2* are maintained on a *ScxGFP* transgenic background. The cross sections of zeugopod in the heterozygous embryo (A) and homozygous embryo (B) at E14.5 stained for muscles using myosin heavy chain antibody and ScxGFP tendon cells are in green. White arrow indicates flexor digitorium profundus (FDP) tendon (T1). Yellow arrows indicate FDP muscle.

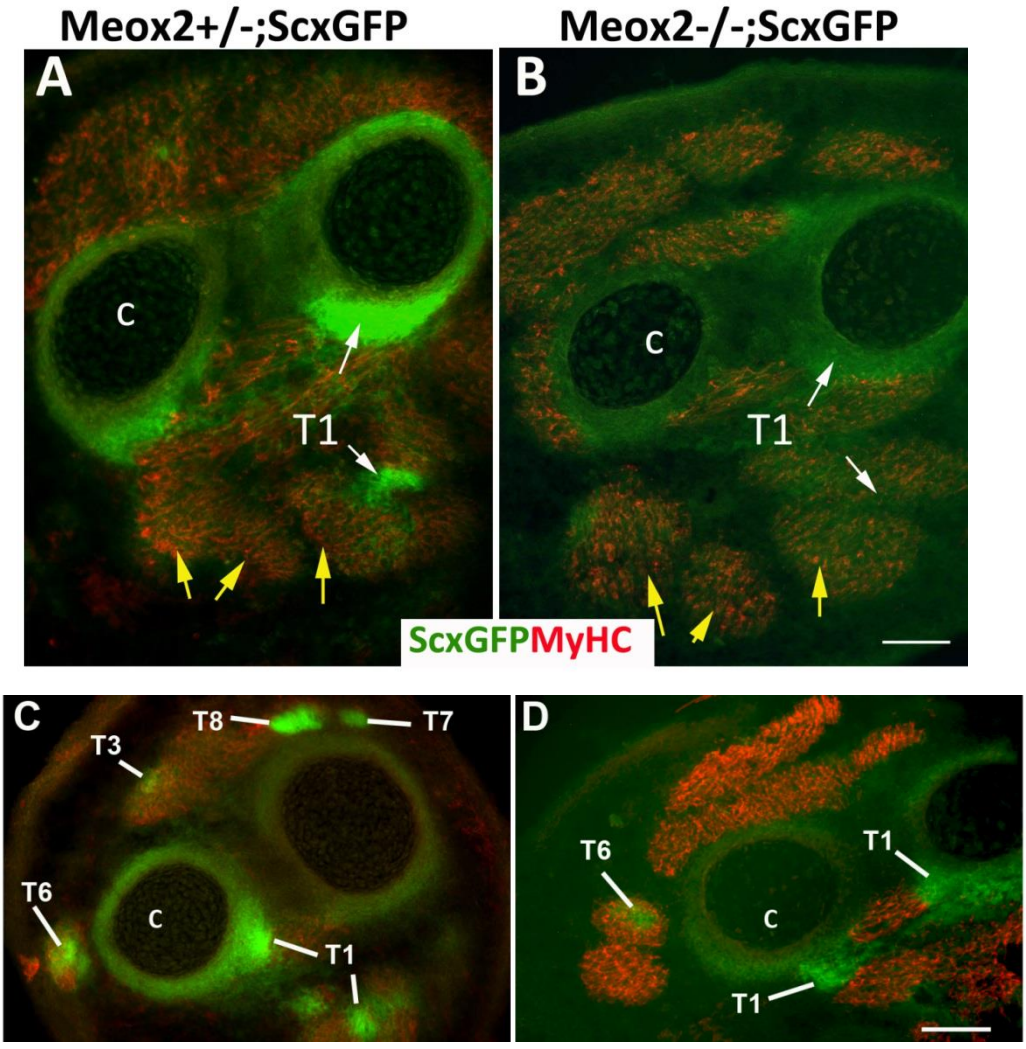
Meox2+/-;ScxGFP
Meox2-/-;ScxGFP
A
B
C
T1
C
T1
ScxGFPMyHC
C
T8
T7
T3
T6
C
T1
D
T6
T1
C
T1

Fig 4.3.11 Disrupted intercostal muscle-tendon unit at E14.5

Frontal sections of the trunk from *Meox2*$^{+/-}$*;ScxGFP* (A,C and E) and *Meox2*$^{-/-}$*;ScxGFP* (B,D and F) embryos stained with myosin heavy chain (MHC;red) which detected intercostal muscles to the ribs. ScxGFP signal (green) from the intercostal tendons were completely lost (A and B, white arrows) in the mutants. Yellow arrowhead represents intercostal muscle in controls (C and E) but absent in mutants (D and F). Scale bars=100um

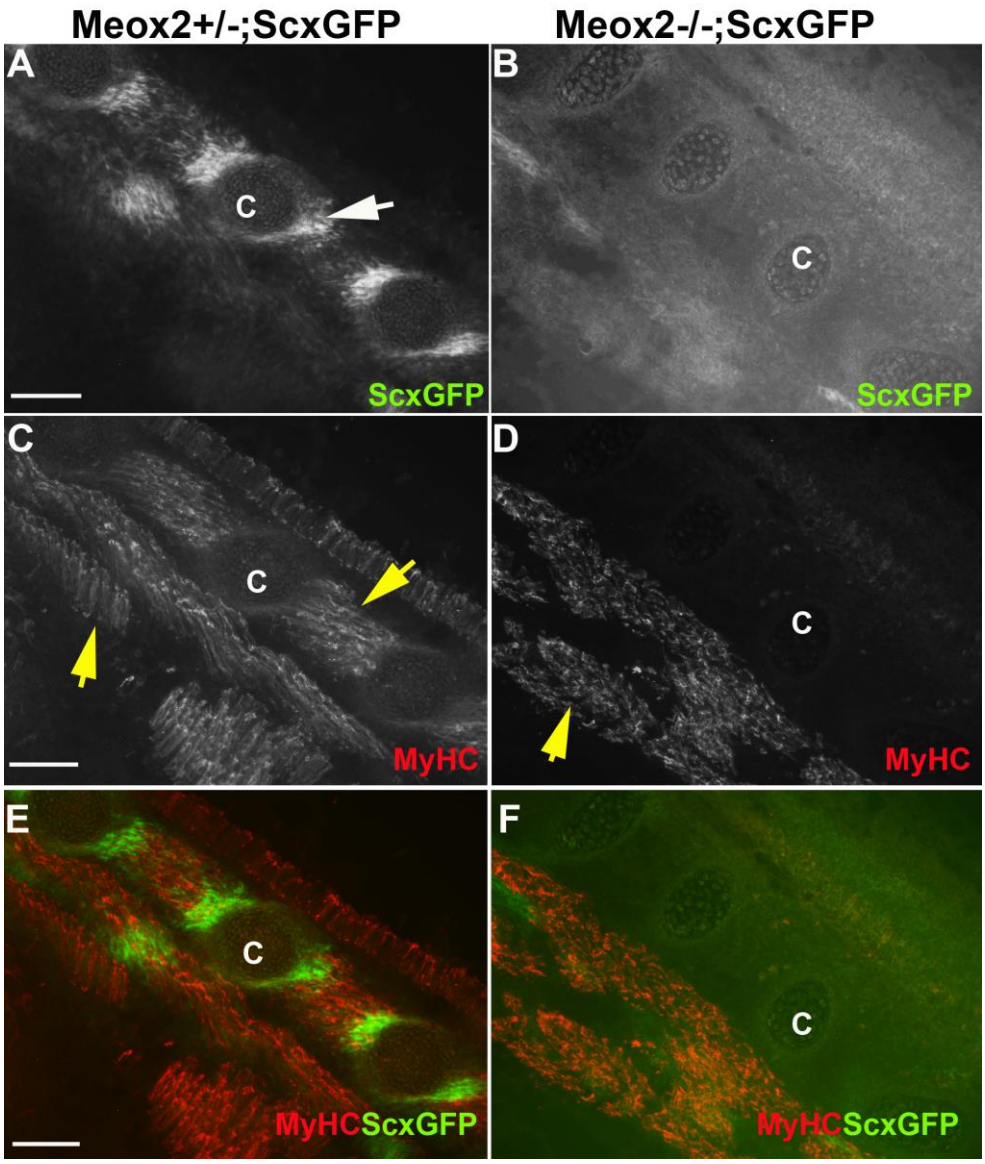
Meox2+/-;ScxGFP
Meox2-/-;ScxGFP
A
C
ScxGFP
B
C
ScxGFP
C
C
MyHC
D
C
MyHC
E
C
MyHCScxGFP
F
C
MyHCScxGFP

Fig 4.3.12 Disrupted zeugopod tendon progenitor cells in *Sp*^{d} embryos at E12.5

Whole-mount in situ analysis for Scx at E12.5 in a *Pax3*$^{+/Sp}$ heterozygous forelimb dorsal and ventral (A and C) and in the *Pax3*$^{Sp/Sp}$ homozygous mutant embryo (B and D) was performed. Yellow arrowheads indicate a reduced chevron-shaped Scx expression domain that was similar in the *Meox2* mutants.

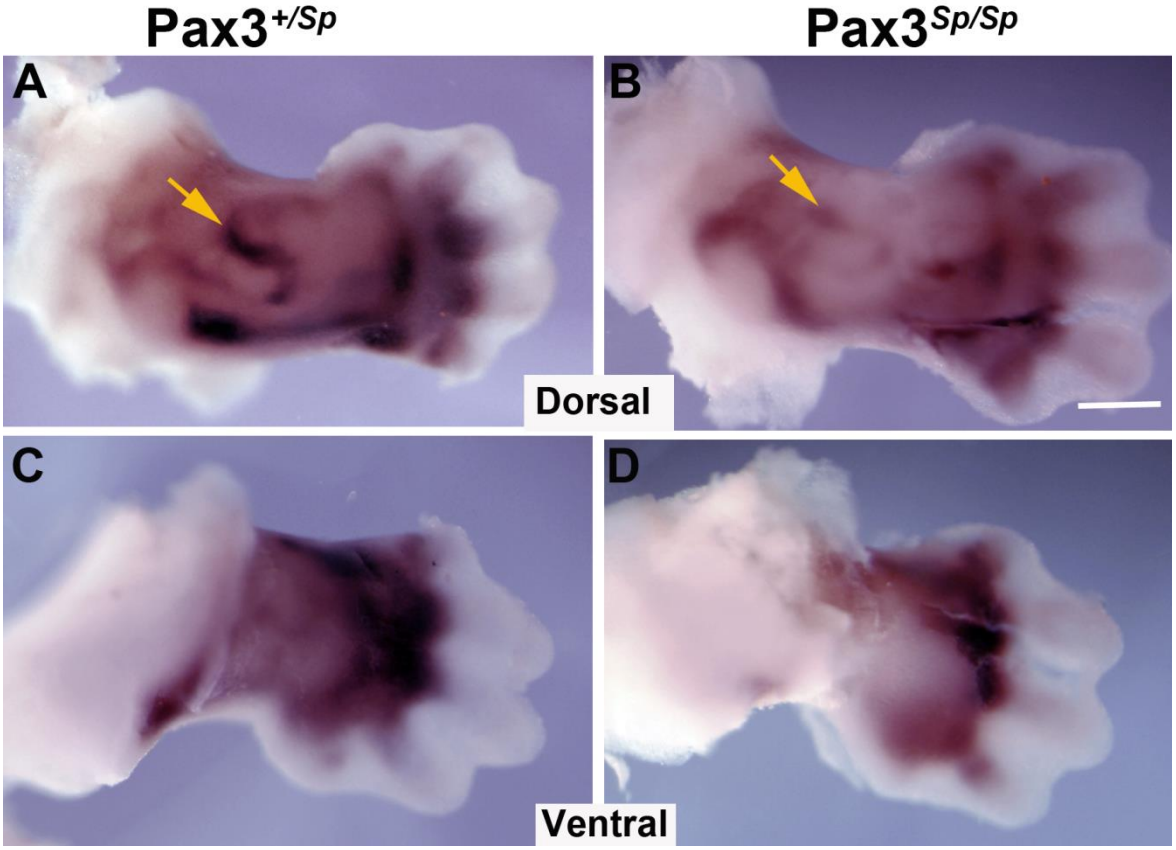
Pax3+/Sp
Pax3Sp/Sp
A
B
Dorsal
C
D
Ventral

Fig 4.3.13 Normal cartilage development in the absence of Meox2 at embryonic day (E) 12.5

Whole-mount in situ analysis for *Sox9* at E12.5 in a *Meox2*$^{+/-}$ heterozygous embryo (A,C) and in *Meox2*$^{-/-}$ homozygous mutant embryo (B,D). The left and right sides of the embryos showed normal *Sox9* expression in the somites and limbs in controls and mutants. The heads were removed in the *Meox2*$^{-/-}$ homozygous mutant embryo to distinguish them from controls.

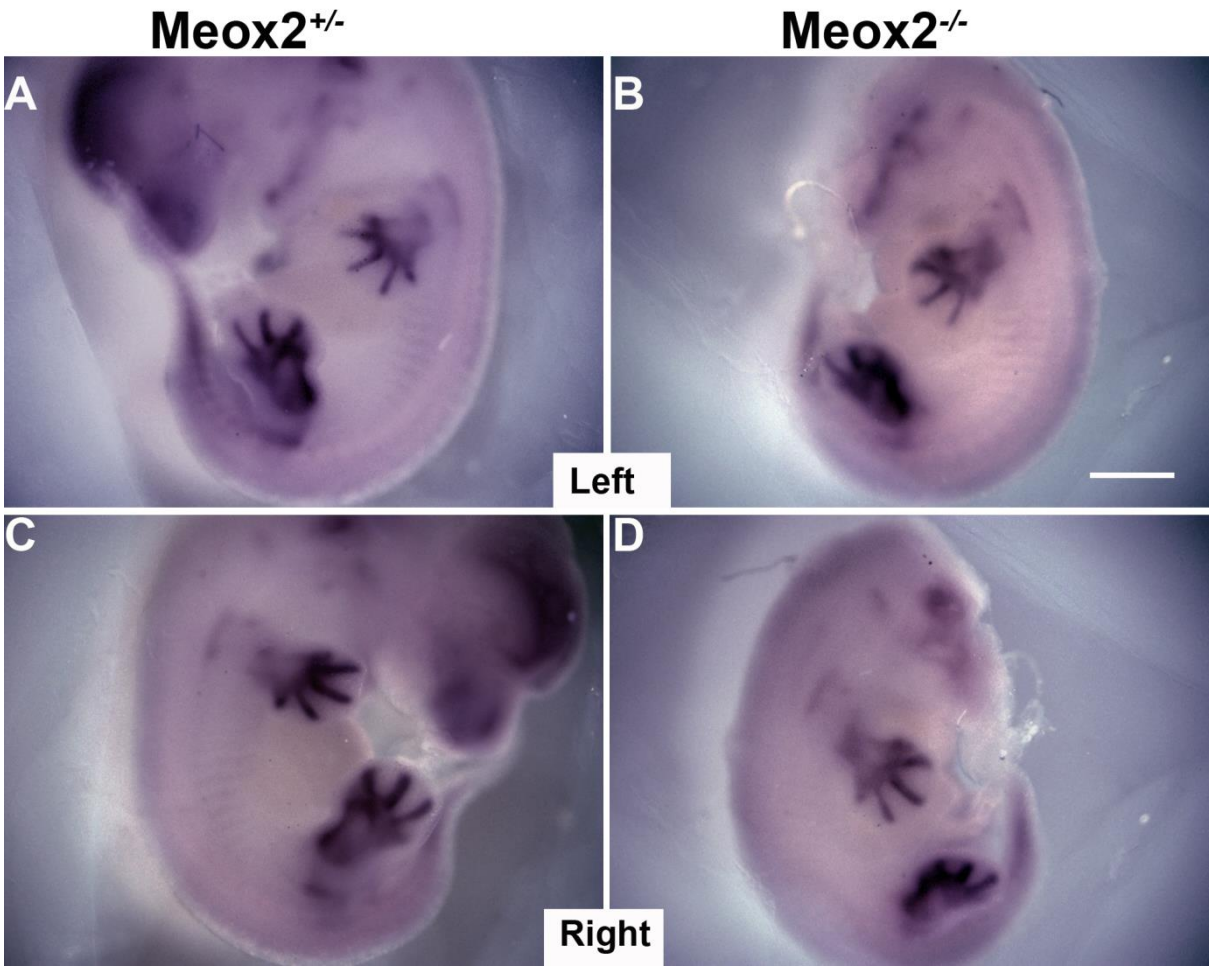
Meox2+/-
Meox2-/-
A
B
Left
C
D
Right

Chapter 5

Cellular and molecular mechanisms of *Meox2* function in tendon development

5.1 Introduction

Several studies have shown the chain of events ongoing during tendon development. Despite this progress, we still lack a fundamental understanding of many aspects of tendon development, such as the molecular regulators that control all tendon categories in a similar fashion. In previous chapters, we showed that in the absence of *Meox2*, all tendon categories are affected. We also show that the tendon defect is embryonic in origin. In addition, the expression of the *Scx* transcription factor is down regulated in *Meox2*$^{-/-}$ mutant embryos. In the previous chapter, we concluded that the first manifestation of the embryonic tendon phenotype in the *Meox2*$^{-/-}$ mutant embryos occurred at E12.5 in axial tissue.

Tendon fate commitment and induction (E10.5-11.5), alignment and organisation (E12.0-12.5), condensation and aggregation (E13.5) and lastly, tendon differentiation, growth and maturation (E14.5 onwards continuing after birth) are well-coordinated events. The early specification and induction of committed axial tendon progenitors occurs inside the syndetome and are dependent on FGF signalling emanated from the adjacent myotome(Brent and Tabin, 2004; Edom-Vovard et al., 2002). This extrinsic signal is necessary and sufficient to promote *Scx* expressing tendon precursors thereby expanding them in the sclerotome. The tendon precursors are induced at the expense of *Sox5/6* expressing chondrogenic progenitors that also share common origins in the sclerotome (Brent et al., 2003). Interestingly, a recent study showed that the sclerotome acts as host for multipotent chondrotendo progenitors expressing both *Scx* and *Sox9* (Sugimoto et al., 2013). Under the influence of extrinsic cues, the relative proportions of *Scx*$^{+}$*/Sox9*$^{+}$ inside the sclerotome are maintained and as the development proceeds, they diverge into a *Scx*$^{-}$*/Sox9*$^{+}$ cell population that is retained inside the sclerotome, whereas *Scx*$^{+}$*/Sox9*$^{-}$ expressing cells are concentrated in the syndetome.

Moreover, the TGFβ signalling pathway is also shown to coordinate cartilage and tendon differentiation (Lorda-Diez et al., 2009). It favours tendon formation by leading to the robust induction of *Scx* and tenomodulin, a type II transmembrane protein (Furumatsu et al., 2010; Lorda-Diez et al., 2009; Pryce et al., 2009). In addition, unlike in somites, the initial *Scx* induction for limb tendons is independent of the requirement of myogenic factors and is achieved by mutual repression between BMP and FGF signalling. Thus, FGF and TGFβ signalling pathways modulate the $Scx^{+}/Sox9^{-}$ cell population at the myotendinous junction and repress $Sox9^{+}$ cartilage cells in the limb. Conversely, BMP signalling pathways favour cartilage progenitors and repress tendon precursors at the site of skeletal condensations (Edom-Vovard and Duprez, 2004; Edom-Vovard et al., 2002; Schweitzer et al., 2001).

TGFβ signalling is crucial for the orderly alignment and organisation of limb tendon progenitors to maintain the integrity of the musculoskeletal system at E12.5 (Pryce et al., 2009). The same study also showed that the ectopic expression of the TGFβ2 protein could induce *Scx* in both vivo and in vitro systems. Moreover, the TGFβ signals are also required for maintaining the tenoblastic identity of the committed precursor, thereby restricting them from adopting alternative cell fates, such as cartilage formation. Evidence also suggests that TGFβ signals recruit a second wave of tendon progenitor cells at E12.5 (Pryce et al., 2009).

From E13.5, *Scx* is required for the tendon progenitor cells to undergo condensation and differentiation(Murchison et al., 2007). Additionally, another transcription factor, *Mohawk* (*Mkx*) is also expressed in tendon cells at E13.5 (Anderson et al., 2006); yet, it has no functional role at this stage of tendon development (Anderson et al., 2006; Ito et al., 2010; Liu et al., 2010).

Our earlier chapters showed that in the *Meox2* null mice, almost all diverse groups of tendon tissue, i.e. short tendons (intercostal tendons), long tendons (limb and tail tendons) and fascia were profoundly affected. The first manifestation of the tendon phenotype in the forelimbs occurs at E12.0 and thus precedes the tendon defects found in *TGFβ2/3* knockouts (E12.5)(Pryce et al.,

2009), *TGFβRII* mutants (E12.5)(Pryce et al., 2009), and *Scx* null mutants (E13.5)(Murchison et al., 2007). Conversely, in axial tissues, the failure of tendon machinery in the absence of *Meox2* was first detectable at E12.5, coinciding with the *TGFβ2/3* mutant axial tendon phenotype (Pryce et al., 2009). Moreover, *Scx* expression domains were overall reduced in both mutant mice models at E12.5. Therefore, with an aim to unravel the molecular mechanisms involving *Meox2* in tendon genesis, at this point, we hypothesized that *Meox2* and TGFβ signalling pathways act in a complementary manner to modulate *Scx* expression in tendon development. And that *Meox2* and *TGFβ* signals are coordinated for the proper alignment, organisation, and recruitment of additional tendon progenitor cells during the assembly of the musculoskeletal system.

5.2 Aims

First, we aimed to account for the considerable loss of *Scx* expression in *Meox2*$^{-/-}$ mutant embryos at E12.5. For this, we analysed changes in cell proliferation and cell death using anti-Ki-67 and anti-Caspase 3 antibodies. Second, we aimed to characterise the expression domains of *Meox2* and *Scx* during embryonic stages. This would be the key to understanding whether *Meox2* acts intrinsically or extrinsically on *Scx*$^{+}$ tendon progenitor cells. We utilised the *ScxGFP* transgene to identify tendon cells on cross sections obtained from E12.5 (only in axial tissue), E13.5, and 14.5 embryos. We used *Scx* in situ hybridization for the limbs at E12.5. Third, using *Meox2-nLacZ* tool, we observed the derivatives of *Meox2* expressing cells in *Meox2* heterozygous embryos and therefore lineage tracing analysis was performed using salmon-gal staining to detect β-galactosidase activity at embryonic stages. Subsequently, we also performed X-gal staining on *Meox2*$^{nLacZ/+}$ heterozygous control and *Meox2*$^{nLacZ/nLacZ}$ homozygous foetuses at E16.5. At this point, we also hypothesised that *Meox2* and *TGFβ* signals are coordinated for the proper alignment, organisation, and recruitment of additional tendon progenitor cells during the assembly of the musculoskeletal system. For this, we investigated the interaction between *Meox2* and TGFβ2 signalling by analysing endogenous

Tgfβ2 expression in *Meox2*$^{-/-}$ embryos at E12.5 and by in vitro assays, which included the evaluation of ectopic expression of TGFβ2 protein on *Meox2* expression in C3H10T1/2 mesenchyme cell line.

5.3 Results

5.3.1 IMPAIRMENT OF CELLULAR PROLIFERATION IN MEOX2$^{-/-}$ MUTANT EMBRYOS AT E12.5

Here we tested the hypothesis that failure of cell proliferation could be responsible for the reduction in *Scx* expression in *Meox2*$^{-/-}$ embryos at E12.5. For this purpose, we performed immunostaining for anti-Ki67 (cell proliferation marker) on longitudinal trunk sections obtained from *Meox2*$^{+/-}$*; ScxGFP* heterozygous and *Meox2*$^{-/-}$*; ScxGFP* homozygous mutant embryos at E12.5 (Fig. 5.3.1A-D). We were able to detect the active proliferation of cells by bright red fluorescence for Ki67 staining (Fig. 5.3.1A and B). Conversely, a severe loss of proliferating cells was observed in the absence of Meox2 (Fig. 5.3.1C and D). An overall failure of cell proliferation was found evenly throughout the section. ScxGFP expression was used to locate the tendon progenitors in the syndetome (Fig. 5.3.1B and D). This suggests a necessary role of the *Meox2* transcription factor during cell proliferation of all tissue types that label various regions within somites.

Furthermore, we also evaluated the expression of *Meox2* on an equivalent longitudinal section by antibody staining of the *Meox2*$^{+/-}$ embryo heterozygous control at E12.5 (Fig. 5.3.1E and F). We found a strong *Meox2*$^{+}$ signal in cells situated at distinct region away from the syndetome (Fig. 5.3.1E, white arrow).

Taken together, these findings reveal that the failure of cell proliferation indeed accounted for the defective tendon genesis and therefore reduced *Scx* expression at E12.5 in *Meox2*$^{-/-}$ embryos.

5.3.2 NORMAL LEVELS OF APOPTOSIS IN *MEOX2*$^{-/-}$ EMBRYOS AT E12.5

We also suspected that the loss of *Scx* levels in the somites could be due to apoptotic cell death. To test the attribution of *Meox2* role in this pathway, we examined the expression of active caspase3 on longitudinal sections obtained from *Meox2*$^{+/-}$*; ScxGFP* heterozygous controls and *Meox2*$^{-/-}$*; ScxGFP* homozygous mutant embryos (Fig. 5.3.2). The cells of neural tube progenitors showed cell death in a pattern indistinguishable between controls and mutants serving as an internal positive control for the experiment (Fig. 5.3.2A and D, white arrowheads). Moreover, the expression of caspase3 remained unchanged in the somites of *Meox2*$^{-/-}$ mutant embryos (Fig. 5.3.2B and E, white arrowheads). Therefore, these data suggest that *Meox2* dependent signals play no role in the normal cell death machinery, which is an important cellular event during embryonic development of musculoskeletal development.

5.3.3 MEOX2 EXPRESSION IN NON-TENOGENIC CELLS AT E12.5

The *ScxGFP* transgenic reporter labels all tendon cells in axial tissue (Pryce et al., 2007). To compare the expression domains of *Meox2*$^{+}$ cells in detail, we performed antibody staining for Meox2 and GFP on frozen sections obtained from *Meox2*$^{+/-}$*;ScxGFP* embryos at E12.5. The syndetome exhibited overlapping expression patterns for Meox2^{+} and ScxGFP^{+} cells when observed under a fluorescence microscope (Fig. 5.3A and B, white arrowheads). To investigate if *Meox2* expression was expressed within tendon progenitor cells, we performed confocal analysis. Importantly, we found that ScxGFP+ cells were predominantly found in the syndetome (Fig. 5.3B and E, yellow arrows). In contrast, the majority of *Meox2*$^{+}$ cells were found in the regions of the sclerotome (Fig. 5.3A and D, white arrows). However, there were few double

positive cells (*Meox2*$^{+}$/*ScxGFP*$^{+}$) identified at the interface of the two exclusive domains (Fig. 5.3C and F, yellow arrowheads).

Therefore, these data indicate that *Meox2* is widely expressed in the sclerotome that hosts the chondro-tenogenic progenitors (*Scx*$^{+}$/*Sox9*$^{+}$). It also shows the absence of *Meox2* expression from *ScxGFP*$^{+}$ tendon progenitors at E12.5 in the axial tissue.

5.3.4 NON-OVERLAPPING EXPRESSION OF *MEOX2*$^{+}$ AND *SCX*$^{+}$ CELLS IN THE LIMB TENDON CELLS AT E12.5

Since the ScxGFP reporter only corresponds faithfully to endogenous *Scx* expression for limb progenitors from E13.5 onwards(Pryce et al., 2007), we decided to evaluate the expression of *Scx* and *Meox2* at E12.5 limbs by in situ hybridisation for *Scx* combined with immunostaining for Meox2. Due to lack of *Scx* antibody, we used this feasible approach of combination of in situ hybridisation and immunofluroscence and thereby demonstrating the expression domains of *Meox2*$^{+}$ and *Scx*$^{+}$ tendon cells. We observed that location of *Meox2*$^{+}$ cells adjacent to the *Scx*$^{+}$ cells and surrounding the cartilage primordia (Fig. 5.3.4A, white arrows). Moreover, *Scx* expression was found in dorsal and ventral patches in the mesenchyme of developing limb bud (Fig. 5.3.4B, white arrows) (Schweitzer et al., 2001). In order to achieve the comparison of both cell populations on same section, a false colour image for *Scx* expression was produced using photoshop and merged with the fluorescent image of Meox2 antibody staining. Similar to axial tendon cells at E12.5, limb tendon progenitors also showed non-overlapping expression domains for *Scx*$^{+}$ and *Meox2*$^{+}$ cell populations (Fig. 5.3.4C).

Hence, we can infer that the *Meox2* gene is specifically expressed in the regions that are closely associated with tendon precursors in the limbs at E12.5 but never co-expressed with *Scx*.

5.3.5 EXPRESSION PATTERN OF *MEOX2* IN THE FORELIMB AT E13.5

The severe loss of autopod tendons and the expanded domain of *Scx* transcripts in the metacarpal region at E13.5 (Fig. 4.3.6 in chapter 4), prompted us to examine endogenous *Meox2* expression during tendon cell condensation. The comparison of *Meox2* and *Scx* transcripts in the digit tendons showed partially overlapping expression domains (Fig. 5.3.5A-D, red arrowheads). This could be a plausible explanation for the reduced *Scx* expression in the digit tendons of *Meox2*$^{-/-}$ embryos at E13.5.

Furthermore, *Scx* labelled tendon cells in the zeugopod showed overlapping and non-overlapping expression domains with *Meox2* throughout the proximodistal axis. Specifically, *Meox2* transcripts were detected in the cells immediately beneath the ectoderm and overlaid the broader *Scx*$^{+}$ domains (Fig. 5.3.5, A-D, black arrows). Although tendon progenitor cells in the prospective metacarpal region were clearly identified as a broad patch of *Scx* expression, this cell group does not express *Meox2* transcripts (Fig. 5.3.5, yellow arrows). Interestingly, despite the absence of *Meox2* expression in the prospective metacarpal tendon progenitors, a patterning defect in these tendon cells was found in *Meox2*$^{-/-}$ embryos (see Fig.4.3.6 in chapter 4, red arrowheads).

In summary, the partially overlapping expression patterns of *Meox2* and *Scx* in the distal digit tendons could explain the failure in the formation of these tendons cells and therefore an intrinsic role of *Meox2* in autopod tendon cells. On the contrary, wrist tendon cells and zeugopod tendons do not express *Meox2* suggesting an extrinsic role of *Meox2* for zeugopod tendon development.

5.3.6 CHARACTERISATION OF *MEOX2* EXPRESSION IN THE AUTOPOD AT E13.5

Previously, it was reported that *Meox2*$^{+}$ cells showed non-overlapping expression patterns with *MyoD*$^{+}$ muscle cells in the chick embryos at stage 25 (Reijntjes et al., 2007). Similarly, in the mouse embryos at E13.5, it was observed that the *Meox2-nLacZ*$^{+}$ signal could not be detected in muscle cells (B. Mankoo, unpublished observation). Therefore, here we investigated the expression pattern of *Meox2* using antibody staining on forearm autopod cross sections at E13.5. The results showed strong antibody staining inside the cells surrounding flexor digitorium profundus tendons (Fig. 5.3.6A-D, white arrows). Closer examination revealed that *Meox2* expression was also observed in the regions nearby tendons and cartilage (Fig. 5.3.6C, D white arrowheads). This expression is likely to be from the muscle connective tissue that contributes to maintain a functional musculoskeletal system.

Collectively, *Meox2* is strongly expressed in the cell group located at the circumference of the flexor digitorium profundus tendons. These cells could be tendon sheath, which are an elastic connective tissue that surrounds tendons. Meox2 expression is also in the muscle connective tissue at E13.5.

5.3.7 DISTINCT EXPRESSION PROFILES FOR *MEOX2*$^{+}$ AND *SCXGFP*$^{+}$ IN THE ZEUGOPOD AND STYLOPOD AT E13.5

Examination of transverse sections through the zeugopod and stylopod of a *Meox2*$^{+/-}$*; ScxGFP* embryo at E13.5 revealed the distribution of *Meox2*$^{+}$ cells along the proximodistal axis of the limb segment. Using the Meox2 antibody and the ScxGFP expression to label tendon cells, we found that *Meox2*$^{+}$ cells were positioned adjacent to the surface ectoderm and at the circumference of the cartilage condensations (Fig. 5.3.7A, D and G, white arrows). *ScxGFP* expression was found strongest in the regions surrounding the radius and ulna

in the zeugopod and the humerus in the stylopod (Fig. 5.3.7A, D and G, yellow arrows). The exclusive domains of *Meox2*$^{+}$ and *ScxGFP*$^{+}$ cells were obvious and paralleled our observation recorded for both cell populations at E12.5.

Hence, *Meox2*$^{+}$ cells exhibit non-overlapping expression territories when compared with the ScxGFP^{+} tendon cells.

5.3.8 *MEOX2* IS EXPRESSED IN THE DIGIT TENDONS AT E14.5

By E14.5, tendon differentiation and individualisation was clearly observed in the forelimb by performing whole mount in situ hybridisation for *Scx* in a *Meox2*$^{+/-}$ control embryos (Fig. 5.3.8A). The profound loss of *ScxGFP* expression in the mutants led us to investigate the Meox2 expression in the forelimb autopod at E14.5. Once again we performed immunostaining using the Meox2 antibody on cross section obtained from *Meox2*$^{+/-}$*;ScxGFP* control embryos (Fig. 5.3.8B-H). The observation was performed for the digit tendons and tendon anlagen at the metacarpal level. In the distal autopod segment, the Meox2 protein was strongly confined to the FDP (T1) and EDC (T3) tendon bundles (Fig. 5.3.8B-E, white arrows, white arrowheads). Noticeably, a cell population near the tendon tissue also expressed *Meox2*; however, these were restricted near the tendon periphery (Fig. 5.3.8B-E, pink arrowheads).

Furthermore, at the metacarpal level, the expression patterns of both genes showed striking differences compared to the distal region. A robust expression of *Meox2* was found in the cell population that was present near the cartilage condensation and found in between the cartilage and *ScxGFP*$^{+}$ EDC tendon cells (T3 in Fig. 5.3.8H, white arrowheads). The FDP tendon was found at the wrist region as an expanded ScxGFP^{+} domain and few *Meox2*$^{+}$ cells were interspersed in this region (T1 in Fig. 5 5.3.8H, white arrow).

Together, the molecular diversity among the tendon cells was exhibited by the distinct expression of *Meox2* in the distal and proximal autopod segments.

5.3.9 *MEOX2* EXPRESSION IN THE ZEUGOPOD AND STYLOPOD AT E14.5

We analysed *Meox2* expression and tendon cells by the ScxGFP transgene in the zeugopod and stylopod at E14.5. On the cross sections obtained from *Meox2*$^{+/-}$*;ScxGFP* control embryos, we observed exclusive domains of Meox2 and ScxGFP expression along the proximodistal axis of the forearm (Fig. 5.3.9). We found a close proximity of both cell populations in the zeugopod segment (Fig. 5.3.9C and F, white and yellow arrowheads). Conversely, in the stylopod both of these cell groups are positioned as two distinct cell population that were situated far apart on the section, i.e. *ScxGFP*$^{+}$ cells were found adjacent to the cartilage whereas *Meox2*$^{+}$ cells were located beneath the ectoderm (Fig. 5.3.9G-I, white and yellow arrowheads).

Collectively, these data demonstrate that in the zeugopod and stylopod, *Meox2*$^{+}$ cells represent non-ScxGFP tendon cells, however, a close proximity with ScxGFP labelled tendon cells only in the zeugopod. It also strongly implies the important role of *Meox2* in the modular development of tendons in autopod and zeugopod.

5.3.10 *MEOX2* DERIVED CELLS CONTRIBUTE TO TENDONS AND MUSCLE CONNECTIVE TISSUE

To facilitate a temporal-spatial characterisation of *Meox2* derived cells during key stages of tendon morphogenesis, we utilised mice carrying insertion of a *LacZ* cassette into the *Meox2* locus. The *Meox2-nLacZ* transgene created a null allele of *Meox2* by nuclear localised expression of lacZ gene under the control of *Meox2* regulatory elements. Expression of the *Meox2-nLacZ* transgene faithfully outlines *Meox2* expression in the progeny cell populations inside axial and appendicular tissues throughout developmental stages. As previously shown that Meox2 proteins were recruited in the autopod tendons by E14.5,

using genetic fate mapping approach we hypothesized an intrinsic role of Meox2 in tendon precursors during development.

Therefore, in order to address the mechanisms that account for the tendon phenotype in the absence of *Meox2*, we used Salmon-gal staining for visualising β-galactosidase activity in the cells that were expressing *Meox2-nLacZ* gene. We obtained transverse sections of the forelimb from *Meox2*$^{nLacZ/+}$ embryos at two developmental stages i.e. at E13.5, the phase when tendon cell condensation is ongoing, and at E15.5, when all mature tendon bundles are formed.

Our results show that at both stages, S-gal positive cells were found in EDC (T3) and FDP (T1) tendons in the distal autopod sections (Fig. 5.3.10A and E). FDS tendon development is considered almost complete by E15.5 and it surrounds the FDP tendon tissue in the autopod segment (Watson et al., 2009). S-gal staining was also present in FDS tendon cells (T2 in Fig. 5.3.10E, F, G and J). Furthermore, we found a broader staining of S-gal positive cells in the proximal autopod at both embryonic stages (Fig 5.3.10 B, G and J). This cell group must be classified as loose connective tissue cells due to following reasons: (i) *Meox2-nLacZ* cells are never present in muscle cells as revealed by non-overlapping expression of LacZ^{+} cells and MyHC expression at E13.5, and (ii) *Meox2* derived cells never contribute to cartilage cells of the digits (Fig. 5.3.10A).

In the proximal zeugopod segment, Meox2-nLacZ labelling was observed in all tendon groups and in a broader zone closer to the cartilage condensation that appears to be the muscle connective tissue (Fig. 5.3.10C, D, H, and I). Notably, S-gal staining was not observed in radius and ulna at both developmental stages. This observation is consistent with our line of reasoning that Meox2 progeny do not contribute to the cartilage.

Taken together, these data confirm that β-galactosidase reporter at the *Meox2* locus labelled both dense (tendon) and loose (muscle connective tissue)

connective tissue in the forelimb at E13.5 and E15.5 during embryonic development.

5.3.11 DISRUPTED MUSCLE CONNECTIVE TISSUE IN *MEOX2*$^{nLacZ/nLacZ}$ FOETUS AT E16.5

Our data showed that tendons and muscle connective tissue express the *Meox2-nLacZ*. Next, we investigated the impact of a *Meox2* mutation on muscle connective tissue. Therefore, in *Meox2*$^{nLacZ/+}$ heterozygous control and *Meox2*$^{nLacZ/nLacZ}$ homozygous foetus, we investigated expression of β-galactosidase gene. We obtained forelimb cross-sections at E16.5 and performed X-gal staining to perform LacZ staining. Strong blue cells were observed in all zeugopod tendons of heterozygous controls (Fig. 5.3.11A, B, black arrow). *Meox2-nLacZ*$^{+}$ cells were also detected in the cell population surrounding stained tendons and unstained cartilage cells, which are grouped as muscle connective tissue (Fig. 5.3.11A, B, red arrows). In addition, all the cells surrounding the individual muscle groups in the proximal zeugopod were stained for strong β-galactosidase activity (Fig. 5.3.11D). Noticeably, X-gal staining was never found in muscle fibres (Fig. 5.3.11D, red asterisks). Collectively, these analyses served to demonstrate the contribution of *Meox2* to muscle connective tissue.

Furthermore, examination of the cross sections obtained from *Meox2*$^{nLacZ/nLacZ}$ embryos demonstrated disruption of blue staining in mature tendon bundles in the zeugopod (Fig. 5.3.11C and E). It is noteworthy that, despite the absence of tendons, the same sections showed lacZ (Meox2) positive cells from the muscle connective tissue. However, finding fields of Meox2-nLacZ positive cells in this tissue group showed severe abnormality in patterning around the muscles that resulted in the fusion of individual loosely organised muscle compartments.

Corroborating our genetic fate mapping data clearly indicated that *Meox2* derived cells are recruited to the individuated tendon cells and muscle connective tissue. The absence of lacZ expression from muscle fibres

confirmed the down regulation of the *Meox2* gene in the myoblasts when they have migrated and are positioned as differentiated muscle groups inside the limb territory(Mankoo et al., 1999).

5.3.12 INTERLIMB SOMITES DISPLAY ATYPICAL EXPRESSION OF *TGFβ2* IN *MEOX2*$^{-/-}$ EMBRYOS AT E12.5

TGFβ2 plays a pivotal role in axial tendon development (Pryce et al., 2009). Therefore, we examined the effect of *Meox2* mutation on *TGFβ2* expression by whole mount in situ hybridization in *Meox2*$^{+/-}$ heterozygous controls and *Meox2*$^{-/-}$ homozygous mutants at E12.5 (Fig. 5.3.12). The expression pattern was similar in most regions of the trunk for both mutants and controls (Fig. 5.3.12A and B, yellow arrowheads). Surprisingly, we found an elevated *TGFβ2* expression in interlimb somites that extended towards the distal sclerotome, whereas, in controls, it was restricted only in the medial regions of sclerotome (Fig. 5.3.12A-F, black arrowheads).

Together, our data here represent an unexpected increase in the level of *TGFβ2* expression only in somites present at interlimb level in *Meox2*$^{-/-}$ mutant embryos.

5.3.13 INCREASED *TGFβ2* EXPRESSION IN THE ZEUGOPOD IN *MEOX2*$^{-/-}$ MUTANTS AT E12.5

Given the critical tendon inducing activity of TGFβ2 signalling in limb tendon development, we analysed *TGFβ2* expression in the dorsal and ventral aspects of *Meox2*$^{+/-}$ heterozygous controls and *Meox2*$^{-/-}$ homozygous mutant forelimbs and hindlimbs (Fig. 5.3.13). While, the evidence showed a decrease in Scx expression in TGFb2-/- mutants (Pryce et al., 2009), the Meox2-/- mutants showed similar down regulation of Scx domains at E12.5. We predicted this

down regulation of Scx could be accompanied by decrease in TGFb2 expression. Surprisingly, we found an increase in the *TGFβ2* within the zeugopod in *Meox2*$^{-/-}$ mutant embryos. Importantly, there was a wider expression domain towards the proximal axis of the forelimb segment on dorsal and ventral aspects (Fig. 5.3.13A-D, red arrowheads). Conversely, we observed similar expression patterns in forelimb autopod segments of control and mutant (Fig. 5.3.13A-D, yellow arrows).

Furthermore, in hindlimbs, we found a similar phenotype with the broader expression pattern of *TGFβ2* in the prospective zeugopod (Fig. 5.3.13E-H, red arrows). However, no evident differences were observed in the autopod of hindlimb (Fig. 5.3.13E-H, yellow arrows). In summary, absence of *Meox2* results in an increase in levels and domains of *TGFβ2* expression in zeugopod segments of the forelimb and hindlimb. This observation does not support our proposed model of Meox2 coordinates with TGFβ signalling that up regulates Scx expression in target cells.

5.3.14 *MEOX2* EXHIBITS VARIABLE LEVELS IN RESPONSE TO TGFβ2 SIGNALLING

After our investigation of TGFb2 up regulation in the absence of Meox2, at this point, we proposed an alternative model that TGFb signalling acts upstream on both Scx and Meox2. Therefore, we decided to use an in vitro assay to investigate if Meox2 is regulated by TGFb signalling as previously described for Scx in C3H10T1/2 cell line by Pryce et al., (2009). We stimulated these cells by adding recombinant TGFβ2 protein and performed semi-quantitative PCR analysis of *Scx* and *Meox2* mRNA at various time points up to 24 hours (Fig. 5.3.14). TGFβ2 protein induced robust expression of *Scx* at 8 hours (Fig. 5.3.14A) (Pryce et al., 2009). We found that *Meox2* levels were initially down regulated after addition of TGFβ2 protein; however, the level sharply increased at 24 hours (Fig. 5.3.14B). We found repeatedly this biphasic response of *Meox2* in response to TGFβ2 protein.

5.4 Discussion

Our evidence indicates that the Meox2 protein is not expressed by *Scx*$^{+}$ tendon progenitors at E12.5-13.5 and E14.5 in the zeugopod of the forearm. However, *Meox2*$^{+}$ cells are present in forelimb autopod tendons at E14.5 revealing a pivotal function of *Meox2* in modular limb tendon development. The aim of our study was to identify whether *Meox2* acts extrinsically or intrinsically in tendon progenitor cells during embryonic tendon development. We employed the co-expression analysis for *Meox2* and *ScxGFP* at E12.5, the stage when profound loss of *Scx* transcripts is evident. For this purpose, first we optimised the IHC protocol using the *Meox2* antibody as described in methods section. Moreover, using a lineage-tracing method, an integrative description for *Meox2* contribution during tendon formation and muscle connective tissue is described. Interestingly, in the absence of Meox2, severe loss of cell proliferation resulted, which could account for the reduction in the number of cells being recruited to express *Scx*.

Various signalling molecules have been demonstrated to influence tendon cell commitment, organisation, and differentiation at all stages of tendon development (Brent et al., 2004; Edom-Vovard et al., 2002; Pryce et al., 2009; Lords-Diez et al., 2009; Mendias et al., 2008; Clark et al., 2001; Eloy-Trinquet et al., 2009). Using *Scx* as a marker for tendon cells, in *Tgfβ2*$^{-/-}$*; Tgfβ3*$^{-/-}$ double knock out mouse embryos, a complete loss of all tendons was reported. In addition, *Tgfβ2*$^{-/-}$ mutant embryos exhibit severe disruption in tendon progenitor cells at E12.5 but no change of *Scx* expression observed in *Tgfβ3*$^{-/-}$ mutant embryos (Pryce et al., 2009). However, deletion of TGFβRII, which is single type II receptor utilised by all the members TGFβ superfamily, affected overall tendon development suggesting a wider role of the signalling pathway in tendon morphogenesis.

Likewise, *Meox2*$^{-/-}$ mutant embryos also show first manifestation of axial tendon phenotype at E12.5 whereas limb phenotype was apparent at E12.0 (see chapter 4). All these facts point to the existence of a reciprocal interaction

between *Meox2* and *TGFβ2* signals in regulating *Scx* expression and thereby suggest their significant contributions in maintaining tendon architecture. For this study, we employed analysis of two experimental approaches: (i) *TGFβ2* expression in *Meox2*$^{-/-}$ mutant embryos (ii) response of *Meox2* by over expressing *TGFβ2* proteins under in vitro conditions.

Characterization of *Meox2* expression during tendon development

Given the satisfactory results of *Meox2* expression in limb buds during optimization protocols, we next characterised the expression of *Meox2* from E12.5-14.5 that are the key developmental phases to form load bearing functional tendons. We then compared these expression patterns with ScxGFP fluorescence to identify tendon progenitor cells. Thereby, we proposed two alternative hypotheses: (i) *Meox2* is co-expressed in *ScxGFP*$^{+}$ cells and thereby causing an intrinsic defect in tendon cells at E12.5 in the knockouts. (ii) Alternatively, *Meox2* is never co-expressed with *ScxGFP*$^{+}$ tendon cells and is part of extrinsic cues necessary for normal tendon morphogenesis. Therefore, we used confocal analysis to identify co-expression of both genes in the tendon cells at E12.5. Our analysis in the syndetome demonstrated that the majority of the *Meox2*$^{+}$ cells are located in the sclerotome and very few cells show co-expression with *ScxGFP*$^{+}$ cells in syndetome.

Furthermore, the study that generated the ScxGFP reporter mouse has shown an expanded GFP expression in the early limbs bud (E10.5-12.5) (Pryce et al., 2009). Therefore, for our limb tendon analysis at this stage, we combined *Scx* in situ hybridization with Meox2 antibody staining on limb cross sections. The non-overlapping domains for both genes are evident (Fig. 5.3.2). However, we speculate that our observations for double positive cells from this method could be challenging. This is because the dense colour precipitates from the whole mount in situ hybridisation protocol in a cell could potentially mask the GFP signals that are localised in the cytoplasm. To ascertain our current observation for limbs at E12.5, in future we will perform double whole mount in situ

hybridization for both genes using fluorescent probe to compare the expression domains using a confocal microscope. Alternatively, the limb tissue specimens can be doubly labelled with Scx and Meox2 antibodies, which will provide a robust conclusion for the limbs. Due to the lack of a Scx antibody, the later approach is not possible at present.

In order to gain a better understanding of *Meox2* expression during further developmental stages of the tendons, we compared whole mount in situ hybridizations for *Meox2* and *Scx* in forelimbs of *Meox2*$^{+/-}$ control embryos at E13.5. The analysis of these results suggests a distinct role of *Meox2* in modularity during tendon development. Both transcription factors showed partially overlapping expression domains in the distal autopod tendon cells, which suggest an intrinsic requirement of *Meox2* by digit tendon precursors. Likewise, the subectodermal mesenchyme region showed overlapping expression patterns in the presumptive zeugopod segment.

Although overlapping within the proximal limb, *Scx* mRNA was expressed in a considerable wider region than *Meox2*. Additionally, the *Scx*$^{+}$ wrist tendon progenitors never expressed *Meox2* (Fig. 5.3.3, yellow arrows). These wrist tendon cells connect the autopod tendons to their corresponding muscle counterparts in the proximal limb region (Huang et al., 2015b). Similar to autopod tendon precursors, the induction of wrist tendon cells is independent of the cues from the muscle cells, however, the maintenance and elongation towards the proximal zeugopod is dependent on the signals derived from muscle cells (Huang et al., 2015b; Huang et al., 2013). Despite the absence of *Meox2* in this unique tendon population, we found severe irregularity in the organisation of wrist tendon anlagen in *Meox2*$^{-/-}$ mutant embryos at E13.5 (see Fig. 4.3.6, red arrowheads). This suggests an extrinsic role of *Meox2* in tendon development whereby *Meox2*$^{+}$ non-tenogenic cells are essential for continuous maintenance of the wrist tendon cells.

The presence of *Meox2*$^{+}$ in non-tenogenic cells is apparent throughout the proximodistal axis that includes zeugopod and stylopod of the developing limb at E13.5 (Fig. 5.3.4 and 5.3.5). Whilst the specific identity of these *Meox2*$^{+}$ cells

was not determined at this point, the fact they are present at the circumference of condensed tendons e.g. in the digits and nearby periphery of tendons suggest that they could be muscle connective tissue cells. Moreover, in the zeugopod and stylopod, cells that populate the regions adjacent to the surface ectoderm express *Meox2* whereas tendon cells (ScxGFP^{+}) are present near the cartilage condensations. This analysis once again exposed an inevitable involvement of *Meox2* in modular limb tendon development due to its distinct expression patterns in autopod, zeugopod and stylopod.

By E14.5, the majority of the *Meox2*$^{+}$ cells are integrated into the autopod tendon cells in the distal digit segment (Fig. 5.3.6). Conversely, the tendon cells at the metacarpal level do not express *Meox2* and this expression pattern persisted in the zeugopod and stylopod regions even at this stage (Fig. 5.3.7).

Altogether, on one hand, *Meox2* plays an intrinsic role for the digit tendon development. On the other hand, for normal wrist tendons and zeugopod tendons, *Meox2* provides extrinsic cues for their maintenance and growth. Similar differential regulations of tendon development is also observed in various mouse models. For instance, *Sox5* and *Sox6* transcription factors are shown to be essential for autopod tendon development only. In *Sox5*$^{-/-}$*;Sox6*$^{-/-}$ double mutant embryos at E12.5, due to a failure in cartilage formation, all autopod tendons are lost, on the contrary, zeugopod tendons remained unaffected (Huang et al., 2015b). This study has shown for the first time a positive cooperative action of cartilage on normal autopod tendon induction. The authors concluded that cartilage is not only necessary but also sufficient for the autopod tendon formation. In the same line of reasoning, it would be worth identifying the mechanisms by which *Meox2* coordinates with *Sox5* and *Sox6* genes for normal digit tendon formation and therefore could be the topic of future investigations.

The *Meox2*$^{+}$ cell lineage contributes to normal tendon development and muscle connective tissue

The proper insight into the consequences of *Meox2* loss-of-function on muscle-tendon interactions and muscle connective tissue was revealed by inserting the *LacZ* gene into the *Meox2* locus (see methods section). The analysis of *Meox2-nLacZ* at embryonic stages revealed that the *lacZ*$^{+}$ (*Meox2*$^{+}$*)* cells contribute to the establishment of tendons and muscle connective tissue at E13.5 (Fig. 5.3.8). In general, the connective tissue can be defined as cells rich in proteoglycan and collagen fibers. Categorically using this definition, they can be divided into two subgroups: (i) dense fibrous connective tissues i.e. tendons and ligaments, which aid in joining muscle to the bone and bone to bone, respectively, (ii) loose fibrous connective tissue i.e. muscle connective tissue and fascia which encompass muscle fibers and individual muscle groups (Gray et al., 2005).

Several studies have shown that the limb mesenchyme contains pools of multipotent progenitor cells that give rise to both categories of connective tissues and are present adjacent to the muscle and cartilage progenitors (Kardon, 1998; Oliver et al., 1995; Suzuki and Kuroiwa, 2002). These lateral plate mesoderm derived connective tissue are shown to regulate various aspects of limb muscle development and patterning (Chevallier and Kieny, 1982) (Chevallier and Kieny, 1982; Grim and Wachtler, 1991; Hasson et al., 2010; Kardon et al., 2003; Mathew et al., 2011; Swinehart et al., 2013).

Furthermore, muscle connective tissue actively coordinates muscle-tendon interactions during embryonic morphogenesis (Hasson et al., 2010; Kardon et al., 2003; Swinehart et al., 2013). All tendons and ligaments express *Scx* that is widely acknowledged as a faithful marker for distinguishing events in dense connective tissue (Schweitzer et al., 2001). Likewise, the *Tcf4* transcription factor, a member of the Tcf/Lef family was identified as a marker for muscle connective tissue (Kardon et al., 2003). A critical role for the muscle connective tissue during myogenesis was demonstrated using *TCF4*, which is a

downstream regulator of the canonical *Wnt-β-catenin* pathway (Mathew et al., 2011). The *TCF4*-dependent signal from the MCT was shown to regulate the muscle fibre differentiation from embryonic to fetal myofibers. In another study, Hasson et al. (2010) reported the forelimb muscle patterning defects including muscle splitting in the absence of *Tbx5* gene. They further reported that *Tbx5* is expressed in the muscle connective tissue and regulates muscle development in a cell non-autonomous manner.

Our lineage tracing data suggest that *Meox2* is expressed by both categories of connective tissues. In the autopod segment, all prominent tendon groups e.g. FDP, FDS and EDC tendons show strong staining for *Meox2-nLacZ* at embryonic stages beginning from E13.5. Moreover, β-galactosidase activity is widely detected in the proximal tendon cells of the zeugopod. Therefore, in dense connective tissue i.e. tendons, *Meox2* seems to play an essential role in the specification of the committed tendon progenitors cells. Interestingly, the close proximity of *Meox2*$^{+}$ cells near the autopod tendons at E13.5 (Figure 5.3.4) and the strong *Meox2-nLacZ*$^{+}$ (Figure 5.3.8) in these tendon groups strongly suggests that *Meox2* expressing cells are later on recruited for autopod tendon formation. Indeed, by E14.5, *Meox2*$^{+}$ cells are detected in digit tendons (Figure 5.3.6).

Additionally, we demonstrated that the differentiated cartilage cell population are not a derivative of the *Meox2* progeny. Despite sharing common origins with tendon progenitor cells in limb mesenchyme, chondrocytes never show β-galactosidase activity at any embryonic stages and hence specify the role of *Meox2* as restricted to tendons and muscle connective tissue only.

By E15.5, defined regions of *Meox2-nLacZ* expression corresponded to the FDS tendon cup formed around FDP tendon cells. In this scenario, *Meox2* performs an intrinsic role in tendon genesis whereby it is involved in commitment and specification of tendon progenitor cells. In addition, the loss of this early *Meox2* dependent tendon precursor specification caused both embryonic and post-natal tendon defects (see chapter 3 and 4). On the contrary, continuous expression of *Meox2* is required for the proper

establishment and functioning of muscle connective tissue. Hence, an indispensable requirement of *Meox2* in muscle connective tissue during muscle patterning and tendon formation in the limbs are concluded.

The possibility of *Meox2* playing a central in tendon cell morphogenesis was further established by carrying out analysis in *Meox2*$^{nLacZ/+}$ heterozygous controls and a *Meox2*$^{nLacZ/nLacZ}$ homozygous mutant fetus at E16.5 that provided two key informations. First, all tendon groups show strong β-galactosidase activity. The majority of tendons were lost in *Meox2*$^{nLacZ/nLacZ}$ embryos, the stage when morphogenesis of all tendon groups are achieved and the muscle-tendon units are well-established. Some tendon tissue that was present showed reduction in tissue mass and fusion of tendon bundles (Fig. 5.3.9).

Second, the loose connective tissue (fascia and muscle connective tissue) was present despite the insertion of the *LacZ* gene at both allelic loci disrupting *Meox2* gene function. However, severe patterning defects of this tissue are evident in the mutants. Strikingly, the *Meox2* mutation in the muscle connective tissue caused intermixing and disruption of individual muscle compartments. Evidently, it demonstrates an important intrinsic function of *Meox2* from muscle connective tissue to regulate muscle patterning and organisation.

Altogether, our data provide strong evidence that the muscle phenotype in *Meox2* mutants is due an abnormality in the muscle connective tissue (see chapter 3 and (Mankoo et al., 1999). It also indicates both intrinsic and extrinsic actions of *Meox2* during tendon development and muscle connective tissue specification.

Meox2 is essential for normal cellular proliferation but not cell death during tendon morphogenesis

The down regulation of *ScxGFP*$^{+}$ tendon cells at E12.0 suggests that the *Meox2* gene act as an even earlier regulatory factor to dictate tendon cell commitment compared to TGFβ signalling and the *Scx* transcription factor. Once specified, these cells no longer need *Meox2* in zeugopod tendons but exhibit a continuous wave of recruitment in autopod tendon formation. During development of a tissue, it is worth considering cell proliferation and cell death that occur in synchronisation to achieve a final functional form of that tissue. Therefore, this fact along with our data on the failure of muscle connective tissue organisation and tendon progenitor specification led us to perform analysis for both important cellular events in *Meox2*$^{-/-}$ mutant embryos. We concluded severe loss of cellular proliferation at E12.5, which occurred due to loss of Meox2 function.

This strongly implies that *Meox2* regulates tendon genesis by promoting cell proliferation and thereby assists in additional recruitment of tendon progenitor cells at the site of condensation. However, there was an overall reduction in cell proliferation among all cell types across the entire compartment in somites suggesting a significant role of Meox2 in cell cycle progression during embryogenesis. Nonetheless, functional roles of *Meox2* in promoting cell cycle events need a rigorous examination during embryonic development.

Moreover, in the absence of *Meox2*, reduction in *ScxGFP*$^{+}$ cells in somites is not due to activation of the cell death machinery at E12.5 (see Fig. 4.3.11 and 5.3.11). We found no change in apoptotic pathways in the mutants at this embryonic stage. Taken together, one of the aspects by which *Meox2* is required for tendon development is through regulating mitotic proteins in the cell cycle of tendon cell proliferation. It also implies that early *Meox2* expression represents a commitment to tendon lineage at E12.5 by regulating only cell proliferation and not cell death.

Increase of *TGFβ2* in interlimb somites in *Meox2*$^{-/-}$ embryos at E12.5

To gain insight into the cooperative molecular functions of *Meox2* and TGFβ2 signals, it was important for us to demonstrate that both molecules are regulating *Scx* expression in a complementary manner. Therefore, to begin with, we sought to validate the expression patterns of TGFβ2 in the absence of *Meox2* at E12.5. Surprisingly, our results demonstrated an increase in TGFβ2 levels in the interlimb somites of *Meox2*$^{-/-}$ mutant embryos. TGFβ2 expression pattern were similar in cervical (contribute towards tongue, neck and shoulder muscles) and lumbar (opposite the hindlimbs) somites.

Various studies have shown that along the rostrocaudal body axis, somites at each levels exhibit some variation in morphological characteristics (Franz et al., 1993; Smith et al., 1994; Tajbakhsh et al., 1996). Interlimb somites differ from the somites located opposite to the limbs that express *Pax3*, *c-met*, *Meox2* and *Lbx1* and thereby leave the lateral dermomyotome and migrate into the developing limb bud (Bober et al., 1991; Mankoo et al., 1999). As a result, the lateral dermomyotome of somites at the limb level is reduced compare to the somites present at the interlimb levels. The migratory behaviour of somite cells opposite to the limb was accompanied by apoptosis in the lateral dermomyotome during later developmental stages of forelimb level somites (Tosney, 1994). From these evidence, we can attempt to interpret the differences found in *TGFβ2* expression only in interlimb somites of *Meox2*$^{-/-}$ mutant embryos.

However, this contradicts our initial hypothesis, as our assumptions were that at E12.5, the expression pattern of TGFβ2 in *Meox2*$^{-/-}$ embryos and *Meox2* in *TGFβ2*$^{-/-}$ mutant embryos would be normal in somites and limbs. Thereby, we predicted a concerted action of *Meox2* and TGFβ2 in providing means of guiding the developing tendons from the site of induction to their appropriate insertions. Furthermore, evidence suggests a complex interaction between *Meox2* and TGFβ signals in epithelial cell biology (Valcourt et al., 2007). Tgfβ1

derived signals synergised with ectopic *Meox2* to arrest proliferation of epithelial cells and, conversely, *Meox2* partially caused blockage of TGFβ-1 derived epithelial-to-mesenchymal transition (EMT) in cultured keratinocytes (Valcourt et al., 2007). Therefore, our results should be considered novel in the course of development, but are unexpected.

Moreover, during development, TGFβ2 expression is localised in the medial domains of the sclerotome that act as primitive sites of cartilage condensation (Pryce et al., 2009). It was shown that this compartment contains a multipotent cell population that expresses both *Scx* and *Sox9* (Sugimoto et al., 2013). Conversely, *TGFβ2* expression was never located in the syndetome, which hosts only $Scx^{+}/Sox9^{-}$ tendon precursors (Pryce et al., 2009; Sugimoto et al., 2013a; Sugimoto et al., 2013b). Moreover, TGFβ2 levels are upregulated in the presumptive zeugopod and stylopod of $Meox2^{-/-}$ mutant limbs at E12.5 (Fig. 5.3.12). On the contrary, the *Meox2* mutation does not affect *TGFβ2* expression in the autopod segment. Finally, unlike in epithelial cells, we could not detect any down regulation of TGFβ2 in the absence of *Meox2*.

Previously, Pryce and co-worker (2009) indicated that the prechondrogenic mesenchymal condensation along the proximodistal axis of the limb bud shows robust expression of *TGFβ2*. In the same work, the authors described a partial but not complete overlap of *TGFβ2* with differentiating muscles and tendon progenitor cells in the limbs. Evidence suggests that the distal tendon progenitor cells of the limb never express *TGFβ2* at E12.5. In the same way, we found non-overlapping expression of *Meox2* and *Scx* in the dorsal and ventral domains of the limb. Collectively, we can deduce two possible ways of interaction between *Meox2* and *TGFβ2* during embryonic development: (i) in a growing limb bud, $Meox2^{+}$ muscle connective tissue and $TGFβ2^{+}$ cartilage cells work in conjunction to guide the Scx^{+} tendon precursors for their organisation and proper insertions to establish a functional musculoskeletal system (Pryce et al., 2009). (ii) During proximodistal differentiation of limb bud and in somites, $Meox2^{+}$ cells in turn also restrict $TGFβ2^{+}$ cells to achieve an integrated musculoskeletal system by limiting $TGFβ2^{+}$ domains.

In the same line of reasoning, we could propose the involvement of *Meox2* along with TGFβ2 for the active recruitment of a second stream of induced tendon progenitor cells. This is because all tendon groups and muscle connective tissue at later embryonic tendon development stages are derived from the Meox2 progeny (see Fig. 5.3.8 and 5.3.9). Nonetheless, in future it would be useful to analyse *Meox2* expression in *TGFβ2*$^{-/-}$ mutant embryos at E12.5. This will help us to conclude if *Meox2* functions upstream of TGFβ2 for regulating *Scx* expression during tendon development.

Transient expression of *Meox2* in response to TGFβ signalling

In this study, effect TGFβ signalling on *Meox2* expression was evaluated using C3H10T1/2 fibroblast cells. We found ambiguous patterns of *Meox2* expression at various time points of the experiment. Initially, upon stimulation of cultured cells, *Meox2* levels were downregulated until 8 hour after which its expression was elevated. We found this behaviour analogous to observations performed in cultured epithelial cells (Valcourt et al., 2007). The authors described that the cytostatic response of TGFβ1 caused an initial suppression of *Meox2* expression but at later time points, a sharp elevation of *Meox2* levels occurred. Furthermore, the functional experiments in keratinocytes suggested *Meox2* forms a complex with Smad proteins and thereby acts as a downstream effector of TGFβ1 induced cell growth arrest.

Collectively, evidence so far suggest a biphasic interaction between *Meox2* and TGFβ signals, however, our next step will be to analyse the expression pattern of known downstream effectors of the TGFβ pathway in *Meox2*$^{-/-}$ mutant embryos e.g. Smad proteins. Thereby, for future studies, we hypothesised that *Meox2* is involved in restricting TGFβ signalling pathways and thereby promotes cellular proliferation during embryonic development.

5.5 Conclusions

In summary, *Meox2* plays an intrinsic role for the distal autopod tendon development, whereas, it exhibits a key extrinsic role for the zeugopod tendons. *Meox2* is also necessary for normal cell proliferation. Additionally, using lineage tracing, we concluded that Meox2 derived cells are incorporated in both tendons and muscle connective tissue. Moreover, our data here represent an unexpected increase in the level of *TGFβ2* expression only in the somites present at interlimb level in *Meox2*$^{-/-}$ mutant embryos. Also, an increase in levels and domains of *TGFβ2* expression in zeugopod segments of the forelimb and hindlimb. There is a biphasic interaction between *TGFβ2* and Meox2 under *in vitro* conditions.

Fig 5.3.1 Failure of cell proliferation in Meox2$^{-/-}$ embryos at E12.5

Sagittal sections were obtained from trunk of a Meox2+/-;ScxGFP (A and C); Meox2-/-;ScxGFP (B and D) and Meox2+/- (E and F) at E12.5. (A-D) Immunostaining was performed to identify actively proliferating cells by Ki67 antibody. ScxGFP fluorescence marked tendon progenitor cells in the syndetome. The profound loss of proliferating cells occurred due to Meox2 mutation. (E and F) An equivalent sagittal section from Meox2+/- embryo was stained using Meox2 antibody. White arrows indicate the Meox2+ expression from a distinct cell population outside the syndetome in E. NT, neural tube.

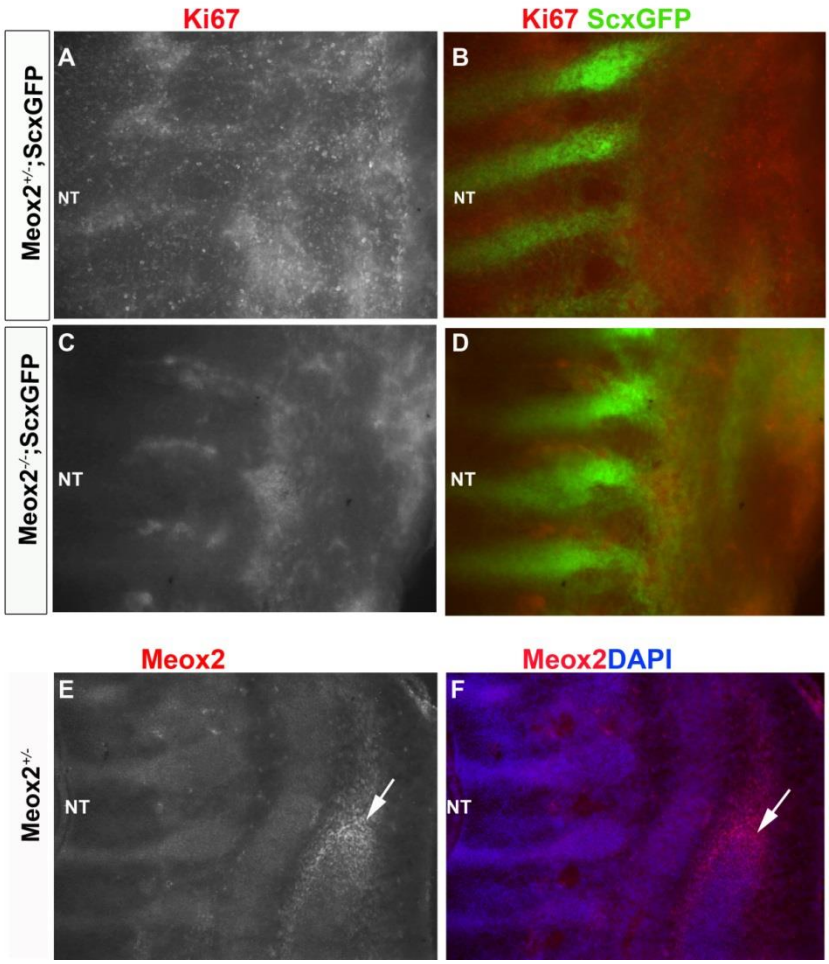
Ki67
Ki67 ScxGFP
Meox2+/-;ScxGFP
Meox2-/-;ScxGFP
A
B
C
D
NT
Meox2
Meox2DAPI
Meox2+/-
E
F

Fig 5.3.2 Normal apoptosis in *Meox2*$^{-/-}$ embryos at E12.5

Sagittal sections were obtained from trunk of a Meox2$^{+/-}$;ScxGFP (A, B and C); Meox2-/-;ScxGFP (D, E and F) at E12.5. Immunostaining was performed for activated caspase 3 by antibody as marker for apoptotic cell death. ScxGFP fluorescence marked tendon progenitor cells in the syndetome. (A and D) high level of apoptosis is observed near neural tube in control and mutant embryos. (B and E) Expression of Caspase 3 staining is found normal in the somite of heterozygous controls and homozygous mutants. (C and F) The caspase 3 staining is merged with ScxGFP expression to detect tendon cells. White arrowheads indicate the expression of Caspase 3 from the cells undergoing apoptosis. nt, neural tube.

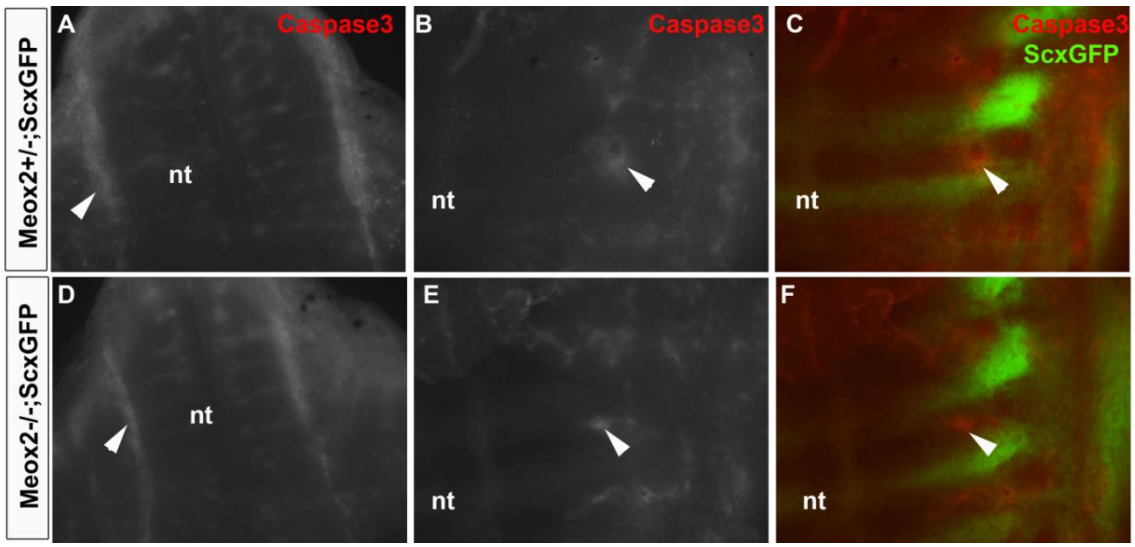
Meox2+/-;ScxGFP
Meox2-/-;ScxGFP
A
Caspase3
nt
B
Caspase3
nt
C
Caspase3
ScxGFP
nt
D
nt
E
nt
F
nt

Fig 5.3.3 Majority of *Meox2*$^{+}$ cells are distributed in the sclerotome

Longitudinally sections from a *Meox2*$^{+/-}$*;ScxGFP* embryo at E12.5 was obtained (A-I). Immunostaining was performed using specific antibodies for *Meox2* and GFP while nuclei were stained with DAPI. (A-C) show overlapping expression domains of *Meox2*$^{+}$ and *ScxGFP*$^{+}$ under fluorescence microscope. The boxes I and II in C show the two regions of the section analysed under confocal microscope. (D-I) show the higher magnification of the same section observed in confocal microscope. *ScxGFP*$^{+}$ cells mark syndetome region in the somite. *Meox2*$^{+}$ cells were mostly located in the sclerotome. White arrowheads in A-C indicate overlapping *Meox2*$^{+}$ and *GFP*$^{+}$ cells; white arrows in D,F and G indicate *Meox2*$^{+}$ cells; yellow arrows in E,F and H show *ScxGFP*$^{+}$ cells; yellow arrowheads show few *Meox2*$^{+}$*;ScxGFP*$^{+}$ double positive cells. NT, neural tube; DRG, dorsal root ganglion.

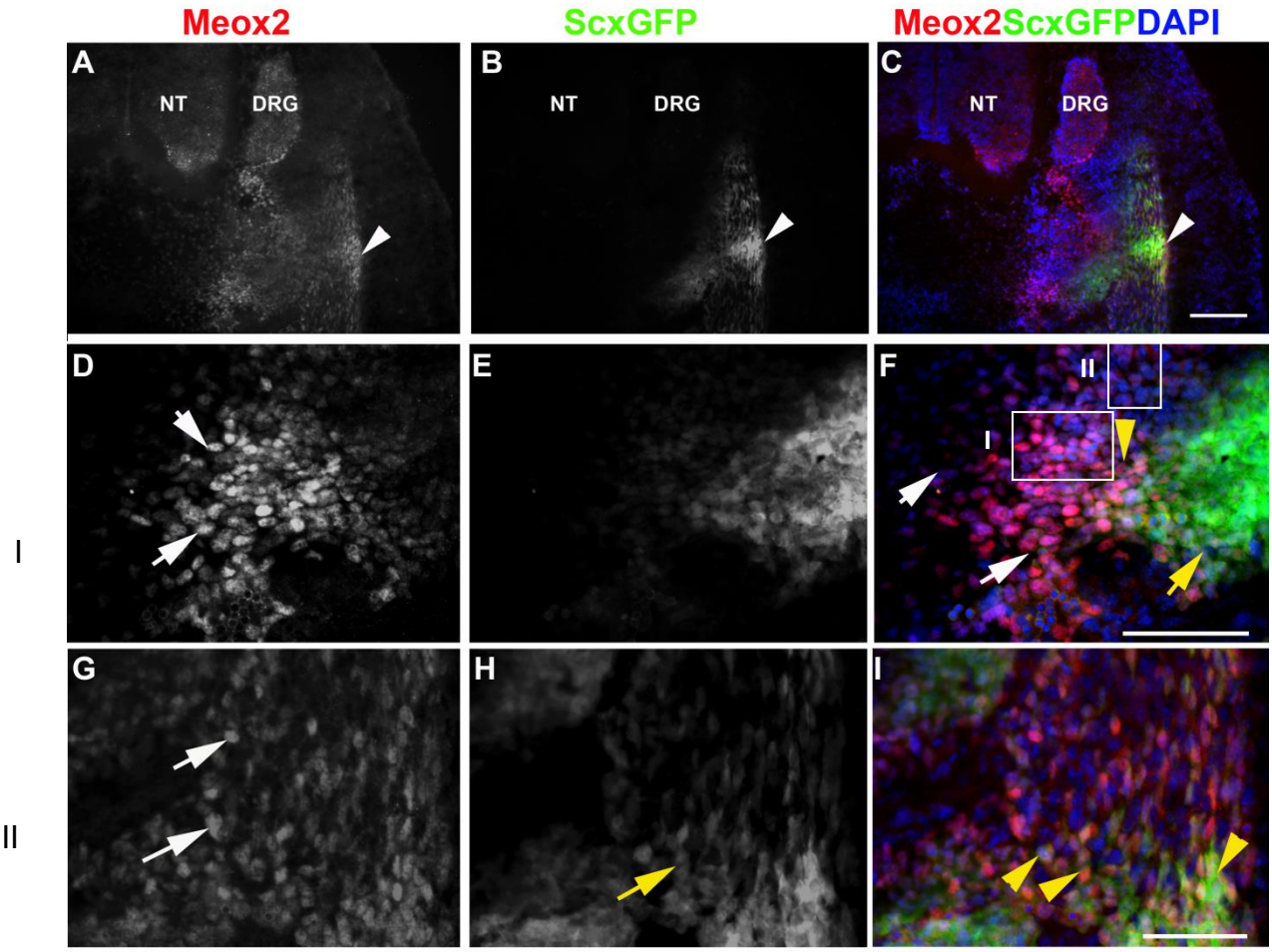
Meox2
ScxGFP
Meox2ScxGFPDAPI
A
NT
DRG
B
NT
DRG
C
NT
DRG
D
E
F
II
I
G
H
I
I
II

Fig 5.3.4 *Meox2*$^{+}$ is not expressed in Scx+ domains in the limbs at E12.5

The transverse section of limbs from an E12.5 *Meox2*$^{+/-}$ embryo was obtained (A-C). In situ hybridisation for Scx was performed to identify tendon progenitor cells in the limb (B) and immunofluorescence for *Meox2* using an antibody was performed (A). The non-overlapping expression domains of *Meox2* and *Scx* were evident on merged image (C). White arrowhead indicates *Meox2*$^{+}$ cells surrounding cartilage primordia; white arrows indicate dorsal and ventral patches of mesenchyme positive for *Scx* transcripts. C, cartilage.

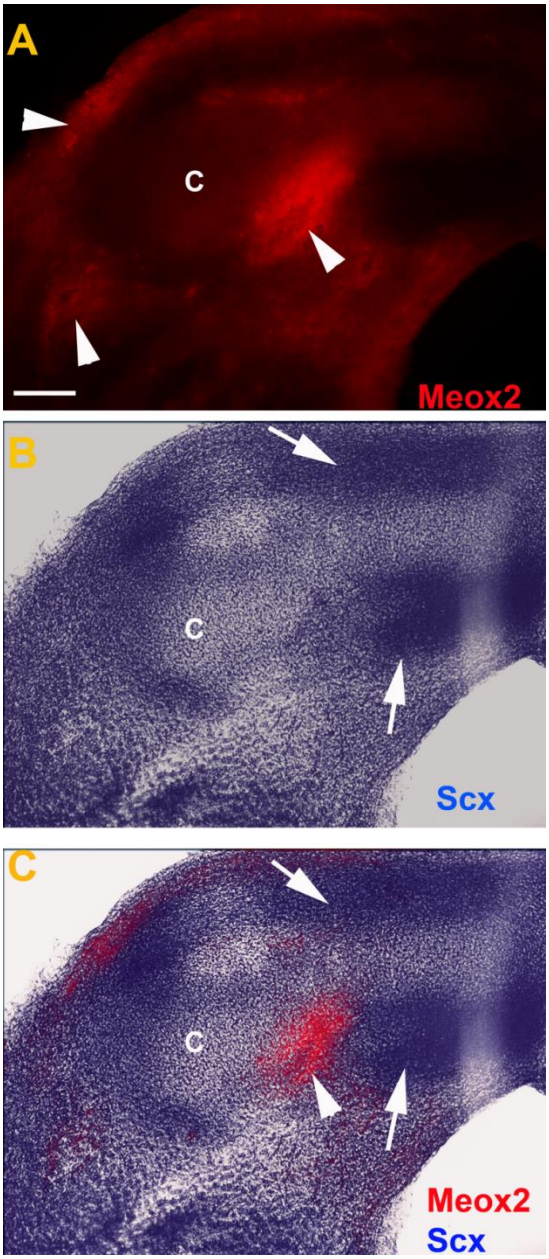
A
C
Meox2
B
C
Scx
C
C
Meox2
Scx

Fig 5.3.5 Expression analysis of *Meox2* and *Scx* in the forelimbs at E13.5

(A-D) Whole mount in situ hybridization of the forelimbs using antisense probe for Meox2 and Scx at E13.5. (A and B) show the dorsal aspect of limbs while (C and D) show the ventral aspects of limbs. Black arrows show similar region of expression in the zeugopod. Red arrows in the autopod show expression of Meox2 transcripts in the digit tendon cells. Yellow arrows represent *Scx* expression in the tendons of metacarpal region of the limb.

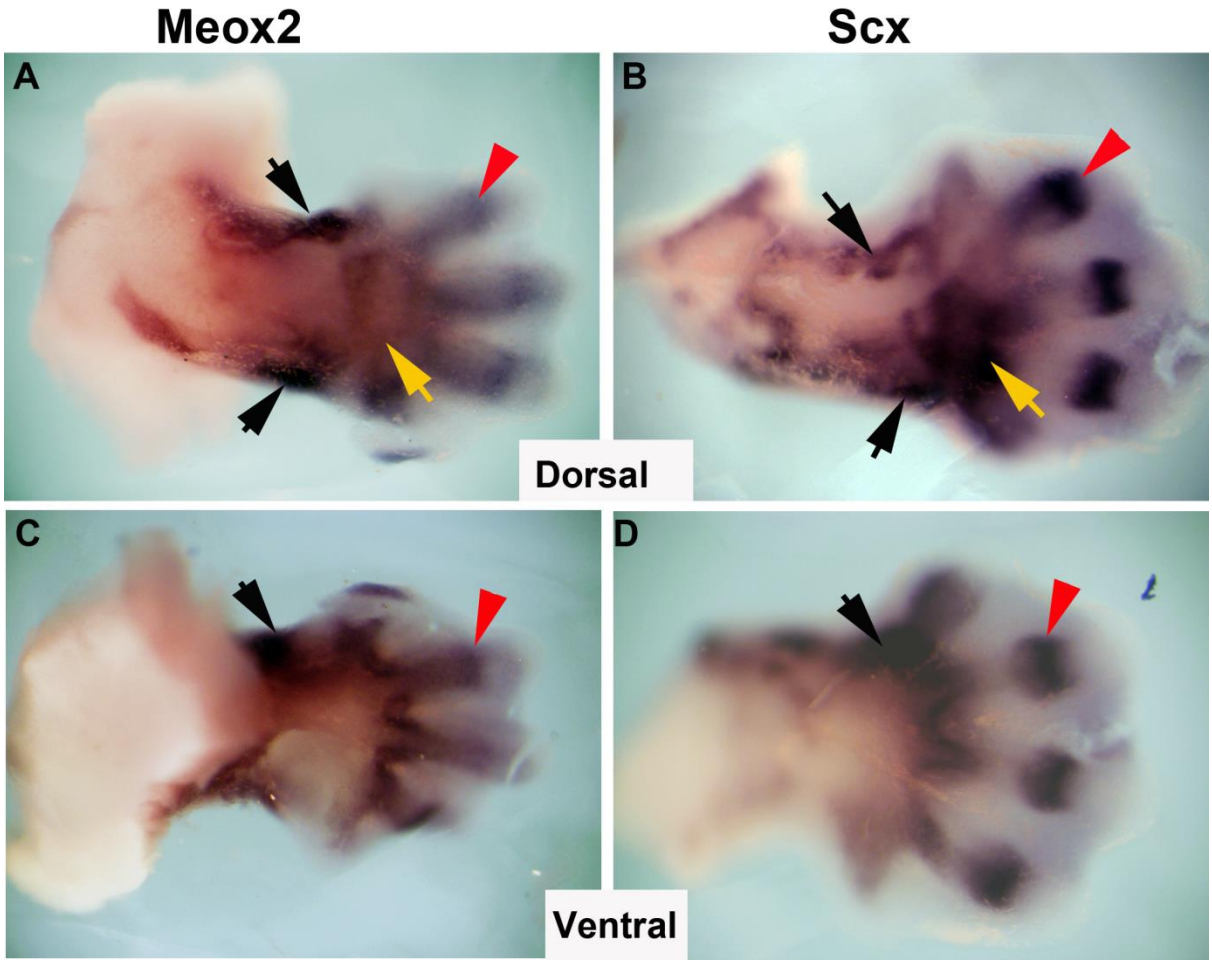
Meox2
Scx
A
B
Dorsal
C
D
Ventral

Fig 5.3.6 *Meox2* expressing cells surround the condensed tendon bundles in the autopod at E13.5

(A-D) Transverse sections of limbs from an E13.5 *Meox2*$^{+/-}$ embryo were stained for Meox2 expression using an antibody. FDP tendons cells were visibly condensed (T1). The higher magnification of a tendon tissue in C and D is from the boxed regions in A and B. *Meox2*$^{+}$ cells were confined at the circumference of tendon tissue and were found in muscle connective tissue. White arrowheads indicate *Meox2*$^{+}$ cells surrounding cartilage primordial and connective tissue; white arrows indicate *Meox2*$^{+}$ cells surrounding tendon condensation; white arrowheads show Meox2+ cells in muscle connective tissue; C, cartilage; T1, flexor digitorum profundus.

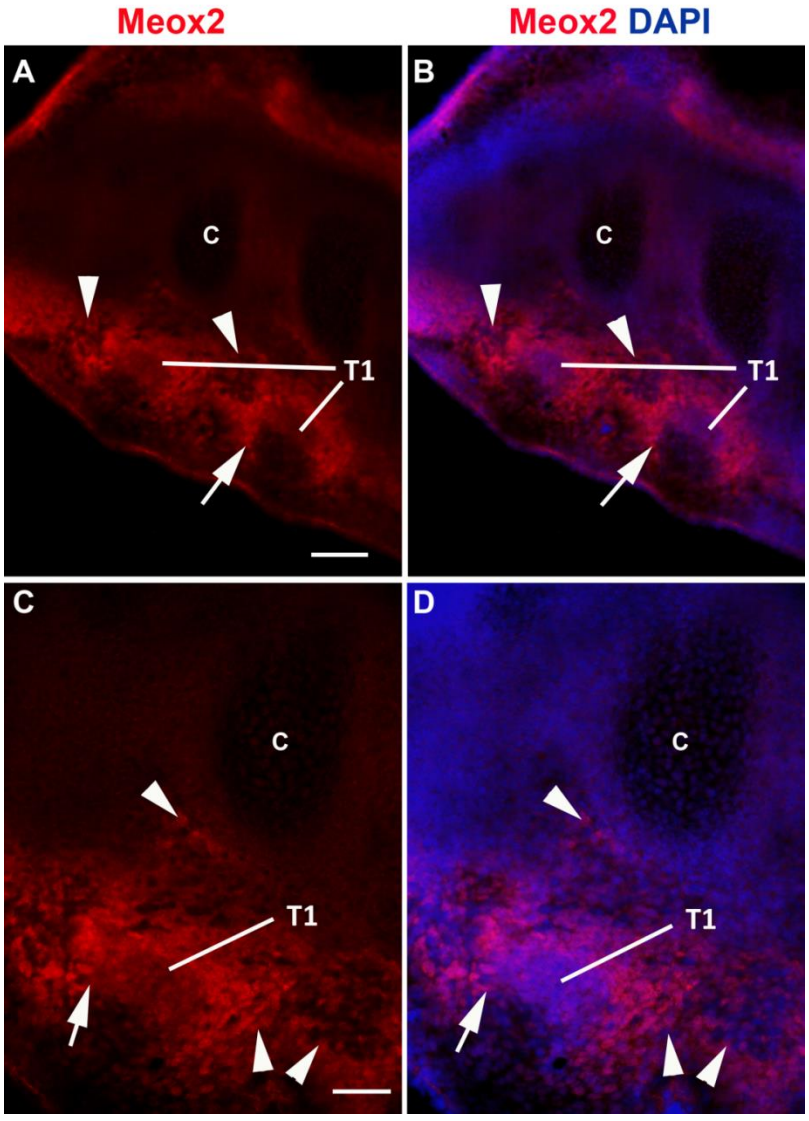
Meox2
Meox2 DAPI
A
B
C
D
C
T1

Fig 5.3.7 Non-overlapping expression of M*eox2+ and ScxGFP+* in the zeugopod and stylopod at E13.5

The transverse section of limbs from an E13.5 *Meox2*$^{+/-}$;*ScxGFP* embryo was obtained (A-D). Immunofluorescence for *Meox2* using an antibody was performed (red) and tendons cells were identified using ScxGFP expression. The higher magnification of a tendon tissue in C and D is from tagged panel in A and B. The *Meox2*$^{+}$ was confined in outer layer of tendon tissue and was found in soft connective tissue. White arrowhead indicates *Meox2*$^{+}$ cells surrounding cartilage primordial and connective tissue; white arrows indicate *Meox2*$^{+}$ cells surrounding tendons; yellow arrowhead show tendons; C, cartilage; D, distal; P, proximal

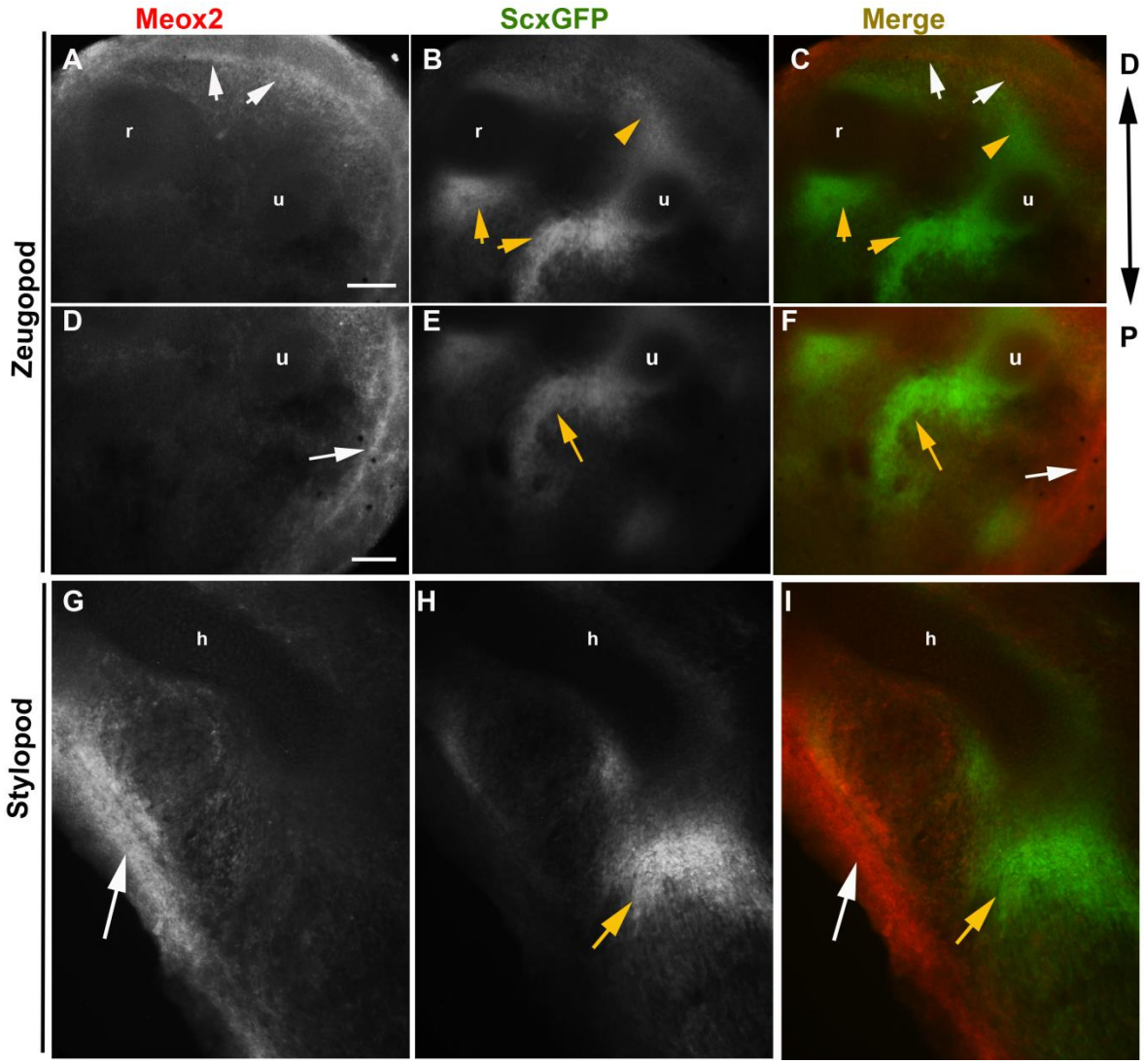
Meox2
ScxGFP
Merge
A
B
C
D
E
F
G
H
I
r
u
h
Zeugopod
Stylopod
D
P

Fig 5.3.8 Distinct expression of Meox2 in distal and proximal autopod tendon compartment at E14.5

(A) Whole mount in situ hybridisation for *Scx* in a Meox2$^{+/-}$ embryo showing individuated tendon groups in the forelimb. (B-E) Immunostaining with antibody for Meox2 (red) and nuclei stained with DAPI (blue) on a transverse section from the digit of a Meox2$^{+/-}$ embryo. The level of section (1) obtained is indicated in panel (1 in A). The boxed areas in B and C is shown in higher magnification in D and E. (F-H) Transverse section through the limb of Meox2$^{+/-}$;ScxGFP was obtained at the metacarpal level indicated in figure (2 in A). Meox2+ cells in red identified by using antibody staining and ScxGFP expression for tendon cells. White arrowheads in B and C indicate EDC tendons (T3); white arrows in B and C show FDP tendons (T1); pink arrowheads in B-E show Meox2 expression in muscle connective tissues; white arrowheads in F and H Meox2+ cells adjacent to EDC tendon (T3) and white arrowheads in F and H show FDP tendons. C, cartilage

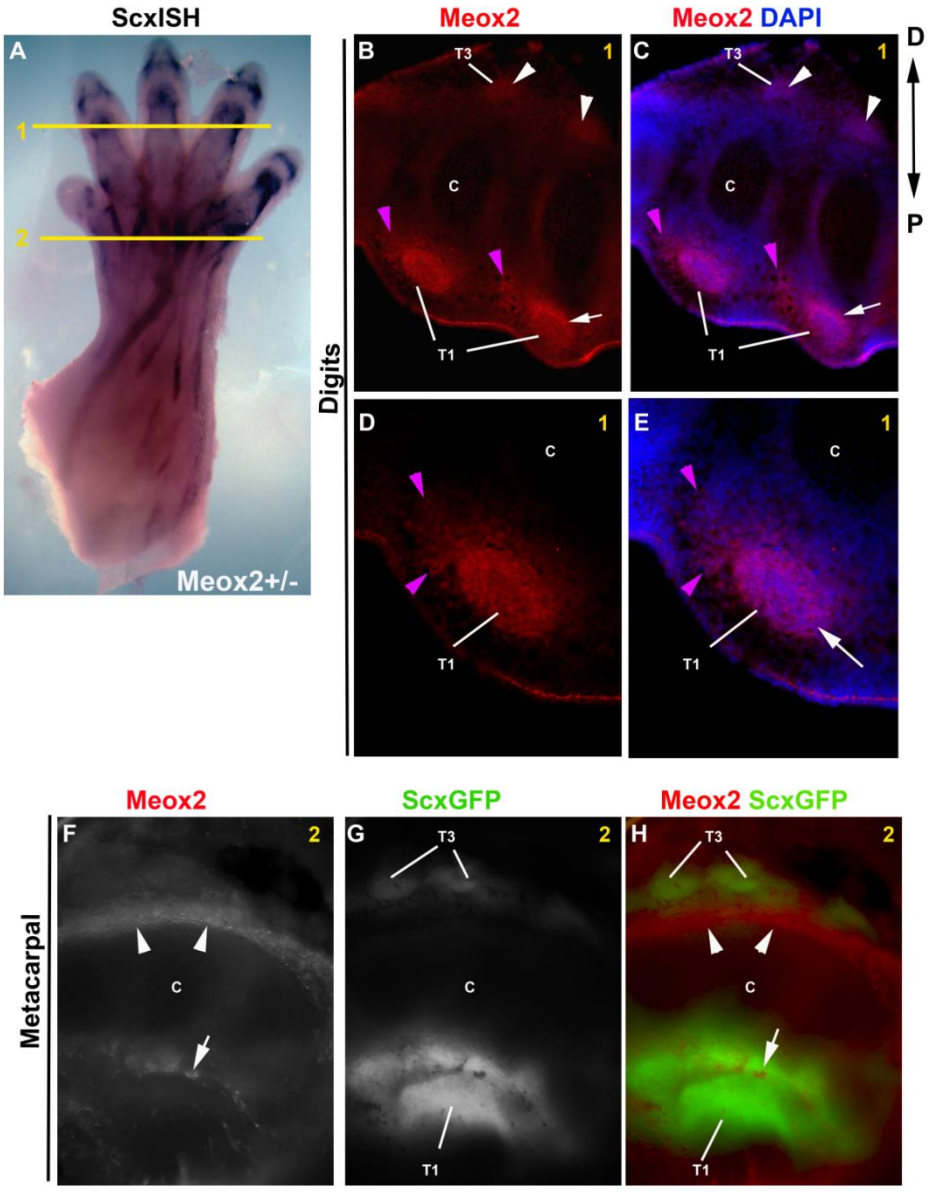
ScxISH
Meox2
Meox2 DAPI
A
1
2
Meox2+/-
B
T3
1
C
T1
D
P
Digits
D
E
Meox2
ScxGFP
Meox2 ScxGFP
F
2
G
H
Metacarpal

Fig 5.3.9 Meox2^{+} cells are not expressed in ScxGFP^{+} tendon cells of zeugopod at E14.5

(A-I) Transverse section was obtained from a forearm zeugopod and stylopod of Meox2$^{+/-}$;ScxGFP at E14.5. Immunostaining was carried out using Meox2 antibody (red) and ScxGFP expression located tendon cells (green). (A-F) represents a cross section from zeugopod segment in which Meox2+ cells marked a non-ScxGP+ regions. The boxed regions in A-C were analysed at higher magnification as shown in D-F. The Meox2+ cells were never found in the regions of ScxGFP+ expression domains. (G-H) represent a stylopod segment following the similar pattern of non-overlapping expression domain of Meox2 (red) and ScxGFP tendon cells (green). White arrows show Meox2+ cells; yellow arrows show ScxGFP+ cells; r, radius; u,ulna; h, humerus

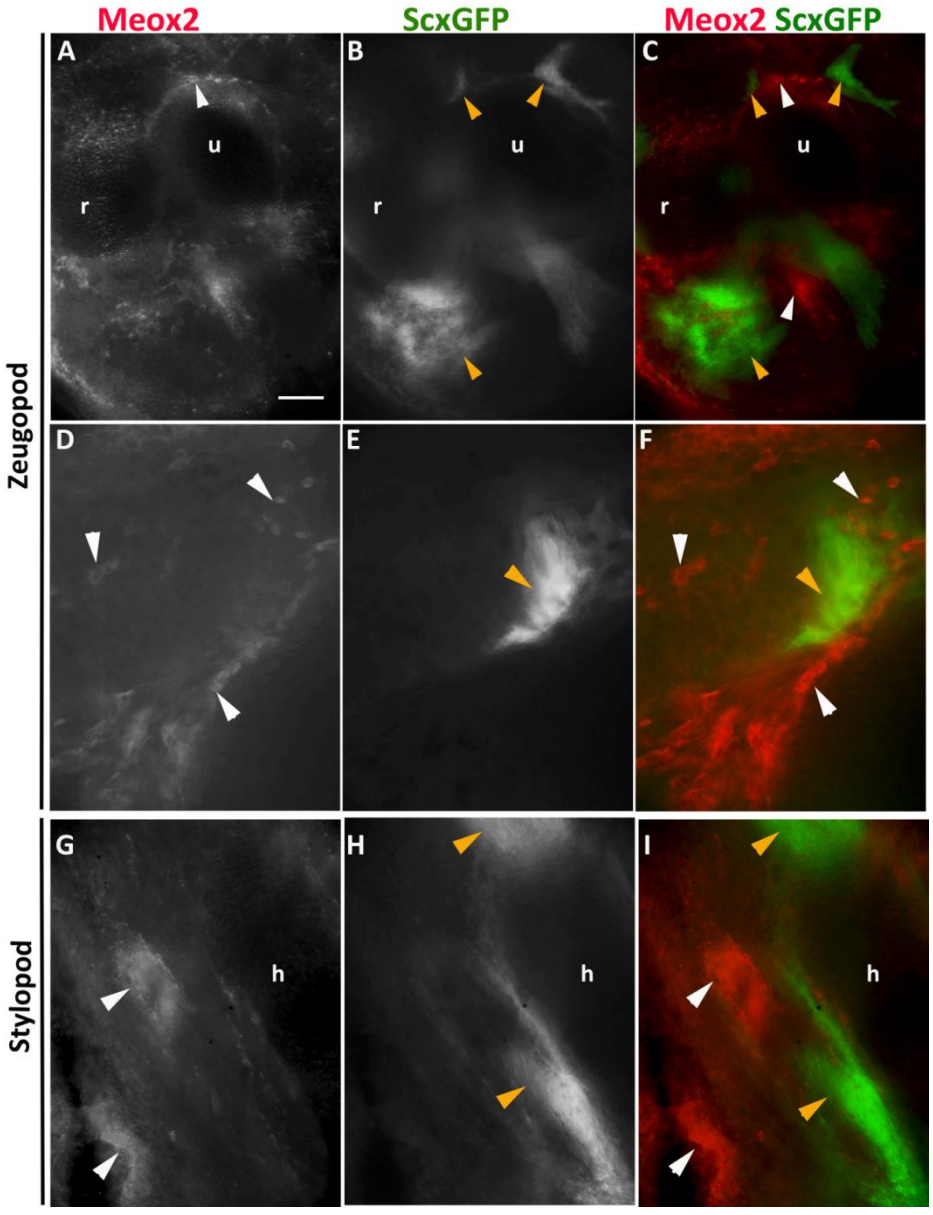
Meox2
ScxGFP
Meox2 ScxGFP
A
B
C
u
r
D
E
F
G
H
I
h
Zeugopod
Stylopod

Fig 5.3.10 Fate-mapping of Meox2^{+} cells during embryonic stages:

β-galactosidase activity was identified from Meox2 locus on transverse sections obtained from the forelimbs of Meox2$^{nLacZ/+}$ embryos at E13.5 (A-D) and E15.5 (E-J). Descendants of Meox2+ cells were visualised by S-gal staining. (A-D) At E13.5, Meox2 derived S-gal^{+} cells are present in the FDP (T1) and EDC (T3) digit tendons. The proximal sections show wider expression from the muscle connective tissue in C and D. (E-J) At E15.5, all digit tendon show S-gal staining. The boxed region in E is shown at higher magnification in F and the boxed region of G is magnified in J. Tendon nomenclature is tabulated in Table 2. Notice, by E15.5, all tendon groups and surrounding cells are showing a strong β-galactosidase activity. The cartilage cells are not S-gal^{+} at both embryonic stages.

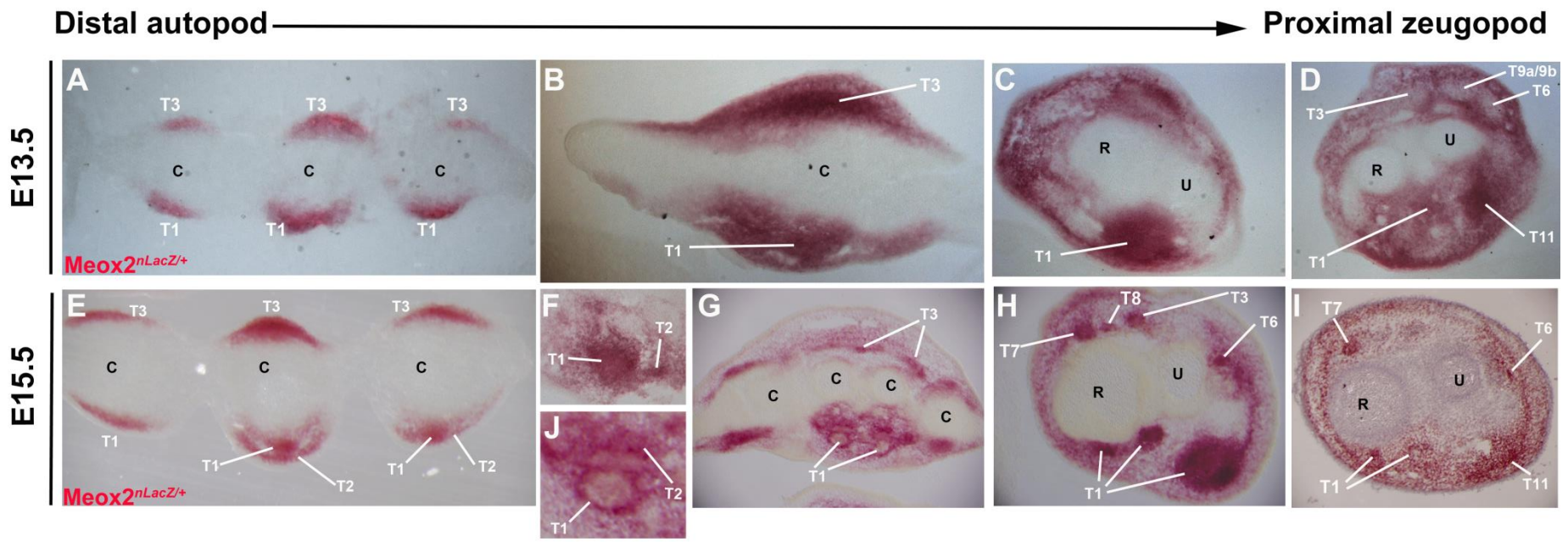
Distal autopod
Proximal zeugopod
E13.5
E15.5
A
B
C
D
E
F
G
H
I
J
T1
T2
T3
T6
T7
T8
T9a/9b
T11
C
R
U
Meox2nLacZ/+

Fig 5.3.11 Meox2^{+} derived cells are present in tendons and muscle connective tissue at E16.5

Transverse sections of forearm zeugopod were obtained from Meox2$^{nLacZ/+}$ (A, B and D) and Meox2$^{nLacZ/nLacZ}$ (C and E). X-gal staining was performed to identify b-galactosidase activity from Meox2 locus. The boxed region in B is magnified in A to show blue tendon cells and muscle connective tissue in heterozygous controls. (C and E) In homozygous mutant, all tendons were lost, however, the muscle connective tissue showed strong X-gal staining. Black arrow in (A) show tendon; red arrows represent muscle connective tissue; asterisks in (D) show muscle fibres; R, radius; U, ulna. Notice, absence of blue cells from muscle fibres in (D).

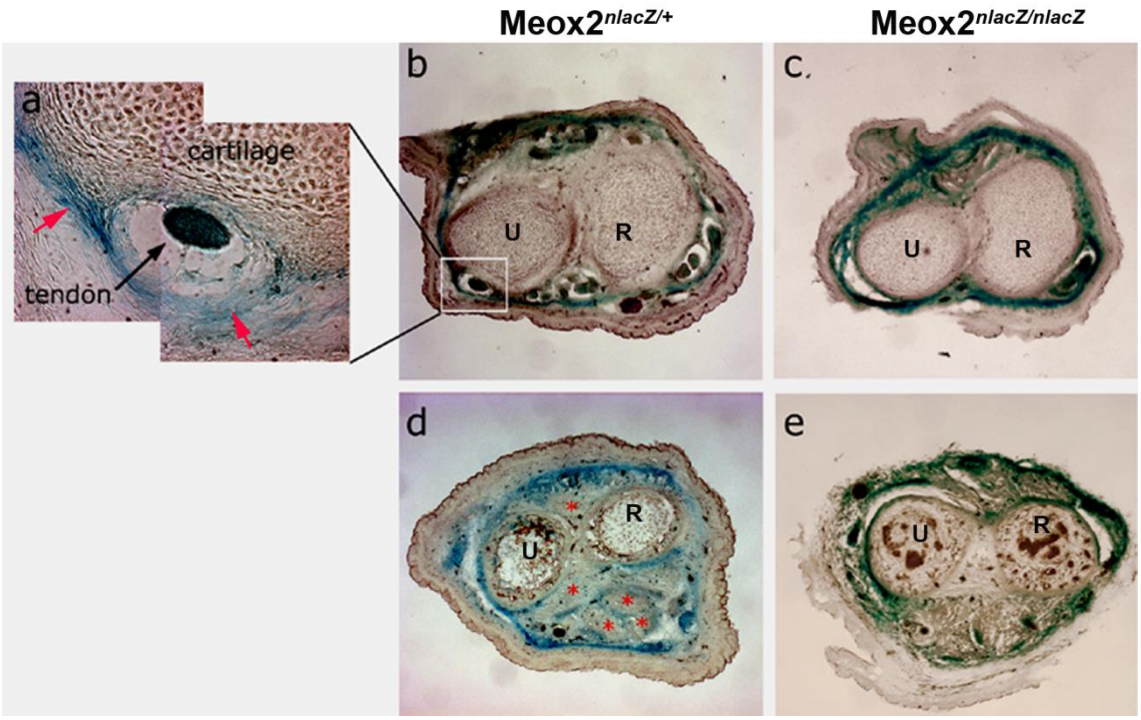
Meox2nlacZ/+
Meox2nlacZ/nlacZ
a
cartilage
tendon
b
U
R
c
U
R
d
U
R
e
U
R

Fig 5.3.12 Interlimb somites showed increase in TGFb2 transcripts in *Meox2*$^{-/-}$ at E 12.5

Whole-mount in situ analysis for TGFb2 at E12.5 on a *Meox2*$^{+/-}$ control embryo (A, C and E) and in homozygous *Meox2*$^{-/-}$ mutant embryo (B, D and F) was performed. Black arrows represent increased TGFb2 expression domain in the interlimb somites whereas yellow arrowhead showed normal expression levels in the other regions of trunk.

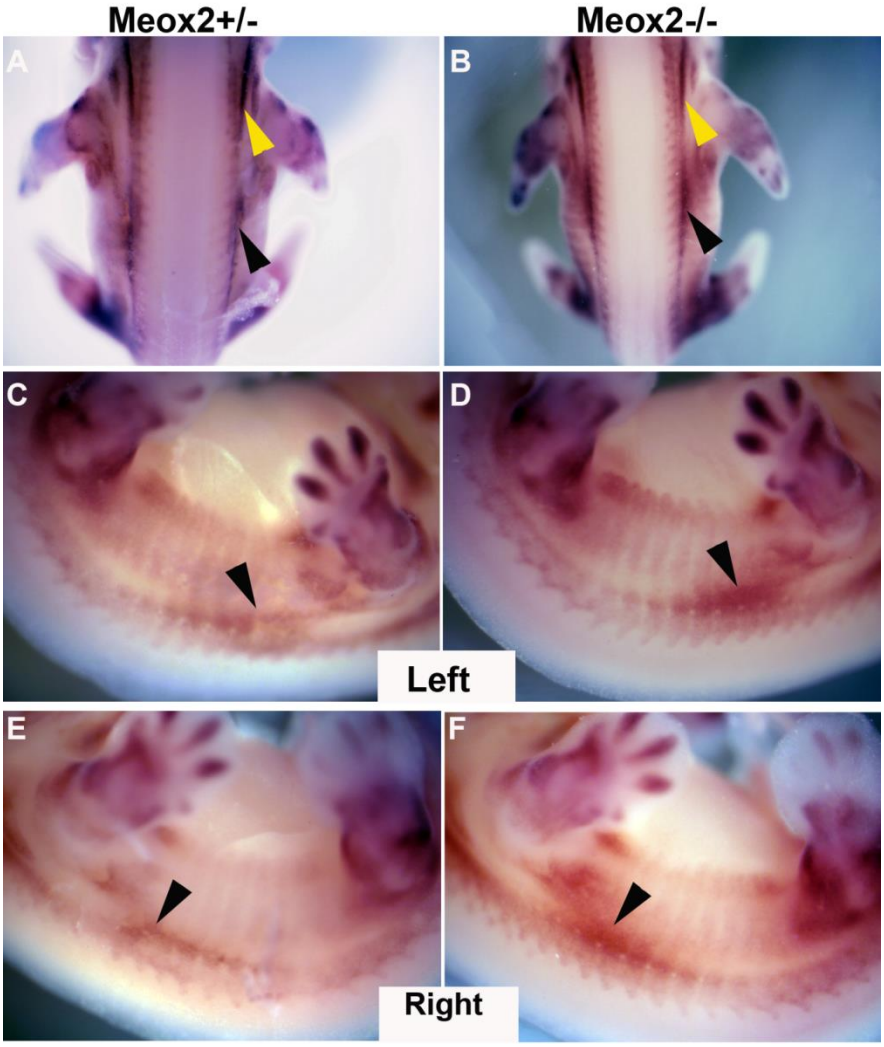
Meox2+/-
Meox2-/-
A
B
C
D
Left
E
F
Right

Fig 5.3.13 Increased TGFb2 expression restricted for only zeugopod and not autopod in *Meox2*$^{-/-}$ at E 12.5

Whole-mount in situ analysis for TGFb2 at E12.5 in a *Meox2*$^{+/-}$ forelimb dorsal and ventral (A and C) and in the *Meox2*$^{-/-}$ embryo dorsal and ventral forelimb (B and D) was performed. Yellow arrows indicates normal TGFb2 expression domain whereas red arrows showed overall considerable increase of TGFb2 expression levels in the absence of *Meox2*. In addition, TGFb2 whole-mount in situ analysis on the *Meox2*$^{+/-}$ control hindlimb dorsal and ventral (E and G) and in *Meox2*$^{-/-}$ embryo dorsal and ventral (F and H) was performed.

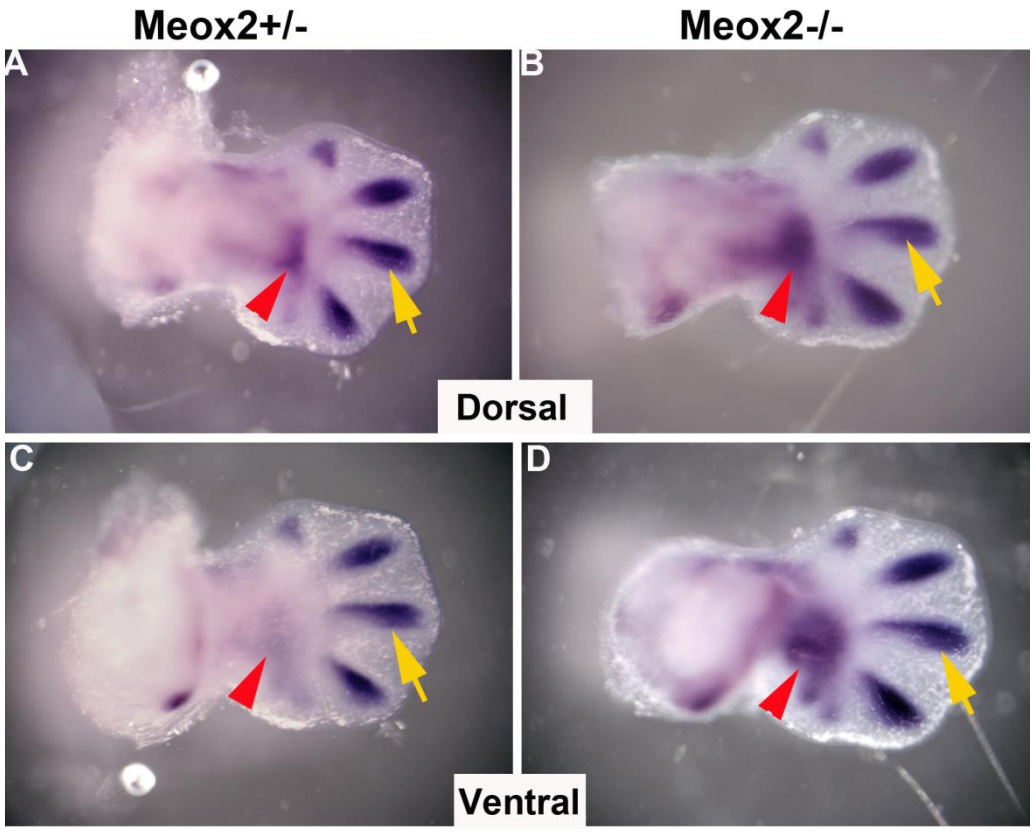

Forelimbs

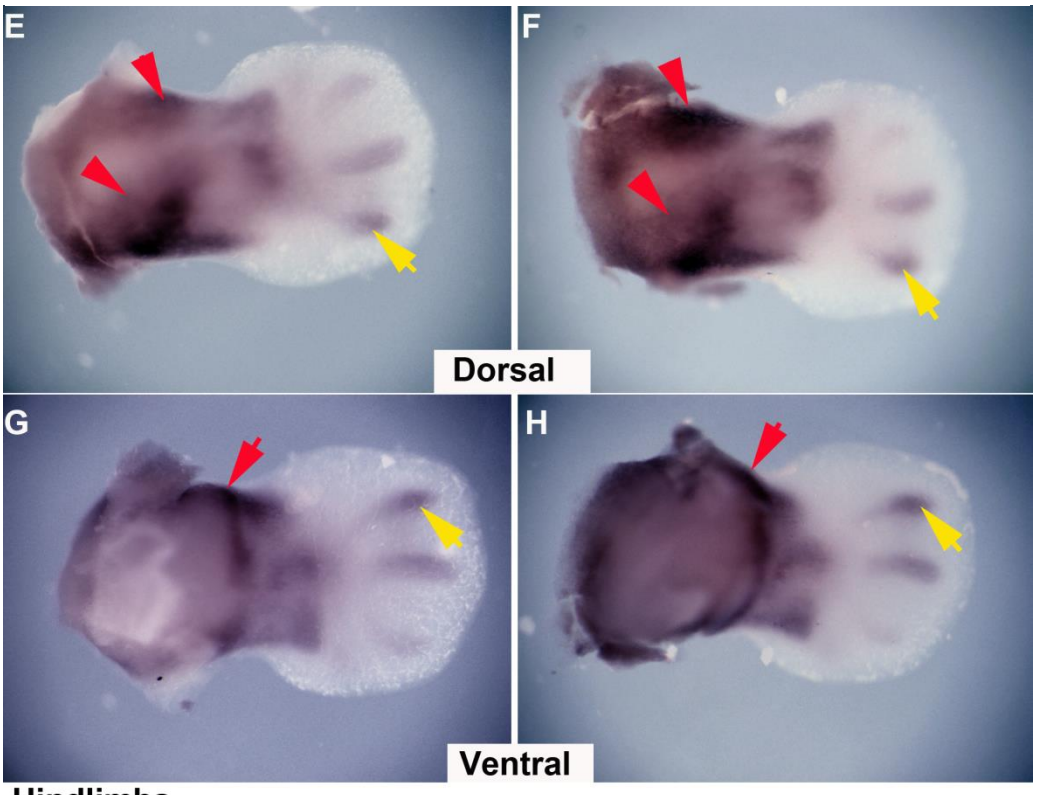

Hindlimbs

Fig 5.3.14 Biphasic interaction between *Meox2* and TGFβ2 signalling in cell culture

Overexpression of TGFβ2 protein was performed in C3H10T1/2 cells. *Scx* and *Meox2* cDNA was monitored by semi-quantitative PCR after 1h, 2h, 6h and 8h of the incubation followed by harvesting cells. Scx was upregulated from 6h onwards whereas Meox2 levels showed biphasic response to the TGFβ2 signalling pathway.

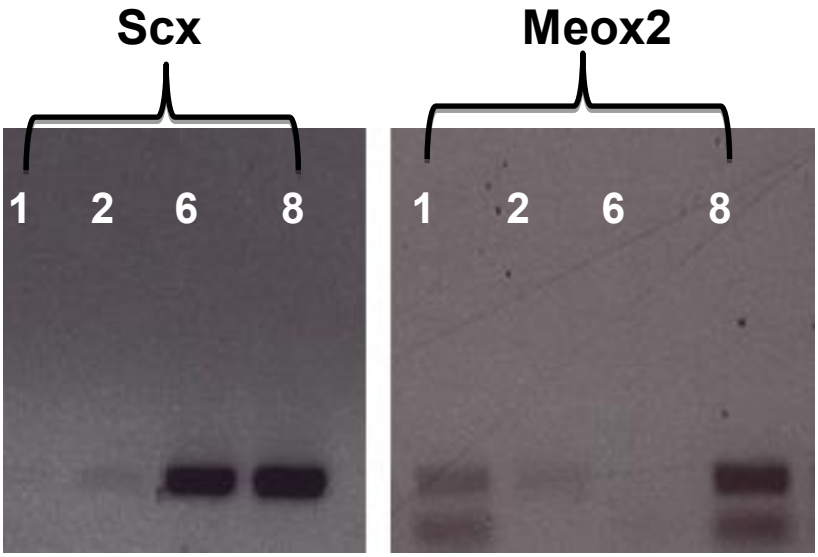
Scx
1
2
6
8
Meox2
1
2
6
8

Chapter 6

General Discussion

6.1 General discussion

During embryonic tendon genesis, the specified tendon cells are positioned between the muscle fibres and bone to form a functional musculoskeletal system. However, the mechanisms underlying precise alignment of tendon cells at their functional sites have just started to be elucidated. Currently, there are only few molecular regulators present to study the development of tendon. Using *Meox2*$^{-/-}$ mutant mice, we show an essential role for the *Meox2* gene in tendon formation. The mutant neonates displayed much thinner and extremely fragile tendons; and these defects were found to be a failure in embryonic tendon development and demonstrated a sustained role for *Meox2* in the alignment and organisation (E12.5), maturation (E13.5), integration, and differentiation (E14.5 onwards) of tendon progenitor cells.. However, the induction of tendon progenitor cells at E11.5 remained unaffected in the mutant embryos, and there was no discernible defect in cartilage cells and ligaments of *Meox2*$^{-/-}$ embryos. Deciphering the tendon phenotype in the *Meox2* mutants, we show that *Meox2* is expressed by the *Scleraxis*$^{+}$ autopod tendons but not in the zeugopod tendon indicating a position specific roles of *Meox2* in the autopod and zeugopod. Furthermore, *Meox2* ablation affected cell proliferation but not cell death. In mice, TGFβ2 signalling is crucial for the embryonic tendon development where it maintains tendon cell identity and recruits additional specified tendon progenitor cells. We found a biphasic interaction between *Meox2* and TGFβ2 signalling *in vitro* whereby, initially *Meox2* levels were up regulated and then weakly repressed at later time points. Therefore, it raises the possibility of direct interaction between *Meox2* and TGFβ2 signalling during embryonic tendon development. Interestingly, in Meox2 mutant embryos we observed an increase in TGFb2 expression in interlimb somites and limbs.

Meox2$^{-/-}$ mutant animals have profound limb tendon defects

Broadly, connective tissues are categorized into two groups: (i) dense connective tissue (tendons and ligaments) and (ii) loose connective tissue (fascia and muscle connective tissue). Using the *ScxGFP* transgene as a tendon marker, we showed that mutant neonates lack axial tendons of the trunk, tail tendons and the limbs displayed only thin trails of tendon fibres. In *Meox2*$^{-/-}$ neonates, apart from the substantial defects in all appendicular and axial tendons, there was severe impairment of fascia formation that led to intermixing of muscle groups in the forelimbs and hindlimbs.

An essential requirement of the *Scx* gene has been proposed for FDS tendon development in the forelimb autopod but not in the zeugopod (Huang et al., 2013; Murchison et al., 2007). Our observations in *Meox2*$^{-/-}$ neonates indicated a complete loss of FDS in the autopod and zeugopod. This suggests that *Meox2* also plays a decisive role in the autopod and zeugopod FDS tendon development, *Scx* expressing FDS tendon progenitors in the autopod rely on the cues from meta-carpophalageal joints (MCP) joints for the development (Huang et al., 2015b). This observation was supported by the loss of the autopod FDS tendon unit in *Sox5*$^{-/-}$*; Sox6*$^{-/-}$ double mutant embryos which show complete failure in the cartilage differentiation; and in the Indian hedgehog null embryos (*Ihh*$^{-/-}$) embryos that exhibit skeletal defects (Huang et al., 2015b). Conversely, zeugopod FDS tendon segment does not rely on the cartilage and therefore, it suggests that *Scx* mediates the signals from the cartilage in the FDS tendon progenitors of the autopod.

It is noteworthy that *Meox2*$^{-/-}$ mutant neonates displayed a regular bilateral symmetry of MCP joints in the digits. So why then does a loss of FDS tendon in the digit occur in the mutants despite the presence of normal skeletal elements? We propose the *Meox2* gene is required intrinsically for the normal development of the autopod tendons. The finding that the Meox2 protein is expressed in digit tendons during tendon maturation stage supports this view. Our data showed

similar expression domains of *Meox2* transcripts with *Scx* in the distal autopod tendon cells of the forelimb at E13.5 and Meox2 proteins in the forelimb autopod tendons by E14.5. In this scenario, we propose an intrinsic role of *Meox2* to drive the normal expression of *Scx* gene function inside digits of the forelimb. Interestingly, we have observed the loss of *Scx* mRNA expression in *Meox2*$^{-/-}$ mutant embryos at E13.5. Therefore, we conclude that a *Meox2* function genetically upstream of *Scx* in the autopod tendon progenitors and that *Meox2 is* a member of the intrinsic regulatory mechanisms to control maturation and differentiation of digit tendon progenitors. Therefore, skeletal cues are unable to compensate for the loss of *Meox2* gene function in the autopod.

As development proceeds, FDS tendons residing in the zeugopod (Huang et al., 2015b; Huang et al., 2013) control contraction of differentiated FDS muscle from the autopod towards zeugopod. The muscle inactivity in paralysed *mdg* embryos or absence of muscles in *Sp*^{d} embryos shows loss of FDS tendon in zeugopod but not in autopod (Huang et al., 2015b) suggesting that the cues from the muscles are necessary for the development of FDS tendon inside zeugopod. Likewise, our data revealed a reduction in the FDS tendon in the zeugopod due to *Meox2* loss-of-function. We propose that unlike the autopod, an extrinsic regulation of *Meox2* gene function for the zeugopod tendon development. This is supported by the observation that expression of *Meox2* is not localised to *Scx*$^{+}$ cells throughout zeugopod tendon development.

The morphological characterisation in *Meox2*$^{-/-}$ neonates revealed an overall disruption of flexor and extensor tendons. Other major tendons that were affected throughout the proximodistal axis included other flexor and extensor tendons i.e. FDP and EDC tendons. Lineage tracing analysis has shown that induction and progression of these tendons originates from two separate pools of progenitor cells in the autopod (*Six2*$^{+}$*/Scx*$^{+}$) and zeugopod segments (*Scx*$^{+}$) (Huang et al., 2015b). The same study also showed that extrinsic cues from the muscle cells are required for the tendon development in the metacarpal and zeugopod segments. The subtle changes in FDP tendon morphology and fusion of individuated EDC tendon bundles in the zeugopod of the forelimb in *Meox2*$^{-/-}$ neonates indicate deleterious effects on both of these cell populations in the autopod (*Six2*$^{+}$*/Scx*$^{+}$) and zeugopod (*Scx*$^{+}$). We demonstrate the EDC tendon

phenotype in *Meox2*$^{-/-}$ was similar to that reported for *Sp*^{d} and *mdg* mutant embryos (Huang et al., 2015b). This suggests an indirect role of *Meox2* during zeugopod tendon formation and we conclude that the zeugopod tendon defects are secondary to an initial failure of the normal muscle formation. Significantly, *Meox2* is expressed in limb myoblasts only as they migrate into the limb at E10.5, and is quickly down regulated prior to the expression of myogenic regulators such a MyoD (Mankoo et al., 1999). Furthermore, the same study also showed that in *Meox2* mutants, limb myoblast migration and differentiation are observed to be normal (Mankoo et al., 1999). Therefore, we conclude the tendon defects, although similar to those seen in *Sp* and *mdg* mutants, are unlikely to be a consequence of a loss of *Meox2* in myogenic precursors. Instead, we propose that *Meox2* functions in muscle connective tissues (MCT), affecting muscle development that secondarily impacts on zeugopod tendon development, as previously shown (Hasson, 2011; Kardon et al., 2003; Mathew et al., 2011). Of course, this does exclude the possibility that *Meox2* functions extrinsically to *Scx*$^{+}$ cells in progenitors that are subsequently recruited to tendons. Additionally, we cannot exclude the possibility that a pool of mesoderm cells that are bipotential and can be directed to a MCT or tendon fate; in a mechanism similar to that seen with *Sox9*$^{+}$*; Scx*$^{+}$ cells which can contribute to cartilage or tendon(Lorda-Diez et al., 2014; Lorda-Diez et al., 2009)

Our lineage analysis with the *Meox2-nLacZ* transgene further revealed the muscle connective tissue retains a history of *Meox2* expression. Interestingly, unlike the complete loss of tendons in *Meox2*$^{nLacZ/nLacZ}$ foetus at E16.5, loose connective tissue (fascia and muscle connective tissue) was still present in the mutants. However, development defects of these tissues were evident in the mutants that showed severe mispatterning and reduction in the tissue mass. Importantly, this correlated with the intermixing and disruption of individual muscle compartments at E16.5 and neonatal stage (Mankoo et al., 1999). This demonstrates an important intrinsic function of *Meox2* from muscle connective tissue to regulate muscle patterning and organisation. Muscle connective tissue actively coordinates muscle-tendon interactions and muscle patterning during embryonic morphogenesis (Hasson et al., 2010; Kardon et al., 2003; Swinehart et al., 2013). A critical role for the muscle connective tissue (MCT) during

myogenesis was demonstrated using classic chick-quail experiment and single-cell lineage tracing of myogenic progenitor cells that lacked the capacity to form a particular anatomical muscle (Chevallier et al., 1977; Christ et al., 1977; Kardon et al., 2002). Therefore, the pivotal role of the cells that are derived from limb mesoderm emerged as an extrinsic cue for muscle pattern. In recent years, the *TCF4* transcription factor, a downstream regulator of the canonical *Wnt-β-catenin* pathway is recognised as a marker for MCT (Kardon et al., 2003; Mathew et al., 2011). The *TCF4*-dependent signal from the MCT was shown extrinsically regulating the muscle fibre differentiation as genetic deletion of fibroblast specific *Tcf4* expression led to severe reduction in muscle mass at P0. Same study also showed that *Tcf4*-dependent signals are necessary for the switching of embryonic myofibres to multinucleated foetal muscle fibres. Intriguingly, the authors showed that *Tcf4* positively regulates embryonic and foetal myogenic cells by directly binding to the MyHCI and MyHCIIb enhancers via Wnt/β-catenin signalling pathway and therefore, an intrinsic regulatory *Tcf4* dependent machinery controls muscle fibre switch.

In addition, Hasson et al. (2010) reported that *Tbx* genes are also required for the development of MCT. *Tbx5* knockout mice have forelimb muscle patterning defects including the muscle splitting in the forelimb. The data in the same report also showed that *Tbx5* regulates muscle connective tissue development via N-Cadherin and β-catenin pathway and thereby controls the intrinsic pathway in maintaining integrity of this tissue. The profound disruption in the embryonic development of zeugopod muscle and tendon was also occurred due to the loss of *Hox11* genes in the muscle connective tissue (Swinehart et al., 2013). Using *Hoxa11eGFP* reporter, the study showed that *Hoxa11* gene is expressed in the muscle connective tissue, however, in *Hox11* knock out embryos, tendons and muscle precursors failed to differentiate and thereby an extrinsic role of *Hox* genes from MCT was suggested during tendon morphogenesis.

Evidence for a direct contribution of *Meox2*$^{+}$ cells to developing tendons was obtained from the analysis of *Meox2*$^{nLacZ/+}$ mice limbs which showed that all prominent tendon groups of the autopod e.g. FDP, FDS and EDC tendon

bundles showed strong *LacZ* staining from E13.5 onwards. Similarly, the zeugopod tendons showed β-galactosidase activity indicating that the *Scx*$^{+}$*/Meox2*$^{-}$ tendon cells at these stages are derivatives of *Meox2* progenitor cells. Interestingly, the close proximity of *Meox2*$^{+}$ cells near the autopod tendons and strong *Meox2-nLacZ*$^{+}$ in these tendon groups at E13.5 strongly suggests that *Meox2* expressing cells are recruited in the autopod tendon formation. Indeed, by E14.5, *Meox2*$^{+}$ cells are detected in the digit tendons. Therefore, in dense connective tissue i.e. tendons, *Meox2* seems to play essential role in organisation and recruitment of the committed tendon progenitors cells.

Therefore, on the basis of published data and observations in the present study, we hypothesize that, during tendon development, *Meox2* regulates autopod tendon progenitors intrinsically whilst there is an external cues delivered by *Meox2* for proper zeugopod tendon formation. Our RNA and protein expression data confirmed *Meox2* expression is excluded from domains of *Scx*$^{+}$ tendon progenitors at E12.5-13.5 and by E14.5 in the zeugopod of the forearm, although, significantly, the Meox2^{+} positive areas are adjacent o Scx^{+} domains. These observations indicate an indirect role of *Meox2* and this interpretation is further supported by similarities in the phenotype of *Scx* expression in *Meox2*$^{-/-}$ and *Sp*^{d} embryos at E12.5. Whilst *Meox2* loss-of-function resulted in complete loss of chevron-shaped *Scx* domain in the medial zeugopod; there was a significant reduction of the same expression domain due to the absence of muscles in *Pax3* mutants. The presence of *Meox2-nLacZ*$^{+}$ cells in both MCT and tendons can suggest that a pool of uncommitted progenitors in the limb are bipotential and can be recruited to both MCT and tendon fates.

Embryonic limb tendon development

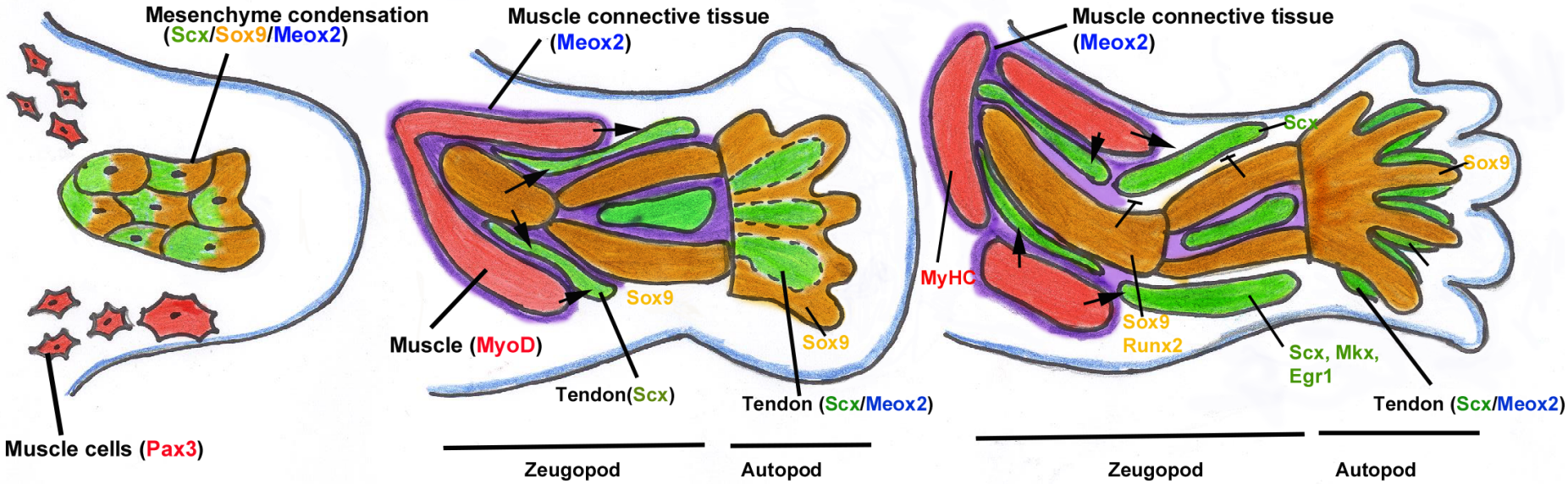

Induction
E10.5-11.5

Organisation and alignment
E12.0-12.5

Aggregation and differentiation
E13.5 onwards

Figure6.1: Diagrammatic summary of research findings in limb tendon development. (A) Induction of initial *Scx/Sox9/Meox2* multipotent limb mesenchyme cells is specified to form tendons under the influence of Wnt and Fgf signalling. (B) Organisation of tendon progenitors requires signals that are derived from *Meox2*$^{+}$ muscle connective tissue, muscle cells and adjacent cartilage condensation in the zeugopod. However, the extrinsic signals from the cartilage and *Meox2* derived cues within the tendon cells are necessary for the autopod tendon formation. (C) *Scx* favours aggregation and differentiation of tendon progenitors to form mature distinct tendon along the proximo-distal axis occurs by E13.5. Additional *Meox2*$^{+}$ cells are recruited to form the autopod tendons. While in the zeugopod, *Meox2*$^{+}$ cells continue to regulate tendon development extrinsically from the muscle connective tissue.

An extrinsic and intrinsic influence of the transcription factors to regulate the development of neuron, blood cell and retinal tissue development has been described before (Cepko, 1999; Nguyen et al., 2014; Tosney et al., 1994). For instance, the extrinsic regulation of *Meox1* from the somite on the endothelial cell derivatives was revealed when the genetic deletion of *Meox1* in the zebrafish embryos resulted in the expansion of haematopoietic stem cells that are derived from endothelial cells (Nguyen et al., 2014). Moreover, during the vertebrate eye development, various cell types (rod and cone photoreceptor cells, bipolar cells and glial cells) though derived from common pool of progenitors, the morphogenesis all cells are affected by extrinsic and intrinsic activities of bHLH transcription factors (Brown et al., 2001; Furukawa et al., 2000; Hatakeyama et al., 2001). For example, bHLH genes *Mash1*, *Mash3* and *Chx10* play an intrinsic role for the bipolar cell morphogenesis. While, *Mash1* and *Mash3* indirectly promoted the formation of rod cell genesis, *Chx10* extrinsically favoured glial cell formation (Cepko, 1999). Such findings support the notion of both intrinsic and extrinsic roles of *Meox2* that governs the molecular mechanisms for the normal differentiation and morphogenesis of tendon tissue.

Furthermore, several line of evidence have demonstrated the modular development of FDS, FDP and EDC tendon groups by two separate groups of

progenitor cells in the autopod and zeugopod; we propose a crucial role of *Meox2* function that controls the regulatory mechanisms in both progenitor populations of the tendons along the proximodistal axis of the forelimb.

A particularly striking finding of our data is the conserved role of *Meox2* along the proximo-distal axis of the limb. Specifically, it indicate that *Meox2* plays an evolutionary conserved function in the genetic regulatory mechanisms that are responsible for the functional and morphological shifts from fish fins to the tetrapod limbs. Using comparative morphology and functional genomics methods, previous studies have shown that the tetrapod limbs develop due to dual phases of *HoxD* and *HoxA* expression. These phases modulate the development of the autopod including wrist and digits that are controlled by cis-acting enhancers (Zakany and Duboule, 2007). A recent study has shown that two topological domains at *Hox* loci are conserved both in the zebrafish and in tetrapods (Woltering et al., 2014). However, functional genomics studies show that the late phase enhancers isolated from teleosts (zebrafish, tetraodon) are able to drive the expression of *Hox* genes only in the proximal structure of the limb but not in the autopod (Spitz et al., 2003). This suggests that the extrinsic roles of *Meox2* in the zeugopod are conserved in the ancestors during early evolution. On the other hand, it also suggests that the intrinsic role of *Meox2* in the autopod is acquired during the late evolution of autopods in the tetrapods.

Therefore- and hindlimb share similar genetic regulations and are evolutionary conserved (Wagner, 1989; Young et al., 2009), so it was not surprising that the FDB in the hindlimb, an analogue of the FDS in the forelimb, was completely missing in *Meox2*$^{-/-}$ neonate. To date, there is no other genetic model described that investigated FDB tendon development. Therefore, our data can be considered as the first report of a conserved genetic mechanism necessary for both FDS (forelimb) and FDB (hindlimb) tendon development.

Meox2$^{-/-}$ neonates showed a significant loss of Achilles tendon mass suggesting a role in both the prenatal and postnatal development and regulation of tendons. The hallmark of postnatal tendon development is the continuous deposition of collagenous matrix. Interestingly, the majority of the molecular

regulators that are important for post-natal tendon formation do not exhibit embryonic tendon defects in the respective mutants. Abnormalities in the collagen fibril organisation of Achilles tendon have been reported in COMP mutants, which display muscle myopathy, bone dysplasia, and reduce tendon thickness (Pirog et al., 2010). The defects in the collagen composition from this tendon group was also observed in *Gdf5*$^{-/-}$ that showed impaired properties of mechanical loading along with delayed in healing properties when observed in injury model. Therefore, it is interesting for us to speculate that the biomechanical properties of individual collagen fibrils in the Achilles tendon of *Meox2*$^{-/-}$ could be altered.

Meox2$^{-/-}$ mutant animals show gross axial tendon defects

Our analysis of the trunk and tail tendons in addition to the limbs indicated that *Meox2* plays an essential role in the tendons that assist in the passive transfer of the force from both epaxial and hypaxial muscles. Whilst epaxial muscles support the back and neck muscles, the hypaxial muscles controls the limb, tongue, diaphragm, intercostal, tail and the entire body wall (Kablar et al., 1997).The somite expression of *Meox1* in the demomyotome and *Meox2* in the sclerotome suggests they regulate epaxial and hypaxial muscle development (Candia et al., 1992; Mankoo et al., 2003).

Using ScxGFP transgene expression, we showed the disrupted tendon fibres of the dorsal back skeleton in the mutant neonates. However, *Meox2* exhibits a crucial role for the maintenance of intercostal at E14.5 and tail tendons that are required by hypaxial muscles of the trunk. Interestingly, the annulus fibrosus ligament in the tail, that also expresses *ScxGFP,* remained unaffected in our mutant model. A similar tail tendon phenotype was also reported in the *ScxGFP*$^{-/-}$ animals (Murchison et al., 2007). Previously, the data showed that *Meox2*$^{-/-}$ animals are born with expected Mendelian frequency and no embryonic lethality observed due to *Meox2* mutation (Mankoo et al., 1999). Such normal survival ratio despite loss of ScxGFP from the intercostal tendons could be explained by

the observation of normal tissue morphology and size of the hypaxial muscles in neonates i.e. intercostal and diaphragm muscles that are essential for the viability of all vertebrates.

Our findings further demonstrated the tendon defects are embryonic and the earliest tendon phenotype was at E12.5 for axial tendon tissues, in contrats to E12.0 in the limbs. Between E12.0- E12.5, the committed axial tendon cells initiate to position between muscle and cartilage cells (Murchison et al., 2007; Schweitzer et al., 2001). It is well known that tenocytes that are positioned near a cartilage arise from *Scx*$^{+}$*/Sox9*$^{+}$ progenitor cells, whereas *Scx*$^{-}$*/Sox9*$^{+}$ cells contribute to the cartilage (Blitz et al., 2013; Sugimoto et al., 2013a; Sugimoto et al., 2013b). The lack of *Meox2* has shown no effect on the cartilage cells that are marked by *Sox9*.

The evidence here further showed that the expression of *Meox2* was predominantly found in the sclerotome that hosts the multipotent *Scx*$^{+}$*/Sox9*$^{+}$ cell progenitors (Sugimoto et al., 2013a; Sugimoto et al., 2013b). However, we also found a narrow overlap between *Meox2*$^{+}$ cells residing in the sclerotome and *ScxGFP*$^{+}$ cells in the syndetome. The syndetome is a sub compartment of the anterior sclerotome (Brent et al., 2003; Schweitzer et al., 2001), which is comprised of *Scx*$^{+}$*/Sox9*$^{-}$ tendon precursors (Sugimoto et al., 2013a). Collectively, we conclude that *Meox2*$^{+}$ cells in the sclerotome selectively affects only *Scx*$^{+}$*/Sox9*$^{-}$ progenitor and not *Scx*$^{+}$*/Sox9*$^{+-}$ cells during tendon morphogenesis population although further analyses are needed to establish this point.

Meox2 regulates cell proliferation but not cell death

We observed that at E12.5 there was an overall reduction in cell proliferation in mutant embryos across the entire compartment in somites suggesting a significant role of Meox2 in cell cycle progression. In contrast, we found no change in programmed cell death in mutants at embryonic stages. This is consistent with our finding that *Meox2* is required for additional recruitment of

tendon progenitor cells at the site of condensation, and suggests the primary role of Meox2 is by regulating the proliferation of progenitors that will be recruited to the tendon pool. Previous data has shown the overlapping expression regions of *Meox* homoeobox genes in the early developing somites of chick and mouse emrbyos (Reijntjes et al., 2007). Moreover, the somites of *Meox1* null embryos showed developmental alterations in cell proliferation (Mankoo et al, 2009). It was shown that in the absence of functional *Meox1*, increased cell proliferation rates were observed in the rostral somitic region at the expense of caudal region. However, ablation of *Meox1* gene caused no significant changes in the cell death. The similarities of the role of *Meox* genes during the somite development highlight the concentrated action of *Meox1* and *Meox2* during the cell proliferation and cell death in developing embryos. Therefore, our data provide a line of evidence that *Meox2* function is essential to maintain the cell densities during embryonic tendon development.

Interaction between *Meox2* and TGFβ signalling

By E12.5, an overall decrease of *Scx* levels was observed in the absence of both TGFβ2 (Pryce et al., 2009) and *Meox2*. TGFβ signalling is essential for the organisation and recruitment of tendon progenitor cells. Using *Scx* as a marker for tendon cells, in *Tgfβ2*$^{-/-}$*; Tgfβ3*$^{-/-}$ double knock out mouse embryos, a complete loss of all tendons was reported (Pryce et al., 2009). In addition, *Tgfβ2*$^{-/-}$ mutant embryos exhibit a severe disruption in tendon progenitor cells at E12.5 but no change of *Scx* expression was observed in *Tgfβ3*$^{-/-}$ mutant embryos (Pryce et al., 2009). However, deletion of the TGFβRII, which is the single type II receptor utilised by all the members of the TGFβ superfamily, affected overall tendon development suggesting a wider role of the signalling pathway in tendon morphogenesis. Therefore, we propose a series of possible models for the interaction of *Meox2* and TGFβ2 in regulating *Scx* expression. First, *Meox2* acts upstream of TGFβ2, and so a loss of Meox2 will lead to a deficit of TGfb2 signalling and impact in turn on Scx expression; second Tgfβ2 functions upstream of Meox2, a loss of Meox2 will therefore impair the TGFb mediated signalling required for Scx expression; last, *Meox2* and TGFβ2 acting

in parallel to regulate the *Scx* expression at E12.5. Consequently, we expected either, a down regulation (model 1) or normal (models 2 and 3) TGFβ2 expression in *Meox2* knock out embryos. Surprisingly, our results revealed an increase in Tgfβ2 transcripts in the interlimb somites and in the zeugopod of *Meox2*$^{-/-}$ mutant embryos. On the contrary, other regions e.g. cervical (contribute towards tongue, neck and shoulder muscles), lumbar (opposite the hindlimbs) somites and presumptive autopod showed similar Tgfβ2 expression pattern. At present we cannot resolve this paradox, and it is essential to investigate expression of TFGb2 protein levels in Meox2 mutants. We have attempted to investigate the expression of Meox2 in TGFBII2 mutants; however these experiments were unsuccessful, due to transport delays of embryos from Dr. Schweitzer's laboratory.

We also investigated the relationship between TGFb signalling and Meox2 using the in vitro culture of C3H10T1/2 mesodermal stem cells. We observed a biphasic interaction of *Meox2* expression due to ectopic TGFβ2 proteins at various time points in the cells. There was a decrease in *Meox2* levels until 8 hours; however, *Meox2* expression was later on increased. Interestingly, it was shown that the *Scx* level was significantly up regulated when TGFβ2 was added in the medium (Pryce et al., 2009). Moreover, a previous study has shown the complex interaction between *Meox2* and TGFβ signals in epithelial cell biology (Valcourt et al., 2007). Tgfβ1 derived signals synergised with ectopic *Meox2* to arrest proliferation of epithelial cells and, conversely, *Meox2* partially caused blockage of TGFβ-1 derived epithelial-to-mesenchymal transition (EMT) in cultured keratinocytes (Valcourt et al., 2007).

We can suggest a possible mechanism by which *Meox2* modulates restriction of TGFβ2 domains to maintain integrity of functional musculoskeletal system. Moreover, the TGFβ signalling pathway promotes programmed cell death during limb formation (Dunker et al., 2002), whereas, *Meox2* stimulates cellular proliferation. Hence, we hypothesize a reciprocal interaction between Meox2 and TGFβ2 could play a role in modulating limb morphogenesis.

6.2 Future perspectives

ScxGFP expression and tissue histology in *Meox2*$^{-/-}$ neonates revealed gross tendon defects in appendicular and axial tissues. The specific loss of tendons, namely, FDS in forelimb and FDB in hindlimb suggest a unique role of Meox2 in these tendon groups. Further investigations are needed in *Meox2* null embryonic and foetal stages to examine the FDS/FDB tendon induction, organisation, and differentiation as these events are delayed in mouse (starting only at E14.5 until E16.5) compare to all other limb tendons (from E10.5 until E14.5) (Huang et al., 2013; Schweitzer et al., 2001). Moreover, during this late developmental phase, FDS muscle differentiates in the autopod and then translocation occurs towards zeugopod. Substantial effects of this translocation are shown to be associated with FDS tendon development because this tendon elongates from the FDS muscle insertion sites within the autopod towards zeugopod (Huang et al., 2013). Therefore, developmental analysis of FDS muscle in Meox2 control embryos from E14.5 to E16.5 will provide a clue for the failure of FDS tendon formation.

Tendon is composed largely of collagen-rich extracellular matrix and secreted by tendon fibroblasts and this has a pivotal role in the normal physiological homeostasis and regulation of the tendon matrix. Therefore, a manifestation of defective collagen fibril organization would be analysed by transmission electron microscopy to investigate collagen fibril diameter and arrangement in the mutant neonates. There are number of individual proteins present in tendon cells e.g. type I and type II collagen and tenomodulin, therefore, these proteins will be observed by immunohistochemistry in the mutant tendons. Collectively, all these analysis will help us to derive the focussed role of Meox2 in determining the post-natal integrity of tendons and regulating tendon homeostasis.

In vitro assays in C3H10T1/2 cells can be validated to identify the levels of Meox2 in response to TGFβ signalling. It was also shown that in the C3H 10T/2

cells, Scleraxis expression increases in response to TGFβ addition over the period of 24 hours. Therefore, our assay will provide an opportunity to identify direct targets of *Meox2* gene. Additionally, we can extrapolate this method to identify response of cell cycle proteins in the fibroblasts as we established that Meox2 positively regulates cellular proliferation during embryogenesis. For this, we could also able to employ the assay in primary fibroblast and monitor their active proliferation in response to ectopic expression of *Meox2*.

Finally, it is necessary to unfold the interaction of *Meox2* and TGFβ2 proteins. As we have already found a regionalised increase of Tgfβ2 transcripts in *Meox2*$^{-/-}$ embryos at E12.5, an *in vivo* analysis of *Meox2* expression in TGFβ2$^{-/-}$ embryos would be important. In limb organ culture, ectopic expression of *Scx* is induced by TGFβ2 soaked beads. Therefore, an *ex vivo* approach using Scx as the positive control, TGFβ2 soaked bead would be implanted in the chick limbs of appropriate stages and *Meox2* expression will be monitored. Our results from this methodology will also enable to describe the dynamic relationships of *Meox2* and TGFβ2 throughout the proximo-distal axis of the limb.

Meox2 mutants in some aspects resemble *Scx* knockouts, with defects associated with the later stages of limb tendon development. As our data from *Meox2-nLacZ* expression analysis provide an evidence that all tendon cells retains *Meox2* expression history during the tendon development, therefore, from our proposed genetic model we aimed to study the *Meox2* gene function in tendon-less model. To analyse the intrinsic regulation of tendon progenitor cells by *Meox2*, we plan to utilize *Prx1-Cre* transgenic mice (Logan et al., 2002) that will be obtained from Prof. Malcolm Logan in the Randall division. The conditional inactivation of *Meox2* in limb mesoderm could then be achieved by mating *Meox2*$^{+/-}$ heterozygous animals with *Prx1-Cre* mice.

6.3 Final conclusion

In summary, our study reveals that *Meox2* is an important regulator of axial and appendicular tendon development. *Meox2* exhibit an intrinsic regulation of autopod tendons whereas it extrinsically regulates zeugopod tendon development. The muscle connective tissue is derivatives of *Meox2* progenitor cells and therefore *Meox2* extrinsically regulate muscle and tendon patterning during embryogenesis. Our study has contributed an additional transcription factor in tendon research that provides novel insights for the new therapeutic methods during tendon pathology and will benefit the tendon tissue healing efforts during stress or injury.

List of references

Ahn, D.G., Kourakis, M.J., Rohde, L.A., Silver, L.M., Ho, R.K., 2002. T-box gene tbx5 is essential for formation of the pectoral limb bud. Nature 417, 754-758.

Anderson, D.M., Arredondo, J., Hahn, K., Valente, G., Martin, J.F., Wilson-Rawls, J., Rawls, A., 2006. Mohawk is a novel homeobox gene expressed in the developing mouse embryo. Developmental dynamics : an official publication of the American Association of Anatomists 235, 792-801.

Ansorge, H.L., Meng, X., Zhang, G., Veit, G., Sun, M., Klement, J.F., Beason, D.P., Soslowsky, L.J., Koch, M., Birk, D.E., 2009. Type XIV Collagen Regulates Fibrillogenesis: PREMATURE COLLAGEN FIBRIL GROWTH AND TISSUE DYSFUNCTION IN NULL MICE. The Journal of biological chemistry 284, 8427-8438.

Benjamin, M., Ralphs, J.R., 1997. Tendons and ligaments--an overview. Histology and histopathology 12, 1135-1144.

Benjamin, M., Ralphs, J.R., 1998. Fibrocartilage in tendons and ligaments--an adaptation to compressive load. Journal of anatomy 193 (Pt 4), 481-494.

Berthet, E., Chen, C., Butcher, K., Schneider, R.A., Alliston, T., Amirtharajah, M., 2013. Smad3 binds Scleraxis and Mohawk and regulates tendon matrix organization. Journal of orthopaedic research : official publication of the Orthopaedic Research Society 31, 1475-1483.

Bi, Y., Ehirchiou, D., Kilts, T.M., Inkson, C.A., Embree, M.C., Sonoyama, W., Li, L., Leet, A.I., Seo, B.M., Zhang, L., Shi, S., Young, M.F., 2007. Identification of tendon stem/progenitor cells and the role of the extracellular matrix in their niche. Nature medicine 13, 1219-1227.

Birk, D.E., Mayne, R., 1997. Localization of collagen types I, III and V during tendon development. Changes in collagen types I and III are correlated with changes in fibril diameter. European journal of cell biology 72, 352-361.

Birk, D.E., Southern, J.F., Zycband, E.I., Fallon, J.T., Trelstad, R.L., 1989. Collagen fibril bundles: a branching assembly unit in tendon morphogenesis. Development (Cambridge, England) 107, 437-443.

Bismuth, K., Relaix, F., 2010. Genetic regulation of skeletal muscle development. Experimental cell research 316, 3081-3086.

Bladt, F., Riethmacher, D., Isenmann, S., Aguzzi, A., Birchmeier, C., 1995. Essential role for the c-met receptor in the migration of myogenic precursor cells into the limb bud. Nature 376, 768-771.

Blitz, E., Sharir, A., Akiyama, H., Zelzer, E., 2013. Tendon-bone attachment unit is formed modularly by a distinct pool of Scx- and Sox9-positive progenitors. Development (Cambridge, England) 140, 2680-2690.

Blitz, E., Viukov, S., Sharir, A., Shwartz, Y., Galloway, J.L., Pryce, B.A., Johnson, R.L., Tabin, C.J., Schweitzer, R., Zelzer, E., 2009. Bone ridge patterning during musculoskeletal assembly is mediated through SCX regulation of Bmp4 at the tendon-skeleton junction. Developmental cell 17, 861-873.

Bober, E., Lyons, G.E., Braun, T., Cossu, G., Buckingham, M., Arnold, H.H., 1991. The muscle regulatory gene, Myf-6, has a biphasic pattern of expression during early mouse development. The Journal of cell biology 113, 1255-1265.

Bonnin, M.A., Laclef, C., Blaise, R., Eloy-Trinquet, S., Relaix, F., Maire, P., Duprez, D., 2005. Six1 is not involved in limb tendon development, but is expressed in limb connective tissue under Shh regulation. Mechanisms of development 122, 573-585.

Boregowda, R., Paul, E., White, J., Ritty, T.M., 2008. Bone and soft connective tissue alterations result from loss of fibrillin-2 expression. Matrix biology : journal of the International Society for Matrix Biology 27, 661-666.
Borello, U., Berarducci, B., Murphy, P., Bajard, L., Buffa, V., Piccolo, S., Buckingham, M., Cossu, G., 2006. The Wnt/beta-catenin pathway regulates Gli-mediated Myf5 expression during somitogenesis. Development (Cambridge, England) 133, 3723-3732.
Borycki, A.G., Li, J., Jin, F., Emerson, C.P., Epstein, J.A., 1999. Pax3 functions in cell survival and in pax7 regulation. Development (Cambridge, England) 126, 1665-1674.
Brand-Saberi, B., Muller, T.S., Wilting, J., Christ, B., Birchmeier, C., 1996. Scatter factor/hepatocyte growth factor (SF/HGF) induces emigration of myogenic cells at interlimb level in vivo. Developmental biology 179, 303-308.
Braun, T., Bober, E., Rudnicki, M.A., Jaenisch, R., Arnold, H.H., 1994. MyoD expression marks the onset of skeletal myogenesis in Myf-5 mutant mice. Development (Cambridge, England) 120, 3083-3092.
Brent, A.E., Braun, T., Tabin, C.J., 2005. Genetic analysis of interactions between the somitic muscle, cartilage and tendon cell lineages during mouse development. Development (Cambridge, England) 132, 515-528.
Brent, A.E., Schweitzer, R., Tabin, C.J., 2003. A somitic compartment of tendon progenitors. Cell 113, 235-248.
Brent, A.E., Tabin, C.J., 2002. Developmental regulation of somite derivatives: muscle, cartilage and tendon. Current opinion in genetics & development 12, 548-557.
Brent, A.E., Tabin, C.J., 2004. FGF acts directly on the somitic tendon progenitors through the Ets transcription factors Pea3 and Erm to regulate scleraxis expression. Development (Cambridge, England) 131, 3885-3896.
Brohmann, H., Jagla, K., Birchmeier, C., 2000. The role of Lbx1 in migration of muscle precursor cells. Development (Cambridge, England) 127, 437-445.
Brown, N.L., Patel, S., Brzezinski, J., Glaser, T., 2001. Math5 is required for retinal ganglion cell and optic nerve formation. Development (Cambridge, England) 128, 2497-2508.
Brukner, P., Connell, D., 2016. 'Serious thigh muscle strains': beware the intramuscular tendon which plays an important role in difficult hamstring and quadriceps muscle strains. British journal of sports medicine 50, 205-208.
Candia, A.F., Hu, J., Crosby, J., Lalley, P.A., Noden, D., Nadeau, J.H., Wright, C.V., 1992. Mox-1 and Mox-2 define a novel homeobox gene subfamily and are differentially expressed during early mesodermal patterning in mouse embryos. Development (Cambridge, England) 116, 1123-1136.
Candia, A.F., Wright, C.V., 1996. Differential localization of Mox-1 and Mox-2 proteins indicates distinct roles during development. The International journal of developmental biology 40, 1179-1184.
Cepko, C.L., 1999. The roles of intrinsic and extrinsic cues and bHLH genes in the determination of retinal cell fates. Current opinion in neurobiology 9, 37-46.
Chapman, D.L., Garvey, N., Hancock, S., Alexiou, M., Agulnik, S.I., Gibson-Brown, J.J., Cebra-Thomas, J., Bollag, R.J., Silver, L.M., Papaioannou, V.E., 1996. Expression of the T-box family genes, Tbx1-Tbx5, during early mouse development. Developmental dynamics : an official publication of the American Association of Anatomists 206, 379-390.
Chaudhari, N., 1992. A single nucleotide deletion in the skeletal muscle-specific calcium channel transcript of muscular dysgenesis (mdg) mice. The Journal of biological chemistry 267, 25636-25639.
Chevallier, A., Kieny, M., 1982. On the role of the connective tissue in the patterning of the chick limb musculature. Wilhelm Roux' Archiv 191, 277-280.
Chevallier, A., Kieny, M., Mauger, A., 1977. Limb-somite relationship: origin of the limb musculature. Development (Cambridge, England) 41, 245-258.

Daston, G., Lamar, E., Olivier, M., Goulding, M., 1996. Pax-3 is necessary for migration but not differentiation of limb muscle precursors in the mouse. Development (Cambridge, England) 122, 1017-1027.
Daubas, P., Duval, N., Bajard, L., Langa Vives, F., Robert, B., Mankoo, B.S., Buckingham, M., 2015. Fine-tuning the onset of myogenesis by homeobox proteins that interact with the Myf5 limb enhancer. Biology open 4, 1614-1624.
Daugherty, R.L., Gottardi, C.J., 2007. Phospho-regulation of Beta-catenin adhesion and signaling functions. Physiology (Bethesda, Md.) 22, 303-309.
Del Buono, A., Chan, O., Maffulli, N., 2013. Achilles tendon: functional anatomy and novel emerging models of imaging classification. International orthopaedics 37, 715-721.
Dietrich, S., Abou-Rebyeh, F., Brohmann, H., Bladt, F., Sonnenberg-Riethmacher, E., Yamaai, T., Lumsden, A., Brand-Saberi, B., Birchmeier, C., 1999. The role of SF/HGF and c-Met in the development of skeletal muscle. Development (Cambridge, England) 126, 1621-1629.
Docheva, D., Hunziker, E.B., Fassler, R., Brandau, O., 2005. Tenomodulin is necessary for tenocyte proliferation and tendon maturation. Molecular and cellular biology 25, 699-705.
Docheva, D., Popov, C., Alberton, P., Aszodi, A., 2014. Integrin signaling in skeletal development and function. Birth defects research. Part C, Embryo today : reviews 102, 13-36.
Edom-Vovard, F., Duprez, D., 2004. Signals regulating tendon formation during chick embryonic development. Developmental dynamics : an official publication of the American Association of Anatomists 229, 449-457.
Edom-Vovard, F., Schuler, B., Bonnin, M.A., Teillet, M.A., Duprez, D., 2002. Fgf4 positively regulates scleraxis and tenascin expression in chick limb tendons. Developmental biology 247, 351-366.
Elliott, D.H., Crawford, G.N., 1965. THE THICKNESS AND COLLAGEN CONTENT OF TENDON RELATIVE TO THE CROSS-SECTIONAL AREA OF MUSCLE DURING GROWTH. Proceedings of the Royal Society of London. Series B, Biological sciences 162, 198-202.
Eloy-Trinquet, S., Wang, H., Edom-Vovard, F., Duprez, D., 2009. Fgf signaling components are associated with muscles and tendons during limb development. Developmental dynamics : an official publication of the American Association of Anatomists 238, 1195-1206.
Engel, J., 1997. Versatile collagens in invertebrates. Science (New York, N.Y.) 277, 1785-1786.
Espira, L., Lamoureux, L., Jones, S.C., Gerard, R.D., Dixon, I.M., Czubryt, M.P., 2009. The basic helix-loop-helix transcription factor scleraxis regulates fibroblast collagen synthesis. Journal of molecular and cellular cardiology 47, 188-195.
Franz, T., Kothary, R., Surani, M.A., Halata, Z., Grim, M., 1993. The Splotch mutation interferes with muscle development in the limbs. Anatomy and embryology 187, 153-160.
Furukawa, T., Mukherjee, S., Bao, Z.Z., Morrow, E.M., Cepko, C.L., 2000. rax, Hes1, and notch1 promote the formation of Muller glia by postnatal retinal progenitor cells. Neuron 26, 383-394.
Furumatsu, T., Shukunami, C., Amemiya-Kudo, M., Shimano, H., Ozaki, T., 2010. Scleraxis and E47 cooperatively regulate the Sox9-dependent transcription. The international journal of biochemistry & cell biology 42, 148-156.
Gotwals, P.J., Paine-Saunders, S.E., Stark, K.A., Hynes, R.O., 1994. Drosophila integrins and their ligands. Current opinion in cell biology 6, 734-739.
Grim, M., Wachtler, F., 1991. Muscle morphogenesis in the absence of myogenic cells. Anatomy and embryology 183, 67-70.
Gross, M.K., Moran-Rivard, L., Velasquez, T., Nakatsu, M.N., Jagla, K., Goulding, M., 2000. Lbx1 is required for muscle precursor migration along a lateral pathway into the limb. Development (Cambridge, England) 127, 413-424.
Guerquin, M.J., Charvet, B., Nourissat, G., Havis, E., Ronsin, O., Bonnin, M.A., Ruggiu, M., Olivera-Martinez, I., Robert, N., Lu, Y., Kadler, K.E., Baumberger, T., Doursounian, L., Berenbaum, F., Duprez, D., 2013. Transcription factor EGR1 directs tendon differentiation and promotes tendon repair. The Journal of clinical investigation 123, 3564-3576.

Harrison, S.M., Whitton, R.C., Kawcak, C.E., Stover, S.M., Pandy, M.G., 2010. Relationship between muscle forces, joint loading and utilization of elastic strain energy in equine locomotion. The Journal of experimental biology 213, 3998-4009.
Hasson, P., 2011. "Soft" tissue patterning: muscles and tendons of the limb take their form. Developmental dynamics : an official publication of the American Association of Anatomists 240, 1100-1107.
Hasson, P., DeLaurier, A., Bennett, M., Grigorieva, E., Naiche, L.A., Papaioannou, V.E., Mohun, T.J., Logan, M.P., 2010. Tbx4 and tbx5 acting in connective tissue are required for limb muscle and tendon patterning. Developmental cell 18, 148-156.
Hatakeyama, J., Tomita, K., Inoue, T., Kageyama, R., 2001. Roles of homeobox and bHLH genes in specification of a retinal cell type. Development (Cambridge, England) 128, 1313-1322.
Hosokawa, R., Oka, K., Yamaza, T., Iwata, J., Urata, M., Xu, X., Bringas, P., Jr., Nonaka, K., Chai, Y., 2010. TGF-beta mediated FGF10 signaling in cranial neural crest cells controls development of myogenic progenitor cells through tissue-tissue interactions during tongue morphogenesis. Developmental biology 341, 186-195.
Huang, A.H., Lu, H.H., Schweitzer, R., 2015a. Molecular regulation of tendon cell fate during development. Journal of orthopaedic research : official publication of the Orthopaedic Research Society.
Huang, A.H., Riordan, T.J., Pryce, B., Weibel, J.L., Watson, S.S., Long, F., Lefebvre, V., Harfe, B.D., Stadler, H.S., Akiyama, H., Tufa, S.F., Keene, D.R., Schweitzer, R., 2015b. Musculoskeletal integration at the wrist underlies modular development of limb tendons. Development (Cambridge, England).
Huang, A.H., Riordan, T.J., Wang, L., Eyal, S., Zelzer, E., Brigande, J.V., Schweitzer, R., 2013. Repositioning forelimb superficialis muscles: tendon attachment and muscle activity enable active relocation of functional myofibers. Developmental cell 26, 544-551.
Hunger, C., Odemis, V., Engele, J., 2012. Expression and function of the SDF-1 chemokine receptors CXCR4 and CXCR7 during mouse limb muscle development and regeneration. Experimental cell research 318, 2178-2190.
Inanlou, M.R., Kablar, B., 2005a. Abnormal development of the intercostal muscles and the rib cage in Myf5-/- embryos leads to pulmonary hypoplasia. Developmental dynamics : an official publication of the American Association of Anatomists 232, 43-54.
Inanlou, M.R., Kablar, B., 2005b. Contractile activity of skeletal musculature involved in breathing is essential for normal lung cell differentiation, as revealed in Myf5-/-:MyoD-/- embryos. Developmental dynamics : an official publication of the American Association of Anatomists 233, 772-782.
Ito, Y., Toriuchi, N., Yoshitaka, T., Ueno-Kudoh, H., Sato, T., Yokoyama, S., Nishida, K., Akimoto, T., Takahashi, M., Miyaki, S., Asahara, H., 2010. The Mohawk homeobox gene is a critical regulator of tendon differentiation. Proceedings of the National Academy of Sciences of the United States of America 107, 10538-10542.
Jepsen, K.J., Wu, F., Peragallo, J.H., Paul, J., Roberts, L., Ezura, Y., Oldberg, A., Birk, D.E., Chakravarti, S., 2002. A syndrome of joint laxity and impaired tendon integrity in lumican- and fibromodulin-deficient mice. The Journal of biological chemistry 277, 35532-35540.
Kablar, B., Krastel, K., Ying, C., Asakura, A., Tapscott, S.J., Rudnicki, M.A., 1997. MyoD and Myf-5 differentially regulate the development of limb versus trunk skeletal muscle. Development (Cambridge, England) 124, 4729-4738.
Kardon, G., 1998. Muscle and tendon morphogenesis in the avian hind limb. Development (Cambridge, England) 125, 4019-4032.
Kardon, G., Harfe, B.D., Tabin, C.J., 2003. A Tcf4-positive mesodermal population provides a prepattern for vertebrate limb muscle patterning. Developmental cell 5, 937-944.
Kjaer, M., 2004. Role of extracellular matrix in adaptation of tendon and skeletal muscle to mechanical loading. Physiological reviews 84, 649-698.

Kuhl, U., Ocalan, M., Timpl, R., von der Mark, K., 1986. Role of laminin and fibronectin in selecting myogenic versus fibrogenic cells from skeletal muscle cells in vitro. Developmental biology 117, 628-635.
Lan, M.A., Gersbach, C.A., Michael, K.E., Keselowsky, B.G., Garcia, A.J., 2005. Myoblast proliferation and differentiation on fibronectin-coated self assembled monolayers presenting different surface chemistries. Biomaterials 26, 4523-4531.
Langen, R.C., Schols, A.M., Kelders, M.C., Wouters, E.F., Janssen-Heininger, Y.M., 2003. Enhanced myogenic differentiation by extracellular matrix is regulated at the early stages of myogenesis. In vitro cellular & developmental biology. Animal 39, 163-169.
Lejard, V., Blais, F., Guerquin, M.J., Bonnet, A., Bonnin, M.A., Havis, E., Malbouyres, M., Bidaud, C.B., Maro, G., Gilardi-Hebenstreit, P., Rossert, J., Ruggiero, F., Duprez, D., 2011. EGR1 and EGR2 involvement in vertebrate tendon differentiation. The Journal of biological chemistry 286, 5855-5867.
Lejard, V., Brideau, G., Blais, F., Salingcarnboriboon, R., Wagner, G., Roehrl, M.H., Noda, M., Duprez, D., Houillier, P., Rossert, J., 2007. Scleraxis and NFATc regulate the expression of the pro-alpha1(I) collagen gene in tendon fibroblasts. The Journal of biological chemistry 282, 17665-17675.
Liu, H., Xu, J., Liu, C.F., Lan, Y., Wylie, C., Jiang, R., 2015. Whole transcriptome expression profiling of mouse limb tendon development by using RNA-seq. Journal of orthopaedic research : official publication of the Orthopaedic Research Society.
Liu, W., Watson, S.S., Lan, Y., Keene, D.R., Ovitt, C.E., Liu, H., Schweitzer, R., Jiang, R., 2010. The atypical homeodomain transcription factor Mohawk controls tendon morphogenesis. Molecular and cellular biology 30, 4797-4807.
Logan, M., Martin, J.F., Nagy, A., Lobe, C., Olson, E.N., Tabin, C.J., 2002. Expression of Cre Recombinase in the developing mouse limb bud driven by a Prxl enhancer. Genesis (New York, N.Y. : 2000) 33, 77-80.
Lorda-Diez, C.I., Montero, J.A., Garcia-Porrero, J.A., Hurle, J.M., 2014. Divergent differentiation of skeletal progenitors into cartilage and tendon: lessons from the embryonic limb. ACS chemical biology 9, 72-79.
Lorda-Diez, C.I., Montero, J.A., Martinez-Cue, C., Garcia-Porrero, J.A., Hurle, J.M., 2009. Transforming growth factors beta coordinate cartilage and tendon differentiation in the developing limb mesenchyme. The Journal of biological chemistry 284, 29988-29996.
Mankoo, B.S., Collins, N.S., Ashby, P., Grigorieva, E., Pevny, L.H., Candia, A., Wright, C.V., Rigby, P.W., Pachnis, V., 1999. Mox2 is a component of the genetic hierarchy controlling limb muscle development. Nature 400, 69-73.
Mankoo, B.S., Skuntz, S., Harrigan, I., Grigorieva, E., Candia, A., Wright, C.V., Arnheiter, H., Pachnis, V., 2003. The concerted action of Meox homeobox genes is required upstream of genetic pathways essential for the formation, patterning and differentiation of somites. Development (Cambridge, England) 130, 4655-4664.
Martin-Bermudo, M.D., 2000. Integrins modulate the Egfr signaling pathway to regulate tendon cell differentiation in the Drosophila embryo. Development (Cambridge, England) 127, 2607-2615.
Mathew, S.J., Hansen, J.M., Merrell, A.J., Murphy, M.M., Lawson, J.A., Hutcheson, D.A., Hansen, M.S., Angus-Hill, M., Kardon, G., 2011. Connective tissue fibroblasts and Tcf4 regulate myogenesis. Development (Cambridge, England) 138, 371-384.
Mayer, U., Saher, G., Fassler, R., Bornemann, A., Echtermeyer, F., von der Mark, H., Miosge, N., Poschl, E., von der Mark, K., 1997. Absence of integrin alpha 7 causes a novel form of muscular dystrophy. Nature genetics 17, 318-323.
Mendias, C.L., Bakhurin, K.I., Faulkner, J.A., 2008. Tendons of myostatin-deficient mice are small, brittle, and hypocellular. Proceedings of the National Academy of Sciences of the United States of America 105, 388-393.

Mikic, B., Rossmeier, K., Bierwert, L., 2009. Sexual dimorphism in the effect of GDF-6 deficiency on murine tendon. Journal of orthopaedic research : official publication of the Orthopaedic Research Society 27, 1603-1611.
Miller, G., Neilan, M., Chia, R., Gheryani, N., Holt, N., Charbit, A., Wells, S., Tucci, V., Lalanne, Z., Denny, P., Fisher, E.M., Cheeseman, M., Askew, G.N., Dear, T.N., 2010. ENU mutagenesis reveals a novel phenotype of reduced limb strength in mice lacking fibrillin 2. PloS one 5, e9137.
Murchison, N.D., Price, B.A., Conner, D.A., Keene, D.R., Olson, E.N., Tabin, C.J., Schweitzer, R., 2007. Regulation of tendon differentiation by scleraxis distinguishes force-transmitting tendons from muscle-anchoring tendons. Development (Cambridge, England) 134, 2697-2708.
Nguyen, P.D., Hollway, G.E., Sonntag, C., Miles, L.B., Hall, T.E., Berger, S., Fernandez, K.J., Gurevich, D.B., Cole, N.J., Alaei, S., Ramialison, M., Sutherland, R.L., Polo, J.M., Lieschke, G.J., Currie, P.D., 2014. Haematopoietic stem cell induction by somite-derived endothelial cells controlled by meox1. Nature 512, 314-318.
Oliver, G., Wehr, R., Jenkins, N.A., Copeland, N.G., Cheyette, B.N., Hartenstein, V., Zipursky, S.L., Gruss, P., 1995. Homeobox genes and connective tissue patterning. Development (Cambridge, England) 121, 693-705.
Pan, T.C., Zhang, R.Z., Markova, D., Arita, M., Zhang, Y., Bogdanovich, S., Khurana, T.S., Bonnemann, C.G., Birk, D.E., Chu, M.L., 2013. COL6A3 protein deficiency in mice leads to muscle and tendon defects similar to human collagen VI congenital muscular dystrophy. The Journal of biological chemistry 288, 14320-14331.
Pirog, K.A., Jaka, O., Katakura, Y., Meadows, R.S., Kadler, K.E., Boot-Handford, R.P., Briggs, M.D., 2010. A mouse model offers novel insights into the myopathy and tendinopathy often associated with pseudoachondroplasia and multiple epiphyseal dysplasia. Human molecular genetics 19, 52-64.
Pryce, B.A., Brent, A.E., Murchison, N.D., Tabin, C.J., Schweitzer, R., 2007. Generation of transgenic tendon reporters, ScxGFP and ScxAP, using regulatory elements of the scleraxis gene. Developmental dynamics : an official publication of the American Association of Anatomists 236, 1677-1682.
Pryce, B.A., Watson, S.S., Murchison, N.D., Staverosky, J.A., Dunker, N., Schweitzer, R., 2009. Recruitment and maintenance of tendon progenitors by TGFbeta signaling are essential for tendon formation. Development (Cambridge, England) 136, 1351-1361.
Rallis, C., Bruneau, B.G., Del Buono, J., Seidman, C.E., Seidman, J.G., Nissim, S., Tabin, C.J., Logan, M.P., 2003. Tbx5 is required for forelimb bud formation and continued outgrowth. Development (Cambridge, England) 130, 2741-2751.
Reijntjes, S., Stricker, S., Mankoo, B.S., 2007. A comparative analysis of Meox1 and Meox2 in the developing somites and limbs of the chick embryo. The International journal of developmental biology 51, 753-759.
Rodrigo, I., Bovolenta, P., Mankoo, B.S., Imai, K., 2004. Meox homeodomain proteins are required for Bapx1 expression in the sclerotome and activate its transcription by direct binding to its promoter. Molecular and cellular biology 24, 2757-2766.
Sakabe, T., Sakai, T., 2011. Musculoskeletal diseases--tendon. British medical bulletin 99, 211-225.
Sanderson, I.R., Ezzell, R.M., Kedinger, M., Erlanger, M., Xu, Z.X., Pringault, E., Leon-Robine, S., Louvard, D., Walker, W.A., 1996. Human fetal enterocytes in vitro: modulation of the phenotype by extracellular matrix. Proceedings of the National Academy of Sciences of the United States of America 93, 7717-7722.
Schafer, K., Braun, T., 1999. Early specification of limb muscle precursor cells by the homeobox gene Lbx1h. Nature genetics 23, 213-216.

Schmidt, C., Bladt, F., Goedecke, S., Brinkmann, V., Zschiesche, W., Sharpe, M., Gherardi, E., Birchmeier, C., 1995. Scatter factor/hepatocyte growth factor is essential for liver development. Nature 373, 699-702.
Schwartz, A.G., Lipner, J.H., Pasteris, J.D., Genin, G.M., Thomopoulos, S., 2013. Muscle loading is necessary for the formation of a functional tendon enthesis. Bone 55, 44-51.
Schweitzer, R., Chyung, J.H., Murtaugh, L.C., Brent, A.E., Rosen, V., Olson, E.N., Lassar, A., Tabin, C.J., 2001. Analysis of the tendon cell fate using Scleraxis, a specific marker for tendons and ligaments. Development (Cambridge, England) 128, 3855-3866.
Schweitzer, R., Zelzer, E., Volk, T., 2010. Connecting muscles to tendons: tendons and musculoskeletal development in flies and vertebrates. Development (Cambridge, England) 137, 2807-2817.
Shukunami, C., Oshima, Y., Hiraki, Y., 2001. Molecular cloning of tenomodulin, a novel chondromodulin-I related gene. Biochemical and biophysical research communications 280, 1323-1327.
Shukunami, C., Takimoto, A., Oro, M., Hiraki, Y., 2006. Scleraxis positively regulates the expression of tenomodulin, a differentiation marker of tenocytes. Developmental biology 298, 234-247.
Silver, F.H., Freeman, J.W., Seehra, G.P., 2003. Collagen self-assembly and the development of tendon mechanical properties. Journal of biomechanics 36, 1529-1553.
Skuntz, S., Mankoo, B., Nguyen, M.T., Hustert, E., Nakayama, A., Tournier-Lasserve, E., Wright, C.V., Pachnis, V., Bharti, K., Arnheiter, H., 2009. Lack of the mesodermal homeodomain protein MEOX1 disrupts sclerotome polarity and leads to a remodeling of the cranio-cervical joints of the axial skeleton. Developmental biology 332, 383-395.
Smith, T.G., Sweetman, D., Patterson, M., Keyse, S.M., Munsterberg, A., 2005. Feedback interactions between MKP3 and ERK MAP kinase control scleraxis expression and the specification of rib progenitors in the developing chick somite. Development (Cambridge, England) 132, 1305-1314.
Smith, T.H., Kachinsky, A.M., Miller, J.B., 1994. Somite subdomains, muscle cell origins, and the four muscle regulatory factor proteins. The Journal of cell biology 127, 95-105.
Soeda, T., Deng, J.M., de Crombrugghe, B., Behringer, R.R., Nakamura, T., Akiyama, H., 2010. Sox9-expressing precursors are the cellular origin of the cruciate ligament of the knee joint and the limb tendons. Genesis (New York, N.Y. : 2000) 48, 635-644.
Spitz, F., Gonzalez, F., Duboule, D., 2003. A global control region defines a chromosomal regulatory landscape containing the HoxD cluster. Cell 113, 405-417.
Stern, M.M., Myers, R.L., Hammam, N., Stern, K.A., Eberli, D., Kritchevsky, S.B., Soker, S., Van Dyke, M., 2009. The influence of extracellular matrix derived from skeletal muscle tissue on the proliferation and differentiation of myogenic progenitor cells ex vivo. Biomaterials 30, 2393-2399.
Subramanian, A., Wayburn, B., Bunch, T., Volk, T., 2007. Thrombospondin-mediated adhesion is essential for the formation of the myotendinous junction in Drosophila. Development (Cambridge, England) 134, 1269-1278.
Sugimoto, Y., Takimoto, A., Akiyama, H., Kist, R., Scherer, G., Nakamura, T., Hiraki, Y., Shukunami, C., 2013a. Scx+/Sox9+ progenitors contribute to the establishment of the junction between cartilage and tendon/ligament. Development (Cambridge, England) 140, 2280-2288.
Sugimoto, Y., Takimoto, A., Hiraki, Y., Shukunami, C., 2013b. Generation and characterization of ScxCre transgenic mice. Genesis (New York, N.Y. : 2000) 51, 275-283.
Suzuki, M., Kuroiwa, A., 2002. Transition of Hox expression during limb cartilage development. Mechanisms of development 118, 241-245.
Swinehart, I.T., Schlientz, A.J., Quintanilla, C.A., Mortlock, D.P., Wellik, D.M., 2013. Hox11 genes are required for regional patterning and integration of muscle, tendon and bone. Development (Cambridge, England) 140, 4574-4582.

Tajbakhsh, S., Buckingham, M.E., 1994. Mouse limb muscle is determined in the absence of the earliest myogenic factor myf-5. Proceedings of the National Academy of Sciences of the United States of America 91, 747-751.
Tajbakhsh, S., Rocancourt, D., Buckingham, M., 1996. Muscle progenitor cells failing to respond to positional cues adopt non-myogenic fates in myf-5 null mice. Nature 384, 266-270.
Theveneau, E., Mayor, R., 2012. Cadherins in collective cell migration of mesenchymal cells. Current opinion in cell biology 24, 677-684.
Tidball, J.G., 1994. Assembly of myotendinous junctions in the chick embryo: deposition of P68 is an early event in myotendinous junction formation. Developmental biology 163, 447-456.
Tidball, J.G., Lin, C., 1989. Structural changes at the myogenic cell surface during the formation of myotendinous junctions. Cell and tissue research 257, 77-84.
Tosney, K.W., Dehnbostel, D.B., Erickson, C.A., 1994. Neural crest cells prefer the myotome's basal lamina over the sclerotome as a substratum. Developmental biology 163, 389-406.
Tozer, S., Duprez, D., 2005. Tendon and ligament: development, repair and disease. Birth defects research. Part C, Embryo today : reviews 75, 226-236.
Trelstad, R.L., Birk, D.E., Silver, F.H., 1983. Cellular and collagen fibrillar polarity in developing chick limb tendon. Progress in clinical and biological research 110 Pt A, 245-249.
Tseng, B.S., Cavin, S.T., Booth, F.W., Olson, E.N., Marin, M.C., McDonnell, T.J., Butler, I.J., 2000. Pulmonary hypoplasia in the myogenin null mouse embryo. American journal of respiratory cell and molecular biology 22, 304-315.
Valcourt, U., Thuault, S., Pardali, K., Heldin, C.H., Moustakas, A., 2007. Functional role of Meox2 during the epithelial cytostatic response to TGF-beta. Molecular oncology 1, 55-71.
Vasyutina, E., Stebler, J., Brand-Saberi, B., Schulz, S., Raz, E., Birchmeier, C., 2005. CXCR4 and Gab1 cooperate to control the development of migrating muscle progenitor cells. Genes & development 19, 2187-2198.
Vogan, K.J., Epstein, D.J., Trasler, D.G., Gros, P., 1993. The splotch-delayed (Spd) mouse mutant carries a point mutation within the paired box of the Pax-3 gene. Genomics 17, 364-369.
Wachtler, F., Christ, B., Jacob, H.J., 1981. On the determination of mesodermal tissues in the avian embryonic wing bud. Anatomy and embryology 161, 283-289.
Watson, S.S., Riordan, T.J., Pryce, B.A., Schweitzer, R., 2009. Tendons and muscles of the mouse forelimb during embryonic development. Developmental dynamics : an official publication of the American Association of Anatomists 238, 693-700.
Welser, J.V., Rooney, J.E., Cohen, N.C., Gurpur, P.B., Singer, C.A., Evans, R.A., Haines, B.A., Burkin, D.J., 2009. Myotendinous junction defects and reduced force transmission in mice that lack alpha7 integrin and utrophin. The American journal of pathology 175, 1545-1554.
Woltering, J.M., Noordermeer, D., Leleu, M., Duboule, D., 2014. Conservation and divergence of regulatory strategies at Hox Loci and the origin of tetrapod digits. PLoS biology 12, e1001773.
Yoon, B.S., Pogue, R., Ovchinnikov, D.A., Yoshii, I., Mishina, Y., Behringer, R.R., Lyons, K.M., 2006. BMPs regulate multiple aspects of growth-plate chondrogenesis through opposing actions on FGF pathways. Development (Cambridge, England) 133, 4667-4678.
Young, M.F., Bi, Y., Ameye, L., Chen, X.D., 2002. Biglycan knockout mice: new models for musculoskeletal diseases. Glycoconjugate journal 19, 257-262.
Zakany, J., Duboule, D., 2007. The role of Hox genes during vertebrate limb development. Current opinion in genetics & development 17, 359-366.
Zhang, G., Young, B.B., Ezura, Y., Favata, M., Soslowsky, L.J., Chakravarti, S., Birk, D.E., 2005. Development of tendon structure and function: regulation of collagen fibrillogenesis. Journal of musculoskeletal & neuronal interactions 5, 5-21.
Zhang, J., Wang, J.H., 2010. Mechanobiological response of tendon stem cells: implications of tendon homeostasis and pathogenesis of tendinopathy. Journal of orthopaedic research : official publication of the Orthopaedic Research Society 28, 639-643.

Zhang, K., Sha, J., Harter, M.L., 2010. Activation of Cdc6 by MyoD is associated with the expansion of quiescent myogenic satellite cells. The Journal of cell biology 188, 39-48.